

**Yield Assessment of Grapes in Drought Prone Areas Using
Satellite Remote Sensing-based Time-Series Datasets and
Machine Learning Approach**

July 2022

SARA TOKHI ARAB

Yield Assessment of Grapes in Drought Prone Areas Using Satellite Remote Sensing-based Time-Series Datasets and Machine Learning Approach

A Dissertation Submitted to
the Graduate School of Life and Environmental Sciences,
the University of Tsukuba
in Partial Fulfillment of the Requirements
for the Degree of Doctor of Philosophy in Agricultural Science
(Doctoral Program in Appropriate Technology and Sciences for Sustainable Development)

SARA TOKHI ARAB

Abstract

Grapes are one of the most sensitive horticultural crops to climate change effects, especially drought. Drought has a significant impact on grape yield and grapevines throughout the world. To minimize drought's impact on vineyards and support farmers' livelihoods from micro to regional scale assessment and interventions are required. The remote sensing datasets consisting of vegetation signatures of grapevines and climatic factors can be trained using machine learning approaches to predict the long-term changes in yield assessments and weather predictions for interventions to support growers. Thus, the primary goal of this study was to develop yield assessment models and drought monitoring systems with numerous agrometeorological factors that can predict drought severity utilizing timescale satellite datasets and machine learning techniques.

First, yield prediction was performed at the micro-scale during drought-affected periods by combining satellite-derived datasets with machine learning methods. The ground reference data were collected during a field survey in the Shakardara district of Kabul Province. The satellite-based vegetation indices such as the normalized difference vegetation index (NDVI), leaf area index (LAI), and normalized difference water index (NDWI) were mapped using Landsat 8 surface reflectance images for the years 2017–2019. Furthermore, moving averages and exponential smoothing techniques was used per-pixel. In 2018, NDVI had the maximum performance ($r^2 = 0.79$) of all the vegetative indices; however, in 2019, the LAI performance was greater than the other indices ($r^2 = 0.79$). Artificial neural network-based machine learning showed that NDVI was the most accurate of all vegetative indices in 2017 ($R = 0.94$), 2018 ($R = 0.95$), and 2019 ($R = 0.92$).

Second, grape yield loss assessment was conducted in drought-affected vineyards at macro-scale using a composite drought index derived from satellite remote sensing-based time-series datasets. Since a single index is not able to predict yield loss, appropriately using a composite index is significant. The primary data were collected during a field survey in Kabul Province, Afghanistan. The composite drought index (CDI) was created for the five years (2016 to 2020) using five indices, such as vegetation condition index (VCI), temperature condition index (TCI), deviation of NDVI (NDVI DEV), normalized difference moisture index (NDMI), and precipitation condition index (PCI). Furthermore, each input parameter was given a weight using the principal component analysis (PCA) method, and the weights of all the indices were then added together to create a composite drought index. Moreover, the yield fluctuation in each damaged vineyard was assessed using Bayesian regularized artificial neural

networks (BRANNs). According to the CDI, there was moderate to severe drought in Kabul Province in 2016 and 2018. The related yield losses were 3.4 tons per hectare and 4.7 tons per hectare.

Third, drought severity analysis was carried out for regional vineyard production management using satellite remote sensing and climate datasets at a regional scale. In this research, the standard vegetation index (SVI) and standardized precipitation index (SPI) for the years 2013–2021 were developed. The results showed that the most drought-affected years were 2018 and 2021. In 2018, 4785.03 ha and in 2021, 1825.83 ha were extremely affected by drought. The multi-linear regression result was better than the linear model for regional drought validation ($r^2 = 0.79$).

Fourth, land suitability analysis was performed from micro to regional scales in drought prone areas using satellite remote sensing and multi-criteria decision analysis. In this context, the main goal of this research is to integrate bio-physical and socio-economic criteria. In this research, the same criteria were used for both micro and macro-scale analysis. However, for regional scale, the socio-economic criteria were not available. Thus, vegetation indices, topographic maps (elevation, aspect), and climatic datasets were used. Finally, a weighted overlay method based on the analytical hierarchy overlay process (AHP) for micro-to-macro scales and a fuzzy overlay method were used for regional suitability determination. Based on the results of both physical and socioeconomic suitability, 46 percent of the micro-scale sites are very suitable. However, on macro scale, highly suitable (13%) areas and on regional scale, highly suitable (23%) regions for grape production were reported.

In conclusion, the integrated models of remote sensing, GIS and machine learning were employed to realize yield variation and water stress on vineyards from micro to regional scales during drought-prone years. The generated models could be applied from micro to regional scales for grape yield prediction, yield loss, and drought severity assessment to identify less productive land. These models will assist policymakers to reduce the effects of drought and design drought-severity-based subsidy programs in drought-prone regions in order to improve farmers' livelihoods.

Keywords: Grape yield assessment, Micro-scale, Macro-scale, Regional-scale, Yield prediction, Composite drought index, Regional drought distribution, Satellite remote sensing, Time-series datasets, Machine learning, Vegetation indices, Physical and socio-economic suitability, GIS

Table of Contents

Abstract.....	i
List of Abbreviations	viii
List of Nomenclatures.....	x
List of Figures	xi
List of Tables	xv
List of Appendices	xvii
Chapter 1	1
Introduction.....	1
1.1 Background of the Research	1
1.2 Justification of the study	4
1.3 Research Objectives.....	5
1.4 Outline of the Thesis	5
Chapter 2.....	7
Review of Relevant Literature	7
2.1 Review of Literature	7
2.1.1 Yield Prediction Methods for Grapes using Satellite Remote Sensing.....	7
2.1.1.1 Parametric Grape Yield Prediction Method.....	7
2.1.1.2 Non-parametric Grape Yield Prediction Method.....	8
2.1.2 Yield Loss Assessment	8
2.1.2.1 Yield Loss Assessment based on Single Index	9
2.1.2.2 Yield Loss Assessment based on Composite Index	9
2.1.3 Drought Severity Evaluation.....	10
2.1.3.1 Normalized Difference Vegetation Index	11
2.1.3.2 Standard Vegetation Index (SVI).....	11
2.1.3.3 Standard Precipitation Index (SPI)	11
2.1.3.4 Recent Research on Drought in Afghanistan.....	11
2.1.4 Land Suitability Analysis.....	11
2.1.4.1 Analytical Hierarchical Process (AHP) Weighting.....	13
Chapter 3.....	15
Prediction of Grape Yield at Micro-scale Drought Prone Areas Using Satellite Remote Sensing-based Time-Series Vegetation Indices and Machine-Learning Approach.....	15
3.1 Background of the Research	15
3.2 Methodology	17
3.2.1 Geographical Extent of the Study Area	17
3.2.2 Dataset Acquisition and Analysis	19
3.2.2.1 Satellite Data Acquisition and Image Preprocessing	19

3.2.2.1.1 Normalized Difference Vegetation Index (NDVI).....	19
3.2.2.1.2 Leaf Area Index (LAI)	19
3.2.2.1.3 Normalized Difference Water Index (NDWI)	20
3.2.2.2 Statistical Analysis.....	20
3.2.2.3 Ground Reference Data.....	21
3.3 Results.....	25
3.3.1 Growth Stages Analysis.....	25
3.3.2 Spatial Correlations among NDVI, LAI and NDWI.....	26
3.3.3 Yield Prediction Models	29
3.4 Discussion.....	32
3.5 Conclusion	36
Chapter 4.....	37
Yield Loss Estimation of Grapes at Macro Scale Using Composite Drought Index from Satellite Remote Sensing-based Time Series Datasets	37
4.1 Background of the Research.....	37
4.2 Materials and Methods.....	40
4.2.1 Study Area	40
4.2.2 Data Description	42
4.2.2.1 Satellite Datasets and Data preprocessing.....	42
4.2.2.2 Composite Drought Indices	43
4.2.2.2.1 Deviation of NDVI (DEV of NDVI)	43
4.2.2.2.2. Vegetation Condition Index (VCI).....	43
4.2.2.2.3 Temperature Condition Index (TCI).....	44
4.2.2.2.4 Normalized Difference Moisture Index (NDMI).....	44
4.2.2.2.5 Precipitation Condition Index (PCI)	44
4.2.2.2.6 Standard Precipitation Index (SPI).....	45
4.2.2.3 Ground Reference Datasets.....	46
4.2.3 Methods.....	47
4.2.3.1 Composite Drought Index.....	47
4.2.3.2 Validation of the Composite Drought Index with SPI.....	49
4.2.3.3 Evaluation of Yield Variations due to Drought using BRANNs	49
4.3 Results.....	50
4.3.1 Drought Assessment using CDI.....	50
4.3.2 Validation of CDI with SPI.....	53
4.3.3 Variation in Table Grape Yield.....	56
4.4 Discussion.....	58
4.5 Conclusion	60

Chapter 5.....	62
Drought Severity Analysis for Regional Vineyard Production Management Using Landsat OLI and CHIRPS Datasets	62
5.1 Background of the Research	62
5.2 Materials and Methods.....	64
5.2.1 Area of Research.....	64
5.2.2 Datasets	65
5.2.2.1 Standard Vegetation Index (SVI) for Drought Monitoring.....	66
5.2.2.2 Standard Precipitation Index (SPI)	66
5.2.2.3 Land Cover Map	67
5.2.2.4 Statistical Data	67
5.2.3 Methods.....	69
5.2.3.1 Vineyard Drought Assessment using the time-series SVI and SPI.....	69
5.2.3.2 Drought Verification with Time-series Grape Yield.....	69
5.3 Results.....	70
5.3.1 Drought severity assessment with the time-series SVI	70
5.3.2 Drought Severity Assessment with Time-series SPI-1	73
5.3.3 Drought Affected Vineyards in Afghanistan	74
5.3.4 Verification of Drought Maps with Grape Yield	74
5.4 Discussion.....	80
5.5 Conclusion	82
Chapter 6.....	84
Land Suitability Analysis for Grapes Production from Micro to Regional Scales in Drought-prone Areas Using Satellite Remote Sensing and Multi-criteria Decision Support Systems	84
6.1 Background of the Research	84
6.2 Materials and Methods.....	87
6.2.1 Description of the Study Area.....	87
6.2.2 Data collection and criteria selection for table grapes land suitability analysis.....	89
6.2.3 Micro to Macro Scales Criteria.....	89
6.2.3.1 Normalized Difference Vegetation Index (NDVI).....	89
6.2.3.2 Normalized Difference Moisture Index (NDMI).....	89
6.2.3.3 Land Surface Temperature (LST)	90
6.2.3.4 Rainfall.....	91
6.2.3.5 Elevation	92
6.2.3.6 Slope	92
6.2.3.7 Aspect	92
6.2.3.8 Distance from River.....	93

6.2.3.9 Soil Components	93
6.2.3.10 Soil pH	96
6.2.3.11 Distance from River	96
6.2.3.12 Soil Salinity	96
6.2.3.13 Soil Organic Matter	97
6.2.3.14 Land Use Map	97
6.2.3.15 Distance from Road	97
6.2.3.16 Population Density	97
6.2.3.17 Benefit-Cost Ratio (BCR)	98
6.2.3.18 Distance from Market	98
6.2.4 Regional Scales Criteria	98
6.2.5 Criteria Reclassification and Weighted Linear Combination for Micro to Macro	99
6.2.6 Analytical Hierarchy Process (AHP)	99
6.2.7 Dataset and Criteria Conversion (Fuzzification)	101
6.2.7.1 Elevation	102
6.2.7.2 Slope	102
6.2.7.3 River	102
6.2.7.4 Road	102
6.2.7.5 Soil datasets	103
6.2.7.6 Normalized Difference Vegetation Index (NDVI)	103
6.2.7.7 Land Use Land Cover (LULC)	103
6.2.7.8 Rainfall	104
6.2.7.9 Fuzzy Overlay	104
6.2.7.10 Validation of Suitability Map with Ground Reference Data	104
6.3 Results	117
6.3.1 Reclassification of Criteria for Micro to Macro Scales	117
6.3.2 Analytical Hierarchy Process Weights (AHP)	117
6.3.3 Land Suitability Analysis	119
6.3.4 Reclassification of Criteria for Regional Scale	122
6.3.4.1 Fuzzy Overlay Analysis	122
6.3.4.2 Fuzzy Suitability Validation	123
6.4 Discussion	123
6.5 Conclusions	126
Chapter 7	127
Overall Conclusions	127
7.1. Yield Prediction using Machine Learning at Micro-scale	127
7.2. Yield loss Assessment Using Composite Drought Index at Macro-scale	127

7.3. Vineyard Drought Severity Assessment at Regional Scale	128
7.4. Land Suitability Assessment from Micro to Regional scales	128
7.5 Future Contributions	129
Acknowledgement	130
References.....	132
Appendices.....	159
Additional Appendices A.....	168
Additional Appendices B.....	171
Additional Appendices C.....	173
Additional Appendices D.....	174
Additional Appendices E.....	174

List of Abbreviations

Aberration	Description
AHP	Analytical Hieratical Process
ANN	Artificial Neural Network
BCR	Benefit Cost Ratio
BRANNs	Bayesian regularized neural network
BT	Brightness Temperature
CDI	Composite Drought Index
CI	Consistency Index
DEM	Digital Elevation Model
DEV	Deviation of Vegetation
EXP	Exponential function
EU	European Union
FAO	Food Agriculture Organization
GIS	Geographical Information System
GNDVI	Green Normalized Difference Index
GPS	Geographical Positioning System
GSMaP	Global Satellite Mapping of Precipitation
Ha	Hectare
K	Kelvin
JAXA	Japan Aerospace Exploration Agency
LAI	Leaf Area Index
LST	Land Surface Temperature
LULC	Land Use Land Cover
M	Mean
m	Meter
MA	Moving average
MADCAT	Mapping Device-Change Analysis System Tool Software Suite
Max	Maximum
Min	Minimum
N	Not Suitable
NDMI	Normalized Difference Moisture Index
NDVI	Normalized Difference Vegetation Index
NDWI	Normalized Difference Water Index
NIR	Near Infra-Red
NN	Neural Network
OLI	Operational Land Imager

OM	Organic Matter
PCA	Principal Component Analysis
PCI	Precipitation Condition Index
PH	Power of Hydrogen
PV	Proportion of Vegetation
RI	Consistency Random Index
S1	Highly Suitable
S2	Moderately Suitable
S3	Marginally Suitable
SPI	Standard Precipitation Index
SVI	Standard Vegetation Index
SWIR	Shortwave Infrared
TCI	Temperature Condition Index
TIR	Thermal Infrared Sensor
TOA	Top of Atmosphere
UN	United Nation
USDA	United States Department of Agriculture
USGS	United States Geological Survey
VCI	Vegetation Condition Index
W	Weight

List of Nomenclatures

Symbol	Description
∞	Alpha
β	Beta scale parameters
$^{\circ}\text{C}$	Celsius Degree
C	Criteria
ε	Emissivity
e	Exponential function
$\Gamma(\alpha)$	Gamma Function
λ	Lambda
μm	Micrometers
Y_{O}	Observed Yield
λ_{max}	Principal Eigen Value
ρ	Rho
α	Shape Parameters
Y_{p}	Simulated Yield or Potential Yield
L	Suitability Lands

List of Figures

Figure		Page
1.1	The world's leading grape producer countries in 2019 (FAO,2019)	1
1.2	The world map depicts the global drought risk based on the WWF report (WWF, 2018)	2
1.3	The annual growth cycle of grapevines	3
1.4	Grape production and cultivation area in Afghanistan between 2006 and 2020	4
1.5	Dissertation main body structure from Chapter 3 to Chapter 6	6
2.1	The AHP multi-criteria hierarchy structure	14
3.1	Geographical scope and maps of the research area: (a) Afghanistan location in world (b) Afghanistan administrative area, (c) Kabul Province, and (d) Shakardara District.	18
3.2	Research flowchart for yield prediction of table grapes.	22
3.3	Artificial neural network (ANN) algorithm for predicting table grape yield	23
3.4	Time-series vegetation indices: (a) NDVI, (b) LAI and (c) NDWI in 2017, 2018 and 2019 before and after moving average and exponential smoothing	27
3.5	NDVI-, LAI- and NDWI-derived growth stage maps of grapes in Shakardara District (a, b and c) in 2017, (d, e and f) in 2018 and (g, h and i) in 2019	28
3.6	Scatterplots showing the regression between the vegetation indices and the yield: yield with NDVI (a), yield with LAI (b) and yield and NDWI (c) in 2017, 2018 and 2019	30
3.7	Scatterplots showing the NN-fit results between NDVI, LAI and NDWI and yield in 2017 (a, d and g), 2018 (b, e and h) and 2019 (c, f and i)	31
3.8	Graphs showing the difference between the predicted yield and the actual yield: (a) comparison of predicted and actual yield by the regression model and ANN model for the year 2017, (b) comparison of predicted and actual yield by the regression model and ANN model for the year 2018 and (c) comparison of predicted and actual yield by the regression model and ANN model for the year 2019.	33
3.9	Predicted yield map with (a) NDVI (2017, 2018 and 2019), (b) LAI (2017, 2018 and 2019), and (c) NDWI (2017, 2018 and 2019) in tons per hectare	35
4.1	The study's geographical scope and maps: (a) Afghanistan administrative map, and (b) Kabul Province land cover map based on FAO data.	41

4.2	Research flowchart for predicting drought and yield losses using CDI and machine learning systems to estimate losses.	48
4.3	Drought severity risk areas based on CDI in Kabul Province during the active growing stages of vines from 2016-2020	52
4.4	Percentage of affected agricultural land and vineyards in extreme to moderate drought conditions in Kabul Province from 2016-2020	53
4.5	Standard Precipitation Index (SPI) using JAXA cumulative rainfall for the years of 2016 to 2020	54
4.6	Yearly time series comparison of the zonal mean CDI value of each district with the mean SPI value (April to October) from 2016 to 2020	55
4.7	Scatterplots showing the BRNN results between the yield and CDI in 2016 (a and b) and 2018 (c and d).	56
4.8	Percentage of yield losses: (a) the yield variations under severe drought conditions in 2016 and (b) the yield variations under moderate drought conditions in 2016	58
4.9	Bar charts showing the percentage of yield loss: (a) the yield variations under severe drought conditions in 2018 and (b) the yield variations under moderate drought conditions in 2018	59
5.1	Afghanistan land cover map	65
5.2	A comprehensive flowchart of the regional vineyard drought detection method	68
5.3	Bar chart showing grape production and line chart showing the area under cultivation from 2013 to 2020 in Afghanistan	69
5.4	The zonal mean SVI value in the berry formation and veraison stages before harvest (June, July, and August) in Afghanistan was calculated from 2013 to 2021	70
5.5	Drought classification based on SVI in the berry formation and veraison stages before harvest (June, July, and August) in Afghanistan from 2013 to 2021	71-72
5.6	Zonal mean SPI values in the berry formation and veraison stages before harvest (June, July and August) from 2013 to 2021 in Afghanistan	73
5.7	Minimum SPI value in the berry formation and veraison stages before harvest (June, July and August) from 2013 to 2021 in Afghanistan	73

5.8	Drought classification based on SPI in the berry formation and veraison stages before harvest (June, July, and August) in Afghanistan from 2013 to 2021	75-76
5.9	SPI and SVI- based proportion of drought-strick areas classes (extreme, severe and modern drought) in Afghanistan from 2013 to 2021	78
5.10	Total drought-affected vineyards in three classes (extreme, severe and modern drought) in Afghanistan from 2013 to 2021	78
5.11	The scoter plot shows the regression between grape yield and drought indices (SVI and SPI). (a) June, (b) July and (c) August	79
6.1	Table grape production from 2006-2020 in Afghanistan	86
6.2	The study area's geographical position, from micro to regional levels: (a) Shakardara District (b) Kabul Province (c) Afghanistan administrative map	88
6.3	Schematic chart shows the methodologies that are applied for land suitability analysis for vineyards under dry conditions in Afghanistan	94
6.4	Research framework for vineyard suitability analysis based on a fuzzy algorithm	95
6.5	Reclassification of criteria for micro- scale (a-o) for physical criterion and from (p-t) for socio-economic criterion for vineyards suitability analysis	107-110
6.6	Reclassification of criteria for macro-scale (a-o) for physical criterion and from (p-t) for socio-economic criterion for vineyards suitability analysis	111-114
6.7	Average yield of table grapes (ton/ha) in Afghanistan during 2020	114
6.8	Reclassification of the criterion used for suitability analysis (a-k)	115-116
6.9	(a) Land suitability analysis for grape production based on physical criterion at micro-Scale (Shakardara District) and (b) pie chart showing the percentage of land for each of the four suitability classes.	120
6.10	(a) Land suitability analysis for grape production based on physical criterion at macro-scale (Kabul Province) (b) pie chart showing the percentage of land for each of the four suitability classes.	120
6.11	(a) Land suitability map for grape production based on socio-economical criterion at mircro-scale and (b) pie chart showing the percentage of land for each of the four suitability classes.	121

6.12	(a) Land suitability map for grape production based on socio-economical criterion at macro-scale and (b) pie chart showing the percentage of land for each of the four suitability classes.	121
6.13	Land suitability analysis combining physical and socio economic for grape production in Shakardara District	124
6.14	Land suitability analysis combining physical and socio economic for grape production in Kabul Province	125
6.15	Suitable areas for table grape production in Afghanistan based on fuzzy multicriteria decision analysis	125
6.16	Validation of fuzzy-based land suitability score referring to average grapes yield from different provinces in Afghanistan	126

List of Tables

Table	Page
2.1 Studies have been done for parametric and non-parametric methods of grape yield prediction	8
2.2 Studies have been used for drought indices for drought distribution assessment	12
2.3 Drought-related studies have recently been conducted in Afghanistan	13
3.1 Ground reference data collected from Shakardara District through surveys	24
3.2 Overall performances of vegetation indices at the growth stages of vineyards in Shakardara District	26
3.3 Artificial neural network designed for yield prediction of table grapes	26
3.4 Regression between yield and maximum/moving average indices during the specific growth stages and active growing stages (April to October)	34
3.5 The expected mean absolute error of the model predictions for 2017-2019 in Shakardara District	34
4.1 Average weight values estimated by PCA for individual indices for 2016-2020.	49
4.2 Drought classification system using the CDI values derived from several indices	53
4.3 The affected areas based on drought classes in agricultural lands and vineyards in Kabul Province from 2016 – 2020	55
4.4 Bayesian regularized neural network (BRANN) results, showing the severely and moderately drought-affected vineyards in 2016 and 2018.	57
5.1 The standardized vegetation index (SVI) is used to classify drought	66
5.2 Standard precipitation index (SPI) categories and values based on McKee for drought monitoring	67
5.3 The percentage of drought-affected regions based on the SVI in Afghanistan from 2013 to 2021	77
5.4 The percentage of drought-affected regions based on the SPI in Afghanistan from 2013 to 2021	80
5.5 Multilinear regression between average yield ton/ha and standard vegetation index and standard precipitation index from 2013 to 2020	82
6.1 Land suitability classes and descriptions based on FAO	87
6.2 List of data and source of datasets for table grapes land suitability analysis	100
6.3 Pairwise comparison matrix for grape based on physical criterion to evaluate in	105

	Kabul Province of Afghanistan	
6.4	Normalized matrix of the criteria for grapes based on socio-economic criterion under the dry condition	106
6.5	Value of random consistency index (RI) (Aguaron, 2003)	106
6.6	AHP weights according the expert's opinions for physical criterion	118
6.7	AHP weights according the expert's opinions for socio-economic criteris	118
6.8	Vineyards suitability classes based on combined physical and socio-economic factors at micro and marco scales	122
6.9	Potential areas belonging to the suitable classes based on fuzzy algorithms for Afghanistan	122
6.10	Vineyard locations of each suitability class in Afghanistan	123

List of Appendices

Appendix		Page
4.1	Yield maps shows the ground reference data and GPS points collected from Kabul Province through surveys.	159
4.2	Variation in yield in severely drought-affected vineyards in percent and tons in 2016	160
4.3	Variation in yield in moderately drought-affected vineyards in percent and tons in 2016	161-162
4.4	Variation in yield in severely drought-affected vineyards in percent and tons in 2018	163
4.5	Variation in yield in severely drought-affected vineyards in percent and tons in 201	164-165
6.1	Criteria classification for vineyard suitability analysis based on physical and socio-economics criterion	166-177

Chapter 1

Introduction

1.1 Background of the Research

Grapes (*Vitis Vinifera* L.) are a widely distributed horticultural fruit in the world. Global grape production was 77.13 million metric tons for the year 2019. Grapes are grown in temperate to Mediterranean climates, with an estimated surface area of 6.9 million hectares in 100 different territories. China is the world's greatest grape producer, with 14.8 million metric tons. Second is Italy, with 8.2 million tons; third is the USA, with 7.01 million tons; eighteenth is Afghanistan, with 874 thousand tons; and fortieth is Japan, with 171 thousand tons of grape production in 2019. (Figure 1.1). It implies that grapes are one of the world's most significant fresh fruits.

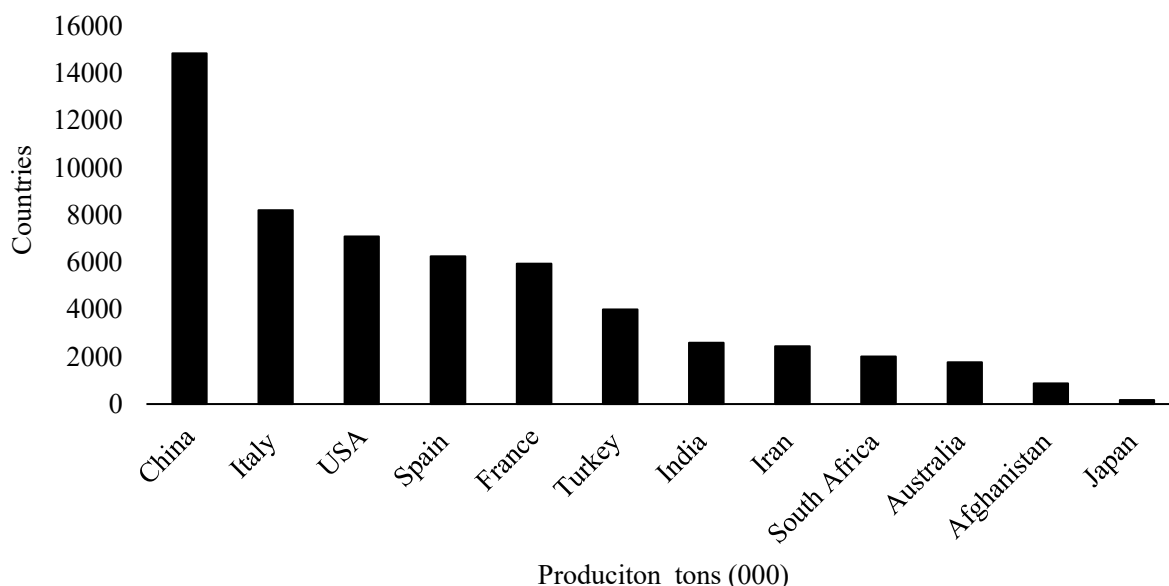


Figure 1.1 The world's leading grape producer countries in 2019 (FAO, 2019)

In recent years, climate change has had a significant substantial effect on worldwide grape output and has posed a substantial threat to vineyards. Many regions around the world are suffering from grape yield losses due to climate change, including Asia, Africa, Australia, Europe and America (Lopez-Fornieles et al., 2022; Field et al., 2012; Paterson and Lima, 2011). Climate variability is a critical issue that requires immediate attention. If we do not reduce our irresponsible actions against the environment now, global warming will approach 1.5 degrees Celsius within the coming decades. In this case, cumulative impacts will be more devastating and irreversible, affecting water quality, severe weather conditions (drought), continuing land degradation, and crop yield losses (Figure 1.2). These challenges are more crucial in developing nations (The Sustainable Development Goals report, 2019) such as the

South Asian regions (Afghanistan, Bangladesh, India and Pakistan), East Asia (China) and Africa (Figure 1.2). Figure 1.1 indicates that drought risk in the most parts of Asia and Africa was very high. Drought occurs in these regions due to decreased rainfall or increased temperatures (Figure 1.1). According to the United Nations Environment Program, when temperature and precipitation rise in a global pattern, production will fall 6% or 16% with carbon fertilization by 2080 (UN Environment Program, 2009). As a result, drought is among the worst environmental calamities that has transpired practically in all climatic zones, causing enormous damage to the ecology and economies of multiple nations, as well as an unprecedented loss of grapes. Afghanistan, like other developing countries, is experiencing drought due to lack of rainfall and rising temperatures. In the country, localized droughts had occurred every two to five years in the last decade. Afghanistan's severe drought occurrences were in 1995, 1998–2006, 2008–2009, 2018 and 2021-2022 (World Bank, 2018; Savage et al., 2009; FAO, 2019). During drought years most of the grape farmers suffered from production loss.

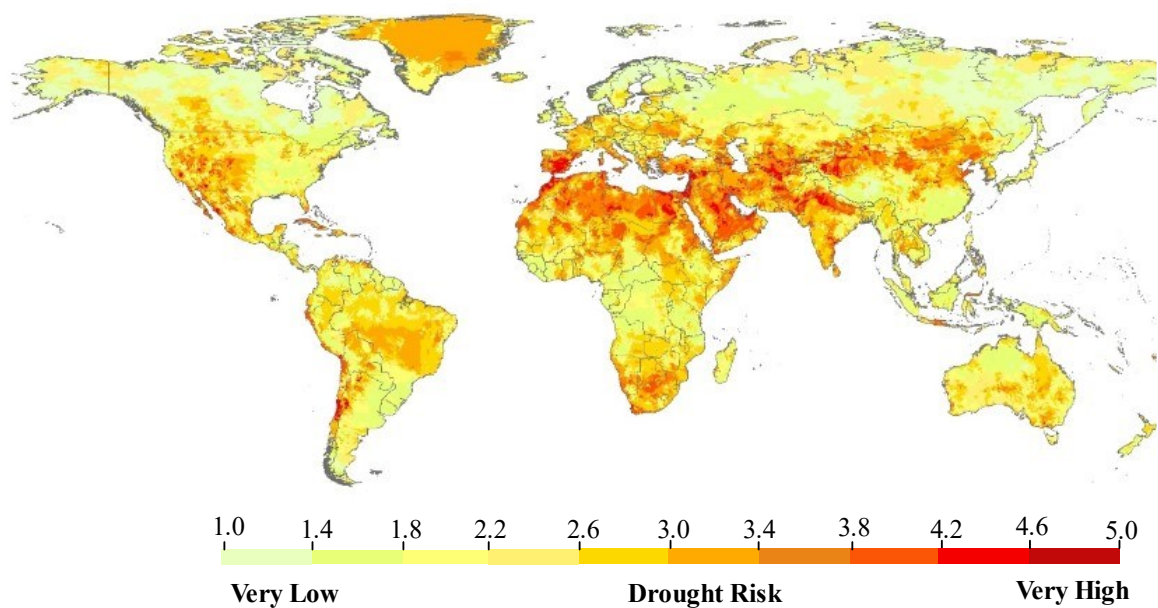


Figure 1.2 The world map depicts the global drought risk based on the WWF report (WWF, 2018)

Drought causes in vines and wine grapes high sugar concentration, acidity reduction and modification of the wine's entire flavor character, which results in less color in red wines. Drought causes stomatal closure, decreased leaf area growth, low flowering, fewer berries, cluster abscission, and ultimately restricted photosynthesis process in vine (Briglia et al., 2020; Patakas et al., 2005). As a result, it decreases the quality and quantity of grapes and changes in the vine's phenological stages (growth stages). These changes cause growth stages to occur earlier such as bud break, flowering, fruit set, and ripening, which can cause changes in a vineyard's entire management system (Figure 1.3). Finally,

drought can affect the fresh grape supply chain, accessibility, and quality of fruit (Delay et al., 2015). Therefore, using the conventional method of yield loss calculation and monitoring is not economically profitable for grape growers. Utilizing models and satellite time series datasets for calculating yield assessment is the best option. In this context, yield evaluation and assessment are essential tasks for farmers and policymakers to ensure farmers' income. It is also crucial in delivering timely information for best vineyard management practices, which includes an early assessment of the import/export strategy and pricing.

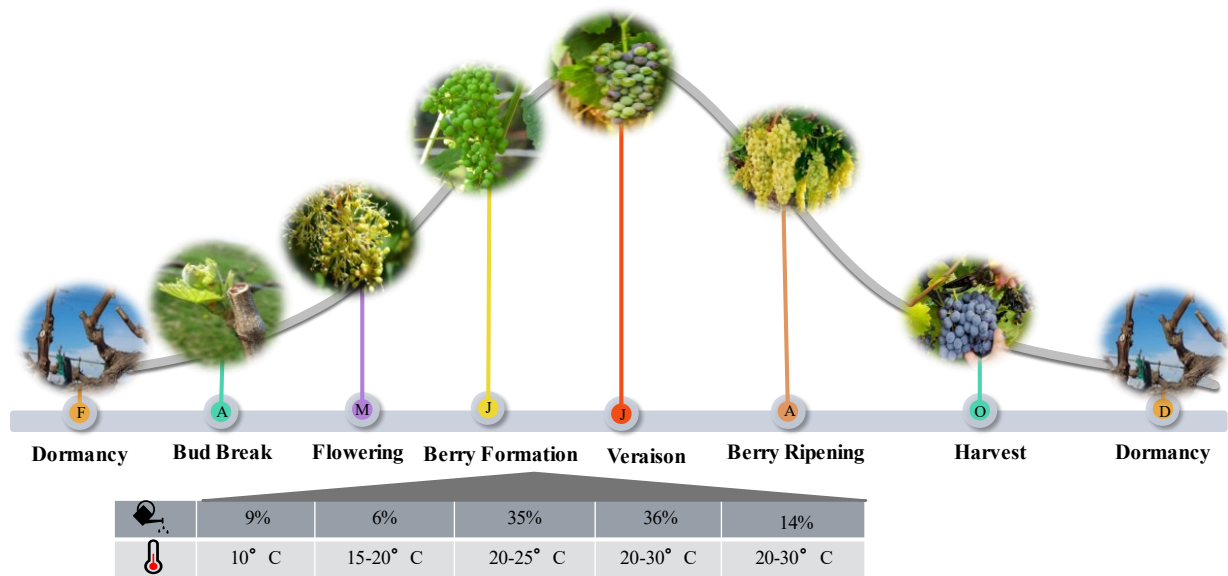


Figure 1.3 The annual growth cycle of grapevines

Satellite remote sensing offers the capacity to identify drought and assess yield in vineyards on a micro-regional scale. For this purpose, different satellites with special and temporal aquations, such as Landsat, MODIS, Sentinel, SPOT, ALOS and others are being utilized by researchers. Satellite time series datasets are essential, particularly in poor nations where data availability is limited. This might assist governments and policymakers in assisting farmers during the dry months preceding harvest by offering training on optimal water usage strategies. In addition, artificial neural networks, fuzzy models, decision trees, clustering, time series analysis, and Markov chain models are examples of machine learning methodologies based on mathematical and statistical methods that are being used for yield assessments. The implementation of these machine learning techniques in yield assessment offers even more benefits owing to the huge volume of data from many sources to extract hidden information.

1.2 Justification of the study

Drought is a serious issue in the agricultural industry, affecting crop yield and productivity, farmers' revenue, and the lives of residents who rely on production, especially in drought prone areas of Southeast Asia. Traditional approaches for drought assessment and determining yield losses due to drought require time and money, which is costly. The conventional methods are due to lack of reliable data, restricted information networks, and technological and institutional capabilities that are exceedingly difficult for most developing nations, including Afghanistan.

The localized drought frequency is between two or three years in Afghanistan, causing enormous damage to the vineyards, agricultural products and environment. Table grapes are the most important horticultural product by value and volume in Afghanistan. It made up 24% of all fresh fruits and is mostly vulnerable to climate variability (**Figure 1.4**). The graph shows the grape's production and vineyard areas from 2006 to 2020 in Afghanistan. The chart in Figure 1.4 indicated due to construction of new vineyards, as a result of that grape production increased from 2006 to 2020 in Afghanistan. However, due to climate change production decreased significantly.

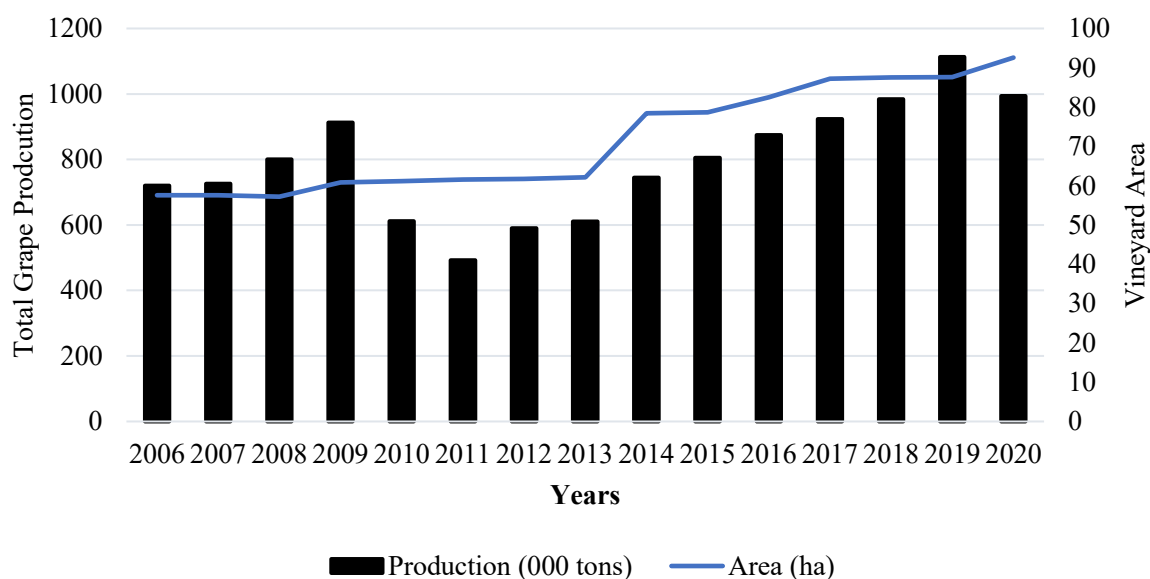


Figure 1.4 Grape production and cultivation area in Afghanistan between 2006 and 2020

Therefore, yield assessment of grapes is a crucial yield fluctuation indicator among vineyards at various stages of development. To overcome the issues mentioned above, it is preferable to rely on satellite sensor data, which is widely available, cost-effective, and capable of detecting the beginning of the drought, including its duration and bounds from micro to regional scales. Because immediate information on the scope and intensity of drought can help to mitigate the effects of drought-related

losses, near real-time evaluation utilizing satellite imagery and real-time satellite rainfall data can help to mitigate its negative effects. Besides, it assists farmers in developing for a suitable management strategy, understanding production variance throughout the farm, quality variation, preventing grape post and preharvest losses, using water conservation strategies, or using varieties with high drought tolerance and improved farm management. Furthermore, policymakers can understand the state of vineyards, mainly throughout times of drought. It could be capable of assisting them by offering technical assistance and subsidies to farmers during extreme events.

1.3 Research Objectives

The overall goal of this study was to use satellite remote sensing and a machine technique to quantify grape output in a drought-prone area. The following precise objectives were pursued to reach this goal:

1. To develop yield prediction models of grapes at the micro-scale during drought-affected periods using satellite remote sensing and machine learning approaches.
2. To estimate yield losses of grapes at the macro-scale using a composite drought index derived from satellite remote sensing-based time series datasets.
3. To conduct drought severity analysis for regional vineyard production management using satellite remote sensing and climate datasets.
4. To conduct a land suitability analysis for grape production from the macro to the regional scale in drought-prone areas using multi-criteria decision analysis and remote sensing sensor datasets.

1.4 Outline of the Thesis

This dissertation has been organized from chapters 1 to 7. Chapter 1 introduces the topic and illustrates current research issues and the importance of grape yield assessment in the vineyard. Chapter 2 reviews the relevant literature: stated the basic concepts of grape yield assessment, such as grape yield prediction, yield loss, drought severity and suitability analysis as an intervention at macro-regional scales in drought-prone areas. Chapter 3 describes the development of a yield prediction model for grapes from time-series vegetation indices using satellite remote sensing and machine-learning approach at a micro-scale in the Shakardar District. Chapter 4 described grape yield loss assessment with the composite drought index using satellite remote sensing and GIS approaches at the macro-scale in Kabul Province. Chapter 5 illustrates drought distribution for regional vineyard production management using Landsat OLI and CHIRPS datasets. Chapter 6 describes land suitability studies for grape cultivation utilizing satellite remote sensing, GIS, and the Analytical Hierarchy approach in dry regions of Afghanistan.

Chapter 7 presents the overall conclusions and highlights the recommendations for further research. Figure 1.5 explains the main body structure of the dissertation.

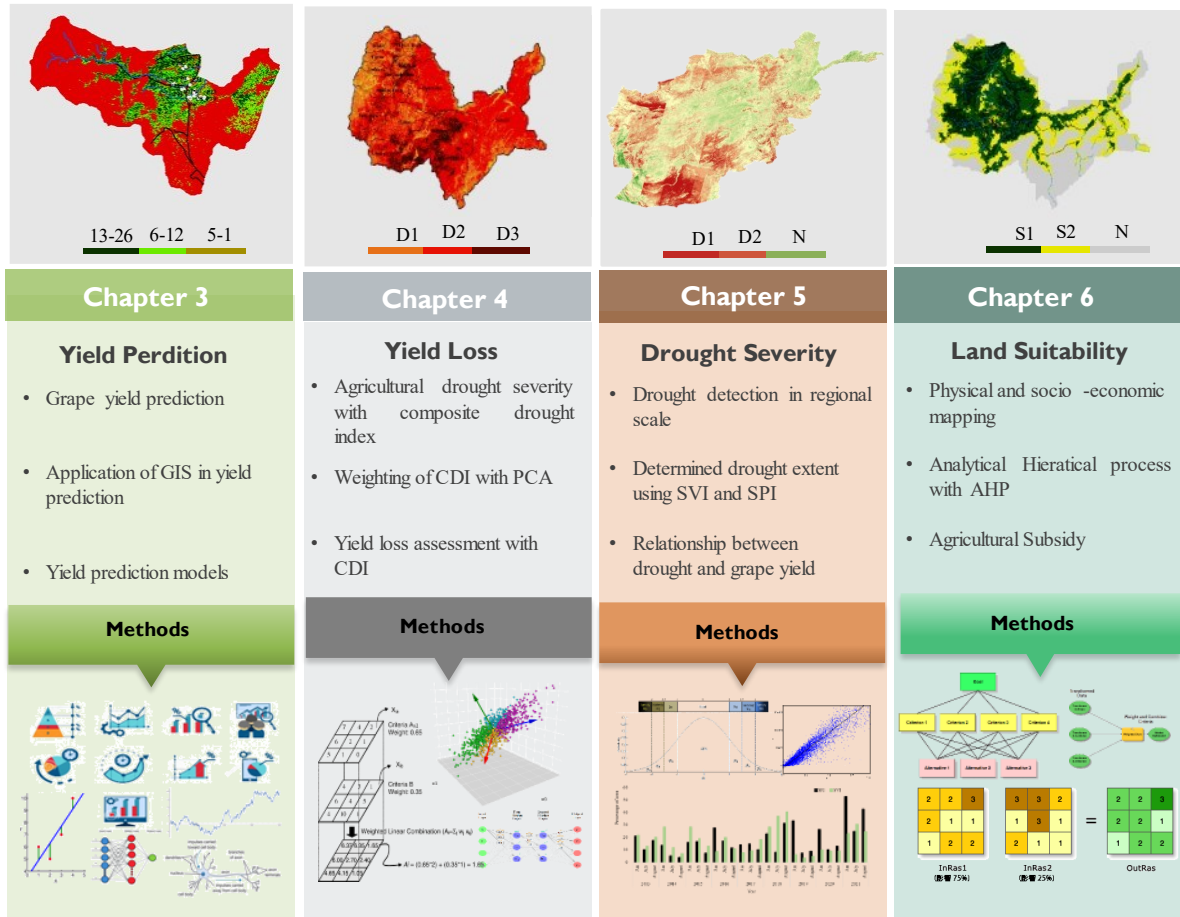


Figure 1.5 Dissertation main body structure from Chapter 3 to Chapter 6

Chapter 2

Review of Relevant Literature

2.1 Review of Literature

This chapter is designed to offer insight and a better picture of what has already been done in terms of yield prediction, yield loss, drought severity, and suitability analysis from micro-to-large scale drought detection for grape production using satellite remote sensing indices and machine learning approaches based on time-series datasets in drought-prone areas.

2.1.1 Yield Prediction Methods for Grapes using Satellite Remote Sensing

Yield prediction is the technique of estimating the number of grapes that will be harvested. These predictions are often made between the planting and harvesting of grapes. Growers must know how much fruit they are producing and if their vines are over-cropping or under-cropping to make the appropriate fruit adjustments through cluster thinning. In ground-based perdition, two main methods have been used for frequent grape yield prediction. The harvesting time cluster weighting method and the lag phase method are two methods for harvesting time cluster weighting. In the harvest time cluster weighting method, the average cluster weight at harvest time per unit of area has been considered. To predict the yield for the following season, in the lag-phase, the berries' weight reaches 50% of their ultimate weight during the lag period. As a result, the average cluster weight measured at this stage may be multiplied by a factor of two to calculate the bunch size at harvest. These two conventional approaches are stressful and time-consuming as well as costly and destructive techniques. Recently, many scientists have developed methods for predicting yield using digital, aerial, and satellite scenes (Arab et al., 2021; Ballesteros, 2020; Sun et al., 2017; Lamb et al., 2004). These output prediction algorithms based on remote sensing may give accurate, accessible, efficient, and timely assessments for grapevine yield monitoring. The successful launch of several sensors (e.g., Landsat, SPOT-VGT, MODIS, and Sentinel) has been credited with this achievement. (Wójtowicz et al., 2016). Based on satellite remote sensing, there are two main methods for grape yield prediction. These methods can be explained as follows:

2.1.1.1 Parametric Grape Yield Perdition Method

Parametric models predict the performance of a parameter based on mathematical or statistical variable. Moreover, the model is based on historical yield and meteorological data. The following model shows that grapes fruit will change when one unit change occurs in environmental parameters.

2.1.1.2 Non-parametric Grape Yield Perdition Method

Non-parametric models refer to the construction of a typology of the environmental conditions that occur during the growing season with the assumption that comparable sorts of seasons result in similar yields. Machine learning is one of the most important non-parametric models that has recently been applied in viticulture and vineyard yield prediction. Due to the processing capacity of computational computers being insufficient in the past, this approach was not applied. One of the main advantages of this technique is that, unlike typical crop simulation models, it does not require mathematical equations or assumptions once the data has been trained (Taylor, 2000). This section highlighted some of the most recent studies on grape yield prediction models using parametric and non-parametric techniques (Table 2.1).

Table 2.1 Studies have been done for parametric and non-parametric methods of grape yield prediction

Year	Country	Methods	Accuracy (%)	References
Parametric methods				
2014	Spain	Correlation and regression analysis	TA 0.62 and IMAD 0.67	Serrano Porta et al. 2014
2017	USA	Correlation analysis	0.8 at the time pick vegetation	Sun et al., 2017
2021	Greece	Pearson's correlation coefficient and regression analysis	0.87	Darra, 2021
Non-parametric methods				
2013	Greece	Cluster analysis and fuzzy	0.5	Tagarakis et al., 2013
2013	Australia	linear regression, fuzzy clustering	0.53, 0.93	Liu et al., 2013
2015	Australia	SVM classifier	0.88, 0.91.6	Liu and Whitty,2015
2020	Spain	ANN	0.90	Ballesteros et at., 2020
2022	Nigeria	Fuzzy c-means, Subtractive Clustering, Grid Partitioning	0.91,0.90, 0.83	Olatunji et al., 2022

2.1.2 Yield Loss Assessment

Drought has a large influence on production and is also a major driver of yield loss. Yield loss assessment is process of comparing the attainable yield from a healthy plant to the amount of yield lost due to a natural disaster. In the remote sensing field, yield reduction assessment is a process to determine the difference between the actual yield of table grapes and the theoretical yield. In my perception, yield loss is an abnormality or decrease in yield due to environmental factors such as temperature, rainfall, pest and disease damage, even due to human activities or other natural disasters. Drought is a natural hazard that limits water supplies and may cause crisis in vineyards as a result of climate variability. Increase in temperate and decrease in rainfall in area harmful for grapevine. Because vineyards are most

susceptible to the climate, particularly temperature, the ideal temperature for grapevines is between 25 and 32 degrees Celsius (in general, it mostly depends on the area). When the temperature falls below the optimum, plant growth is limited, and when the temperature rises higher than the ideal, the rate of photosynthesis is decreased owing to increased respiration. (Ted, 2018). Despite the fact that weather variability is one of the major causes of interannual fluctuations in table grape productivity, estimating how much production is lost due to climate variability is difficult. Researchers have been using different methods for drought-based yield loss calculation based on sensor datasets from remote sensing. Regression is one of the most used methods for assessing the link between each of the influencing characteristics (single or composite drought index) and the observed table grape yield. Besides, using machine learning methods such as random forest and artificial neural networks, the yield loss of table grapes has also been determined (Deo et al., 2017; Leng and Hall, 2019).

2.1.2.1 Yield Loss Assessment based on Single Index

Many multispectral indices have been created for drought monitoring to evaluate crop decrease. The single indices are the normalized difference vegetation index (NDVI) (Tucker, 1979), the normalized difference water index (NDWI) (Gao, 1996), the soil adjusted vegetation index (SAVI) (Huete, 1988), and the vegetation condition index (VCI) (Kogan, 1995a), the temperature condition index (TCI) (Kogan, 1995b), and the standard precipitation index (SPI) (Kogan, 1995c) are the single indices (McKee, 1993). Many studies use a single index to determine the relationship between crop and fruit yields. For example, wheat, barley, rye, oats, oilseed rape, maize, sugar beet, potatoes and grapevine and SPI was 0.52-0.60 for cereals, but 0.31 for grape yield (Potopova et al., 2015). The yield loss was also determined with the help of the vegetation condition index (VCI), temperature condition index (TCI) and vegetation health index (VHI). To quantify the yield loss at the regional level, a correlation analysis was conducted between yield and drought indicators and multiple linear regression (MLR) and artificial neural network (ANN) models were developed. The data revealed a 69% hit rate on yield-losses (Ribeiro et al., 2019).

2.1.2.2 Yield Loss Assessment based on Composite Index

Since 2010, drought monitoring has relied on integrative or composite remotely sensed indicators. At the beginning, researchers utilized an algorithm that combines a drought monitoring model with a crop simulation model (Raksapatcharawong et al., 2020). Later, the VCI and TCI were combined to create a composite index and it was named "vegetation health indexes." (VHI) (Kogan, 1997). In order to combine the indices in the GIS environment, each index needs weight. Therefore, different techniques

of weighting have been used for combinations of drought criteria, such as equal weighting (EW), multiple correspondence analysis (MCA), analytical hierarchy process (AHP), neural network (NN) fuzzy logic (FL), Gaussian mixture model (GMM) and principal component analysis (PCA). Some of the mentioned approaches can still deal with weight matrices that are the same size as the associated dataset (Mainali and Pricope, 2017). Most of these studies combine the metrological indices with soil moisture and satellite-derived drought indices to create a composite drought index. Some of these studies were listed in the following: Du et al. (2013) propose the synthesized drought index (SDI), which combines the vegetative condition index (VCI), temperature condition index (TCI), and precipitation condition index (PCI) using principal component analysis (PCA). Puyu et al. in 2019 developed an integrated drought index from SPI, evapotranspiration, NDVI, and NDWI. The machine learning nonlinear models utilized to validate the relationship between indices and winter wheat. The standardized precipitation evapotranspiration index correlation with grapes is $r = -0.5$ at the district level, and $r = -0.9$ at the county level (Araujo et al., 2016; Yagci et al., 2011). Furthermore, Potopová et al. 2020 applied metrological and agricultural information derived from satellite remote sensing and calculated the yield loss based on multi-linear regression model and Bayesian network for yield loss calculation. Yield loss information was calculated using the annual yield data to indicate the impact of drought years. Yield loss is defined in this study as a decrease in crop yield weight per unit compared to 10 years of statistical data. In this study, the detrend technique and Spearman rank correlation coefficients were determined yield loss by using with grape yield and precipitation, soil wetness, and NDVI variation (Zhang et al., 2017).

2.1.3 Drought Severity Evaluation

Drought is a sophisticated and gradually approaching natural hazard with enormous and widespread agricultural, socio-economic, and environmental repercussions (UN Environment Program, 2009). It causes huge damage and displaces more people than any other natural catastrophe. It is characterized as a climatic, agrarian, hydrology, and socioeconomic dry spell, according to various research. The severity and duration of drought increase as a country progresses from meteorological to socioeconomic drought. Drought severity monitoring in the traditional method over a large area is a complicated task. It needs more time, budget, and equipment. Fortunately, as a result of the advancement of new technologies such as satellite and image analysis software's, this task is now easier than in the past. For example, Google Earth Engine is one of the big data analyzing platforms recently developed by Google. On this platform, researchers, scientists, developers and students can combine and analyze satellite imagery and geospatial datasets to understand changes, trends, and differences on the earth's surface.

Google Engine hosts satellite imagery and preserves it in a public data repository with historical earth photos dating back over four decades. The photos are subsequently made accessible for global-scale data mining after being designed daily. Earth Engine also offers APIs and other tools that make it possible to analyze big databases. Different vegetation-based dryness intensity indices have been established in this respect to monitor drought severity. which will be explained further below.

2.1.3.1 Normalized Difference Vegetation Index

The normalized difference vegetation index (NDVI) is a tool for assessing environmental conditions like drought. The NDVI illustrates how much drought has damaged the plant canopy. NDVI has been utilized in several research projects for dry spell identification and investigation. (Wilhite et al., 2014; Chang et al., 2017) (**Table 2.2**).

2.1.3.2 Standard Vegetation Index (SVI)

Drought monitoring can be done vis SVI (Peters et al., 2002). It shows the deviation of standard NDVI throughout several years (**Table 2.2**).

2.1.3.3 Standard Precipitation Index (SPI)

SPI illustrates the rainfall probability on any time scale. It can monitor drought at one month (SPI-1), three months (SPI-3), six months (SPI-6) and twelve months (SPI-12) (**Table 2.2**).

2.1.3.4 Recent Research on Drought in Afghanistan

Drought monitoring studies on a broad scale have been conducted in South Asian nations, including Afghanistan. In the study area (Kabul Province), only drought monitoring has been done in the Kabul River basin. The majority of studies evaluated the existence and non-existence of drought using single metrological and drought indicators such as temperature and rainfall, MOIDS VCI, TCI, PCI and SPI. None of them evaluate the agricultural drought in vineyards from mic. Table 2.3 lists some of these investigations.

2.1.4 Land Suitability Analysis

A land suitability assessment is required to determine which crops or grape varieties are to be used and how to rotate them on a specific land or vineyard. This assessment may lead to the efficient and optimal spatial arrangement of land and also assess the relative potential for development and modify zoning (Chen-jing et al., 2021). Land suitability assessments can be used for different disciplines. A multi-indicator approach for determining land suitability often includes lots of natural, ecological, socio-

economic aspects (Jafari and Zaredar 2010). Land suitability is also recognized as a multi-criteria evaluation (MCE) method. weighted linear combination (WLC) (Dai et al., 2001), analytic hierarchy process (AHP) (Alsafadi et al., 2022), analytic network process (ANP) (Purnamasari et al., 2019a), fuzzy weighting (FW) (Jiang and Eastman, 2000), and other approaches are used to weight the criteria. Geographical information systems (GIS) have been more important in LSA because they enable the analysis of different geographical datasets. By combining remote sensing (RS) datasets, composite land evaluation systems can increase the accuracy and reliability of land suitability. Some of the weighting approaches that has been used in our study are listed in table 2.1.

Table 2.2 Studies have been used for drought indices for drought distribution assessment

Index	Title	Type of crop	References
	Mapping stressed wheat plants by soil aluminum effect using C-band SAR images: implications for plant growth and grain quality	Wheat	Hernandez et al. 2022
NDVI	Monitoring of drought condition and risk in Bangladesh combined data from satellite and ground meteorological observations	Rice	Prodhan et al., 2022
	Evapotranspiration estimates derived using thermal-based satellite remote sensing and data fusion for irrigation management in California vineyards	Grape	Knipper et al., 2019
	Investigate the sensitivity of the satellite-based agricultural drought indices to monitor the drought condition of paddy and introduction to enhanced multi-temporal drought indices.	Paddy	Jayawardhana & Chathurange, 2020
SVI	Impacts of climate change on drought risk of winter wheat in the North China Plain	Wheat	Zhang et al., 2021
	Utilizing TVDI and NDWI to Classify Severity of Agricultural Drought in Chuping, Malaysia	Oil palm	Shashikant et al., 2021
	Standardized relative humidity index can be used to identify agricultural drought for summer maize in the Huang-Huai-Hai Plain, China	Maize	Wu et al., 2021
SPI	Development of an integrated weighted drought index and its application for agricultural drought monitoring	Rice	Niaz et al., 2021
	Assessment and monitoring of agricultural droughts in Maharashtra using meteorological and remote sensing-based indices	Grapes, oranges, mangos, and bananas	Aswathi et a., 2018

Table 2.3 Drought-related studies have recently been conducted in Afghanistan

Research Titles	Year
Spatial and temporal trend analysis of groundwater levels and regional groundwater drought assessment of Kabul, Afghanistan	2021
The Role of Large Dams in a Transboundary Drought Management Cooperation Framework— Case Study of the Kabul River Basin	2021
Meteorological Factors in Afghanistan Comparison of Multi-Year Reanalysis, Models, and Satellite Remote Sensing Products for Agricultural Drought Monitoring Over South Asian Countries	2021
Climate Change impacts on vegetation and agricultural drought in the basin of Panjshir River in Afghanistan	2020
Assessing Meteorological and Agricultural Drought in Chitral Kabul River Basin Using Multiple Drought Indices	2020
Assessing the Vegetation Condition of Herat Province, Afghanistan Using GIS	2019
Characterization of drought monitoring events through MODIS- and TRMM-based DSI and TVDI over South Asia during 2001–2017	2019
Assessment of Irrigation Performance in Large River Basins under Data Scarce Environment—A Case of Kabul River Basin, Afghanistan	2018
Proposing a Popular Method for Meteorological Drought Monitoring in the Kabul River Basin, Afghanistan	2017

2.1.4.1 Analytical Hierarchical Process (AHP) Weighting

The Analytic Hierarchy Process (AHP) is a mathematical and psychologically based system for managing and analyzing complex situations. It was introduced in 1971 by Thomas L. Saaty. It consists of three main parts: the goal or problem, the criteria and alternatives. The priorities of each aspect in the AHP analysis are primarily computed using the Saaty scale, which is based on the views of experts and other sources. The third step is to integrate the overall priorities of all of the choices. The final step is the sensitivity analysis. The basic ideas in using AHP to solve issues, such as elaboration, valuation comparison, priority synthesis, and sensitivity analysis. The following steps are followed by AHP:

- Establishing an interconnected decision-making hierarchy and pairwise comparison
- The relative weights of decision factors are calculated using an eigenvalue approach.
- Combining the relative weights at the top of the hierarchy to get a composite weight that indicates the decision maker's choice option based on an assessment of the relative importance

After collecting the relative weights, overlaying all of the criteria using the weight of each map in the ArcGIS interface, and creating the final suitability map (**Figure 2.1**).

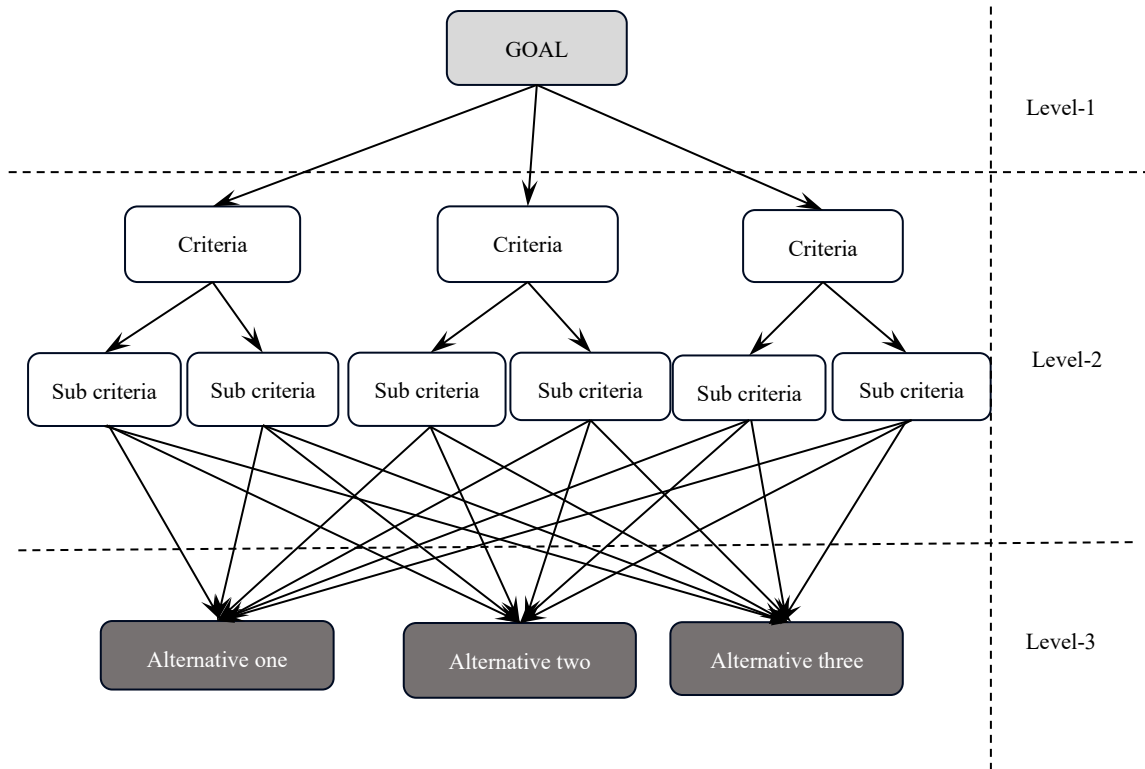


Figure 2.1 The AHP multi-criteria hierarchy structure

Chapter 3

Prediction of Grape Yield at Micro-scale Drought Prone Areas Using Satellite Remote Sensing-based Time-Series Vegetation Indices and Machine-Learning Approach

3.1 Background of the Research

Predictions of yield are a useful mechanism used in the growth of the horticulture industry to prevent an excess or deficiency of fruit on vines and maximize the quantity of fruit produced during each growing season. In addition, grape production is dependent on the optimal ratio of exposed leaves and the link between this ratio and the number of clusters produced by a specific vine (Bobeica et al., 2015). At various phases of plant development, vegetation indices may be used to assess the exposed leaves, which have a substantial impact on grape output (Dokoozlian and Hirschfeld, 1995). Accurate and timely measurement of the vegetation indices at each of these phases is critical for trimming, watering, and scheduling harvesting activities within the ideal time windows (Dokoozlian and Hirschfeld, 1995; Shahab et al., 2020). However, there is geographical heterogeneity across vineyards in various nations and locations, and even within a single field, there is spatial diversity between vines at various development phases (Tisseyre et al., 2007).

The predicted yield is a key predictor of yield variation at various development stages in vineyards (Bramley and Hamilton, 2004). In many poor nations, large postharvest losses are linked with table grape production owing to inadequate storage and inventory planning (Parfitt et al., 2010). In addition, grapevines are susceptible to insect infestation and temperature and moisture extremes (Yin et al., 2019; Iltis et al., 2020; Andresen and Baule, 2020; Pathak et al., 2018; Teixeira et al., 2007). Consequently, yield assessment is crucial for inventory planning in supply chain management, minimizing postharvest losses, and assisting grape producers during natural catastrophes with subsidies or insurance.

Vineyard yield projections have been made using a variety of approaches, the majority of which are based on ground measurements. The traditional and lag phase techniques are two examples of these approaches. Vine density, number of clusters per vine, and cluster weight are all used to estimate grape output in a typical manner. A double cluster's mass is used during lag phase to anticipate the weight of a cluster at harvest time in the lag phase approach. Ground sampling is required for all of these old procedures, which is time-consuming, expensive, and labor-intensive (Bramley and Hamilton, 2004). Mathematical models and statistical regressions are used in the same way in these conventional procedures. While traditional ground-based measurements require a longer period of time, satellite

remote sensing has the potential to cover a much larger area in a shorter period of time, and machine-learning algorithms such as random forests and neural networks have been used to predict yield from satellite vegetation indices (Jones et al., 2020; Pôças et al., 2020).

Vegetation indices developed from satellite data, such as the normalized difference vegetation index (NDVI), are being used to predict table grape production and identify distinct types in vineyards by analyzing phenolics and color (Lamb et al., 2004; and Meggio et al., 2010). In addition to NDVI and LAI, yield calculations are also based on these two parameters. The direct approach and the distant sensing method are often employed to measure LAI (Morisette et al., 2006). A variety of techniques, such as linear modeling (Law and Waring, 1994), physical models, and artificial neural networks (ANNs), are used to create LAI from satellite photos in the indirect remote sensing approach (Morisette et al., 2006). Quality and quantity of grapes are influenced by the aforementioned two factors, as well as the availability of water on the farm (Sun et al., 2017). When it comes to grape productivity, water is a crucial factor, particularly during the expansion of the canopy and the ripening process. Water molecules in plant canopies interact with solar radiation to produce NDWI, which is a normalized difference water index (NDWI) (Gao, 1996). Table grape yield estimates can be improved by utilizing NDWI (the water content of leaves) with NDVI and LAI to analyze the impacts of water management on canopy management and the water content of leaves.

Recently, agricultural production prediction methods based on machine learning and computer vision have seen some usage (Tian et al., 2020). Nonparametric approaches such as these may be applied to noisy data and used to decipher nonlinear connections. It is possible to construct complicated and nonlinear patterns between predictors and response variables by machine learning (Pôças et al., 2020). The standard crop simulation model's mathematical equations and assumptions aren't necessary with the machine-learning technique after the data training is over. Instead of one algorithm, it is a collection of algorithms working together. Once the linkages between the input and output data have been established, machine learning may simply be carried out with complicated data. Different machine-learning algorithms have been used to determine white and red cultivars by looking at their berries' color (Kamir et al., 2020; Kurtser et al., 2020). Automated grape cluster recognition in vineyards is further aided by machine learning, which uses methods such as fitting and k-means clustering to accurately estimate yields (Liu and Whitty, 2015). Therefore, the main objective of this research is to employ a machine-learning approach to develop rapid yield prediction models for table grapes using vegetation indices collected from satellite remote sensing datasets.

3.2 Methodology

3.2.1 Geographical Extent of the Study Area

The research was carried out in Shakardara District, Afghanistan's primary grape-growing area (**Figure 3.1 (a-c)**). Table grapes account for 68 percent of the country's total fresh fruit output. In 2019, 106,464 metric tons of grapes were produced in 2019, covering an area of 10,646 hectares, with an average yield of 9,800 kilos per hectare. Grapes were grown on 1,475 hectares of land in the Shakardara District, with a total yield of 35,479.5 tons (ACSO, 2019). To make use of the non-fermented versions of the goods, such as dried grapes, table grapes, and grape juice (FAO and OVI, 2016). Afghanistan exports a significant number of grapes as well. Fresh and dried grapes were worth around \$132 million in exports in 2018. Grapes were sent to the US, Pakistan, India, Russia, the United Kingdom, the United Arab Emirates, Europe, and China (ACSO, 2019). 2018 was one of the driest years in the area, which had a negative impact on the production of table grapes. Since most of the precipitation (snowfall and rain) falls between January and May, this area is classified as desert or semiarid by the Kabul metrological station, which also notes that summer precipitation is very low (a maximum of 20 millimeters). According to the facts, 2018 was a drought-stricken year in Afghanistan and the Shakardara District. In addition, the district's current irrigation systems include subhorizontal tunnels that are fed by snowfall and utilized to provide water for irrigation and domestic use in nearby communities, as well as deep wells and rivers (UNHCR, 2002; Macpherson et al., 2015). Day-to-night and season-to-season temperature changes are also present; the mean temperatures in December, January, and February are each 7 degrees Celsius; 3 degrees Celsius; and 4 degrees Celsius, respectively. The average spring temperatures in March, April and May are all 13°C, 18°C, and 24°C (Aich et al., 2017).

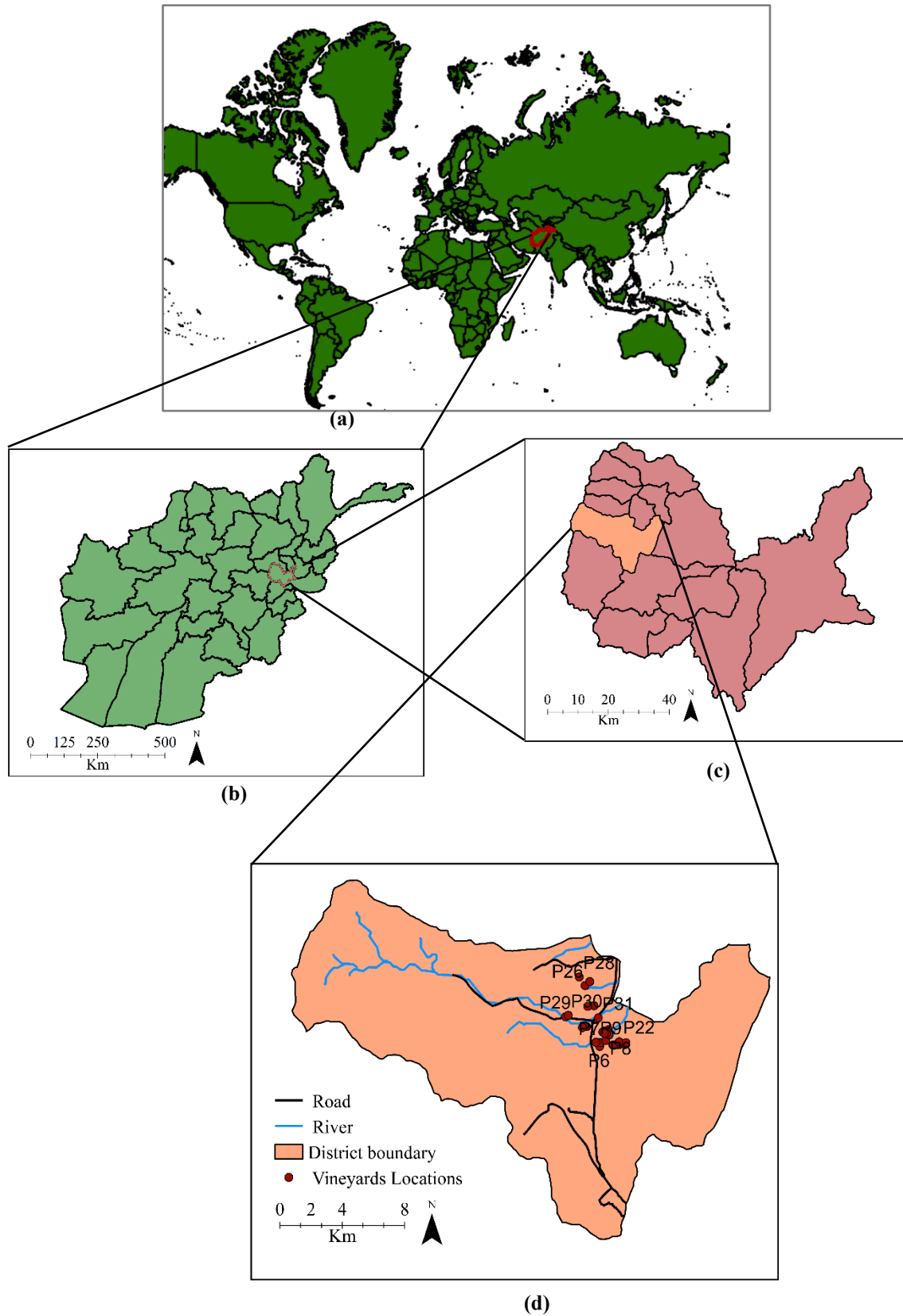


Figure 3.1 Geographical scope and maps of the research area: (a) Afghanistan location in world (b) Afghanistan administrative area, (c) Kabul Province, and (d) Shakardara District.

3.2.2 Dataset Acquisition and Analysis

3.2.2.1 Satellite Data Acquisition and Image Preprocessing

For 2017, 2018, and 2019, Landsat 8 OLI time series were used to gather spectral datasets. Bands 2 to 4 (visible light), 1, 6, 7 and 9 (infrared light) of the OLI sensor has a spatial resolution of 30 meters. It is possible to study coastal and aerosol processes with the use of the ultra-blue band 1. Detection of vegetation and water bodies may be accomplished with the help of shortwave infrared bands 7 and 6, while cloud detection can be accomplished with the help of cirrus band 9. The scene had an about 170-km north-south by 183-km east-west measurement (Sellers, 1985). The OLI/TIRS C1 level-1 with route 153 and row 36 was used to collect and refer to Landsat 8 spatial and temporal scenes. From the USGS Earth Explorer website, all 50 Landsat 8 OLI time series scenes were downloaded and processed to acquire the whole growth cycle over three years. In addition, the ArcGIS® quality assessment tool was tasked with removing the cloud cover and only taking into account the scenes' clean pixels. In order to get sufficiently clear Landsat 8 scenes for subsequent analysis and map development, the QA is constructed via the 'CF mask' technique (Zhu and Woodcock, 2012).

3.2.2.1.1 Normalized Difference Vegetation Index (NDVI)

NDVI primarily assesses the status of vegetation and is directly proportional to a plant canopy's photosynthetic capability and energy absorption (Sellers, 1985). NDVI is computed as the ratio of the red band and near-infrared (NIR) band values and may be represented as follows (Rouse et al., 1974; Quarmby et al., 1993):

$$\text{NDVI} = \frac{\rho_{\text{NIR}} - \rho_{\text{Red}}}{\rho_{\text{NIR}} + \rho_{\text{Red}}} \quad (3.1)$$

where NIR is the near-infrared wavelength reflectance between 0.85 and 0.88 microns and Red is the wavelength reflectance between 0.64 and 0.67 microns (Rouse et al., 1974). Monitoring seasonal variations in plant development (growing, blooming, harvesting, and senescence) using time-series NDVI information. In addition, the NDVI has been used to studies of land use and land cover changes linked to soil type or climate (Quarmby et al., 1993). This indicator has uses for agricultural production estimation and the research of above-ground dry biomass (Tanre et al., 2005).

3.2.2.1.2 Leaf Area Index (LAI)

LAI is the most important parameter in many ecosystems' productivity models and in global climate, hydrologic and biogeochemical models (Enquist and Ebersole, 2006). The leaf area to ground area ratio in broadleaf canopies is known as LAI and could be represented as follows:

$$\text{LAI} = \frac{\text{Leaf area}}{\text{ground area}} = \frac{\text{m}^2}{\text{m}^2} \quad (3.2)$$

where LAI stands for leaf area index. Previous studies have referred to the correlation between NDVI and LAI values derived from satellite data and monthly field observations to develop regression curves. NDVI and LAI values acquired from satellite data and monthly field measurements have been used to create regression curves in previous research. This equation was calculated using the least squares approach. An example of how to express LAI is as follows: (Tewari et al., 2003):

$$\text{LAI} = 0.57 \times \exp(2.33 \times \text{NDVI}) \quad (3.3)$$

3.2.2.1.3 Normalized Difference Water Index (NDWI)

NDWI is used to track variation in water content of leaves by utilizing spectral data from of the near-infrared and shortwave infrared bands (Gao, 1996). NDWI can be expressed as:

$$\text{NDWI} = \frac{\rho_{\text{NIR}} - \rho_{\text{SWIR}}}{\rho_{\text{NIR}} + \rho_{\text{SWIR}}} \quad (3.4)$$

where SWIR is the shortwave infrared reflectance ranging from 1.57-1.65 μm . The liquid water molecules in the plant canopy that interact with solar radiation are measured by NDWI. Water not only acts as a main reactant, but it also regulates stomatal opening and closure. Water scarcity causes a decrease in photosynthesis (Enquist and Ebersole, 2006). Water stress reduces fruit size at any time, but plant development is most vulnerable during the period of quick berry growth during 2 to 3 weeks following bloom (Etchebarne et al., 2009). Over three years, all of these vegetation indices were generated from satellite data with more than 20% clear observations and evaluated in the ArcGIS® environment. The procedures used in this investigation are summarized in Figure 3.2.

3.2.2.2 Statistical Analysis

Per-pixel moving average and exponential smoothing algorithms were utilized to identify the various development phases of a vineyard. After identifying the various phases, correlation analysis was used to evaluate the correlations between the NDVI, LAI, and NDWI. In addition, a time-series moving average model was developed to eliminate the seasonality of the active growth seasons (April to October) and to get a single representative mean score in each model. The moving average scores (NDVI, LAI, and NDWI) throughout the active growth season were then correlated with the ground reference yield using regression analysis. The moving average is defined as:

$$MA_n = \frac{\sum_{i=1}^n VI_i}{n} \quad (3.5)$$

where MA is the moving average, VI is the vegetation index in period i , and n is the number of periods. The forecast vegetation index can be calculated as follows:

$$F_t = \alpha A_{t-1} + (1-\alpha) F_{t-1} \quad (3.6)$$

where F_t is the forecast vegetation index for month t , α is the smoothing constant, A_{t-1} is the observed value of the vegetation index in each vineyard in period t , and F_{t-1} is the previous forecast for period t . For the purpose of determining the most accurate way to forecast yield, both a parametric and a nonparametric approach were used in tandem. In this case, the ANN model was used since it can describe linear and highly nonlinear interactions between datasets (**Figure 3.3**). ANNs are essentially made up of a single input layer, a single output layer, and one or more hidden layers that are utilized to tackle difficult issues. Mathematica (MATLAB) was used to do the neural network analysis and construct various neural networks for NDVI, LAI, NDWI and ground reference yield data for the years 2017-2018 and 2019. The nonlinear prediction model was built using the Levenberg–Marquardt forward propagation training procedure. In the beginning, 70% of the data was randomly selected for training, 15% for validation, and the remaining 15% for testing. The 10 hidden layers were used to choose different numbers of neurons (Khan et al., 2020) (**Figure 3.3 and Table 3.3**).

3.2.2.3 Ground Reference Data

Vineyards in the Shakardara District were surveyed between October 2018 and 2019, and it was found that the majority of farmers were cultivating four varieties of *Vitis Vinifera* L. Hussaini, Kishmishi, Shunderkhani, and Tahaifi are the native grape varieties' names. In loamy and sandy loam soils, furrow irrigation was employed in the vines examined. Using a combination of surveys and portable GPS devices (e-trex, Garmin, USA), the locations of 31 vineyards spread across 11 towns were gathered (**Table 3.1**). In the field survey, we recorded the x and y coordinates of each vineyard in the Shakardara District. Vineyard positions were recorded using a Garmin e-trex portable GPS device by the surveyors. Finally, Google Earth Pro® was used to build polygons based on the waypoints for each vineyard in Shakardara District. The questionnaire was also used to gather information on vineyard management strategies related to pest infestations, drought, and flooding.

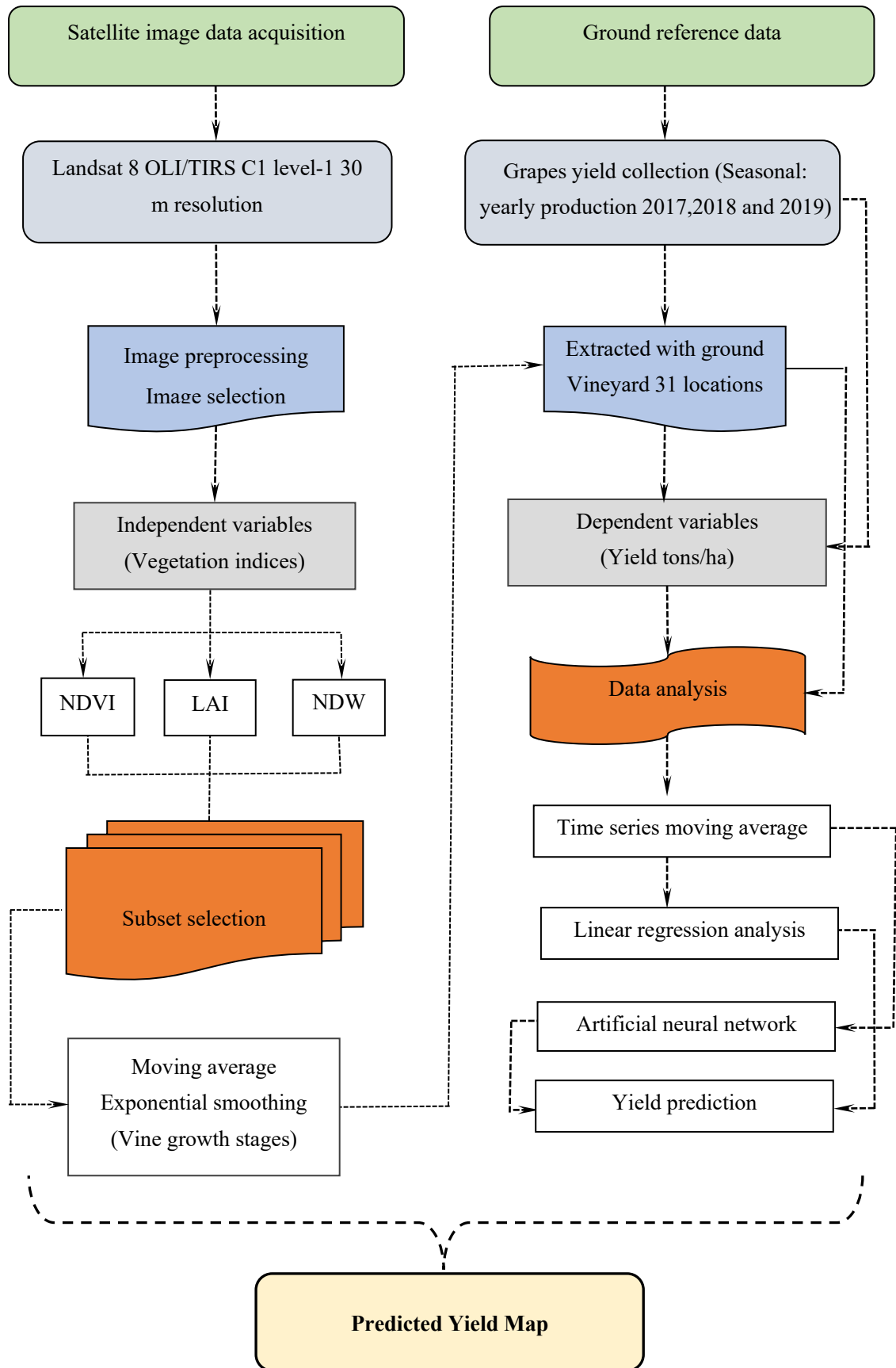


Figure 3.2. Research flowchart for yield prediction of table grapes.

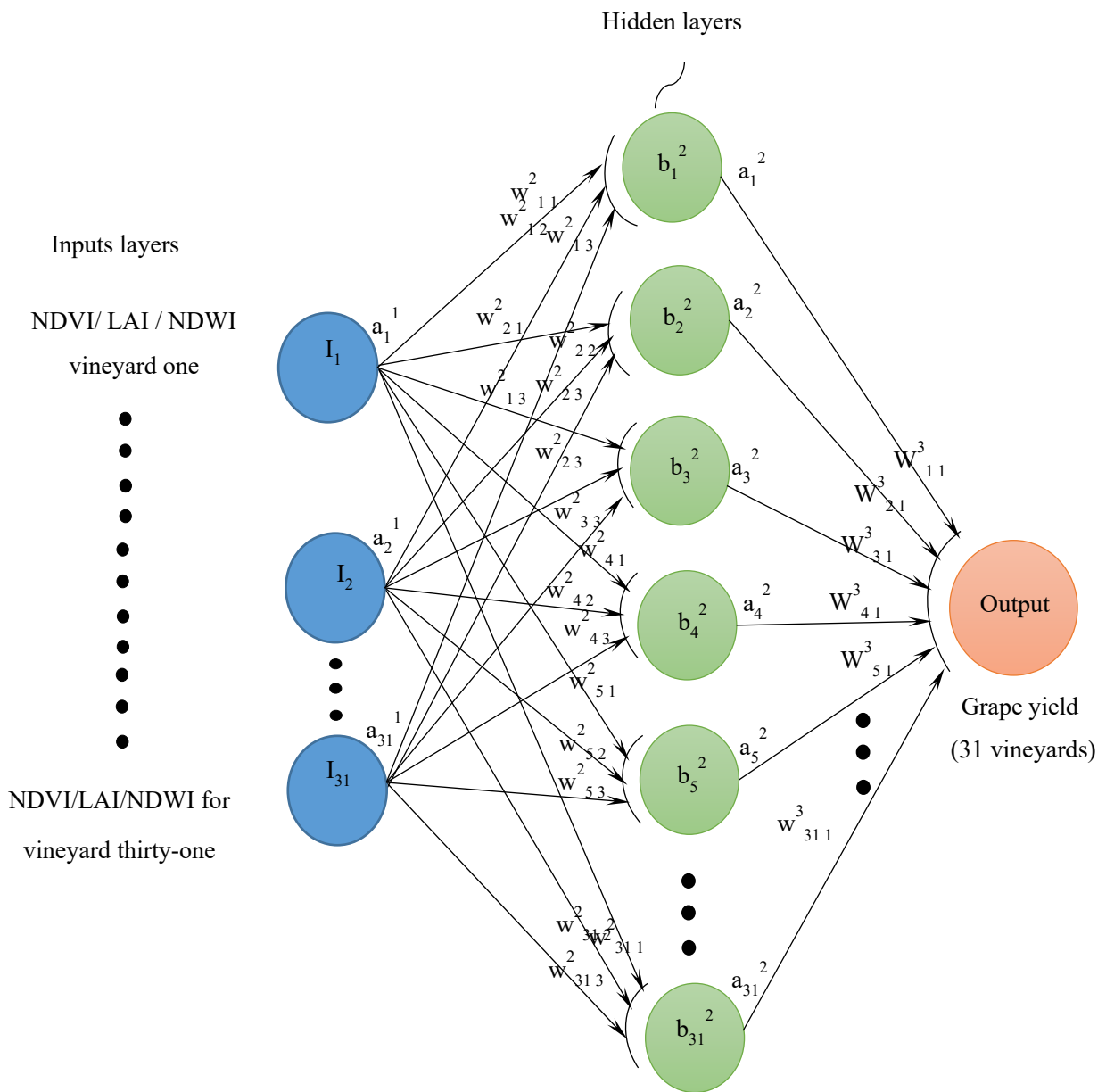


Figure 3.3. Artificial neural network (ANN) algorithm for predicting table grape yield

Table 3.1. Ground reference data collected from Shakardara District through surveys

Field ID	Vineyard Latitude	Vineyard Longitude	Total Area of Vineyard (ha)	Yield (ton/ha) 2017	Yield (ton/ha) 2018	Yield (ton/ha) 2019
1	34.668994	69.084394	0.9	6.1	5.3	6.1
2	34.668281	69.086158	0.2	21.1	16.7	20.0
3	34.667442	69.085032	0.8	6.8	6.4	6.8
4	34.669679	69.086774	0.4	20.3	20.3	20.2
5	34.667765	69.087248	0.7	24.3	22.5	23.3
6	34.660265	69.080597	1.1	21.1	16.8	17.8
7	34.662367	69.081009	0.4	15.3	15.0	15.8
8	34.663537	69.084815	1.1	19.8	20.0	20.4
9	34.662573	69.077955	1.1	9.0	10.0	10.9
10	34.671508	69.071413	0.4	16.9	13.3	16.1
11	34.671532	69.071319	0.9	16.9	15.0	15.8
12	34.670977	69.068530	0.4	15.6	11.2	16.3
13	34.668176	69.086552	0.6	21.6	19.2	21.3
14	34.666888	69.087083	1.1	16.2	17.5	18.6
15	34.667448	69.085100	0.4	19.8	11.2	17.6
16	34.668471	69.082697	0.3	25.6	12.2	23.3
17	34.667748	69.083963	1.1	8.9	5.6	8.7
18	34.661407	69.094569	0.7	18.0	16.7	17.8
19	34.661360	69.098233	1.3	20.0	16.7	17.8
20	34.661026	69.089905	0.4	14.6	16.3	20.6
21	34.660955	69.090309	0.9	24.4	21.9	24.2
22	34.662859	69.094164	0.7	5.6	9.3	9.7
23	34.662363	69.098960	4.4	19.8	20.0	20.2
24	34.683351	69.076653	1.3	11.2	10.0	10.9
25	34.682978	69.072256	0.2	20.3	19.5	20.4
26	34.694788	69.070378	1.3	5.6	8.9	8.9
27	34.697056	69.073670	1.8	18.9	18.8	19.2
28	34.699674	69.066259	1.6	20.0	17.9	19.3
29	34.677100	69.056635	0.9	14.4	14.0	14.4
30	34.677909	69.058587	0.9	14.2	12.2	14.3
31	34.676439	69.079604	0.2	15.6	13.7	15.0

3.3 Results

3.3.1 Growth Stages Analysis

The growth stages of table grapes are noted as bud break (in this stage, tiny buds on the vine start to swell, and green leaves start to appear; the appearance of the first green leaves through the bud scales is referred to as the bud break stage), flowering (in this stage, grapevine flowers are born in a cluster (or bunch), and the main axis of the cluster is called the rachis; when spring temperatures rise to 15-20°C, the flowers typically begin to bloom, and the time between bud break and bloom is usually six to nine weeks, depending on the temperature), fruit set (this initial period of growth is rapid due to cell division and cell enlargement; in this stage, the grape berries are green, hard to the touch, and enlarge rapidly, and they have very little sugar and are high in organic acids) (Ted, 2018; USAID, 2016), maximum canopy expansion, ripening and harvesting time. To identify these growth stages in vineyards per pixel, moving average and exponential smoothing methods were used to develop growth trajectories. A sequence of three years of NDVI, LAI and NDWI data (2017-2019) was used. Seasonality was removed from the time series of the NDVI, LAI and NDWI datasets (**Figure 3.4 (a-c)**). In Figure 4, block dashed lines represent the time-series NDVI, LAI and NDWI per-pixel values, the blue line refers to the moving average and the red line represents exponential smoothing. The green dot indicates the start of the season (SOS), the dark green dot represents the maximum canopy expansion, and the yellow dot indicates the end of the growing season (**Figure 3.4 (a-c)**). Therefore, 97, 193 and 287 days of year for 2017; 115, 210, and 272 days of year for 2018; and 101, 228 and 275 days of year for 2019 were selected as the day of the SOS, maximum canopy expansion, and end of growing season, respectively, according to the acquired satellite data. The days of growth were referred to as the start, middle and end of the growing season of table grapes in Shakardara District (**Table 3.2**). NDVI, LAI and NDWI (30×30 m) pixel growth stage maps were developed for 2017, 2018 and 2019. **Figure 3.5 (a-i)** shows the different growing stages of grapes, which start in April and end at the end of October in Shakardara District, Kabul Province. The white color illustrates restricted areas such as build-up, roads, rivers, and rocks. The light green color represents the start of the season, the dark green color indicates the maximum canopy expansion, and the light-yellow color shows the end of the season.

Table 3.2 Overall performances of vegetation indices at the growth stages of vineyards in Shakardara District

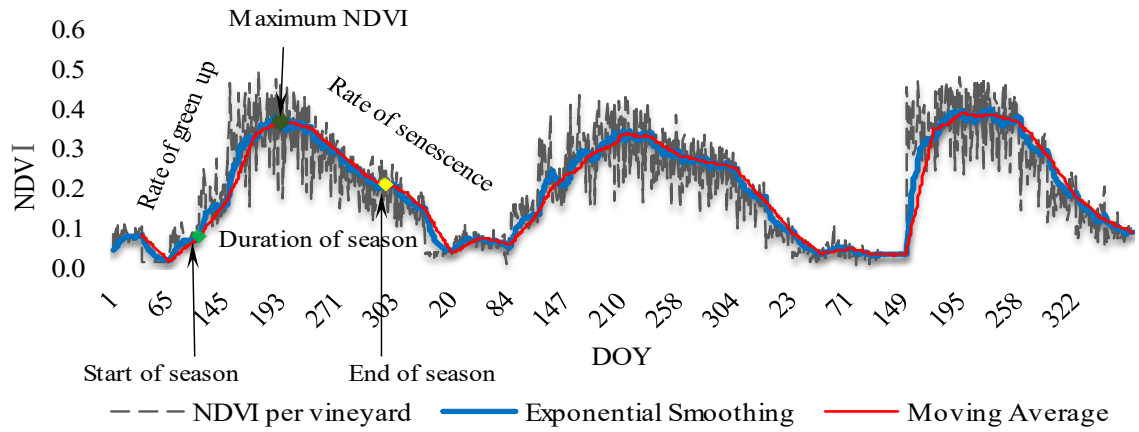
Year	Number of Vineyards	Growth Stages					
		Bud break	Flowering	Fruit Set	Max- Canopy Expansion	Ripening	Harvest
2017	31	97	145	161	193	239	287
2018	31	115	147	163	210	227	272
2019	31	101	145	165	193	228	287

3.3.2 Spatial Correlations among NDVI, LAI and NDWI

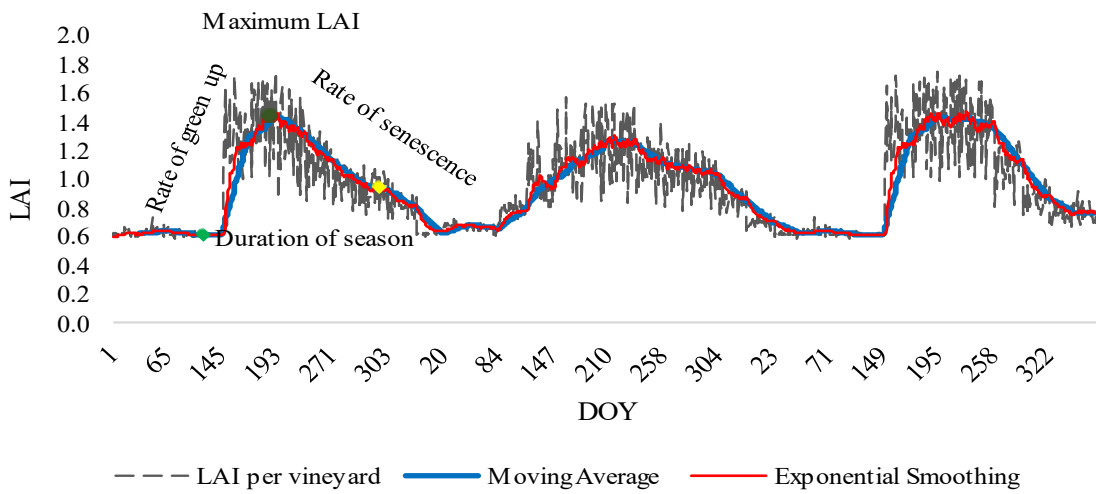
NDVI and NDWI had the highest correlations with the timing of the maximum canopy expansion. To have one mean for each month representing the entire vineyard growth cycle, the time-series moving average was used to calculate the spatial correlations among the vegetation indices. Positive and strong correlations were observed between NDVI and LAI ($r^2=0.99$), NDVI and NDWI ($r^2=0.98$), and LAI and NDWI ($r^2=0.98$) in 2017; between NDVI and LAI ($r^2=0.99$), NDVI and NDWI ($r^2=0.94$), and LAI and NDWI ($r^2=0.93$) in 2018; and between NDVI and LAI ($r^2=0.99$), NDVI and NDWI ($r^2=0.92$), and LAI and NDWI ($r^2=0.92$) in 2019.

Table 3.3 Artificial neural network designed for yield prediction of table grapes

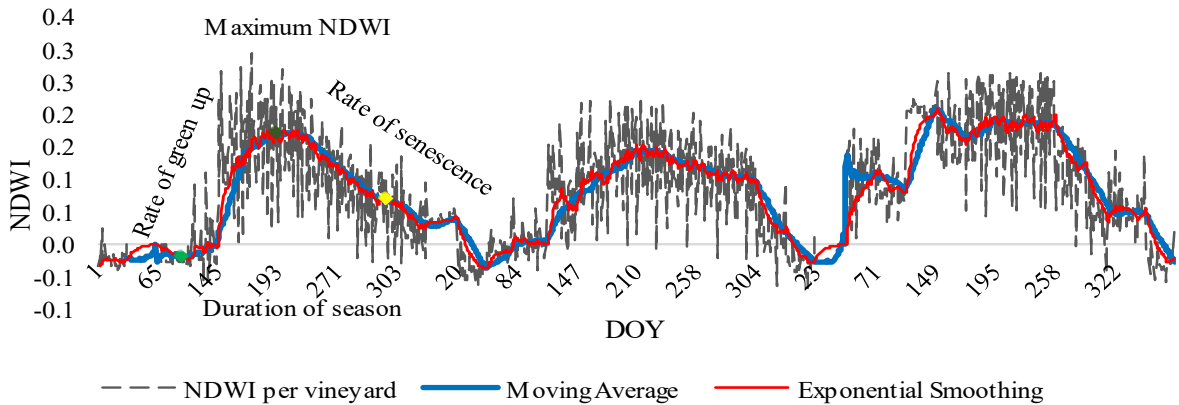
Vegetation Indices	ANN	Parameters (%)	MSE			R -Value		
			2017	2018	2019	2017	2018	2019
NDVI	Training	70%	0.32042	0.14604	0.35970	0.93	0.96	0.93
	Validation	15%	0.23458	0.27474	0.19126	0.96	0.86	0.87
	Testing	15%	0.67756	0.27184	0.95999	0.92	0.97	0.84
	Overall	100%	0.36114	0.18081	0.42959	0.94	0.95	0.92
LAI	Training	70%	0.39939	0.28436	0.33738	0.92	0.93	0.93
	Validation	15%	0.72213	0.10877	0.68186	0.97	0.90	0.95
	Testing	15%	0.58297	0.30864	0.85838	0.93	0.95	0.98
	Overall	100%	0.51819	0.41787	0.47620	0.92	0.89	0.90
NDWI	Training	70%	0.38066	0.31367	0.35211	0.94	0.91	0.94
	Validation	15%	0.53943	0.41758	1.45495	0.76	0.94	0.76
	Testing	15%	0.74658	1.07930	1.61168	0.92	0.93	0.89
	Overall	100%	0.47022	0.45392	0.73170	0.92	0.90	0.85



(a)



(b)



(c)

Figure 3.4 Time-series vegetation indices: (a) NDVI, (b) LAI and (c) NDWI in 2017, 2018 and 2019 before and after moving average and exponential smoothing

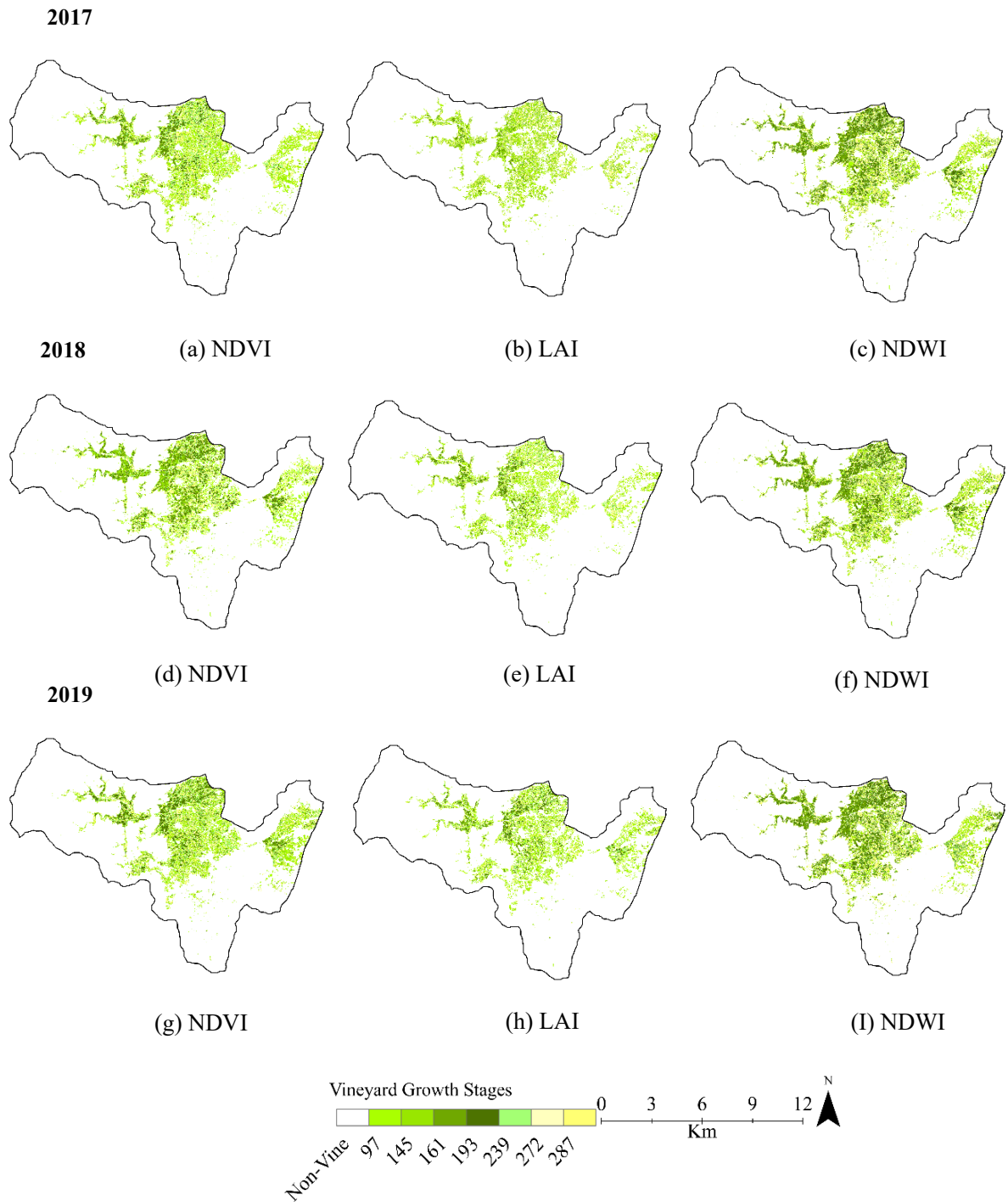


Figure 3.5 NDVI-, LAI- and NDWI-derived growth stage maps of grapes in Shakardara District (a, b and c) in 2017, (d, e and f) in 2018 and (g, h and i) in 2019

3.3.3 Yield Prediction Models

NDVI, LAI and NDWI images were used to carry out regression analyses with the yield data collected from 31 vineyards in Shakardara District in 2017, 2018 and 2019. The results showed that the coefficients of determination for the 2017 yield with NDVI, LAI and NDWI were 0.79, 0.78 and 0.74, respectively. Similarly, the coefficients of determination for the 2018 yield and NDVI, LAI and NDWI were 0.77, 0.78 and 0.72 and for the 2019 yield were 0.79, 0.79 and 0.69, respectively (**Figure 3.6 (a-c)**). LAI had similar performances in terms of r^2 in 2017 and 2018; NDVI had the same performance in 2017 and 2019. In addition, the linear model and nonlinear model were employed for yield predictions. In the nonlinear model, ANN was employed for further predictions using the MATLAB[®] environment. In the ANN analysis, the vegetation indices (NDVI, NDWI and LAI) were referred to as the inputs, and the yield data collected from Shakardara District were referred to as the outputs. The generated results showed relationships between yield and NDVI ($R= 0.94$), yield and LAI ($R= 0.92$) and yield and NDWI ($R= 0.92$) in 2017; between yield and NDVI ($R= 0.95$), yield and LAI ($R= 0.89$), and yield and NDWI ($R= 0.90$) in 2018; and between yield and NDVI ($R= 0.92$), yield and LAI ($R= 0.90$) and yield and NDWI ($R= 0.85$) in 2019 (**Figure 3.7 (a-i)**). NDVI had higher accuracy values in the machine-learning approach in all three years than did the other vegetation indices (**Table 3.3**).

The ground reference yield data were used to evaluate the yield values predicted by conventional statistics and machine-learning (**Figure 3.8 (a-c)**). The line charts in Figure 8 (a-c) indicate the comparison of the ground reference yield data with the predicted yield from conventional statistics in 31 vineyards, and the dash charts illustrate the comparison of the ground reference yield data with the predicted yield from the ANN approach in 31 vineyards for the years 2017-2019. The error bars in Figure 8 (a-c) show that the difference between the ANN-predicted yield and the ground reference yield was much less than the difference between the yield predicted by conventional statistics and the observed data. Finally, a vineyard yield map was generated from the best model to show the variability of table grapes among the various vineyards in Shakardara District, Kabul Province (**Figure 3.9 (a-c)**). The red areas in the predicted yield maps show restricted regions, and the light green and dark green areas show the yields in tons per hectare (**Figure 3.9**).

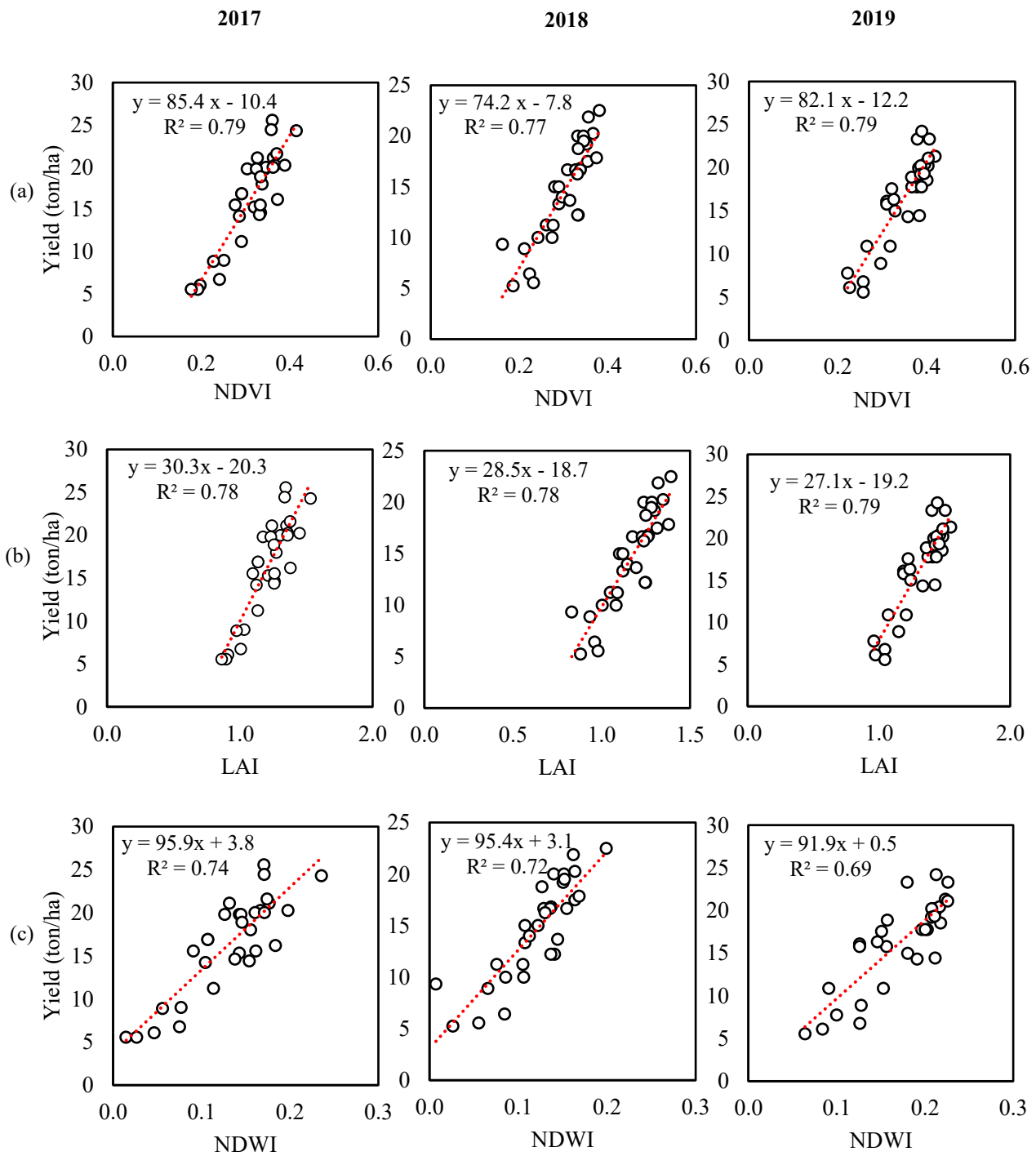


Figure 3.6 Scatterplots showing the regression between the vegetation indices and the yield: yield with NDVI (a), yield with LAI (b) and yield and NDWI (c) in 2017, 2018 and 2019

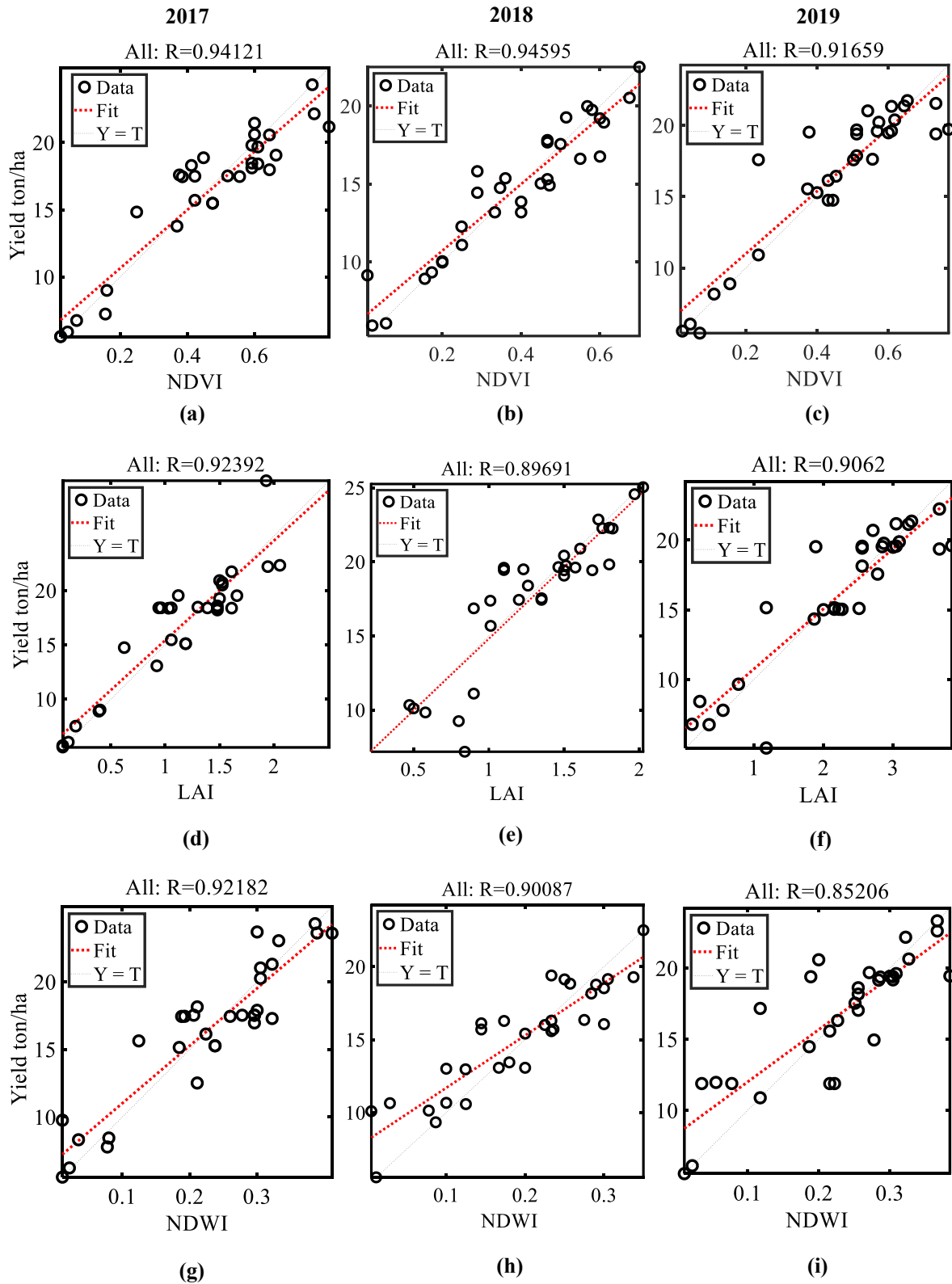
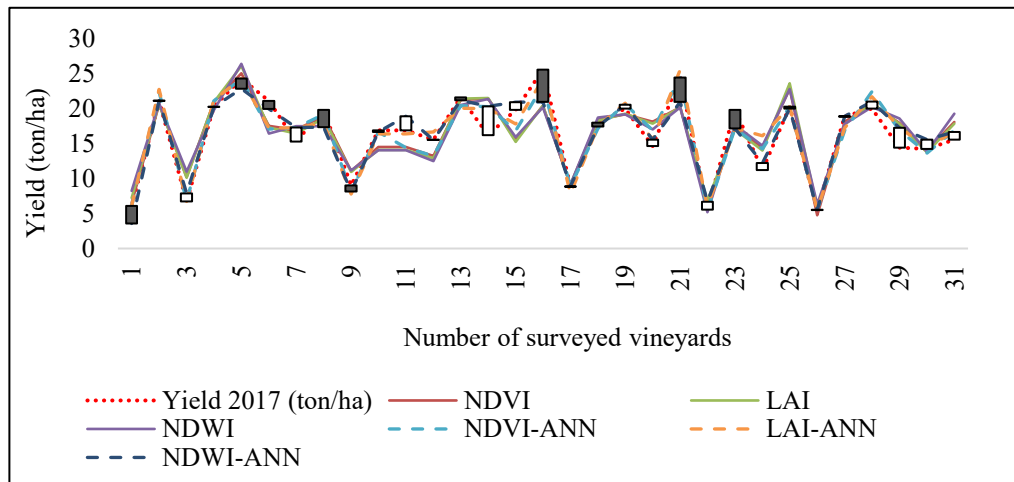


Figure 3.7 Scatterplots showing the NN-fit results between NDVI, LAI and NDWI and yield in 2017 (a, d and g), 2018 (b, e and h) and 2019 (c, f and i)

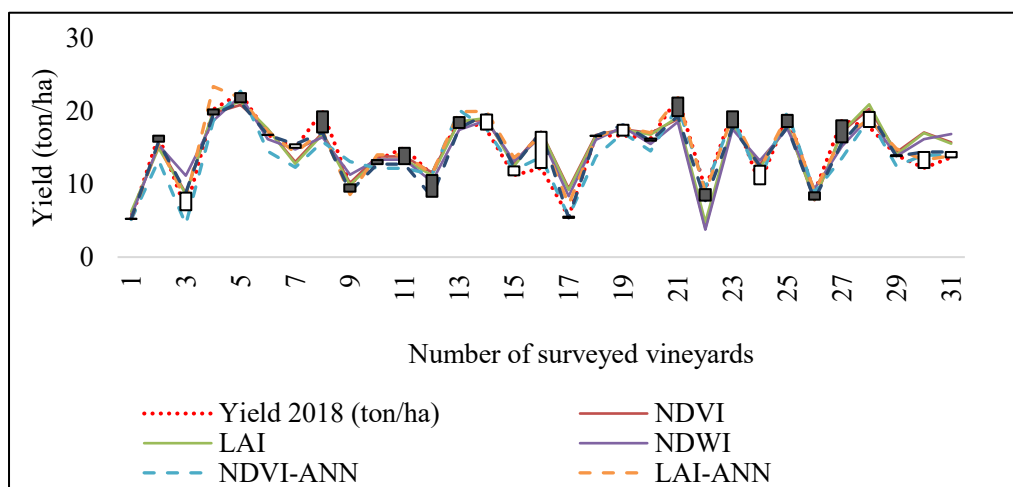
3.4 Discussion

Table grapes are a perishable product. To reduce postharvest losses via logistics arrangements in the supply chain, yield predictions are important. The goal of this study was to create a yield prediction model for table grapes using satellite-based remote sensing vegetation indices and machine-learning methods. Certain growth stages were most important for evaluating the vineyard variability throughout the growing season. Landsat 8 datasets were used to determine the vineyard-based table grape growth stages such as bud break, flowering, maximum canopy expansion and harvest time. According to the crop calendar, after July, the vegetation vigor decreased, and grape berries reached the final stage of ripening. Data about the occurrence times of these stages were considered to be indicators revealing the characteristics of the vegetation at the surface that were essential for yield estimation (Junges et al., 2017; Sun et al., 2017). Moreover, vegetation indices such as NDVI, LAI, and NDWI are important parameters that can reflect near real-time information about the canopy development, crop calendar, water stress, plant condition and grape yield.

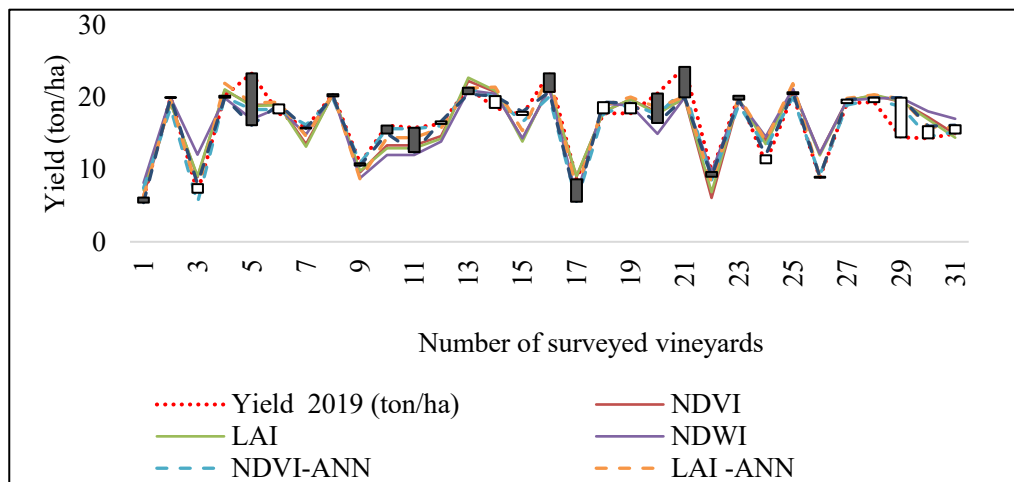
Previous research found that there is a significant correlation between NDVI and vine canopy vigor (Johnson et al., 2003). Sun et al. (2017) evaluated the relationship between yield and different NDVI and LAI combinations and found that although the cumulative NDVI and LAI values were not as good as the NDVI and LAI values from the optimal date at predicting yield, they were better than the maximum NDVI and LAI values and were more stable across two years in two vineyards in the USA. Anastasiou et al. (2018) found that satellite based GNDVI values at the time of harvest presented higher correlations with crop quality characteristics ($r = 0.522$ for berry diameter, $r = 0.537$ for pH, and $r = 0.629$ for berry deformation) than did NDVI (Lamb et al., 2004). However, grape yield prediction is a very challenging process due to environmental and field management factors. Hence, it is very difficult to find the best correlation day and then to determine a single grape yield prediction model based on remotely sensed data (Johnson et al., 2003). Therefore, in this study, we evaluated the correlations between yield and all maximum indices in all months and found that the associations between grape yield and the studied indices (NDVI, LAI and NDWI) were very low during the flowering and harvest periods but relatively high during maximum canopy expansion (**Table 3.4**). Finally, a time-series moving average was employed to represent all growing stages, which provided better results than did the other methods.



(a)



(b)



(c)

Figure 3.8 Graphs showing the difference between the predicted yield and the actual yield: (a) comparison of predicted and actual yield by the regression model and ANN model for the year 2017, (b) comparison of predicted and actual yield by the regression model and ANN model for the year 2018 and (c) comparison of predicted and actual yield by the regression model and ANN model for the year 2019.

Table 3.4 Regression between yield and maximum/moving average indices during the specific growth stages and active growing stages (April to October)

Indices	Growth stages	R ² value		
		2017	2018	2019
NDVI	Flowering	0.15	0.12	0.004
	Max-canopy expansion	0.74	0.69	0.78
	Harvest	0.41	0.72	0.21
	Active growth stages	0.79	0.77	0.79
LAI	Flowering	0.12	0.12	0.004
	Max-canopy expansion	0.71	0.70	0.76
	Harvest	0.42	0.73	0.21
	Active growth stages	0.78	0.78	0.79
NDWI	Flowering	0.06	0.07	0.02
	Max-canopy expansion	0.70	0.62	0.72
	Harvest	0.41	0.62	0.40
	Active growth stages	0.74	0.72	0.69

Table 3.5 The expected mean absolute error of the model predictions for 2017-2019 in Shakardara District

Parameters	Mean Absolute Error (ton/ha)		
	2017	2018	2019
Predicted Yield (NDVI in Max canopy expansion stage)	2.4	2.2	1.9
Predicted Yield (LAI in Max canopy expansion stage)	2.6	2.3	2.1
Predicted yield (NDWI in Max canopy expansion stage)	2.6	2.5	2.2
Predicted yield (NDVI in active growth stages linear regression)	2	1.8	1.9
Predicted yield (LAI in active growth stages linear regression)	2.1	1.7	1.9
Predicted yield (NDWI in active growth stages linear regression)	2.3	1.9	2.3
Predicted yield (NDVI ANN)	1.4	1.4	1.3
Predicted yield (LAI ANN)	1.3	1.2	1.5
Predicted yield (NDWI ANN)	1.3	1.5	1.5

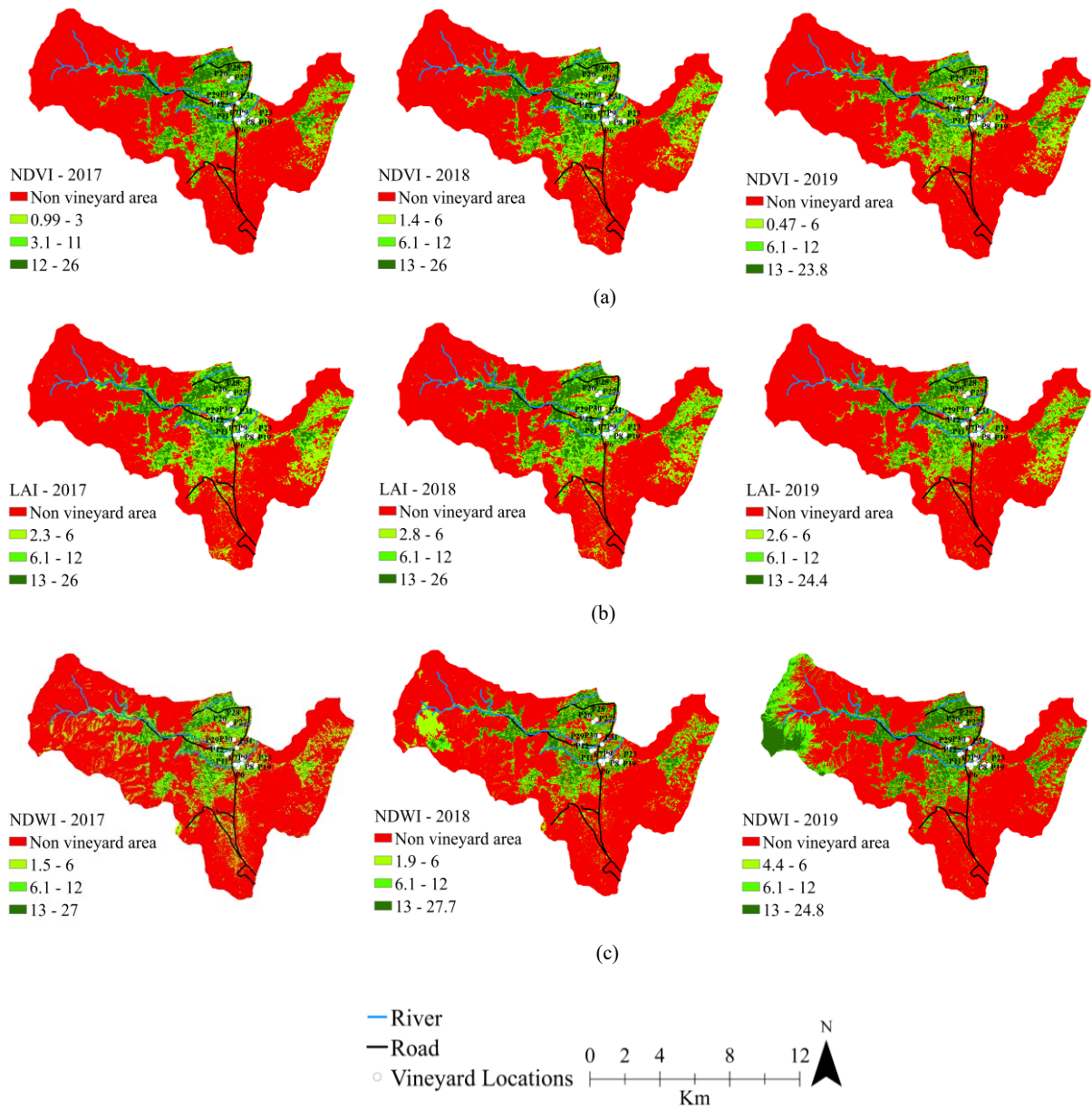


Figure 3.9 Predicted yield map with (a) NDVI (2017, 2018 and 2019), (b) LAI (2017, 2018 and 2019), and (c) NDWI (2017, 2018 and 2019) in tons per hectare

The results indicated that NDVI had higher accuracy in the machine-learning approach in all three years than did the other vegetation indices; NDVI explained almost 79% of the variability in two years, and the predicted yields from NDVI exhibited RMSE values of 2.5, 2.6 and 2.8 tons per hectare in 2017, 2018 and 2019, respectively. The RMSE values obtained for LAI were 2.3, 2.2 and 2.4 tons per hectare in 2017, 2018 and 2019 and those for NDWI were 2.3, 2.4 and 2.9 in 2017, 2018 and 2019, respectively (Figure 3.8 (a-c)). The analysis of the mean expected absolute errors revealed that the ANN mean absolute error was much lower than those of the other prediction methods (Table 3.5). Previous studies

used a machine-learning approach for grape yield predictions by creating a CNN to detect grape clusters from ground images (Santos et al., 2020).

It is worth mentioning that the ANN model performance for the prediction of grape yields had better performance than did the conventional statistical regression (**Figure 3.8 (a-c)**). In addition, in this study, the predicted yield maps were developed at the regional level (**Figure 3.9 (a-c)**). To increase the model accuracy, increasing the size of the training set, including more predictor variables, and using time-series data with shorter revisit cycles are essential. The main constraint in this research was the absence of more seasonal datasets from field observations, which is due to a lack of resources and field security. However, three years of ground reference yield prediction datasets along with satellite remote sensing data could help the government and stakeholders develop a better marketing strategy to decrease pre- and postharvest losses of grapes.

3.5 Conclusion

Vineyard yields may be assessed using NDVI, LAI, and NDWI at various phases of table grape development. To track the progression of growth phases and pinpoint the stages of table grape production, we used moving average and exponential smoothing to eliminate seasonality from the time data. This is why April was referred to as bud break in the development trajectory research. The month of May was found to be the **lushest** (thus, the time for flowering). The vegetation peaked in July, and harvesting may begin at the end of September or the beginning of October. To further anticipate grape production throughout the season, several vegetation indexes (NDVI, LAI, and NDWI) were utilized. The satellite-based remote sensing yield estimations were evaluated using ground reference data. In addition, the coefficients of determination were used to assess the prediction models. In both 2017 and 2019, NDVI had the most accuracy ($r^2=0.79$) of all the vegetative indices, while in 2018, LAI had the highest accuracy ($r^2=0.79$) of all the indices. For 2017 ($R=0.94$), 2018 ($R=0.95$) and 2019, machine learning findings suggested that NDVI had the best accuracies ($R=0.92$). Using this model, grape yields may be estimated and yield maps with regional variability can be developed. Predicting table grape production at various development stages was made possible by the use of satellite-derived vegetation indicators (NDVI, LAI, and NDWI). This study aids farmers in determining the ideal time to harvest and helps stakeholders better understand the many development phases of grapes for site-specific management.

Chapter 4

Yield Loss Estimation of Grapes at Macro Scale Using Composite Drought Index from Satellite Remote Sensing-based Time Series Datasets

4.1 Background of the Research

A drought is a natural catastrophe caused by a lack of precipitation and high temperatures over an extended time or in a single season as a result of climate change (Shukla et al., 2019; IPCC, 2019; FAO, 2019; Pokhrel et al., 2021; Hermans and McLeman, 2021). The agriculture sector, water resources, socioeconomics, and environment are impacted by precipitation shortfalls and extended hot temperatures (Schwalm et al., 2017; Sun et al., 2019; Touma et al., 2015; Badamassi et al., 2020). Therefore, drought causes losses of irrigated and nonirrigated agricultural crops, food shortages, famines, migration, and depletion of natural resources in the afflicted area (Matsa, 2021; Adger et al., 2021; Xu et al., 2021; Lesk et al., 2016).

The first industry affected by drought is agriculture. Drought risk and danger on irrigated and nonirrigated agricultural areas vary considerably across continents and nations. West, Central, and South Asia, Eastern Africa, and the eastern portion of Brazil are believed to have a high drought risk and susceptibility (Meza, et al., 2020). In drought-prone regions such as Afghanistan, Uzbekistan, Portugal, Spain, Burkina Faso, and Tanzania, agricultural output losses of more than 40% are anticipated (Li et al., 2009; Guo et al., 2021).

Drought continues to be an uncontrollable element influencing the amount and quality of agricultural products (Rotter et al., 2013; Potopová et al., 2015). Among all agricultural goods, table grapes are one of the most extensively spread fruits in the world. Table grape (*Vitis vinifera* L.) yields are most vulnerable to climatic variability, including temperature and water availability (Biasi, 2019). The optimal temperature range for grapevines is thus between 25 °C and 32 °C. If a fall in temperature below the ideal range limits plant development or if the temperature rises above the optimum, the photosynthesis rate is lowered owing to the increased respiration (Goldammer, 2018). Under drought circumstances, water stress has an impact on photosynthesis, yield, and crop quality. Water stress mostly affects vines during the phenological phases of bloom to pea-sized berry production (late spring to early summer), resulting in the development of smaller berries. Between veraison and harvest, grapevines are very vulnerable to water shortages and drought conditions (Hoheisel and Moyer, 2015). It not only reduces production, but also affects the ripening and quality of fruits throughout the

following season (Chalmers et al., 2008). As a result, supplying appropriate water supplies for plants permits adequate rates of photosynthesis and sugar synthesis, hence boosting growth and increasing cluster weight. In order to limit the effects of drought on vineyards, it is essential to forecast drought risks and loss estimates.

Conventional techniques for performing drought assessments and identifying drought-affected regions are time-consuming, costly, and subject to logistical restrictions. Due to a lack of communication between academics and grape farmers and a lack of technical and institutional skills for horticulture crops, underdeveloped nations face more logistical challenges. Satellite sensor datasets offer the ability to overcome such logistical limitations since they are regularly accessible, inexpensive, and may be used to anticipate the beginning, length, and severity of drought occurrences. Near-real-time evaluations via effective monitoring utilizing satellite imagery and real-time satellite rainfall data play a crucial role in limiting the negative effects of drought, since timely knowledge on the extent and severity of drought may mitigate its effects (Qureshi and Akhtar, 2004). Therefore, agricultural drought leads in decreased crop and fruit yields, decreased forage, local pasture, and animal production, severe food and nutrition insecurity, and other economic losses (Sepulcre-Canto et al., 2012; Han et al., 2021). Predicting drought based on normalized time series satellite datasets of drought indicators has the ability to help irrigation needs.

Predicting drought using normalized indices may provide result for continuous spatial and temporal resolutions using historical datasets that cover large geographic areas. Climatic variables such as SPI and PCI provide tremendous opportunity for assessing precipitation insufficiencies at particular places across several periods (Mckee et al., 1993). These variables have been used to characterize spatiotemporal differences in drought features, such as drought event extent, severity, and frequency (Yao et al., 2020). In addition, the VCI and deviation of NDVI from its long-term mean have been used for agricultural drought monitoring. Furthermore, TCI may be utilized to identify vineyard stress due to high temperatures (Kogan, 1995a). In addition, crop water stress is closely correlated with the NDMI (Baluja et al., 2012), and this indicator is essential for vineyard drought forecasts since water stress has a significant impact on the quality of table grapes (Goi et al., 2011; Di Vittori et al., 2018). Individually, these vegetative indexes have been used to monitor drought. As drought includes several elements, however, confidence in the capacity of a single measure to forecast drought severity is lacking. Using a mathematical model to combine drought-related indicators into a composite drought index, each

parameter may have a greater impact on detecting drought-affected vineyards and estimating yield losses.

PCA has an advantage over other mathematical models in that it may include weights into the parameter values, which can then be used as an index to anticipate the results of the model assessment. On the other hand, the majority of remote sensing and GIS-based (Geographic Information System) research has used the analytic hierarchy process (AHP) as well as fuzzy logic techniques. Weights are used as judgements in accordance with the views of experts to imply the likelihood of bias when using AHP procedures (Muhsin et al., 2018). In addition, fuzzy sets on their own lead to poorly managed weights for each component or parameter, and they are dependent on a multicriteria decision making (MCDM) method, which is still another kind of subjectivity (Purnamasari et al., 2019b). In hydrological and atmospheric science research, principal components analysis (PCA) is an objective method that is employed to extract the effects of factors in the observed datasets (Barnston and Livezey, 1987; Bayissa et al., 2019). In light of this capacity, the principal component analysis (PCA) technique was included in this investigation as an alternate approach to the task of quantitatively determining the weights of input variables in order to produce a composite drought index.

In very few cases, the CDI has been utilized to differentiate between years of drought and years without drought (Bayissa et al., 2019). In addition to the establishment of the CDI (Han et al., 2019) for the purpose of monitoring agricultural and meteorological droughts, a new station-based integrated index (Jia et al., 2019) has been developed for the purpose of monitoring drought conditions across a wide range of climate conditions. In addition, a combined drought index known as CDI M was established in order to monitor the agricultural drought that has been plaguing India and to offer information that can be used to better manage agricultural drought. In addition, a variety of statistical methods have been used in order to arrive at estimates of the losses in yield that have been attributed to the drought.

The quadratic equation, multivariate regression model, and the logistic function are all examples of these approaches (Zhang, 2004; Zhu et al., 2020; Ming et al., 2015; Chen et al., 2019). Using regression analysis, one of the most common methods is used to identify the relationship between each influencing variables and the observed table grape yield loss. However, conventional statistical methods are not strong enough to estimate accurately vineyard output losses. Table grape and other agricultural crop yield estimate and yield loss calculations have lately employed machine learning, such as random forest and ANN algorithms (Monteiro et al., 2021; Zhu et al., 2020; Arab et al., 2021). When it comes to

machine learning approaches, the use of artificial neural networks (ANNs) to assess yield loss estimate performance in short time frames has become a common methodology. According to a single indicator, very few research have been done on drought-related yield loss estimations using machine learning algorithms. For winter wheat yield reductions, random forest algorithms (Monteiro et al., 2021) and Bayesian network (BBN) algorithms were used to calculate the frequency of yield reductions (Potopová et al., 2020) in the southeastern European region, where the SPEI is used for maize, sunflower, and grapevine losses. Both research indicated that when analyzing drought persistence, machine learning is a useful strategy as the primary driver of yield loss predictions. ANNs do not need previous knowledge of the statistical distribution of the studied data to create patterns (Mollalo et al., 2018). Few studies have been done on the use of an ANN model to forecast drought yield losses.

Therefore, the purpose of this study was to assess grape production losses during drought-affected years using Bayesian regularized artificial neural networks (BRNNs) and a composite drought index generated from vegetation, soil moisture, and precipitation weighted using principal component analysis (PCA).

4.2 Materials and Methods

4.2.1 Study Area

The research location was chosen one of the most drought-prone areas in Southeast Asia; major losses in grape production have happened in Kabul Province, which is situated in Afghanistan's center region. Afghanistan had severe droughts from 1998 to 2006, 2008 to 2009, and 2018 as a result of extremely high temperatures and below-average precipitation, with catastrophic effects for agriculture and food security (World bank, 2018; Savage et al., 2009; FAO, 2019; Arab et al., 2019). More than 85% of Afghanistan's population depends on money earned by agricultural goods for living (ACSO, 2019). The area has a dry and continental climate, with an annual rainfall total of 400 mm, most of that falls between May to November, and an annual snowfall total of 15-30 cm, most of that falls during the winter. The average high temperature in July is +25° C, while the average low temperature in January is about -12 °C. Climate change has caused mean temperature rises of roughly 2 °C through 2050 and 6.3 °C until the end of the century in recent years (Aich and Khoshbeen, 2016).

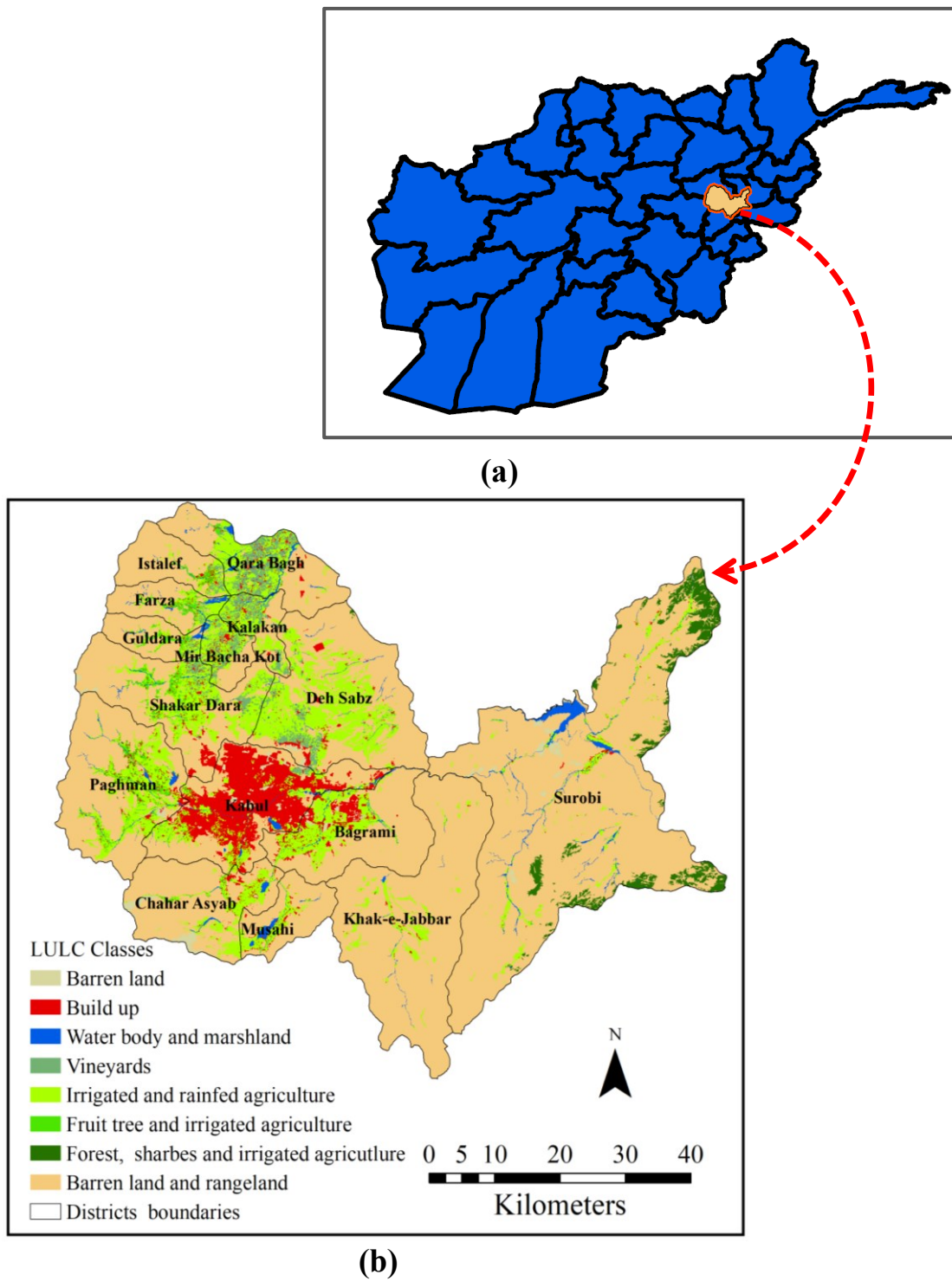


Figure 4.1 The study’s geographical scope and maps: (a) Afghanistan administrative map, and (b) Kabul Province land cover map based on FAO data.

Based on the local climate and temperatures Kabul Province is a single crop region (regional rural economic regeneration strategies (RRERS) provincial profile) and the environment is ideal for cultivating a variety of vegetables and fruits. Table grapes are one of the most important fresh fruits and are grown in practically every area in this province. Kabul Province has 71,088 hectares of agricultural land (irrigated and nonirrigated), 4,000 ha of fruit trees, and 10,599 ha of vineyards, according to the FAO land use categorization (**Figure 4.1**). As a result, agricultural and perennial crops play important roles in the country's economy and rural existence. As a result, table grapes were chosen as the research item in this study. The entire grape output in the research region was around 115,450 tons in 2020 (ACSO, 2020), accounting for 77% of Kabul Province's total fresh fruit production. Table grapes are farmed primarily for family use in certain places rather than for commercial objectives. Table grape output and quality are mostly determined by weather conditions in certain years. The existing growth practices, along with inadequate irrigation water management, have resulted in major production issues that did not exist prior to the drought years. Drought has had the greatest impact on yield in this area because the region is landlocked, and the availability of water for irrigation purposes is primarily determined by rainfall and snowfall, which feed surface and ground water resources, which are primarily determined by the amount and distribution of precipitation (Qureshi, 2002). As a result, drought affects grape harvests, livelihoods, and revenue in this densely populated area; nonetheless, severe and extended droughts have substantial effects for food security (Arab et al., 2019).

4.2.2 Data Description

4.2.2.1 Satellite Datasets and Data preprocessing

Downloads of Landsat 8 datasets were made from the official USGS website (<http://usgs.gov/>). Landsat 8 OLI and TIRS images from April to October of each year were utilized for the years 2016 to 2020. The recent five years were used because the climate variability increased from 1991-2020 in Afghanistan. Landsat 8 OLI sensor has nine reflective bands, and a TIRS sensor with two TIR bands (Band 10 and Band 11). The spatial resolution of these thermal bands is 100 meters; however, they are resampled using cubic convolution at a resolution of 30 meters before being distributed by the USGS (Gemitizi et al., 2021; Loveland and Irons, 2016). The Landsat 8 OLI and TIRS collection has 2 Level-1 (C1 Level-1) daytime images were used. Many data processing tasks, including radiometric calibration and atmospheric correction, were carried out for this product. The scenes were located in the 152 and 153 paths with 36 rows. Two tiles were mosaiced to cover the whole research area since it was positioned in two separate satellite tracks. The active growth season of the grape vines, which begins in April and ends in October before harvesting the table grapes, was affected by the drought.

The drought indicators were calculated using 114 photos for the seventh month, all taken on the same day or nearby same dates. Data from the global satellite mapping of precipitation (GSMap) from JAXA for the years of 2016 to 2020 were also used in this study. Each millimeter per hour measurement on the JAXA real-time rainfall watch website (<https://global.jaxa.jp/>) was given. This was done by analyzing land cover maps for all vineyards in Kabul Province. There are 11 standardized and self-explanatory land cover classifications defined by the FAO (**Figure 4.1**). For research purposes, the similar classes were combined into similar classes.

4.2.2.2 Composite Drought Indices

The composite drought index was formulated using five input parameters. These parameters included the DEV, VCI, TCI, PCI and NDMI.

4.2.2.2.1 Deviation of NDVI (DEV of NDVI)

The drought severity index was calculated using the normalized differential vegetation index data acquired over the growing seasons of 2016 to 2020. First, NDVI values were computed using the near-infrared and red bands of the Landsat 8 imaging data collection (Sellers, 1985). The deviation of NDVI from its long-term mean can be utilized to understand vegetational changes caused by climatic influences. This deviation is determined as the difference between the current NDVI value and the long-term monthly mean NDVI for each pixel (Johnson et al., 1993). The following equation was used:

$$DEV_{NDVI} = NDVI_i - NDVI_{mean, m} \quad (4.1)$$

where $NDVI_{i,j}$ is the current NDVI image for pixel i at time j and $NDVI_{max}$ and $NDVI_{min}$ are the absolute maximum and minimum NDVI values, respectively, calculated for each pixel using the entire NDVI record (2016-2020).

4.2.2.2.2. Vegetation Condition Index (VCI)

The VCI approach was suggested by Kogan (1990, 1995a). This index indicates how near the current month's NDVI value is to the lowest NDVI determined from long-term data. It was created by transforming the NDVI values of each location and pixel from 0 to 1 (Kogan et al, 2019). The VCI can be expressed as follows:

$$VCI = \frac{NDVI_{i,j} - NDVI_{min}}{NDVI_{max} - NDVI_{min}} \quad (4.2)$$

where $NDVI_{i,j}$ is the current NDVI image for pixel i at time j and $NDVI_{max}$ and $NDVI_{min}$ are the absolute maximum and minimum NDVI values, respectively, calculated for each pixel using the entire NDVI record (2016-2020).

4.2.2.2.3 Temperature Condition Index (TCI)

Kogan (1990, 1995a) has proposed the TCI, which is computed in the same way as the VCI but is based on the land surface temperature (LST) normalization of each pixel using the maximum and lowest temperatures in the provided time series (the higher the temperature, the more severe the drought) (Kogan et al, 2019). Using the thermal bands of Landsat 8 TIRS data, the LSTs were computed (Tariq et al., 2020). The TCI can be expressed as follows:

$$TCI = \frac{LST_{max} - LST_{i,j}}{LST_{max} - LST_{min}} \quad (4.3)$$

where $LST_{i,j}$ is the actual land surface temperature for pixel i at time j and $LST_{i,min}$ and $LST_{i,max}$ are the minimum and maximum LSTs, respectively, of pixel i at time j for the entire study period (2016-2020).

4.2.2.2.4 Normalized Difference Moisture Index (NDMI)

This variable has a strong relationship with canopy moisture content (Hardisky et al., 1983). It was generated from NIR and SWIR bands and can be represented as follows:

$$NDMI = \frac{NIR - SWIR}{NIR + SWIR} \quad (4.4)$$

where NIR is the near-infrared wavelength reflectance ranging from 0.85-0.88 μm and SWIR is the shortwave infrared wavelength reflectance ranging from 1.57-1.65 μm in Landsat 8 OLI images.

4.2.2.2.5 Precipitation Condition Index (PCI)

The PCI was calculated by comparing the current precipitation values with the long-term maximum and minimum precipitation values. The JAXA rainfall GSDataset datasets were used to calculate the PCI (Zhang and Jia, 2013). It can be derived from the expression shown below:

$$PCI = \frac{PCI_{i,j} - PCI_{min}}{PCI_{max} - PCI_{min}} \quad (4.5)$$

Where PCI_{ij} is the precipitation at the current date and month for each zone and PCI_{max} and PCI_{min} are the maximum and minimum precipitation, respectively, calculated for each pixel using the entire NDVI record from 2016 to 2020.

4.2.2.2.6 Standard Precipitation Index (SPI)

To measure precipitation shortfalls at a specific place across various periods, McKee developed SPI index in 1993. Finding the probability density function that most accurately describes the distribution of the precipitation data across the various time periods is the first step in the SPI computation. The hourly rainfall information from the global rainfall map (GSMap, JAXA) was applied independently for each month over the course of five years, from 2016 to 2020. The link between probability and precipitation is defined by fitting each data point to the gamma probability density function with the shape and scale parameters. The gamma cumulative distribution function transforms to the standardized normal cumulative distribution function using an equal-probability transformation, which has a mean and standard deviation of zero and one respectively. The benefit of this standardization is that it ensures that the frequency of severe dry and wet occurrences has constant values throughout time and place. A continuous random variable X is connected to a gamma distribution. This is how the X 's of p.d.f are explained:

$$g(x) = \frac{1}{\beta^\alpha \times \Gamma(\alpha)} x^{\alpha-1} \times e^{-\frac{x}{\beta}} \quad \text{for } x > 0 \quad (4.6)$$

where $\alpha > 0$ is a shape parameter, $\beta > 0$ is a scale parameter, $x > 0$ is the quantity of rainfall, and $\Gamma(\alpha)$ is the gamma function. This is how the gamma function is defined in the following.

$$\Gamma(\alpha) = \int_0^{\infty} x^{\alpha-1} e^{-x} dx \quad (4.7)$$

Adjusting the gamma distribution to the data set requires the α and β parameters to be estimated through the maximum likelihood estimation using the following approximation:

$$\hat{\alpha} = \frac{1}{4A} \left(1 + \sqrt{1 + \frac{4A}{3}} \right) \quad (4.8)$$

$$\hat{\beta} = \frac{\bar{x}}{\hat{\alpha}} \quad (4.9)$$

$$A = \ln \bar{x} - \frac{\sum \ln x}{n} \quad (4.10)$$

where n represents the observations. By integrating the probability density function with respect to x and inserting the estimates of the α and β yields, an expression for the cumulative probability $G(x)$ of an observed amount of precipitation occurring for a given month and time scale can be obtained.

$$G(x) = \int_0^x g(x) dx = \frac{1}{\beta^{\hat{\alpha}} \Gamma(\hat{\alpha})} \int_0^x x^{\hat{\alpha}-1} e^{-x/\hat{\beta}} dx \quad (4.11)$$

Substituting t for $x/\hat{\beta}$ reduces the equation shown above to the following expression.

$$G(x) = \frac{1}{\Gamma(\hat{\alpha})} \int_0^{x/\hat{\beta}} t^{\hat{\alpha}-1} e^{-t} dt \quad (4.12)$$

The gamma distribution is undefined when $x = 0$ and $q = P(x = 0) > 0$, while $P(x = 0)$ is the probability of zero (null) rainfall. As a result, the cumulative probability distribution function is written as follows.

$$H(X) = q + (1-q) \times G(x) \quad (4.13)$$

The above approach, while simple, is not practical for computing SPI values for large numbers of data points. Following Edwards and McKee (1997), we employ the approximate conversion provided by Abramowitz and Stegun (1965) as an alternative.

$$Z = \text{SPI} = - \left(t - \frac{c_0 + c_1 t + c_2 t^2}{1 + d_1 t + d_2 t^2 + d_3 t^3} \right) \quad \text{for } 0 < H(x) \leq 0.5 \quad (4.14)$$

$$Z = \text{SPI} = + \left(t - \frac{c_0 + c_1 t + c_2 t^2}{1 + d_1 t + d_2 t^2 + d_3 t^3} \right) \quad \text{for } 0.5 < H(x) < 1 \quad (4.15)$$

4.2.2.3 Ground Reference Datasets

A field survey was conducted in the Kabul Province during November and December of 2020 to collect information on the yield of vineyards. Therefore, a GPS receiver (Garmin®) was used to capture the geographical position of each vineyard (**Appendix 4.1**). 100 vines in 44 villages and eight regions were chosen at random to compile the data. During the field survey, waypoints (x, y coordinates) were gathered for every vineyard in Kabul Province (Specifically from Farza, Shakardara, Deh Sabz, Istalif, Qarabagh, Mir Bacha Kot, Guldara and Kalakan Districts). These waypoints were used as Landmarks to determine vineyard placement. Then, each vineyard in Kabul Province was represented by a polygon created using Google Earth Pro®. End of September and beginning of October is the optimal season to harvest grapes in the Kabul province.

The process of harvesting was done conventionally in Kabul Province, according to the results of the field survey. With shears, a minimum of four centimeters of stem was removed from the grape cluster.

Crates were used to transport the grapes. After harvesting, the grapes were kept in a covered location until they were ready to be packed. As soon as feasible after harvesting, the grapes must be packaged and chilled to storage temperature. It's difficult to store fresh grapes for an extended amount of time since they have a limited shelf life, particularly without refrigeration.

4.2.3 Methods

4.2.3.1 Composite Drought Index

In this study, agricultural and climatic parameters (DEV, VCI, TCI, SPI and NDMI) were used to develop drought maps for drought affected years (2016-2020) (**Figure 4.2**). Landsat 8 OLI and TIRS scenes were used to develop the drought indices, and JAXA rainfall data were used to calculate the PCI and SPI values. The drought periods considered in this research were within in the active growing period of the vines, which started in April and ended in October of each year. Thus, grapes are a perennial crop that were selected to determine the effects of drought on yield and to evaluate the relationships between composite drought indices and table grape yields during the vine growing season (April-October). To determine the contribution of each parameter, the drought layers were weighted by PCA to create a composite drought indicator (**Table 4.1**). The PCA must build a square ($p \times p$), where p is the number of variables, and a symmetric correlation matrix to describe the correlation matrices. Therefore, a 5×5 correlation coefficient matrix was developed using the zonal mean values of five input parameters. The matrix was used to compute the eigenvectors, which were then used to transform the input parameters into different orthogonal principal components (PCs). Since the PCs are orthogonal vectors, it is impossible to combine them into a single vector by applying mathematical expressions (Keyantash and Dracup, 2004; Avena et al., 1999; Bayissa et al., 2019). The eigenvectors reveal the relationships between the principal components and the original data. The first PC1 showed the most variability among all input parameters. The following expression was used to combine all input parameters, and the contribution of each parameter is explained in **Table 4.1** The CDI developed is as follows:

$$CDI_y = W_{vci,y} \times VCI_{ym} + W_{DEV,y} \times DEV_{ym} + W_{NDMI,y} \times NDMI_{ym} + W_{pci,y} \times PCI_{ym} + W_{tci} \times TCI_{ym} \quad (4.14)$$

where CDI is the composite drought index, y is the year (2016-2020), m is the zonal mean, W_y is the PCA weight of each parameter for a specific year (2016-2020), VCI is the vegetation condition index, DEV is the deviation of NDVI from the long-term mean, NDMI is the normalized difference moisture index, PCI is the precipitation condition index and TCI is the temperature condition index.

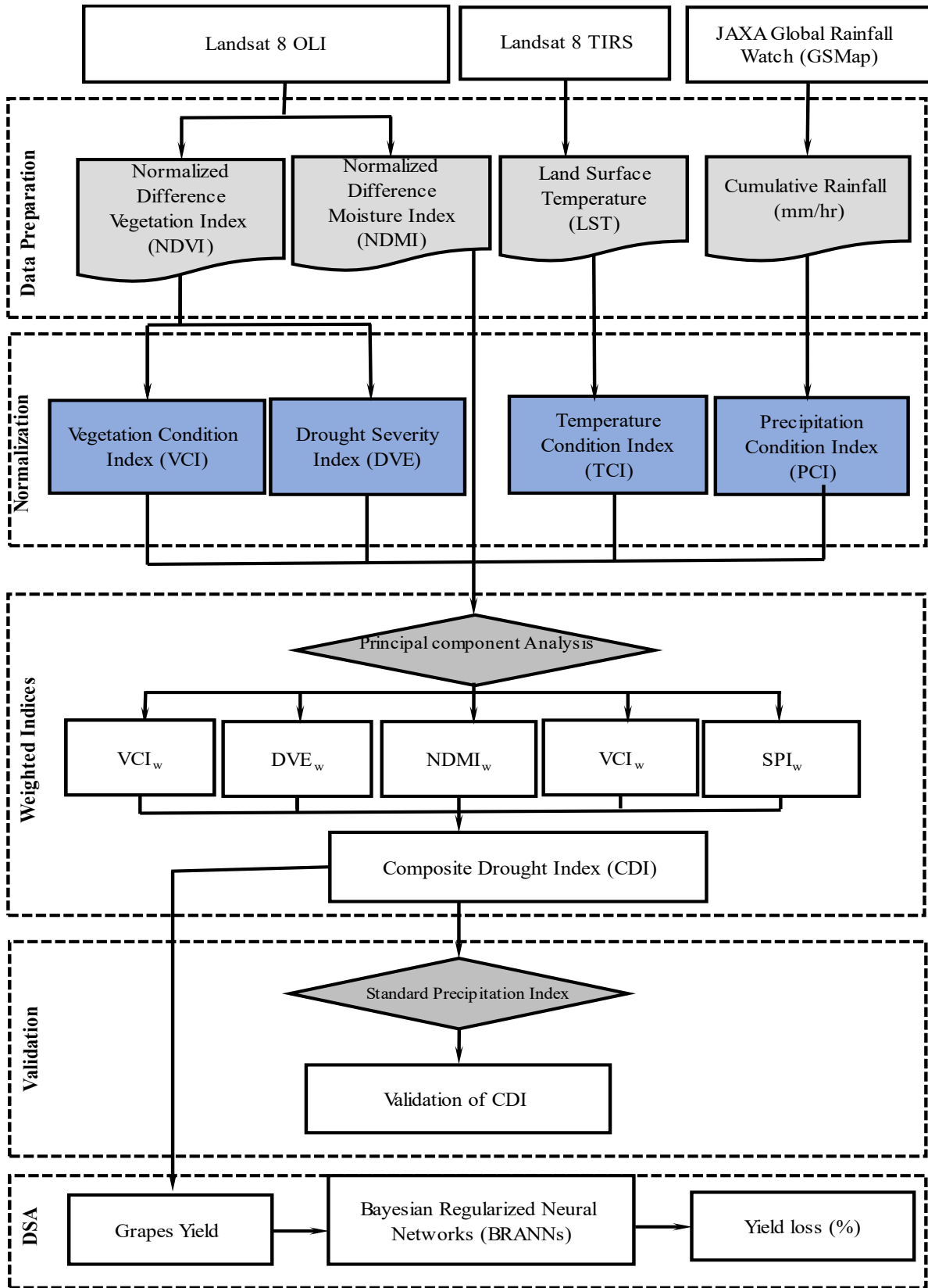


Figure 4.2 Research flowchart for predicting drought and yield losses using CDI and machine learning systems to estimate losses.

4.2.3.2 Validation of the Composite Drought Index with SPI

In this study, an independent variable (standard precipitation index) was used for the CDI validation. The SPI was developed by McKee in 1993 to quantify precipitation deficits at a given location over multiple timescales. The SPI shows the rainfall deficit of a given region. The first step in the SPI calculation involves finding the probability density function that best describes the distribution of the precipitation data over the different considered time scales. This method was applied separately for the hourly rainfall datasets obtained for each month from the global rainfall map (GSMap, JAXA) over the five years from 2016-2020. To maintain the seasonal effect of rainfall on vegetation, the monthly SPI was calculated. Each data point was fitted to the gamma probability density function with shape parameter α and scale parameter β to define the relationship of the probability of precipitation. With an equal-probability transformation, the gamma cumulative distribution function converged to the standardized normal cumulative distribution function with a mean of zero and a standard deviation of one. This standardization provides the advantage of spatially and temporally consistent values of the frequency of extremely dry and wet events (Edwards and McKee, 1997). SPI-1 represents the short-term conditions of soil moisture and crop stress on a relatively short time scale. In this case, for SPI-1, hourly rainfall datasets from a global rainfall map were used to investigate the drought association with the composite drought indicator. Since the drought period was considered from April to October in each vineyard, a 7-month mean SPI was used for comparison with the composite drought index. In this study, all analyses were performed by using ArcGIS 10.8, Microsoft Excel, MATLAB and the SPSS interface® for the geospatial and remote sensing analyses, and the weighted overlay technique was applied for the multiple indices, mathematical and statistical analyses (**Figure 4.2**).

Table 4.1 Average weight values estimated by PCA for individual indices for 2016-2020

Year	VCI	DEV	NDMI	TCI	PCI	Total
2016	0.26	0.20	0.18	0.25	0.10	1
2017	0.25	0.17	0.26	0.16	0.16	1
2018	0.30	0.24	0.14	0.17	0.16	1
2019	0.14	0.23	0.30	0.29	0.04	1
2020	0.17	0.27	0.28	0.19	0.10	1

4.2.3.3 Evaluation of Yield Variations due to Drought using BRANNs

According to the FAO, different factors affecting agricultural yield cause yield losses, such as weather, extreme factors, policy, innovations, and management trends (FAO, 1999). In this study, only drought-

related yield variations were considered. In this regard, first, all vineyards overlaid over the CDI drought map and affected vineyards under extreme to moderate drought were masked. Subsequently, a Bayesian regularized neural network (BRANN) model was run in each drought category to calculate the yield loss during the drought periods of 2016 and 2018. Bayesian ANNs incorporate Bayes' theorem into the regularization scheme. This scheme is more robust than standard backpropagation nets and can reduce or eliminate the need for lengthy cross-validations. BRANNs are powerful mathematical models that provide solutions with a number of problems to reduce the potential for overfitting (Burden and Winkler, 2008; Mackay, 1992). These models consist of a number of neurons in the input, hidden and output layers. The number of hidden layers was chosen based on the performance of each model (1-10). In this regard, the CDIs based on the VCI, TCI, NDMI, DEV, and PCI were selected as the input layer, and the grape yield in each vineyard was selected as the output layer. The number of hidden layers was selected based on the performance of each model. Finally, 10 hidden layers were selected for each model. The number of neurons corresponded to the number of selected predictors in each model, and the number of iterations was equal to the number of observations. Therefore, we chose 70% of the data for training and 30% for testing. The performance of each model was evaluated using the MSE value and R-value. The table grape yield losses that occurred due to drought were calculated in each vineyard in 8 surveyed districts of Kabul Province for the periods of 2016 and 2018. The variations were observed based on the predicted yield and observed yield. The table grape yield loss was calculated using the difference between the predicted yield and observed yield from the CDI values using BRANN techniques. It is worth mentioning that the impacts of pests, diseases and flooding were ignored in the yield loss calculation because this study considered only yield losses that occurred due to extreme weather or drought conditions. The yield loss percentage was calculated using the following expression:

$$\text{Yield loss} = \frac{Y_o - Y_p}{Y_o} \times 100 \quad (4.17)$$

where Y_o is the observed yield collected from the field survey and Y_p is the simulated yield obtained from the CDI during 2016 and 2018 (Wang et al., 2020).

4.3 Results

4.3.1 Drought Assessment using CDI

In this study, drought conditions were monitored in the vineyards of Kabul Province from 2016-2020 using composite drought indices. First, the CDI was developed from input parameters (VCI, TCI, PCI, DVE and NDMI) at the district level and composite by PCA weight for the period 2016 to 2020. The

PCA assigned weights were the highest for VCI (26%) and TCI (25%) for 2016, VCI (25%) and NDMI (26%) for 2017, VCI (30%) and DEV (24%) for 2018, NDMI (30%) and VCI (29%) for 2019 and DEV (27%) and NDMI (28%) for 2020. To determine the drought intensity and severity, the drought maps were classified based on the Kogan drought classification method, and the classes are explained in Table 4.2. According to Kogan, when all parameter values are less than 10% (0.10), an area is affected by extreme drought; however, when all parameter values are above 40% (0.40), wet conditions are observed (**Table 4.2**). The CDI result indicated that 2016 and 2018 were drought and 2017, 2019 and 2020 were wet or lower wet observed (**Figure 4.3**). According to the obtained results, 2018 was the most extreme drought period in Kabul Province, and the extreme drought intensity in this year was higher in the southern, central and northern regions (Bagrami, Khak-e-Jabbar, Musahi, Chara Asyab, some parts of Kabul city, Shakardar, Kalakan and Qara Bagh) of the province than in other regions. However, the severe drought condition was also high in all 14 districts (Bagrami, Chahar Asyab, Deh Sabz, Farza, Guldara, Istalif, Kalakan, Khaki Jabbar, Mir Bacha Kot, Mussahi, Paghman, Qarabagh, Shakardara and Surobi) include the Kabul city. In contrast, in 2016, almost all parts (Bagrami, Chahar Asyab, Deh Sabz, Farza, Guldara, Istalif, Kalakan, Khaki Jabbar, Mir Bacha Kot, Mussahi, Paghman and Qarabagh) of Kabul Province, including Kabul city, experienced severe to marginal stress of drought (**Figure 4.3**).

In the dry years of 2016 and 2018, the total agricultural areas (agricultural lands including all irrigated and nonirrigated lands, fruit trees, vineyards, rainfed and nonrainfed rangelands, forest, and shrubs) affected by extreme drought and moderate drought were 17,264 ha and 36,337.5 ha, respectively. However, 1,053 and 1,290.9 ha of vineyards were observed to be affected by extreme to marginal drought, respectively, from 2016 to 2018 (**Figure 4.4**). Wet years were observed in 2017, 2019 and 2020 in the study area (**Figure 4.3**). According to the obtained results, the affected areas were 0, 0 and 0.9 ha in 2017, 2019 and 2020, respectively. Figure 4 shows the affected area as a percentage of the total area and indicates that the drought-affected areas in 2016 and 2018 were 68% and 90% of the total area of all districts, comprising 18.6% and 40% in agricultural fields and approximately 10% and 13% in vineyard fields, respectively (**Figure 4.4 and Table 4.3**). However, the total affected areas in the wet years of 2017, 2019 and 2020 were 5%, 1.7% and 8.3% respectively. Since the percentage of affected areas were less than 10%, we considered them as a wet year.

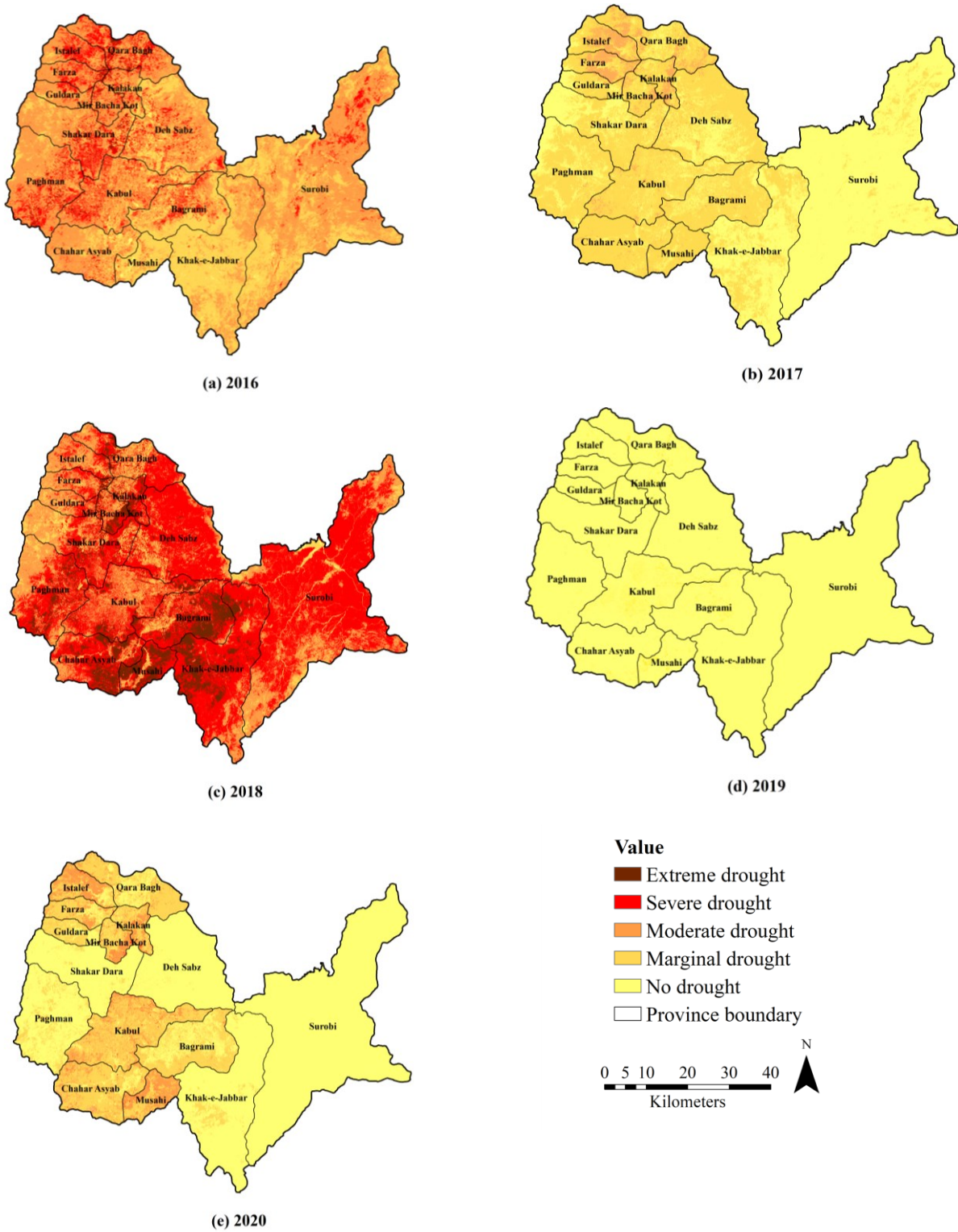


Figure 4.3 Drought severity risk areas based on CDI in Kabul Province during the active growing stages of vines from 2016-2020

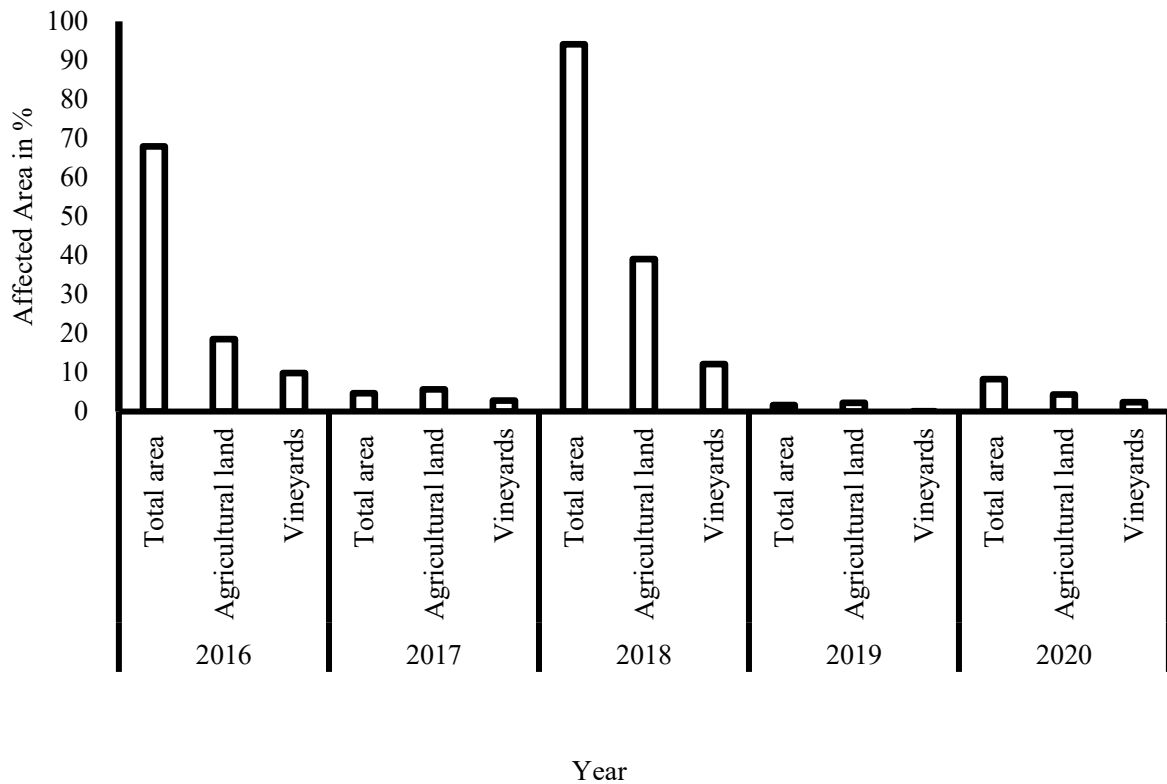


Figure 4.4 Percentage of affected agricultural land and vineyards in extreme to moderate drought conditions in Kabul Province from 2016-2020

Table 4.2 Drought classification system using the CDI values derived from several indices

Drought classes	VCI, TCI, DEV, PCI and NDMI	CID
Extreme drought	$VCI < 0.10$	$VCI < 0.10$
Severe drought	$0.10 \leq VCI < 0.20$	$0.10 \leq VCI < 0.20$
Moderate drought	$0.20 \leq VCI < 0.30$	$0.20 \leq VCI < 0.30$
Marginal drought	$0.30 \leq VCI < 0.40$	$0.30 \leq VCI < 0.40$
No drought	$VCI > 0.40$	$VCI > 0.40$

4.3.2 Validation of CDI with SPI

The SPI-1 result indicated that in February 2016 Bagرامي, Chahar Asyab, Guldara, Deh Sabz and Shakardara districts experienced severe to extreme drought conditions and the SPI values were -2.5, -1.3, -1.2, -1.2 and -1.3 respectively. However, in December 2016 only two districts Bagرامي and

Paghman were experienced extreme dry conditions -2.5 and -1.03 respectively. Besides, in January 2018 Bagrami and Surobi have experienced extremely dry conditions -2.5 and -1.02. respectively.

Moreover, June, July, August, November and December were experienced mild dry conditions. Although in 2017, 2019 and 2020 all the provinces experienced mild dryness during the summer especially in June because Afghanistan is a dry country and there is no rainfall during the summer in Kabul Province (**Figure 4.5**). Subsequently, the CDI values were validated with the time series of SPI from 2016 to 2020, which was developed using JAXA rainfall data. Since Afghanistan is a landlocked and dry country, it is dry almost all summer and lacks rainfall to lessen the effect of the existence of severe drought in all years; thus, to determine the effect of drought in the entire table-grape-growing season, we averaged the data over the entire growing season (April to October). The results indicated that the zonal mean CDI and 7-month mean SPI-1 were significantly highly correlated during the active growing stages of vineyards ($r^2= 0.64$) (**Figure 4.6**). The highly correlation of CDI with the SPI-1 indicated the potential use of CDI for developing a drought evaluation and early warning systems for Kabul Province in Afghanistan.

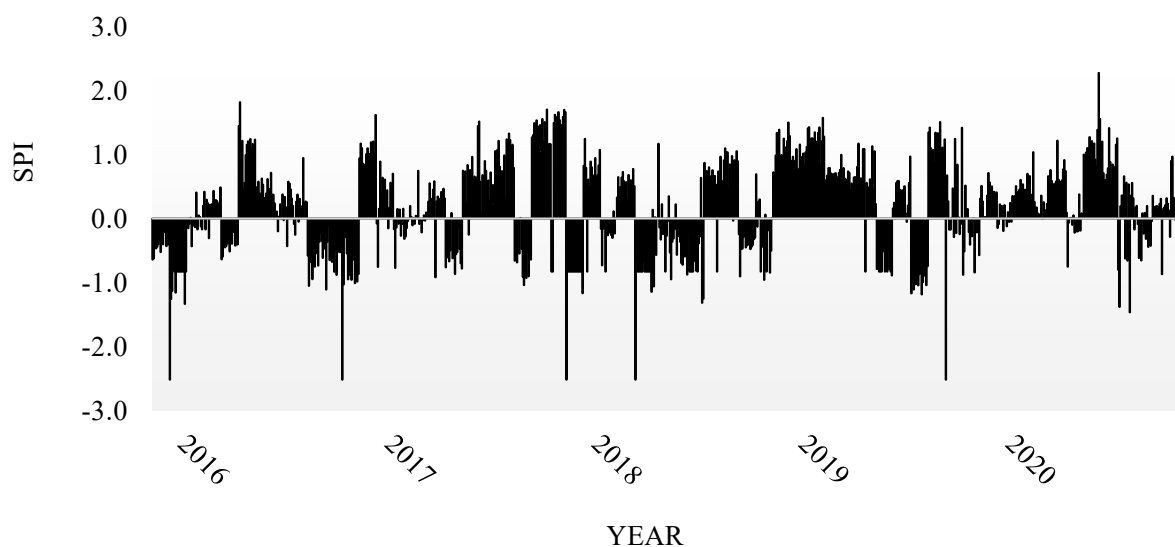


Figure 4.5 Standard Precipitation Index (SPI) using JAXA cumulative rainfall for the years of 2016 to 2020

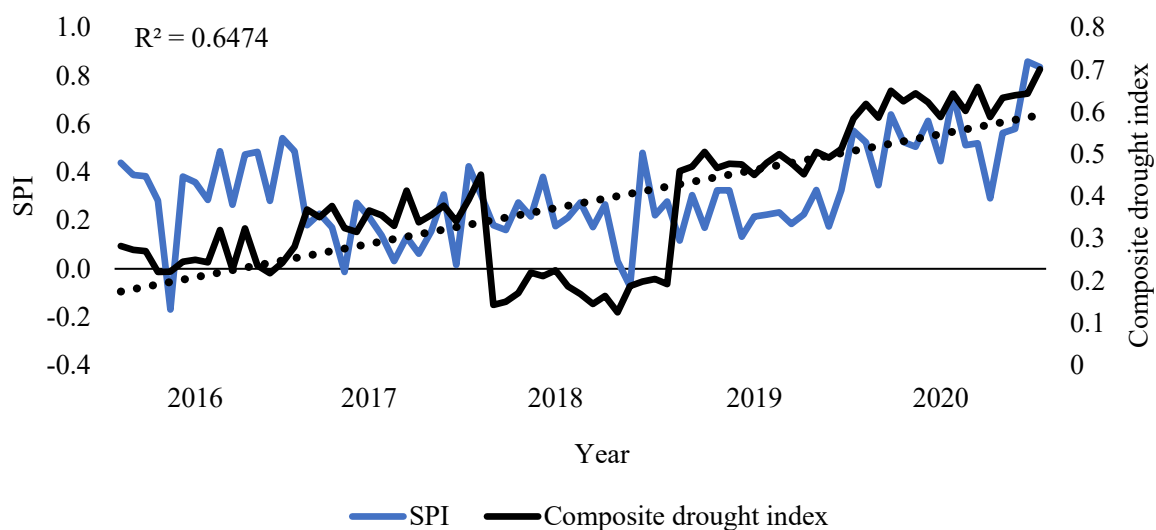


Figure 4.6 Yearly time series comparison of the zonal mean CDI value of each district with the mean SPI value (April to October) from 2016 to 2020.

Table 4.3 The affected areas based on drought classes in agricultural lands and vineyards in Kabul Province from 2016 – 2020

Years	Classes	Extreme drought	Severe drought	Moderate drought	Total area (ha)
2016	Total area	2792.97	55379.25	256739.9	314912.2
	Agricultural land	607.8	3823.9	12832.3	17264
	Vineyards	13.1	145.7	894.6	1053.4
2017	Total area	0	4.5	21787.47	21791.97
	Agricultural land	0	1.98	5357.52	5359.5
	Vineyards	0	0	303.03	303.03
2018	Total area	45511.56	262928.8	127616.9	436057.3
	Agricultural land	797.5	11538.3	24001.7	36337.5
	Vineyards	14.6	271.4	1004.9	1290.9
2019	Total area	0	0.09	14.49	14.58
	Agricultural land	0	0.09	8.9	8.9
	Vineyards	0	0	0.18	0.18
2020	Total area	8.91	573.93	37943.28	38526.12
	Agricultural land	0.9	147.5	3937.9	4086.3
	Vineyards	0.18	15.8	234.4	250.4

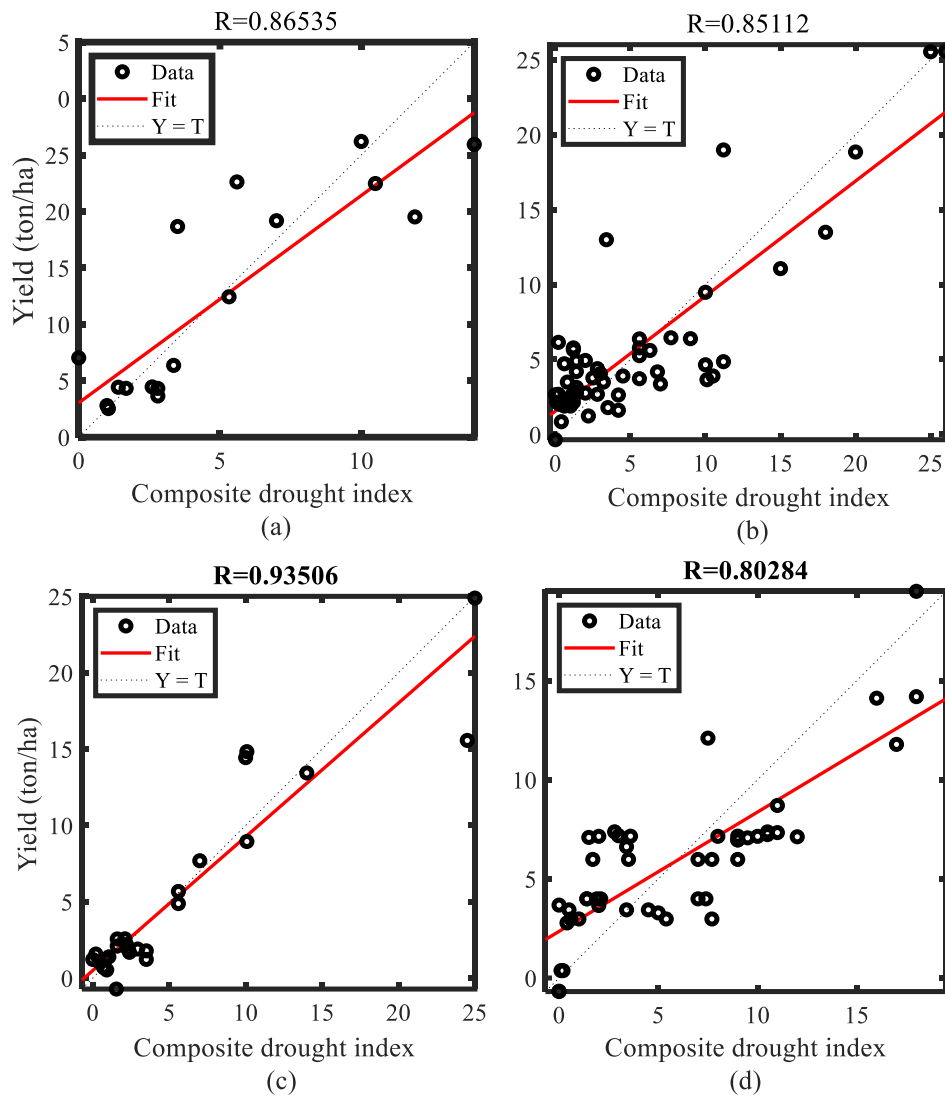


Figure 4.7 Scatterplots showing the BRNN results between the yield and CDI in 2016 (a and b) and 2018 (c and d).

4.3.3 Variation in Table Grape Yield

The yield variations or losses were calculated in each surveyed vineyard at the farm level using BRANNs for the drought-affected years of 2016 and 2018. The yield losses were calculated in vineyards affected by extreme to moderate drought (It means that only three drought categories were considered such as extreme, severe and moderate categories). According to the results, no vineyards were under extreme drought conditions; therefore, we only considered severe and moderate drought conditions categories for further analysis. Before, running the BRANNs model the affected vineyards were found by extracting each vineyard with CDI map. The result indicated that 17 and 26 vineyards were in severe drought categories out of 100 vineyards in 2016 and 2018, respectively. Though, 55 and 45 vineyards

were in moderate drought categories out of 100 vineyards in 2016 and 2018 respectively (**Table 4.4**). The BRAAN-generated results showed the spatial and temporal relationships between the yield and CDI in 2016 and 2018 ($R=0.87$ and $R=0.94$, respectively) under severe drought conditions and between the yield and CDI in 2016 and 2018 ($R= 0.85$ and $R=0.80$, respectively) under moderate drought conditions (**Table 4.4**). The results indicated that higher accuracies were obtained for severe drought areas in 2018 than in 2016. However, in moderately drought-affected areas, the accuracy in 2016 was greater than that in 2018 (**Figure 4.7**).

Table 4.4 Bayesian regularized neural network (BRANN) results, showing the severely and moderately drought-affected vineyards in 2016 and 2018.

Year	Number of vineyards	CDI Classes	BRNNs	Parameters	Hidden layers	
					MSE	R -Value
2016	17	0.1-0.2	Training	70%	5.1	0.86
			Testing	30%	0.74	0.97
			Overall	100%	4.2	0.87
	55	0.2-0.3	Training	70%	0.95	0.77
			Testing	30%	1.9	0.93
			Overall	100%	0.99	0.85
2018	26	0.1-0.2	Training	70%	3.1	0.94
			Testing	30%	2.3	0.96
			Overall	100%	5.5	0.94
	45	0.2-0.3	Training	70%	0.98	0.79
			Testing	30%	6.9	0.84
			Overall	100%	0.89	0.80

In Kabul Province, within the 2-year drought periods, there significant deficits were measured in the table grape yields the highest rate of loss 3.4 ton/ha and 4.9 ton/ha under severe drought conditions in 2016 and 2018, respectively (**Figure 4.8 and 4.9**). However, 2016 had the highest rate of loss of 4.1 ton/ha, and 2018 had a loss of 4.6 ton/ha in the moderate drought classes (**Appendix 4.2, 4.3, 4.4 and 4.5**). This result indicates that farmers learned from past drought conditions and used coping strategies such as high-efficiency irrigation systems.

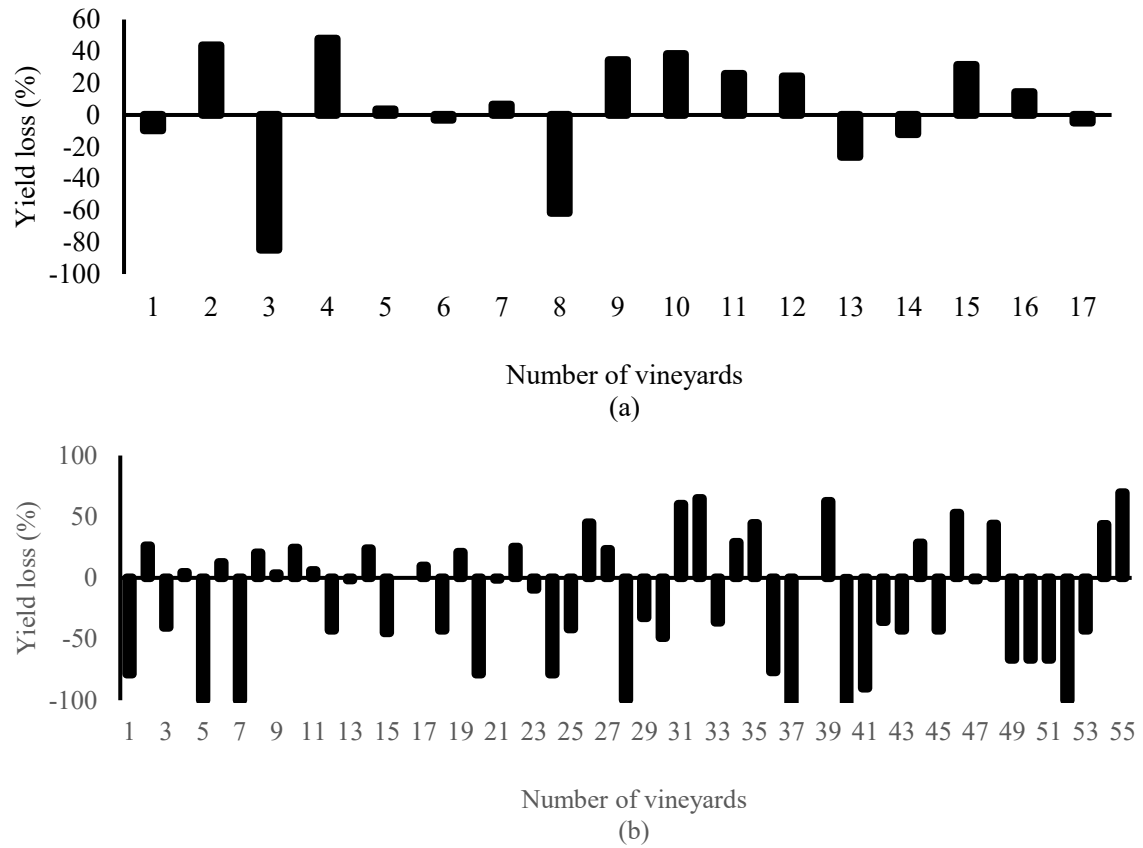


Figure 4.8 Percentage of yield losses: (a) the yield variations under severe drought conditions in 2016 and (b) the yield variations under moderate drought conditions in 2016

4.4 Discussion

Drought is one of the major problems in the world and significantly impacts agricultural products and farm returns. To support farmers during extreme drought periods, it is important to identify drought-affected fields and the extent of the yield losses. In this research, a drought-affected vineyard-based CDI was developed from the VCI, TCI, NDMI, DEV and PCI. The active growth stages of table grapes were considered because table grapes are perennial crops that need water throughout their different growth stages. Water shortages that occur due to drought decrease the yield and quality of table grapes (Permanhani et al., 2016). Furthermore, Landsat 8 OLI and TIRS and JAXA rainfall datasets were used to develop the composite drought index. The CDI results indicated that 2016 and 2018 were drought years; however, 2017, 2019 and 2020 were observed as wet and mildly wet years (**Figure 4.3**). The CDI values were validated using the SPI-1 values for each district of Kabul Province. The results indicated that the CDI was highly associated with the SPI. Therefore, when the SPI increased, the CDI also increased. Similarly, when the SPI decreased, the CDI also decreased, indicating the drought severity (**Figure 4.6**). Based on validations conducted in previous studies that combined drought

monitoring index values based on precipitation, temperature, evapotranspiration, and vegetation, the correlations between the vegetation drought synthesized index and SPI1, SPI3 and SPI6 ($r = 0.20, 0.26$ and 0.50) were found to be relatively higher than the correlations of the single indices (Han et al., 2019).

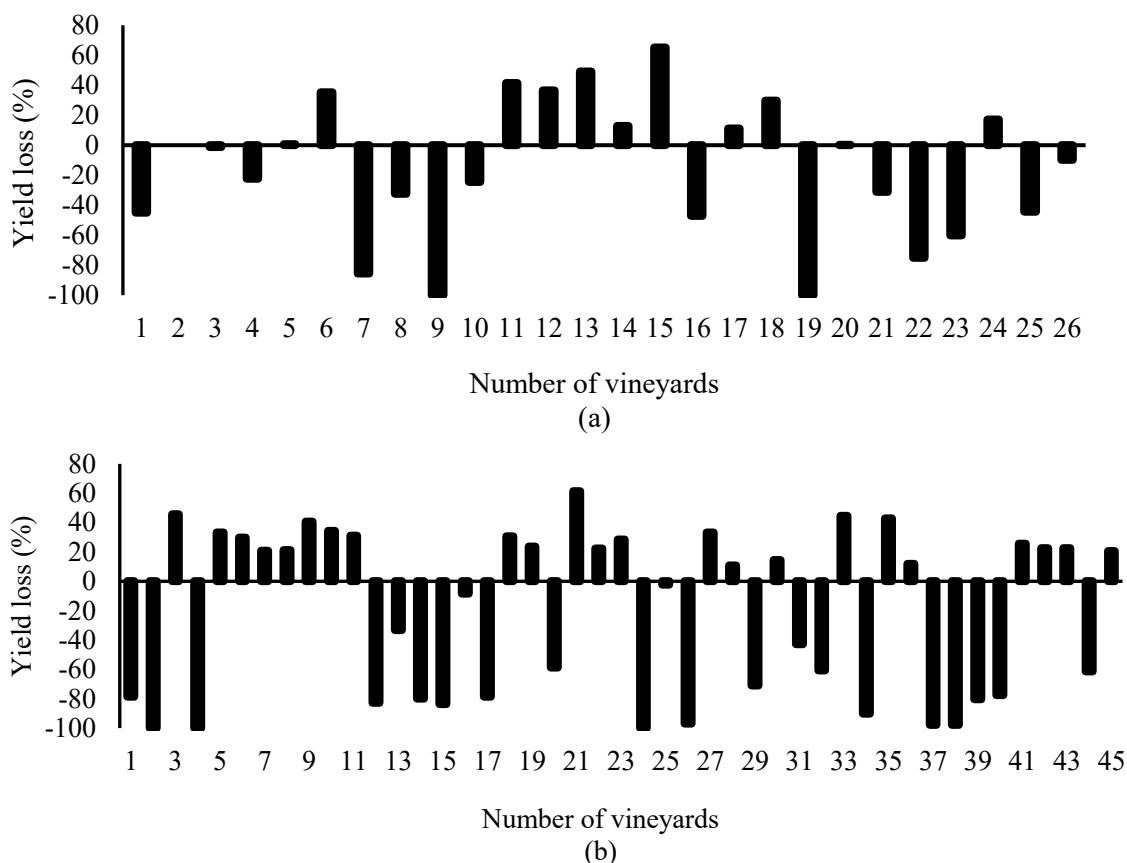


Figure 4.9 Bar charts showing the percentage of yield loss: (a) the yield variations under severe drought conditions in 2018 and (b) the yield variations under moderate drought conditions in 2018.

Good agreement between the combined drought indicator for Ethiopia (CDI-E) and Enhancing National Climate Services (ENACTSS) 3-month SPI values was obtained over most parts of Ethiopia with a correlation coefficient greater than 0.6 during the Kiremt season (Bayissa et al., 2019), and the validation of a new agricultural drought index (ADCI) (incorporating precipitation, the vegetation condition index, the temperature condition index and the evapotranspiration index) with the SPI showed a significantly strong correlation with an r^2 value of 0.60 (Badamassi et al., 2020).

In this study, after identifying drought-affected years, the CDI was classified into 5 drought categories. Based on these categories, affected pixel values were converted to areas (hectares), and then the

percentage of each affected area in each year was calculated. During 2018, almost 39% of the agricultural area was affected by drought (**Figure 4.4**). Furthermore, a nonlinear machine learning ANN model was used to estimate the yield losses in the 2016 and 2018 drought-affected years (**Figures 4.8 and 4.9**). The results showed that the simulated yields had good performances when compared with the observed yields, and the r^2 values were 0.87 and 0.94 in the severe drought class and 0.85 and 0.80 in the moderate drought class for 2016 and 2018, respectively (**Figure 4.7**). According to the results, some vineyard yields were significantly correlated with the simulated yields. The yield variation results indicated that the yield losses in Kabul Province varied from year to year, with the drought intensity and from one cultivar to another. The yield variations in each class in both years indicated that in drier atmospheric conditions, the risk of yield loss was higher. Some varieties of grapes were resistant to drought. However, in general, the water contents of fruit and the size of fruit decrease due to drought. Once the quality of the fruit decreases, farmers usually suffer from lower returns.

4.5 Conclusion

Satellite remote sensing information has the ability to be used to detect droughts and gather data during droughts. The CDI was created in this study to monitor agricultural dryness in Kabul Province's vineyards from 2016 to 2020. The agricultural drought in Afghanistan's Kabul Province was studied using five different input parameters, including the VCI, TCI, DEV of the NDVI from five years of data, the NDMI, and the PCI. Weighting each parameter was done using PCA, an adaptive data analysis approach. Models that are more resilient than ordinary back-propagation nets minimize cross-validation time for calculating grape yield loss. The BRANN is one of these robust models. In comparison to regression models, the Artificial Neural Network (ANN) model is more adaptable and can calculate, predict, and classify data with more precision (Ali et al., 2016). Using JAXA rainfall data and one meteorological station, the CDI was calculated. Short-term soil moisture and crop stress data were disclosed by SPI-1 measurements. Kabul Province had moderate to severe drought in 2016 and 2018, according to the CDI data. Finally, yield losses were computed for vineyards that had been afflicted by moderate and severe drought. The study discovered that the drought had severely harmed vineyards in 2018, with crop losses in 2018 being much higher than in 2016.

It is more useful to monitor droughts using satellite remote sensing rather than traditional approaches. Ground- or station-based meteorological and hydrological measurements, such as precipitation; air temperature; soil moisture; evapotranspiration; and surface runoff; are often used in conventional drought monitoring techniques. Computed drought maps may help producers, government agencies,

and non-profit organizations estimate the impact of lower agricultural outputs on table grape yields. Also, crop insurance companies may use this strategy to estimate the size of payments. Additionally, tracking the losses caused by droughts may help find effective strategies to adapt to changing weather patterns, such as growing drought-resistant vines and implementing water saving tactics.

Chapter 5

Drought Severity Analysis for Regional Vineyard Production Management Using Landsat OLI and CHIRPS Datasets

5.1 Background of the Research

Drought is a complex environmental phenomenon that appears within a territory due to the absence of rainfall, which causes water scarcity in a region or in a continent (Heim, 2002). Droughts could be investigated from different angles: (a) climatic, (b) agrarian, (c) hydrological, and (d) socioeconomic. Meteorological drought reduces precipitation, agricultural drought reduces soil moisture, hydrological drought increases runoff and reduces water storage, and socioeconomic dry spell reduces water resource and increase need in a region. All types of droughts have an impact on the environment, agriculture, and society (Wilhite and Glantz, 1985; Wilhite, 2000; Dai, 2011; Zhang et al., 2022). The impact of drought on the agriculture sector is nearly 82% greater than that on other sectors, at only 18%. Drought causes more than 34% of crop and animal production losses in the underdeveloped countries as well as nations with low and moderate incomes (FAO, 2021). Asia is the most vulnerable region, with a drought loss of approximately four billion USD, followed by Africa at three billion USD and Latin America and the Caribbean at two billion USD. Therefore, agricultural drought assessment indicates an increase in drought occurrence from spring to summer, which is the typical time for agricultural and vineyard growth. (Meng et al., 2017; Spinoni et al., 2018; Arab et al., 2021).

dryness assessments in vineyards are essential because grapevines are one of the most sensitive fruits in the world and are susceptible to water stress. During the summer, when high evapotranspiration is combined with extremely low precipitation, grapevines suffer severe growing issues. Different methods have been utilized for dry spell evaluation and monitoring all over the planet, including (1) in situ measurements and (2) remote sensing-based observations. Agriculture drought monitoring in the field is the most appropriate and ancient style (Maes and Steppe, 2012; Ford and Quiring, 2019). They are dependent on field observations during drought periods in order to have information regarding hydro-climatic, agronomic and plant requirements during climate fluctuations (Kanellou et al., 2008). Most drought assessments require precipitation information; however, many parts of the world have insufficient rain-gauge networks (Anderson et al., 2011). In this circumstance, remote sensing sensors spatial and temporal scenes (Landsat 8, 30 m resolution, 15-day interval; MODIS 250 m, 16-day interval; and Sentinel 2 m resolution, 10-day interval; JAXA and CHIRPS rainfall) have the potential to capture the spectral signature of the soil surface and canopy information for drought assessment, particularly in the red, near-infrared, shortwave infrared, and temperature spectral bands. Since 1999,

the United States Geological Survey (USGS) and the Climate Hazard Center (CHC) have been developing CHIRS datasets at the University of California to produce long-term rainfall maps all around the world, particularly in areas where ground data are scarce. CHIRS has a long-term precipitation record from 1981 to the present day (Funk et al. 2015). The usage of remote sensing images and CHIRPS rainfall in agronomic dryness assessment is based on the notion that drought can influence soil and vegetation biophysical and chemical parameters of soil, soil moisture, organic matter, vegetation biomass, chlorophyll, canopy and soil temperature (Anjum et al., 2011; Shahzaman et al., 2021; Arab et al., 2022). Dry spell can induce a decrease in plant growth that can be seen by satellite. Globally, the assessment of drought impacts on vegetation and agricultural fields is a challenging and difficult task. However, satellite-based drought indices overcome some of these limitations, especially in large areas.

The utilization of sensor-oriented plant growth indicators for drought analysis on a broad scale began in the 1980s (Tucker et al., 1986). Since then, various indices, including the normalized difference vegetation index (NDVI) (indices derived from NDVI such as standard vegetation index (SVI) and vegetation condition index (VCI)), normalized difference moisture index (NDMI), normalized difference water index (NDWI), standard precipitation index (SPI), temperature condition index (TCI), vegetation health index (VHI), and others, have been employed to measure drought on regional and global scales for wheat, maize, paddy, soybean, tea, and other crops (Aulia et al., 2016; Agutu et al., 2017; Wang et al., 2019, Das et al., 2020; Arab et al., 2022). The SVI has occurred for drought assessment since 2002 (Petars et al., 2002) and is an excellent predictor of vegetation response in the short term. Moreover, the SPI is the most common precipitation deficit index used in describing drought conditions. From 1993, the SPI has been applied for mapping and monitoring of dry spell (Mckee et al., 1993) and indicates precipitation deficiency at a specific site over several periods of time. SPI can be calculated for the long- and short term. In the short term, it is used for soil moisture monitoring and is crucial for agricultural production for drought detection on a large scale. In this case, many researchers have investigated the relationship between drought indices and the yield of agricultural crops. For instance, regression between yield and 12-month SPI is described as 0.64 of the sigmoid connection output fluctuation (Yamoah et al., 2000). Drought had a 0.71 influence on winter wheat throughout the main growing season (Zhang et al., 2016). These indices are essential for drought monitoring on small and regional scales, especially in regions where ground-referenced data are limited.

There are very few studies that use the SVI and SPI for drought assessment on a small scale. Therefore, increased efforts toward large-scale drought assessment are required to aid in better understanding

climatic variability and the evolution of droughts, particularly in regions (especially those in underdeveloped countries) with unique vulnerabilities and complicated geographies. In this regard, there is no similar study for vineyards' regional-scale drought assessment.

Vineyard drought assessment and monitoring on a regional scale is challenging due to the large-scale satellite datasets and vineyard variability during the growing season. In this regard, several cloud computing sources are available for spatial big data processing. Amazon Web Service debuted in 2006 as a fee-based cloud computing platform that allows customers to create their own virtual data center (Tamiminia et al., 2020). In 2008, the Google Cloud platform began as a public cloud-computing platform with a multidata base of satellite images and a geographical data analysis interface for data storage, data analysis, machine learning, and mapping systems. (Gorelick et al., 2017, Krishnan and Gonzalez, 2015).

Drought assessment using modern technology and techniques can support policy-makers and regional governments in assessing grape growers whose livelihood depends on grape production. Therefore, the main focus of this assessment was to determine the severity of drought in vineyards using the SPI and SVI indices within the fruit set and berry formation stages using satellite remote sensing and CHIRPS rainfall datasets.

5.2 Materials and Methods

5.2.1 Area of Research

The research was carried out in Afghanistan, which is located between latitudes 29°35' and 38°40' and longitudes 60°31' and 74°55' and is known as the Asia Crossroads. Afghanistan's total area is 652,864 km² with a total population of 40.2 million (United Nations Children's Fund, 2019). The country consists of 34 provinces. The country's highest peak rises to 7,492 m above sea level, with arid lowland and rich and fertile valleys. Lowlands (300-500 m), which include rivers, valleys, and desert regions, may be found in the country's northern, western, southwestern, and southeastern parts, while highlands (200–7500 m) can be found in the country's center. Of all the large areas in Afghanistan, only 11.7% is arable land, which includes irrigated (3,600,210 ha) and nonirrigated agricultural land (3,734,494 ha), fruit trees (117,642 ha), vineyards (82,450 ha), and forest and shrubs (1,781,045 ha). The country's forest and shrubs cover 2.8% of the land, while the remaining 85% is soil, sand, and rocky areas (FAO, 2016) (**Figure 5.1**).

The climate in Afghanistan differs around the country. Yearly temperatures in the highlands (mountainous regions) are below zero, while temperatures in the lowland and plain areas are well over 35 °C. Precipitation in the highlands exceeds 1000 mm; in the lowlands, it is less than 150 mm. As a result of reduced precipitation, droughts erupted across the country. Afghanistan suffered severe drought from 1998–2006, 2008–2009, 2018, and 2021, had major implications for food security (World Bank, 2018; FAO and MAIL, 2019). Based on community need assessment, drought-related shortages of water for agriculture were the most significant impediment to food production across the country in 2021 (IOM, 2021). In this case, drought and other natural calamities have a major influence on regular livelihoods and agricultural output (FAO and MAIL, 2019).

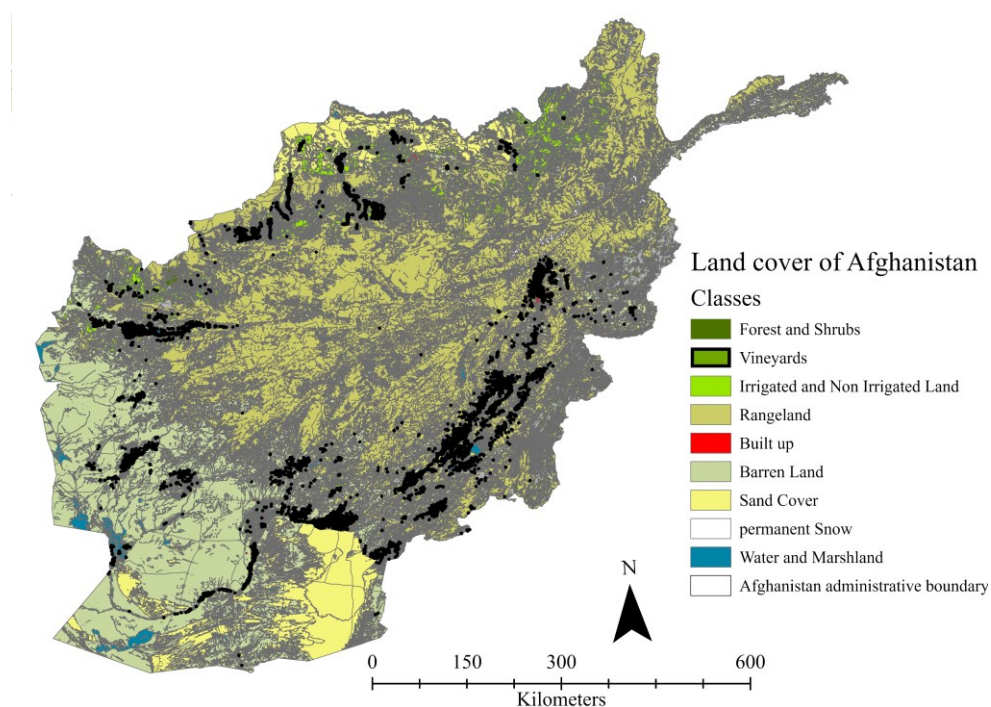


Figure 5.1 Afghanistan land cover map

5.2.2 Datasets

In this study, secondary and primary datasets were used. Time-series primary datasets were downloaded from the USGS and Google Earth Engine, and time-series secondary datasets were used from statistical yearly books of the Islamic Republic of Afghanistan (**Figure 5.2**). Each of the datasets is explained as follows:

5.2.2.1 Standard Vegetation Index (SVI) for Drought Monitoring

To calculate the standard vegetation index for drought monitoring, the Landsat 8 (Collection 1 T1RE 1 eight-day composite) composite NDVI scenes were processed from Google Earth Engine from 2013-2021. ArcGIS 10.8 and ArcGIS Pro 2.7® were used for further analysis. The SVI showed the likelihood of deviation from the typical NDVI over time (Peters et al. 2002). The following equation refers to the SVI calculation:

$$Z_{ijk} = \frac{VI_{ijk} - \mu_{ij}}{\sigma_{ij}} \quad (5.1)$$

where Z_{ijk} is the z number for each unit of pixel i during month j for year k , VI is the NDVI unit of pixel i in month j for year k , and σ_{ij} is the standard deviation of pixel i in month j for n years.

Table 5.1 The standardized vegetation index (SVI) is used to classify drought

Classes	Range of Values
Extremely dry	≥ -2
Severely dry	-2 to -1.5
Moderately dry	-1.5 to -1
Normal	-1 to 0
Moderately wet	0 to 1
Very wet	1 to 1.5
Extremely wet	≥ 2

5.2.2.2 Standard Precipitation Index (SPI)

The standard precipitation index is a basic indicator of dryness measurement. It shows cumulative precipitation for a certain time compared to the long-term average perception that period developed by (McKee et al., 1993). This indicator was determined from CHIRPS rainfall in the Google Earth Engine platform. The SPI can be expressed as follows:

$$SPI_{ijk} = \frac{P_{ijk} - \bar{P}_{ij}}{\sigma_{ij}} \quad (5.2)$$

where SPI_{ijk} is the z unit for pixel i during timeframe j for year k , P_{ijk} is the rainfall unit for pixel i through interval j for year k , \bar{P}_{ij} is the mean for pixel i through interval j over n years, and σ_{ij} is the standard deviation of pixel i for the period of j over n years.

5.2.2.3 Land Cover Map

The map was generated by FAO based on the globally accepted Land Cover Classification System (LCCS) and modern image analysis techniques implemented in the Mapping Device-Change Analysis System Tool software suite (MADCAT) in 2016. The land cover map consisted of 25 initial classes of land cover, which were combined into 11 self-explanatory and generic classes. In this study, the land cover map of Afghanistan was classified into 8 classes based on the study purpose (**Figure 5.1**).

5.2.2.4 Statistical Data

The statistical datasets regarding grape production and cultivation area were collected from the National Statistical Book of the Islamic Republic of Afghanistan. (**Figure 5.3**) (Afghanistan Central Statistics Organization, 2013-2020).

Table 5.2 Standard precipitation index (SPI) categories and values based on McKee for drought monitoring

Drought Category	SPI values	Probability %
Extreme drought	$\leq - 2.00$	2.3
Severe drought	-1.50- to -1.99	4.4
Moderate drought	-1.00 to -1.49	9.2
Mild drought	0- to -0.99	34.1
Near normal	1 to 0.99	34.1
Moderately wet	1.0 to 1.49	9.2
Very wet	1.5 to 1.99	4.4
Extremely wet	2 and above	2.3

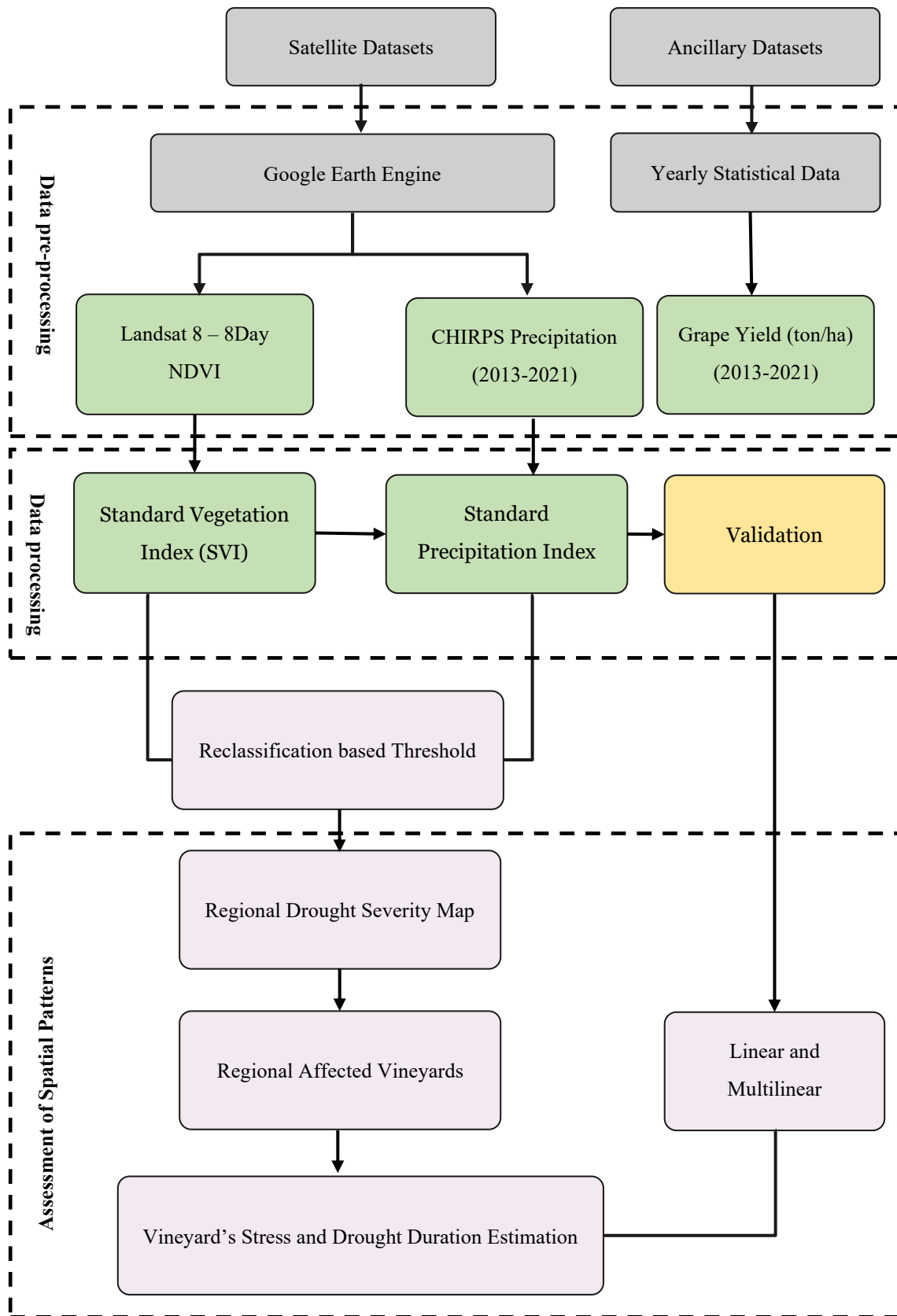


Figure 5.2 A comprehensive flowchart of the regional vineyard drought detection method

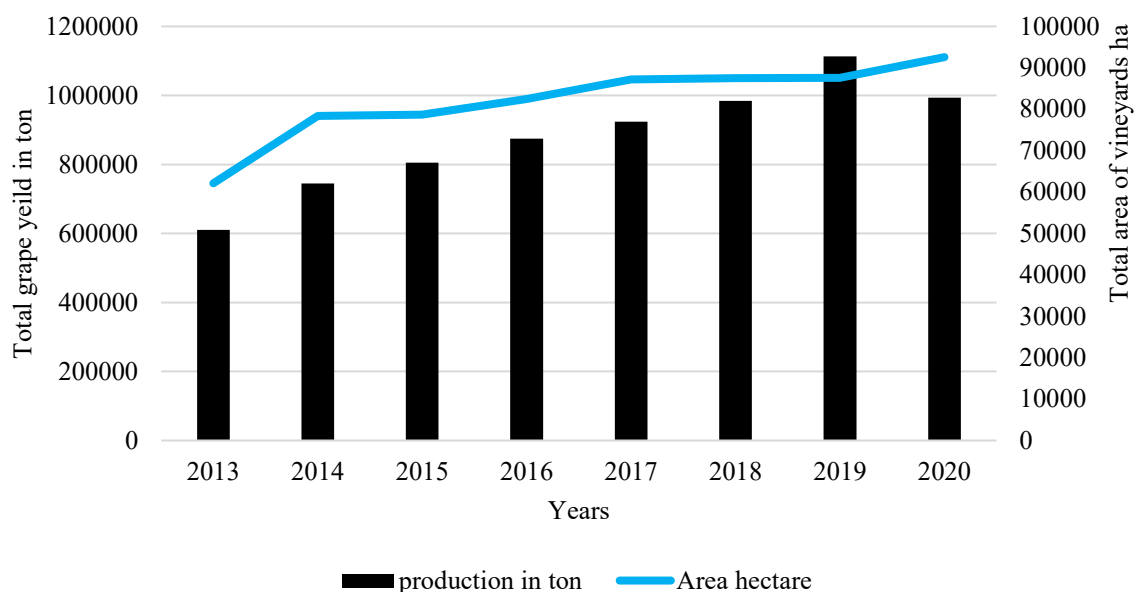


Figure 5.3 Bar chart showing grape production and line chart showing the area under cultivation from 2013 to 2020 in Afghanistan

5.2.3 Methods

5.2.3.1 Vineyard Drought Assessment using the time-series SVI and SPI

The vegetation index and climatic variables (SPI and NDVI) were calculated on the Google Earth Engine from 2013–2021. After downloading the Landsat 8 OLI, the 8-day composite NDVI in the berry formation and veraison stages was evaluated. The three months standardized vegetation index was calculated for 2013 to 2021 in ArcGIS. Maps were classified into seven classes based on the threshold referred to by Peters et al. (2002) (extremely dry, severely dry, moderately dry, normal, moderately wet, very wet, and extremely wet). The standard precipitation index (SPI) was calculated from CHIRPS rainfall in the Google Earth Engine from 2013–2021. After downloading the SPI data, the maps were classified in the ArcGIS environment using the Mackee classification (extreme drought, severe drought, moderate drought, near normal, moderately wet, very wet, and extremely wet). Finally, the vineyard shapefiles were masked with the SPI and SVI to identify the drought-affected vineyards. Since the 2016 land use land cover was available, we used that for all years from 2013 to 2021.

5.2.3.2 Drought Verification with Time-series Grape Yield

Two independent variables were used for drought validation. In this regard, SVI and SPI were considered dependent variables, and grape yield was used as an independent variable to validate the drought periods before harvest (June, July, and August). The independent variables (pixelwise zonal average) were calculated on the ArcGIS platform. The dependent variable, grape yield tons per hectare,

was taken from the statistical book of the Islamic Republic of Afghanistan from 2013 to 2020. Due to internal political instability, the statistical department was not able to release the 2021 statistical book. Therefore, in this research, we used yield datasets from 2013 to 2020. After that, the zonal average drought indices were determined all over Afghanistan from 2013 to 2020. Linear and multilinear regression analyses were performed on a regional scale for validation.

5.3 Results

5.3.1 Drought severity assessment with the time-series SVI

In this research, the SVI values were calculated for all of Afghanistan using NDVI downloaded from the Google Earth Engine Platform. The periods were considered to be the berry formation and veraison stages before the harvest of table grapes from 2013 to 2021. To identify the drought-affected pixels, the SVI map was classified based on drought classes recommended by Peters et al. 2002 (Table 5.1). The results of utilizing the SVI to determine the years when droughts occurred are specified in Figure 4. The results suggested that extreme dryness occurred in 2013 (June and July), 2014 (July and August), 2015 (June and July), 2016 (July), 2018 (Jun, July and August) and 2021 (June, July and August). The intensity of drought was very high in 2018 and 2021, which mostly affected all provinces in Afghanistan. Droughts during 2018 and 2021 had become a very serious societal impact during these times because of the severe water scarcity crisis for irrigation and daily water consumption (Figure 5.4 and Figure 5.5).

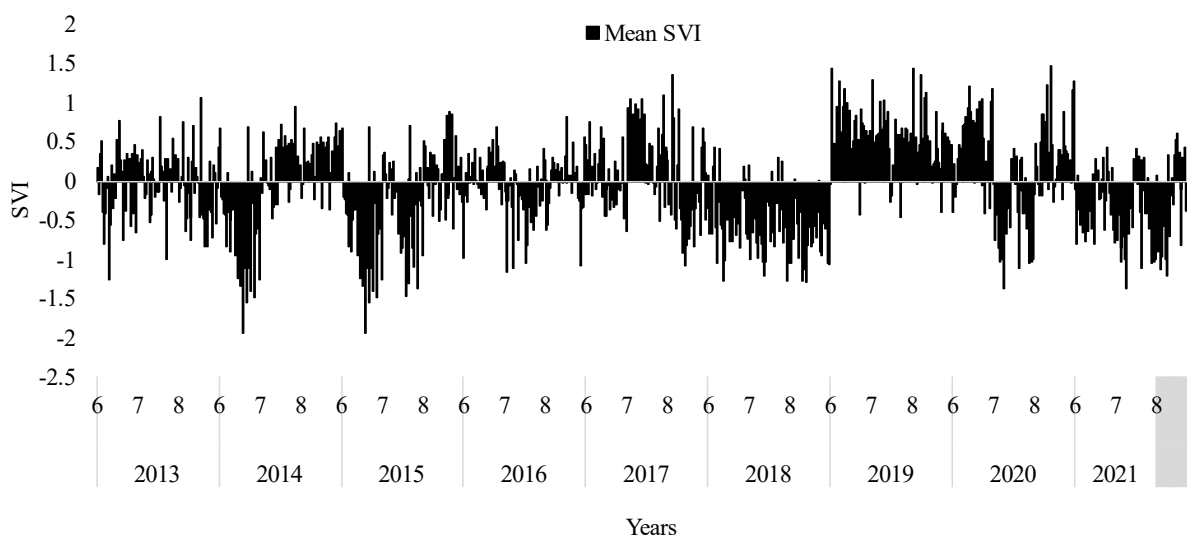
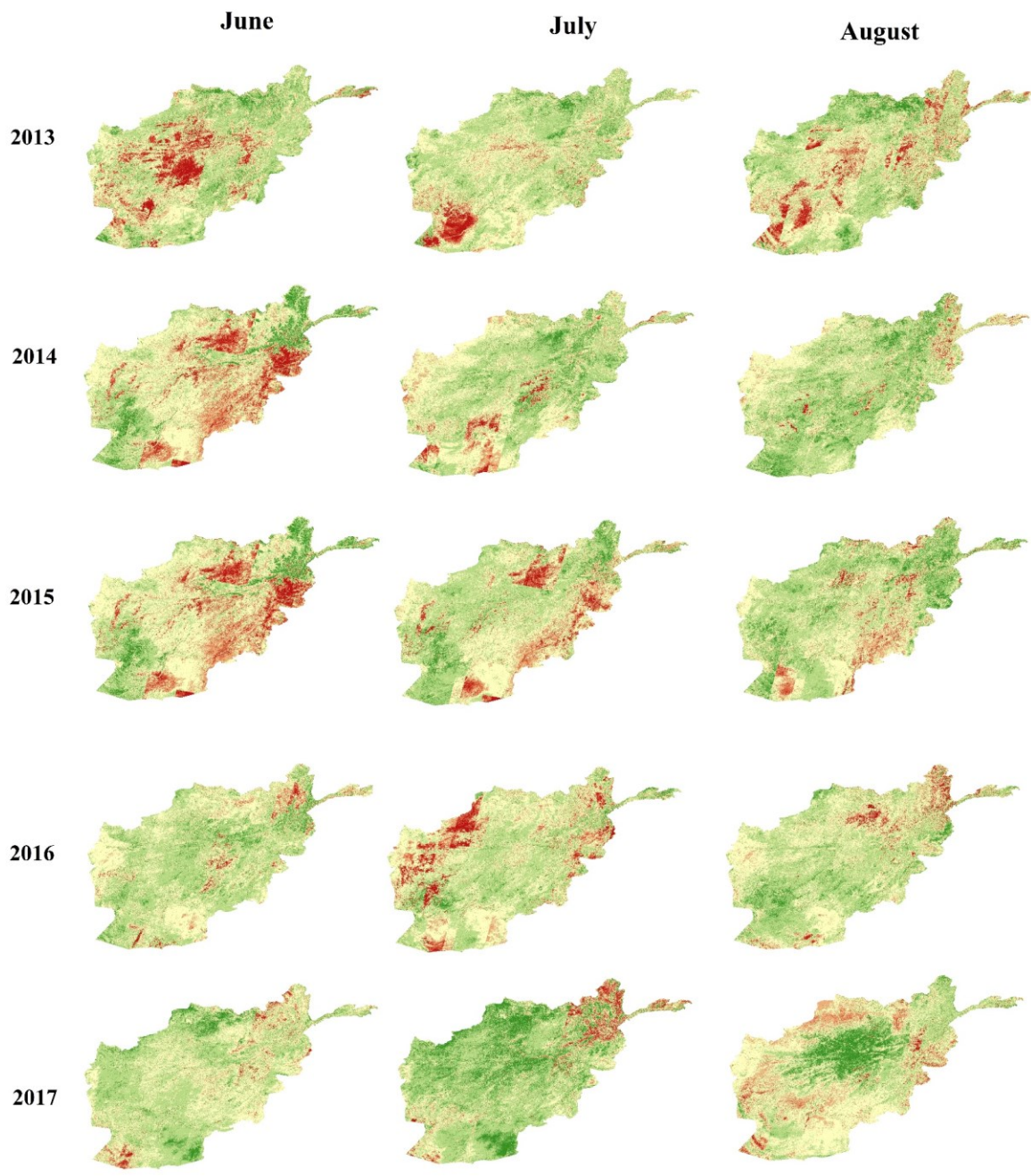
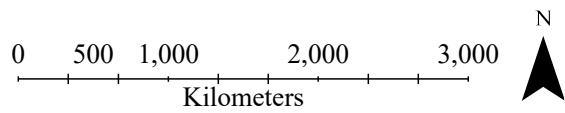


Figure 5.4 The zonal mean SVI value in the berry formation and veraison stages before harvest (June, July, and August) in Afghanistan was calculated from 2013 to 2021



■ Extramely dry
 ■ Moderately dry
 ■ Moderately wet
 ■ Extremely wet
■ Severely dry
 ■ Normal
 ■ Very wet



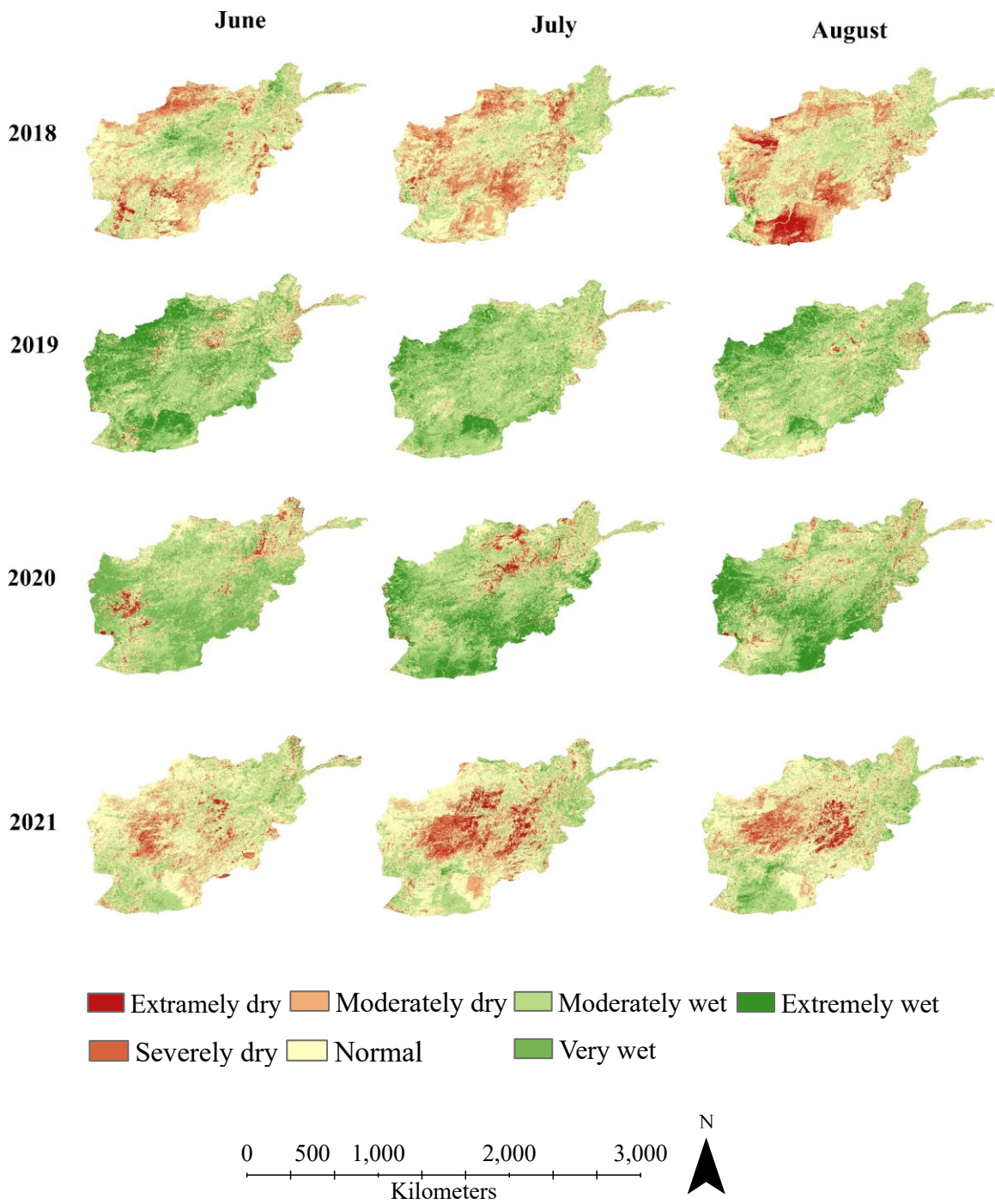


Figure 5.5 Drought classification based on SVI in the berry formation and veraison stages before harvest (June, July, and August) in Afghanistan from 2013 to 2021

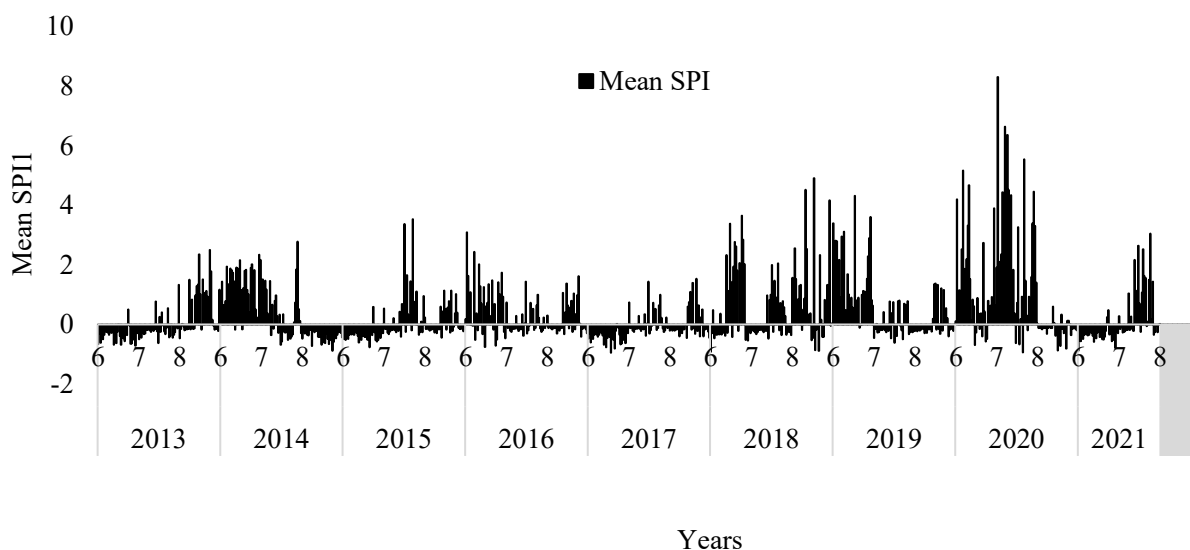


Figure 5.6 Zonal mean SPI values in the berry formation and veraison stages before harvest (June, July and August) from 2013 to 2021 in Afghanistan

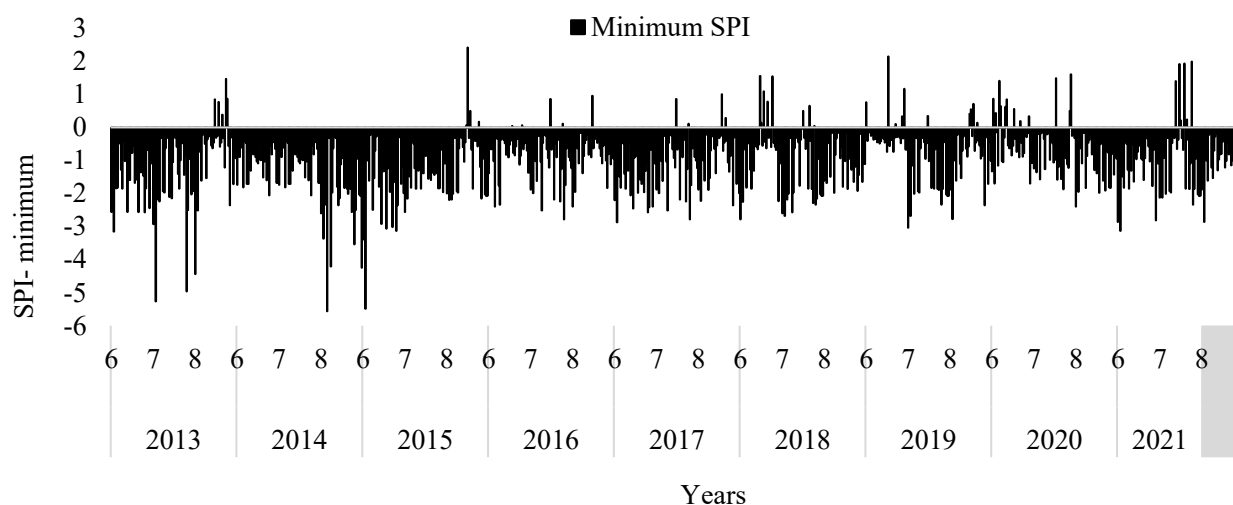


Figure 5.7 Minimum SPI value in the berry formation and veraison stages before harvest (June, July and August) from 2013 to 2021 in Afghanistan

5.3.2 Drought Severity Assessment with Time-series SPI-1

SPI-1 was calculated from CHIRPS precipitation in the Google Earth Engine Interface. After that, datasets were downloaded and classified based on the Mackee drought classification scheme (**Table 5.2**). SPI-1 was used to examine the dry and wet situations in the research region during 2013–2021 June, July and August before grape harvest. The three-month minimum value of SPI-1 indicated that

almost all 9 years were very dry because Afghanistan has a very arid climate. For normalization in this context, we used the SPI-1 average for all nine years. It was found that in 2013 (June, July and August), 2014 (August), 2015 (June and July), 2016 (August), 2017 (June), 2018 (June, July and August), 2019 (August) and 2021 (June, July and partly August), Afghanistan experienced an extreme dry spell (**Figures 5.6, 5.7 and 5.8**).

5.3.3 Drought Affected Vineyards in Afghanistan

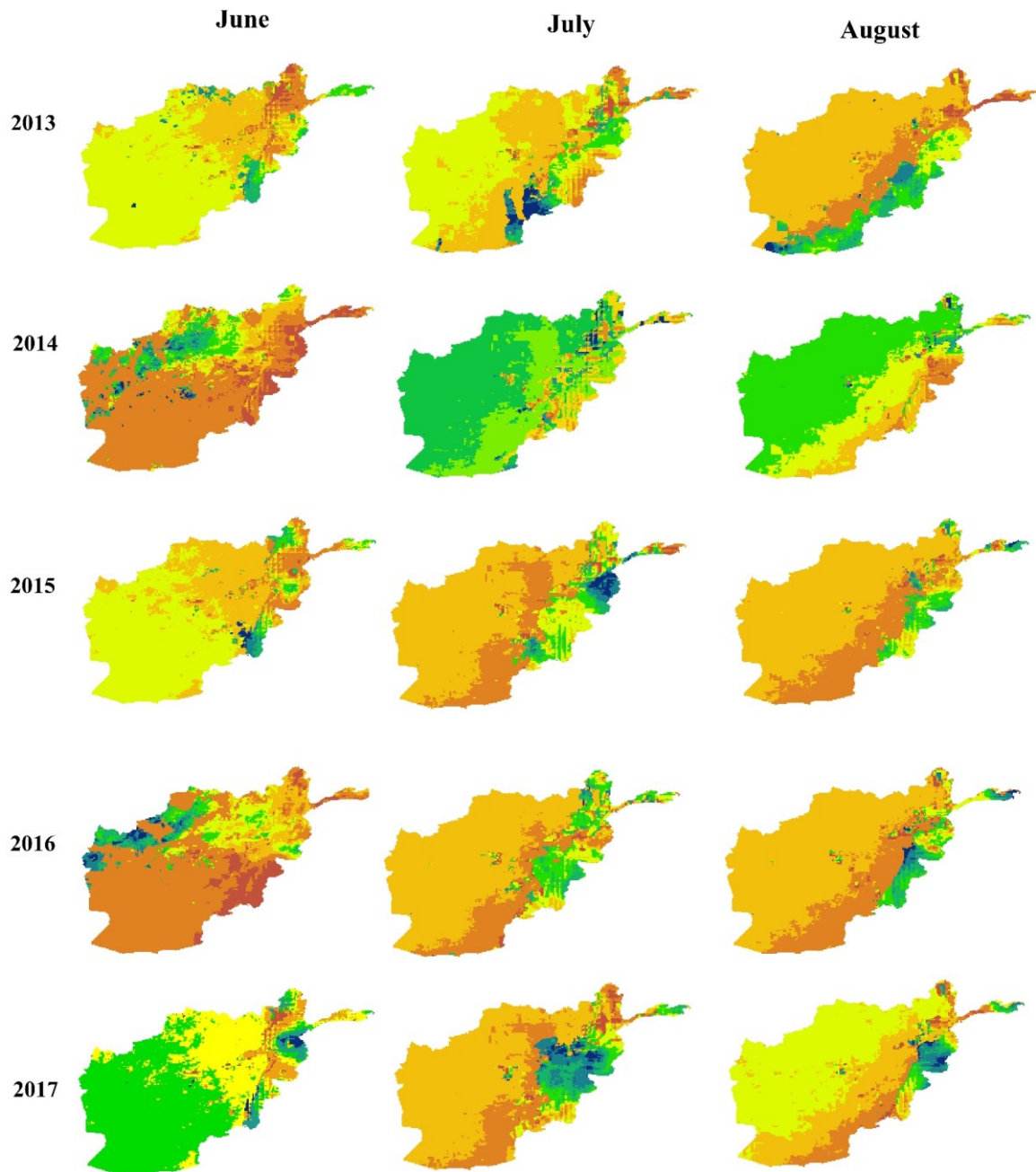
Dry spell conditions were evaluated in Afghanistan vineyards from 2013 to 2021. To quantify the drought occurrence, the drought maps of the SVI and SPI were numerically evaluated. It is used to calculate the proportion of drought occurrences within each three-month period over the past nine years and to identify the years and periods that were severely affected. In this regard, the total affected pixels in each drought class (SVI and SPI) were used to identify the drought-affected pixels. Finally, the percentage of each class was calculated. The results showed that the appearance of drought varied depending on the year and month. Among all the drought-stricken years, it was indicated that the 2021 drought was 52.5% in June and 42.6% in August, affecting the entirety of the country based on SPI. However, in 2018, 22.8% in June and 33.3% in August were affected based on the SPI. The affected area based on the SVI revealed 36.5% in June and 40.3% in August. Nevertheless, in 2021, the prevalence was 30.4% in July and 24.4% in August (**Figure 5.9, Tables 5.3 and 5.4**).

To identify the drought-affected vineyards, the vineyard shapefiles from all over Afghanistan were masked with drought maps. The results demonstrated that 2018 and 2021 were the most drought-affected years. In 2018, extremely drought-affected vineyards accounted for 4785.03 hectares; severely affected vineyards accounted for 13240.26 hectares; and moderately affected vineyards accounted for 22732.02 hectares in June, July, and August. In 2021, 1825.83 hectares were extremely affected, 7448.13 hectares were severely affected, and 15456.78 hectares were moderately disturbed by dryness in June, July, and August, respectively (**Figure 5.10**).

5.3.4 Verification of Drought Maps with Grape Yield

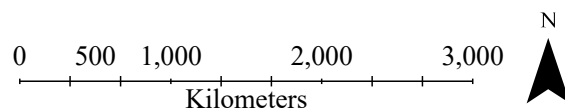
To validate the accuracy of the drought indices (SVI and SPI), regression was observed with grape yield. Afghanistan's yearly statistical book provides the total yield and area under cultivation from 2013-2020. The regression results indicated that the model had higher accuracy in June and July than in August. The coefficient of determination between table grape average yield and average SVI was $r^2 = 0.42$, $r^2 = 0.62$ and $r^2 = 0.03$ for June, July, and August, respectively. However, the coefficient of determination

between table grape yield and SPI was $r^2=0.60$, $r^2= 0.54$ and $r^2=0.02$ for June, July, and August, respectively.



Extreme drought
 Moderate drought
 Near normal
 Very wet

Severe drought
 Mild drought
 Moderately wet
 Extremely wet



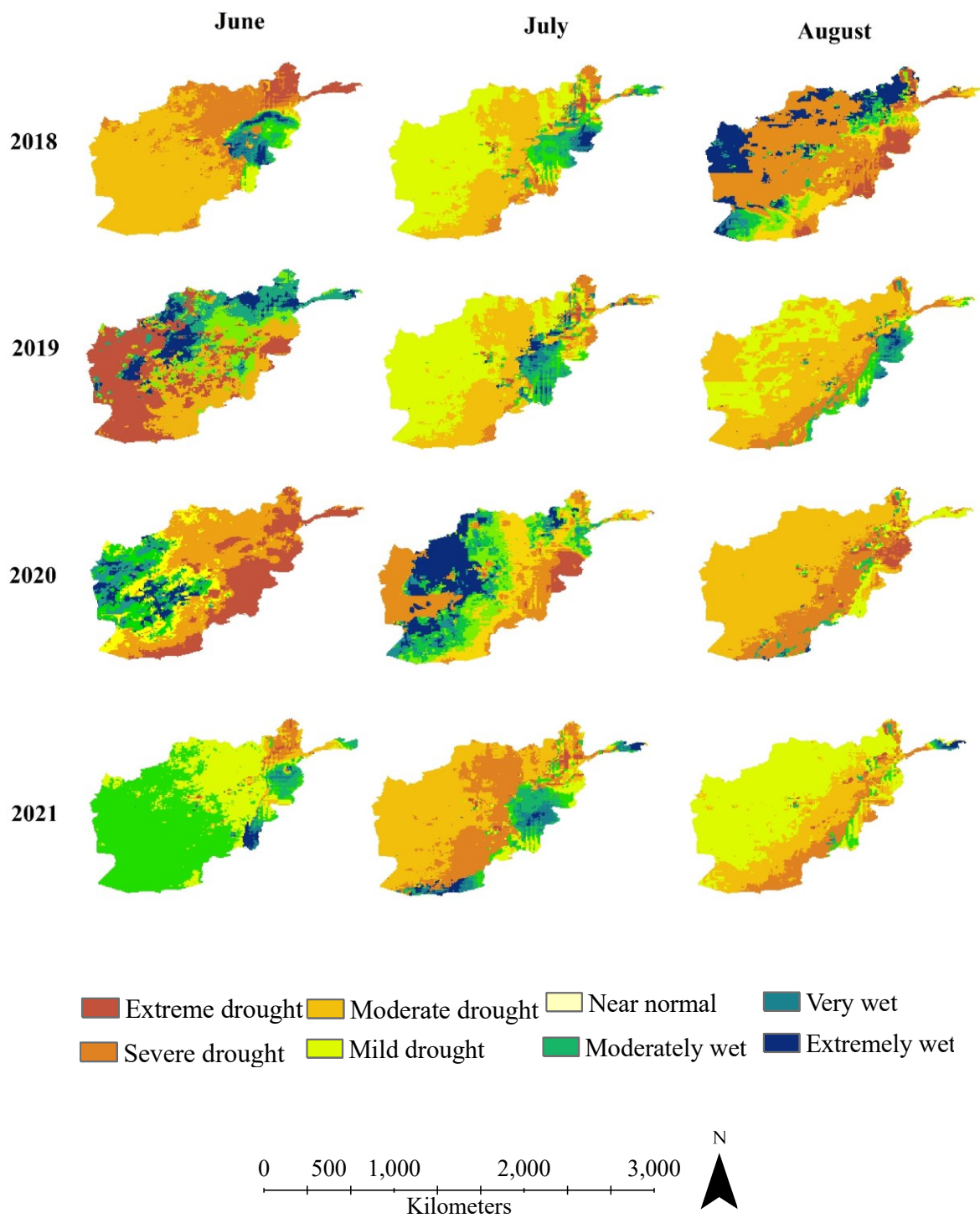


Figure 5.8 Drought classification based on SPI in the berry formation and veraison stages before harvest (June, July, and August) in Afghanistan from 2013 to 2021

Table 5.3 The percentage of drought-affected regions based on the SVI in Afghanistan from 2013 to 2021

Year	Month	Drought Level							Total
		Extremely Dry	Severely Dry	Moderately Dry	Normal	Moderately wet	Very Wet	Extremely Wet	
2013	Jun	6.0	6.5	9.1	31.0	35.7	8.0	3.7	100
	July	2.6	3.4	6.8	37.4	40.3	6.6	2.9	100
	August	3.9	6.1	10.0	34.1	34.3	7.3	4.3	100
2014	Jun	4.7	8.9	14.6	39.9	21.3	5.5	5.0	100
	July	1.5	2.7	7.6	37.3	38.8	8.5	3.6	100
	August	1.0	1.6	4.2	31.1	43.6	12.6	5.8	100
2015	Jun	4.7	8.9	14.6	39.9	21.3	5.5	5.0	100
	July	3.1	5.5	10.3	35.2	34.9	7.6	3.4	100
	August	1.7	3.6	7.7	32.1	39.3	10.1	5.5	100
2016	Jun	1.0	2.1	5.3	36.7	43.8	8.1	2.9	100
	July	4.2	5.7	9.9	38.6	34.1	5.2	2.2	100
	August	1.9	2.7	6.1	37.4	40.8	7.9	3.1	100
2017	Jun	0.8	1.9	5.0	35.2	46.1	7.6	3.4	100
	July	2.3	2.9	4.1	18.5	42.1	17.4	12.7	100
	August	1.0	3.7	13.5	42.5	24.8	6.6	7.9	100
2018	Jun	2.0	7.3	19.0	41.9	23.9	3.9	2.0	100
	July	1.8	10.2	24.5	42.4	18.0	2.3	0.8	100
	August	5.5	11.3	23.5	38.7	18.2	1.8	1.0	100
2019	Jun	0.8	1.6	3.6	15.6	35.9	22.0	20.5	100
	July	0.2	0.7	2.3	15.9	49.2	20.6	11.1	100
	August	0.6	1.2	3.1	21.4	43.7	17.0	13.1	100
2020	Jun	1.9	2.7	5.3	19.8	36.4	33.5	0.5	100
	July	2.1	2.7	4.1	17.4	36.7	19.9	17.0	100
	August	1.3	2.5	5.3	21.5	34.4	15.8	19.2	100
2021	Jun	1.7	5.9	15.3	46.3	25.5	3.7	1.6	100
	July	5.6	9.2	15.5	42.6	21.6	3.6	1.7	100
	August	3.8	7.3	13.3	42.3	25.0	5.6	2.6	100

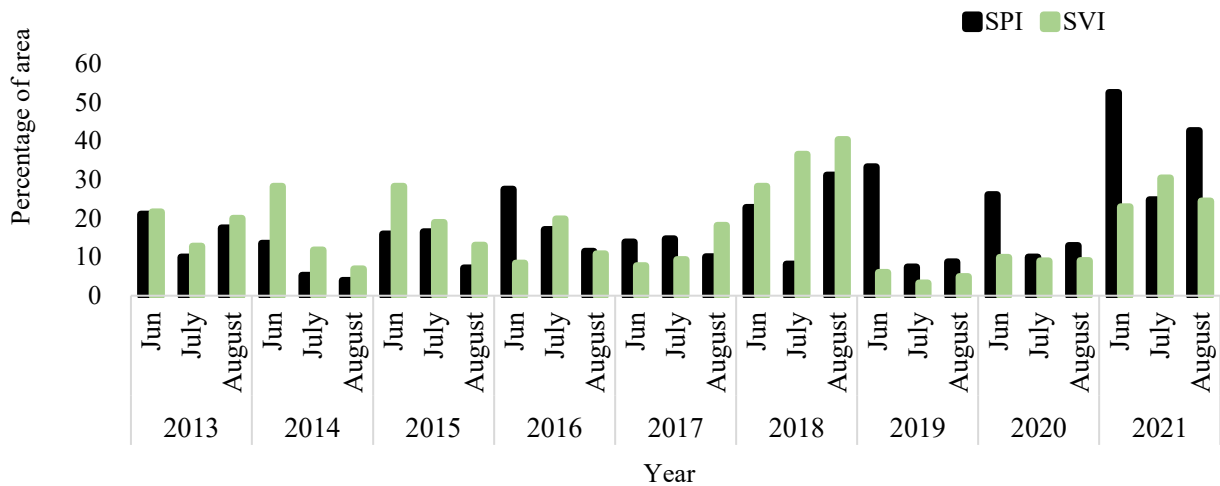


Figure 5.9 SPI and SVI- based proportion of drought-strick areas classes (extreme, severe and modern drought) in Afghanistan from 2013 to 2021

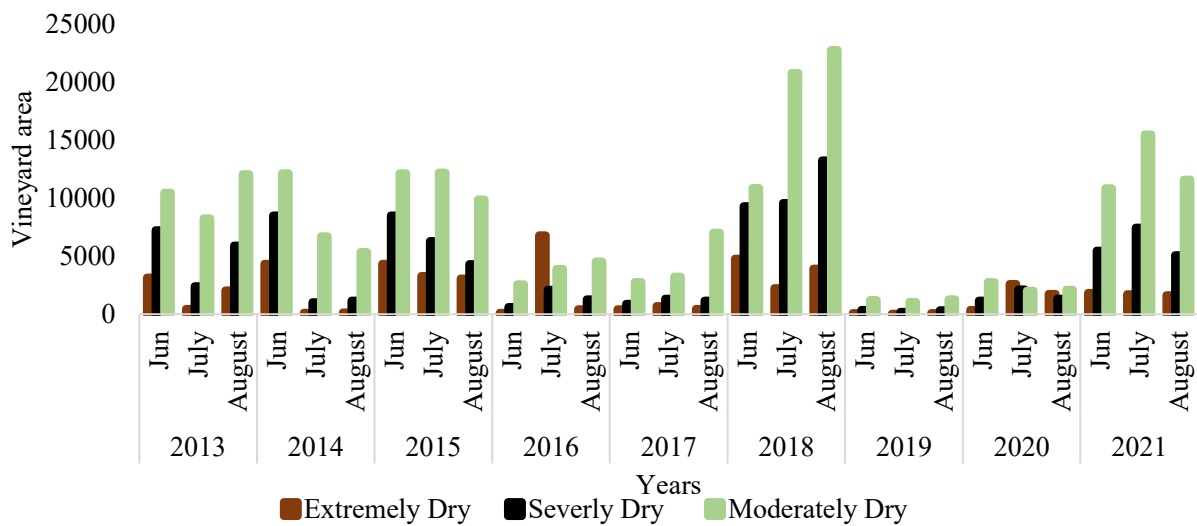


Figure 5.10 Total drought-affected vineyards in three classes (extreme, severe and modern drought) in Afghanistan from 2013 to 2021

The significance test indicated a p value less than 0.05 for June and July. However, the multilinear results indicated higher accuracies of $r^2=0.79$, $r^2=0.71$ and $r^2=0.05$ for June, July and August, respectively (Figure 5.11 and Table 5.5).

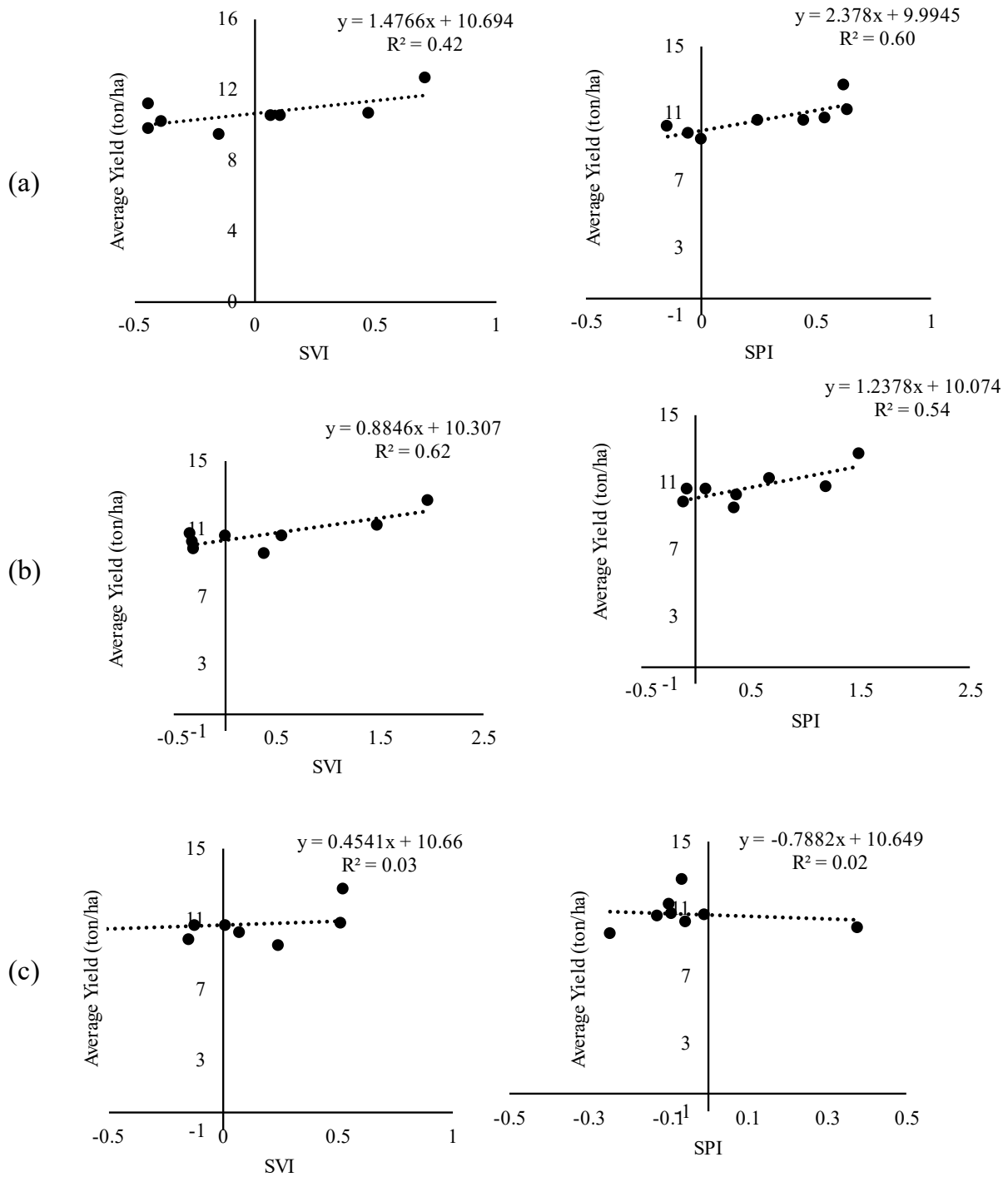


Figure 5.11 The scatter plot shows the regression between grape yield and drought indices (SVI and SPI). (a) June, (b) July and (c) August

Table 5.4 The percentage of drought-affected regions based on the SPI in Afghanistan from 2013 to 2021

Year	Month	Drought Level								Total
		Extreme drought	Severe drought	Moderate drought	Mild drought	Near normal	Moderately wet	Very wet	Extremely wet	
2013	Jun	1.96	5.57	13.49	15.46	57.33	2.96	2.98	0.24	100
	July	1.14	3.05	5.73	3.86	59.84	17.62	4.86	3.91	100
	August	0.64	2.51	14.31	8.88	52.63	8.11	10.69	2.24	100
2014	Jun	3.47	1.62	8.40	10.91	53.91	8.18	7.22	4.63	100
	July	0.14	1.49	3.56	6.25	11.98	25.37	35.36	15.85	100
	August	0.21	0.84	2.89	4.48	10.87	17.45	37.73	25.52	100
2015	Jun	0.62	4.71	10.59	21.86	30.31	28.23	3.06	0.62	100
	July	0.89	2.80	12.83	16.91	46.41	12.51	4.68	2.96	100
	August	0.21	0.59	6.35	9.54	15.13	33.03	27.95	7.21	100
2016	Jun	7.26	2.39	17.88	37.11	21.32	4.39	4.58	3.06	100
	July	0.47	2.70	13.94	36.20	30.65	10.29	5.11	0.64	100
	August	1.29	2.25	7.93	12.31	16.47	31.14	20.03	8.59	100
2017	Jun	1.24	4.54	8.09	20.87	29.38	32.06	2.99	0.84	100
	July	1.04	2.46	11.14	26.71	24.96	16.99	6.98	9.72	100
	August	0.49	1.98	7.56	10.39	15.47	33.48	25.64	4.99	100
2018	Jun	3.47	3.26	16.08	32.52	31.37	5.31	4.42	3.56	100
	July	1.10	2.69	4.32	13.84	26.73	24.69	18.19	8.44	100
	August	3.38	7.12	20.65	33.22	10.54	5.76	2.52	16.80	100
2019	Jun	1.35	21.72	10.24	17.62	26.14	10.46	9.00	3.48	100
	July	0.90	2.26	4.25	14.44	27.16	25.02	16.26	9.72	100
	August	0.38	1.53	6.76	11.62	13.97	30.46	27.25	8.03	100
2020	Jun	4.71	8.32	13.09	17.82	35.00	9.35	6.15	5.56	100
	July	0.84	1.13	7.97	33.18	36.65	7.02	8.88	4.33	100
	August	1.18	3.12	8.67	18.17	42.60	19.21	5.01	2.04	100
2021	Jun	0.18	2.80	49.50	42.91	2.08	1.02	1.33	0.19	100
	July	1.26	1.18	22.33	53.26	6.00	2.75	8.88	4.33	100
	August	0.33	3.39	38.94	54.39	1.07	0.48	0.22	1.20	100

5.4 Discussion

Drought severity assessment is a challenging task for vineyard growers. Monitoring vineyards throughout the season on a regional scale is time-consuming and costly. Therefore, satellite remote sensing drought indices and climatic variables have the potential to cost-effectively evaluate drought in

a region. First, the performance of CHIRPS precipitation for dry surveillance was assessed. After that, the drought impacts on vegetation are also analyzed by SVI. These drought indices (SVI and SPI) were calculated for the time series from 2013 to 2021. This research was conducted in all Afghanistan's vineyards for nine years (2013–2021). Because of the political instability in the country, the 2021 yield data and acreage were not available. Validation was performed on eight-year yield datasets with SVI and SPI.

The SVI and SPI results indicated that in 2018 and 2021, the intensity of drought was very high in the berry formation and veraison stages (**Figures 5.9 and 5.10**). The highest area affected by drought was 43.3% in August 2018 and 52.5% in June 2021 (**Figure 5.9**). Perimeter studies indicated that in the summer months when the SPI value was below zero, severe drought was found at the study sites (Dukat et al., 2022). Furthermore, the SPI responds accurately to drought conditions (Almadani, 2022; Hashemzadeh et al., 2022). Additionally, the SVI correlation with other drought indices in the Fars Province of Iran indicated a higher correlation, and this study showed that SVI is a good parameter for drought detection on a regional scale (Mikaili and Rahimzadegan, 2022). Another study conducted in Cambodia discovered that the SPI and SVI worked effectively in analyzing climatic and agricultural droughts (Sok et al., 2022). Various investigations have found that water scarcity has a major impact on grape yield and quality in the berry formation and veraison stages prior (June, July, and August). Previous studies also indicated that extreme drought events have a critical effect on grapevine plant mortality; an increase in embolism in stems and trunks causes canopy and crop failure, decreases photosynthesis, and decreases berry size and water content (Bota et al., 2016; Tombesi et al., 2018; Gambetta et al., 2020). Climate change, especially the dry spell, also has a substantial influence on viticulture management and wine quality (Cook and Wolkovich, 2016). Our study also proved, based on regression between grape yield and drought indices from satellite datasets, that in June and July, water shortages have a significant impact ($r^2 = 0.79$ in June and $r^2 = 0.71$ in July) (**Figure 5.11**). The study results also indicated that the years 2013, 2014, 2015, 2016, 2018, and 2021 were characterized by drought across the region within the berry formation and veraison stages of table grapes. This shows that drought frequency and occurrence have significantly upsurge in recent years due to global warming. Because most grape growers' livelihood sources are vineyard in the research region, the drastically rising number of drought events has a substantial effect on farming system and the livelihood security of farm families. Livelihoods are vulnerable to increased drought. In this regard, supporting farmers during severe drought conditions based on drought severity classes is the most important way for policy-makers and local governments to support farmers.

The limitation of this research was it used the LULC of the shapefile for 2016 for all years due to the unavailability of vineyard shapefiles for other years. In addition, climate data have a greater level of uncertainty connected with the spatiotemporal distribution of precipitation. As a result, strong downscaling approaches to obtain rainfall information at finer resolution are required to decrease the related ambiguity. Although the results of the validation model showed sufficient accuracy (70%) and drought-impacted fields were in good agreement with yield data, there is still a need for larger validation in the future. In the future, adding soil, water, and more vegetation indices for the evaluation of drought assessment on a regional scale would be useful. This research has shown that CHIRPS is a useful dataset for drought monitoring in Afghanistan. The SPI obtained from CHIRPS performed well in detecting drought events by characterizing different regions of Afghanistan.

Table 5.5 Multilinear regression between average yield ton/ha and standard vegetation index and standard precipitation index from 2013 to 2020

Parameters	June	July	August
R Square	0.789798	0.709841	0.04671578
Number of Observations	8	8	8
P-value	0.020258	0.045351406	0.88727

5.5 Conclusion

The new technology such as satellite sensors has the capability for drought assessment in vineyards on a regional scale. In this research, drought assessment and classification were performed based on a regional scale for vineyards in the berry formation and veraison stages before table grape harvesting. Two main drought indicators, the SVI and SPI, were calculated from NDVI and CHIRPS rainfall in the Google Earth Engine platform for 2013 to 2021. A linear and multilinear regression analysis was performed between grape zonal yield and drought indices to validate the drought effect on vineyards. The drought severity results indicated that the years 2013, 2014, 2015, 2016, 2018, and 2021 were characterized by drought across the region within the berry formation and veraison stages of table grape. In particular, drought severity was high in 2018 and 2021 (40% and 52%, respectively) all over Afghanistan. Moreover, severe drought affected 4785.03 hectares and 1825.83 hectares of vineyards in 2018 and 2021, respectively. The validation result indicated that the model coefficient of determination

for table grape average yield and average SVI was $r^2 = 0.42$, $r^2 = 0.62$, and $r^2 = 0.03$ for June, July and August, respectively. However, the coefficients of determination between table grape yield and SPI in June, July, and August were $r^2 = 0.60$, $r^2 = 0.54$, and $r^2 = 0.02$. Meanwhile, the multilinear findings showed higher accuracy for June and July ($r^2 = 0.79$, $r^2 = 0.71$) than for August ($r^2 = 0.05$). The finding suggests that the multilinear model result had higher accuracy than a linear model for drought severity assessment. Therefore, the combination of both indices could be a more accurate result. This research could help governments and policy-makers develop a subsidy plan based on drought severity throughout the country for grape growers.

Chapter 6

Land Suitability Analysis for Grapes Production from Micro to Regional Scales in Drought-prone Areas Using Satellite Remote Sensing and Multi-criteria Decision Support Systems

6.1 Background of the Research

Land suitability analysis is an important tool to maintain the long-term viability of agricultural lands. It is also an important management strategy to identify the ideal farming locations for various crops and vineyards. Land suitability evaluation is also a basis for land use planning, and it helps to establish the most suitable uses of land on micro to regional scales (Akıncı et al., 2013; Habibie et al., 2019; Kılıc et al., 2022). Assessing the potential of land for grapevine extension is very important in order to increase grapes production in a micro to regional scales (Worqlul et al., 2019). It also supports farmer to increase their income and insure livelihood. In recent land suitability analysis, researchers considered GIS-based multicriteria, satellite remote sensing vegetation indices and UAV images to increase the resolutions for higher accuracy in interpretations (Gilliams, 2005; Grassano et al., 2011). Which includes the qualitative and quantitative land evaluations.

The qualitative and quantitative land evaluation is referred to criteria of climate, hydrology, terrain, vegetation, and soil attributes, which are all addressed in the qualitative assessment of land. However, in the quantitative evaluation of land, yield, farmer motivation, cultivation methods, capital, investment capacity, cost-benefit ratio, vineyard location, and other variables are evaluated (Taghizadeh-Mehrjardi et al., 2020). The Food and Agriculture Organization (FAO, 1976) classified land as highly suitable (S1), moderately suitable (S2), marginally suitable (S3), and not suitable (N) (**Table 6.1**). Determination and identification of land suitability categories done based on determination of numerous aspects that influence the quality of land. Since a huge number of criteria has been using in this analysis, it is called multi-criteria decision-making process (Romano et al., 2015).

In land suitability analysis using remote sensing data from micro to regional scale, may increase the complexity of data collection and image processing due to high data volume and diversity that it generates. Incorporating big data analytics with cloud computing, the large-scale scientific applications have shown the advantages of high computational and storage constraints that is simple to implement (Wang et al., 2018). The Google earth engine made this task possible for everyone to access and manipulate this data without cost and large computational facilities (Xie et al., 2019). Besides, rainfall datasets are also difficult to get from micro to regional scales. In the majority countries in the globe,

there is neither a reliable system of weather data nor a homogeneous distribution. Consequently, it is essential to study other data sources for rainfall information, such as satellite-based near real time rainfall information and radar data. In addition, there are products with low latency and extensive records, such as the Climate Hazards Group Infrared Precipitation with Stations (CHIRPS) dataset. This package contains integrated models of terrain-induced precipitation, precipitation estimates from measurement satellites that cover the majority of the globe and have low latency and low polarization, and precipitation estimates from in-situ stations. The CHIRPS dataset contains a lengthy recording period (1981 to the present) with a fine spatial resolution of 0.05° (Funk et al., 2015; Ghozat et al., 2022). Not only the precipitation information is important for vineyard management but also vegetation and soil properties are important to locate further potential areas to increase vineyard cultivation.

Furthermore, other criteria that affect grape production significantly include temperature, rainfall, elevation, slope, soil pH, and soil characteristics. In order to help the farmers, it is necessary to examine the physical and socioeconomic factors that have a significant impact on grape output. Using geographic information systems (GIS), satellite remote sensing datasets, and multi-criteria decision analysis techniques, it is possible to analyze the physical criteria. The farmers may choose acceptable production lands for boosting productivity as well as alternative support systems for marginal and unsuitable land with the aid of the multi-criteria-based suitability analysis. The fundamental advantage of using multi-criteria decision analysis as an analytical hierarchy process (AHP) in land suitability study is that it may be combined with expert judgment (Ridley and Devadoss, 2021). This technique was created by Saaty, who used pairwise comparisons in suitability analysis to assess the criteria significance of two or more than two at once (Saaty 1980).

Among all the suitability overlay methods the Analytical Hierarchy Process (AHP) is the simplest for generation of the weight. Another method is weighted linear combination (WLC) that primarily employs the weighted average operation to combine the appropriateness ratings of several evaluation elements into a single composite score. WLC has become one of the most widely utilized in the land suitability analysis techniques due to its simplicity, adaptability, and effectiveness (Deng et al, 2014; Radočaj et al., 2020). The Fuzzy-AHP approach is also used for generating suitability maps. In this method, the classification was done by the fuzzy membership function and weight of each criterion obtained by AHP, and finally the suitability map was developed by the overlaying method (Elaalem et al., 2011; Kılıc et al., 2022). AHP and Fuzzy suitability analysis is an effective technique with improved precision for land suitability evaluation from micro to regional scales for grape production.

Grapes (*V. vinifera* L.) play a vital role in the worldwide economy. Table grape is one of the major crops in Afghanistan. Afghanistan's table grape production decreased from 15 years ago (**Figure 6.1**). In 2009, it was 15 tons/ha. However, climate change and conflict affected Afghanistan's grape output the most. Climate change, inadequate understanding of production practices, soil quality, and post-harvest losses reduce table grape yields in Afghanistan compared to developed nations. Lack of table grape storages increases post-harvest losses. Strict winery regulations increase farmers' dependence on table grape consumption. The COVID-19 epidemic and climatic variability affected grape production in 2020, and worldwide traders experienced labor constraints and transportation issues.

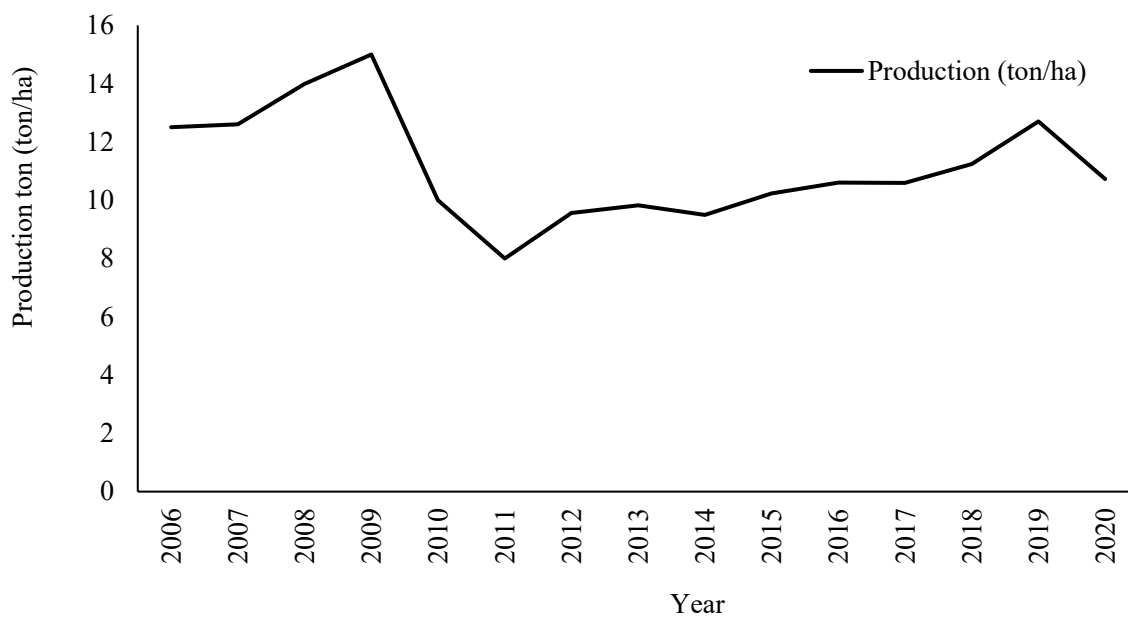


Figure 6.1 Table grape production from 2006-2020 in Afghanistan

Land suitability have been used for different crops such as rice, maize, cassava, grapes and ect(Roy and Saha, 2018; Tashayo et al., 2020; Arab et al., 2022; Purnamasari; et al., 2022). However, vineyard land suitability studies are rare. China evaluated grape site suitability utilizing agricultural land, climate, water regulations, irrigation status, and waste water treatment proximity (Paul et al., 2020). In Italy, soil pH, soil characteristics, elevation, aspect, slope, and heat index are included in land suitability studies (Modica et al., 2014; Cardell et al., 2019). In Afghanistan, no study has used satellite remote sensing datasets and multi-criteria decision-making and fuzzy expert systems to determine grape land suitability.

Table 6.1 Land suitability classes and descriptions based on FAO

Suitability Classes	Description
S ₁ (Highly Suitable)	These types of land having no significant limitations for production
S ₂ (Moderately Suitable)	These types of land having moderate limitations for production. it will reduce productivity by increasing the input into a certain amount can change it to S ₁ .
S ₃ (Marginally Suitable)	These types of lands having marginally limitations. These limitations reduce the productivity by increasing the input the expenditure of land will increase.
N (Not Suitable)	These types of lands having severe limitations with the use of technique and technology we cannot make it suitable.

Therefore, the main objective of this paper was to integrate geographical information systems (GIS) and satellite remote sensing methods for physical and socio-economic criteria using AHP and biophysical, infrastructural, and climate criteria on a regional scale using a fuzzy-based expert system to assess the suitability of lands for increasing grape production from micro to regional scales.

6.2 Materials and Methods

6.2.1 Description of the Study Area

The study was carried out on micro-scale (Shakardara District), macro-scale (Kabul Province) and regional scale (Afghanistan). Kabul Province is a densely populated province of Afghanistan, located between latitudes 34.53330N and longitudes 69.16670E (**Figure 6.2**). It consists of 14 districts, which Shakardara District also includes, and 689 villages with a total population of 5.26 million, which makes up 16% of the total population in Afghanistan. Afghanistan consists of 34 provinces with a total population of 40.2 million (**Figure 6.2**) (ACSO, 2020). Most of the population lives in the fertile valleys. The summers are very hot and dry, but the winters are very cold, especially in high elevations. The area is divided into three parts: the eastern, central, and western parts. In Kabul Province fruit trees are 4000 ha and vines 10,600 ha which makes up about 3.2% of arable land in 2020 (Walt, 2018). However, the total vineyard area is 87,593 ha, which makes up 0.13% of Afghanistan's land (FAO, 2016). Therefore, grape is one of the strategic fruits that produced 115,450 tons in Kabul and 993382 tons in Afghanistan during 2020 (ACSO, 2020).

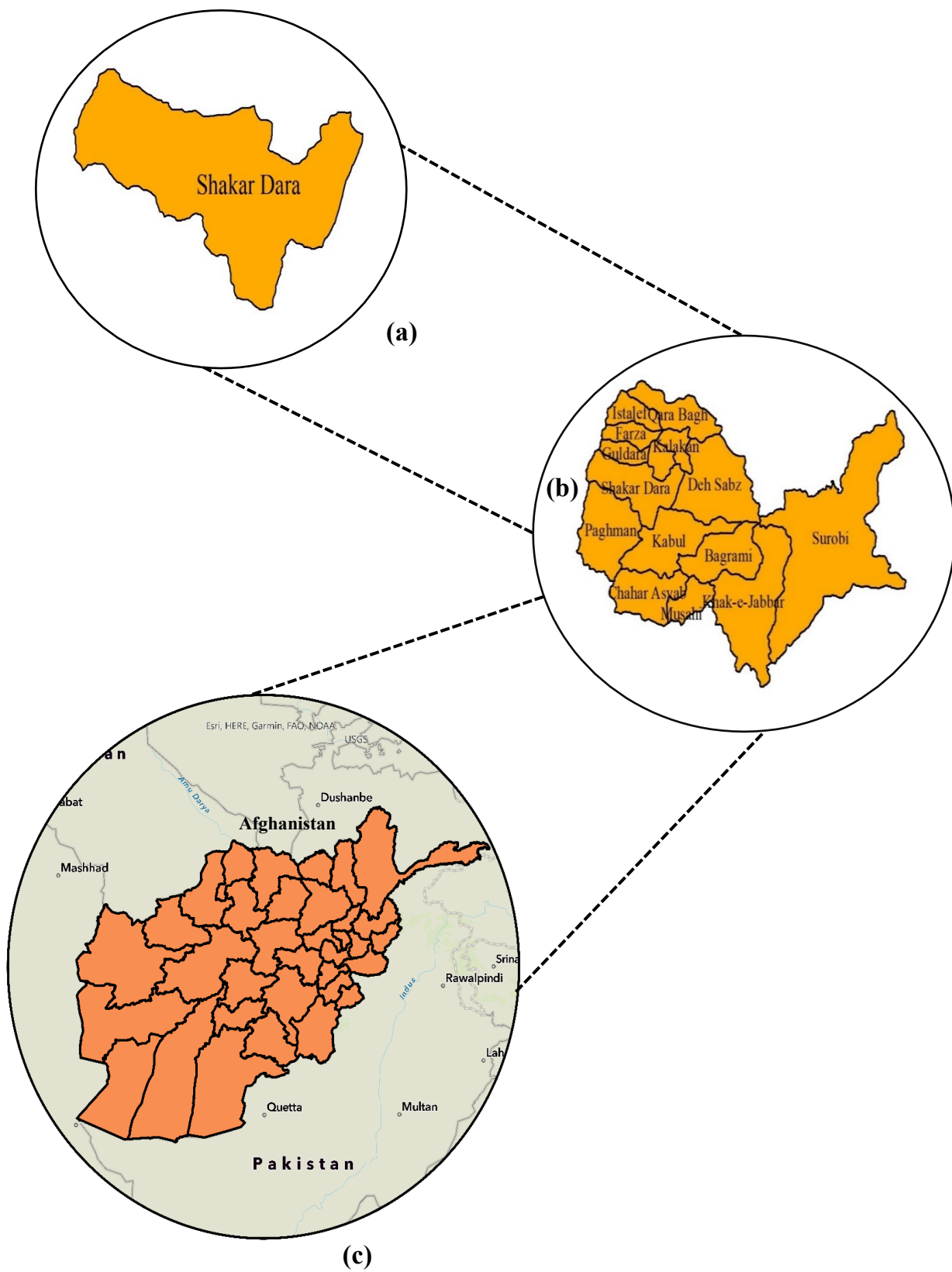


Figure 6.2 The study area's geographical location from micro to regional levels: (a) Shakardara District (b) Kabul Province (c) Afghanistan administrative map

6.2.2 Data collection and criteria selection for table grapes land suitability analysis

The agricultural, metrological, soil and socio-economic data were collected from primary and secondary sources. The criteria for physical suitability were considered NDVI, NDMI, LST, JAXA and CHIRPS rainfall, digital elevation model (DEM), slope, aspect, soil component, soil pH, soil organic matter and soil salinity. Likewise, the socio-economic parameters such as distance from roads, distance from water bodies and population density were collected from the secondary data sources. However, the distance from national and local markets and the benefit-cost ratio of each vineyard were developed from the primary dataset collected during the field survey conducted between November and December 2020 in Kabul Province (**Appendix 4.1**). On a micro-to-macro scale, the geographical location of each vineyard was collected using a Geographic Position System (GPS) Coordinate®. However, for the regional scale, the FAO land use and land cover maps were used. All the datasets and the sources were explained in Table 6.2 and the methods were followed in this research for micro to regional scales explained in the flowchart (**Figure 6.3 and Figure 6.4**).

6.2.3 Micro to Macro Scales Criteria

6.2.3.1 Normalized Difference Vegetation Index (NDVI)

NDVI can be used for real-time plant growth monitoring and estimating the density of greenness (Li et al., 2019). In this study, Landsat 8 multispectral images were used to develop NDVI maps. To ensure an appropriate representation of vegetation evaluation in the study, the images were acquired corresponding to active growing stages of table grapes (April - October) (Anyamba and Tucker 2012; Hadri et al., 2021; Islam et al., 2021) from 2016 to 2020. NDVI can be expressed as:

$$NDVI = \frac{NIR - Red}{NIR + Red} \quad (6.1)$$

where NDVI is the normalized difference vegetation index and NIR is the near-infrared reflectance, ranging from 0.85-0.88 μm , and Red is the wavelength reflectance ranging from 0.64-0.67 μm in Landsat 8 OLI scenes.

6.2.3.2 Normalized Difference Moisture Index (NDMI)

This parameter is very important for vineyards because any variation in the moisture of plants can affect the mesophyll in plants which interact with solar radiation (Bhattacharya et al., 2021). The NDMI was calculated from Landsat 8 OLI images over 5 years from April to October. The NDMI can be expressed as follows:

$$\text{NDMI} = \frac{\text{NIR} - \text{SWIR}}{\text{NIR} + \text{SWIR}} \quad (6.2)$$

where NDMI is the normalized difference moisture index and NIR is the near-infrared wavelength, SWIR is the shortwave infrared reflectance ranging from 1.57-1.65 μm in Landsat 8 OLI scenes.

6.2.3.3 Land Surface Temperature (LST)

LST is the temperature of the surface of the Earth using the Kelvin (K) scale and is an essential criterion for monitoring temperature for crop growth (USGS website and Karnieli et al., 2010). Temperature during the growing season directly impacts the production of sugar in grapes and that this element also influences the type and quality of the grapes produced. The fluctuation of daily temperatures during midwinter is usually more harmful for grapevines than steady cool temperatures (Wolf and Boyer, 2005). Grape vines can be injured or killed by winter cold. Temperatures greater than 30°C can reduce the vine's ability to photosynthetically convert carbon dioxide into sugars and other carbohydrates. Nighttime temperatures greater than about 18°C tend to increase the vine's respiration of this energy. In fact, respiration can consume up to 60% of the energy generated by photosynthesis (Iacono et al., 2000) decreasing the productivity of vines. The LST was calculated from Landsat 8 thermal bands with 30 m resolution in different steps from 2016 to 2020 (Shamsuzzoha et al., 2021). Landsat 8 thermal Infra-Red Scanner (TIRS) has two bands in the TIR region (Band 10 and Band 11). These thermal bands have a 100 m native spatial resolution but are resampled with cubic convolution at 30 m before distribution by United States Geological Survey (USGS) (Loveland and Irons, 2016; Gemitizi et al., 2021). The steps can be explained as following:

The first step of the LST calculation is the top of the atmosphere reflectance (TOA)

$$\text{TOA} = M_L \times Q_{\text{cal}} + A_L \quad (6.3)$$

where M_L represents the band-specific multiplicative rescaling criterion from the metadata, Q_{cal} corresponds to band 10 or 11 Landsat 8 thermal bands and A_L is the band-specific additive rescaling criterion from the metadata.

The second step of this process is the conversion of radiance to sensor temperature. In this, the digital numbers (DNs) are converted to reflection. The TIRS band data should be converted from spectral radiance to brightness temperature (BT). BT can be express as follow:

$$BT = \left(\frac{K_2}{\ln\left(\frac{K_1}{L} + 1\right)} \right) - 273.15 \quad (6.4)$$

where K_1 and K_2 are the band- specific thermal conversion constants from the metadata, and L is the top of atmospheric spectral radiance.

The third step is the calculation of the proportion of vegetation needed to calculate and the P_v is required to calculate the emissivity. Therefore, P_v is determined from NDVI. Therefore, the calculation of the proportion of vegetation is as follows:

$$P_v = \left(\frac{NDVI - NDVI_{min}}{NDVI_{max} - NDVI_{min}} \right)^2 \quad (6.5)$$

where v is the proportion of vegetation, NDVI is the normalized difference vegetation index and max and min is the minimum and maximum NDVI values. Emissivity can be express as follow:

$$\varepsilon = 0.004 + p_v \times 0.986 \quad (6.6)$$

where ε is the emissivity and p_v is the proposition vegetation.

The final step retrieving the LST is computed as follows:

$$T_s = \frac{BT}{1 + \left(\frac{\lambda \times BT}{\rho} \right) \times \ln \varepsilon \lambda} - 273.15 \quad (6.7)$$

where T_s is the land surface temperature in Celsius, BT is the brightness temperature at the sensor, λ is the average wavelength of band 10 or 11 and $\varepsilon \lambda$ is the emissivity.

The satellite datasets were downloaded from the USGS website. Following that, the NDVI, NDMI, and LST from five years of datasets (2016–2020) were calculated using ArcGIS pro[®]. Finally, an average of five years of datasets was used for the final suitability analysis.

6.2.3.4 Rainfall

Rainfall is one of the essential parameters for the production of grapes and lack of rainfall has a severe impact on table grapes productivity. The minimum level of recommended rainfall for vineyards is about 500 mm (Ted, 2018). Therefore, the total water requirement is met through stored winter rainfall,

irrigation, and in-season rainfall. Since the area is arid and semi-arid, the historical average annual rainfall is about 473 mm. In this research, hourly rainfall dataset mm per hour from the global rainfall map (GSMap, JAXA) for each month and districts for five years from 2016-2020 were downloaded. After processing the data, the sum of the cumulative rainfall was calculated for all districts and imported to GIS file. Then, the vector images were converted to raster, and resampling was done for 30m spatial resolution. Finally, an average of five years was used for the final suitability analysis.

6.2.3.5 Elevation

According to previous research, high-elevation regions are more vulnerable to climate change than low-altitude regions (Xu et al., 2016). The highest elevation in Kabul Province is about 4654.4 m above sea level. Furthermore, elevation determined the micro-climate and air temperature variation in a particular area and had a direct influence on the phenology of a vine (Acharya and Yang, 2015). Usually, lower elevations are good for high latitudes, and higher elevations are more desirable at lower latitudes. Increased water stress can reduce the vineyard yield and fruit composition.

6.2.3.6 Slope

The slope has an influence on practicability of agricultural activities, especially referring to the mechanization of vineyards. Vineyards with steep slopes hinder the practical use of machinery, while topography also affects the movement of air and particularly cold air drainage. Therefore, moderate slopes (5–15%) are regarded as optimum (Jones et al., 2009). Besides, the soil water holding capacity can change a slope (Casanova et al., 2000; Bonfante et al., 2015) and that up-slope vines are more prone to water stress, as soils there commonly have lower water holding capacity than down-slope soils (Basile, et al., 2020). Kabul Province slopes ranges are from 0 - 75° the range and between 0 – 10° are optimal slope for vineyard cultivation.

6.2.3.7 Aspect

This criterion directly influences the amount of solar radiation to the soil surface during the growing season. Therefore, this criterion plays a crucial role for high sugar content (Modica et al., 2014). It will also affect the angle that sunlight hits the vineyard and thus its total heat balance. This criterion directly influences the amount of solar radiation to the soil surface during the growing season. Therefore, this criterion plays a crucial role for vineyards which requires very high sugar content for its oenological transformation. (Wolf and Boyer, 2005). *In the southern part of Afghanistan, the intensity of the sun's rays is*

high, and the heat may have a negative effect on the vine. Therefore, north south is the best location for the vineyard's direction (Ghulam Rasoul Samadi. Interview. Conducted by Sara Tokhi Arab, 24th July 2021).

In this study, all topographical parameters such as elevation, slope and aspect were developed from the USGS EROS archive of digital elevation-shuttle radar topography mission (SRTM). The study area had two different paths; therefore, two images were mosaicked using ArcGIS Pro®. Further mask operations were conducted to find the study area.

6.2.3.8 Distance from River

Different rivers and water channels have flow in Kabul Province. Most of these rivers in all districts feed by snowmelt runoffs from the Paghman mountains in the west, the Qorugh Mountain in the southwest, the Shir Darvazeh, Asmayee, and Aliabad mountains are in the center, the Safi Mountain in the northeast, and the southeastern Bagrami, Shina, Lathaband and Tang Gharo dynasties (Series or chain of mountain). The most popular river is the Kabul River that flows from the Paghman Mountain toward South Pass about 70 km west of Kabul. It flows in an easterly direction, past Kabul, through Jalalabad city, and then on to Dakka where it enters Pakistan territory and finally runs into the Indus at the Attock region. The river distance was calculated from the polyline and then changed to raster. After changing to raster, the Euclidean distance was calculated from the nearest river to each vineyard (Purnamasari et al., 2019b). This criterion is important for accessing water for irrigation purposes. According to the expert suggestion, proximity from river or water bodies more than 1 km is the ideal distance. The nearer to river cause more humidity and it will cause fungal disease for the vineyard (Ghulam Rasoul Samadi. Interview. Conducted by Sara Tokhi Arab, 24th July 2021).

6.2.3.9 Soil Components

Soil affects vine productivity and wine quality; soil, like the climate, comprises many components. Soil can be described in terms of its depth, parent rock origin, soil types, organic matter content, texture, chemical properties, hydrology, and in terms of its microbial and other invertebrate fauna density and diversity. All these variables may ultimately affect vine growth and grape quality, but precise relationships are not well characterized for all such variables (Stanchi et al., 2013). The soil datasets were collected from the FAO office branch in Kabul, Afghanistan. Then resampled to 30 m resolution and reclassified based on references to four suitability classes (**Appendix 6.1**).

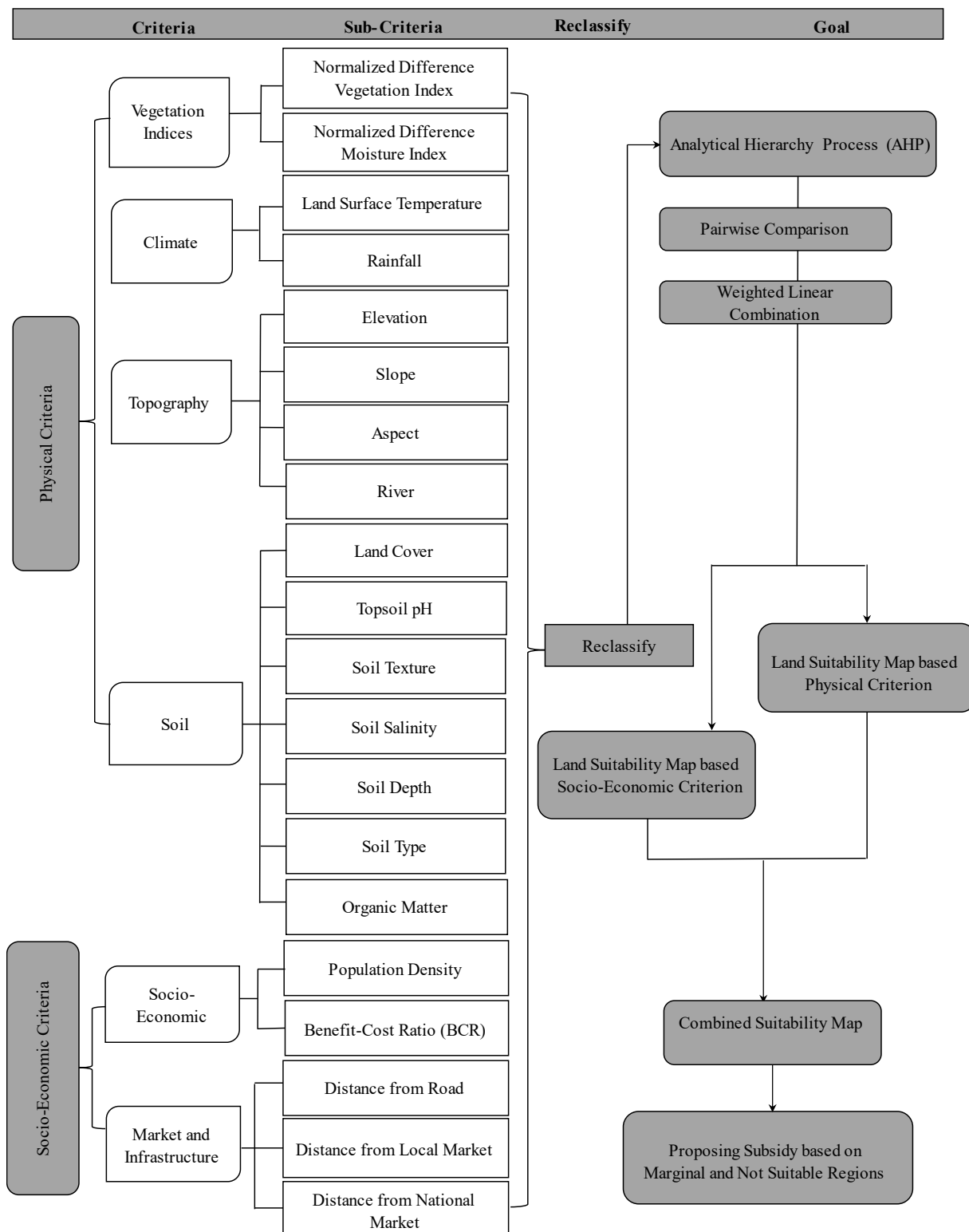


Figure 6.3 Schematic chart shows the methodologies that are applied for land suitability analysis for vineyards under dry conditions in Afghanistan

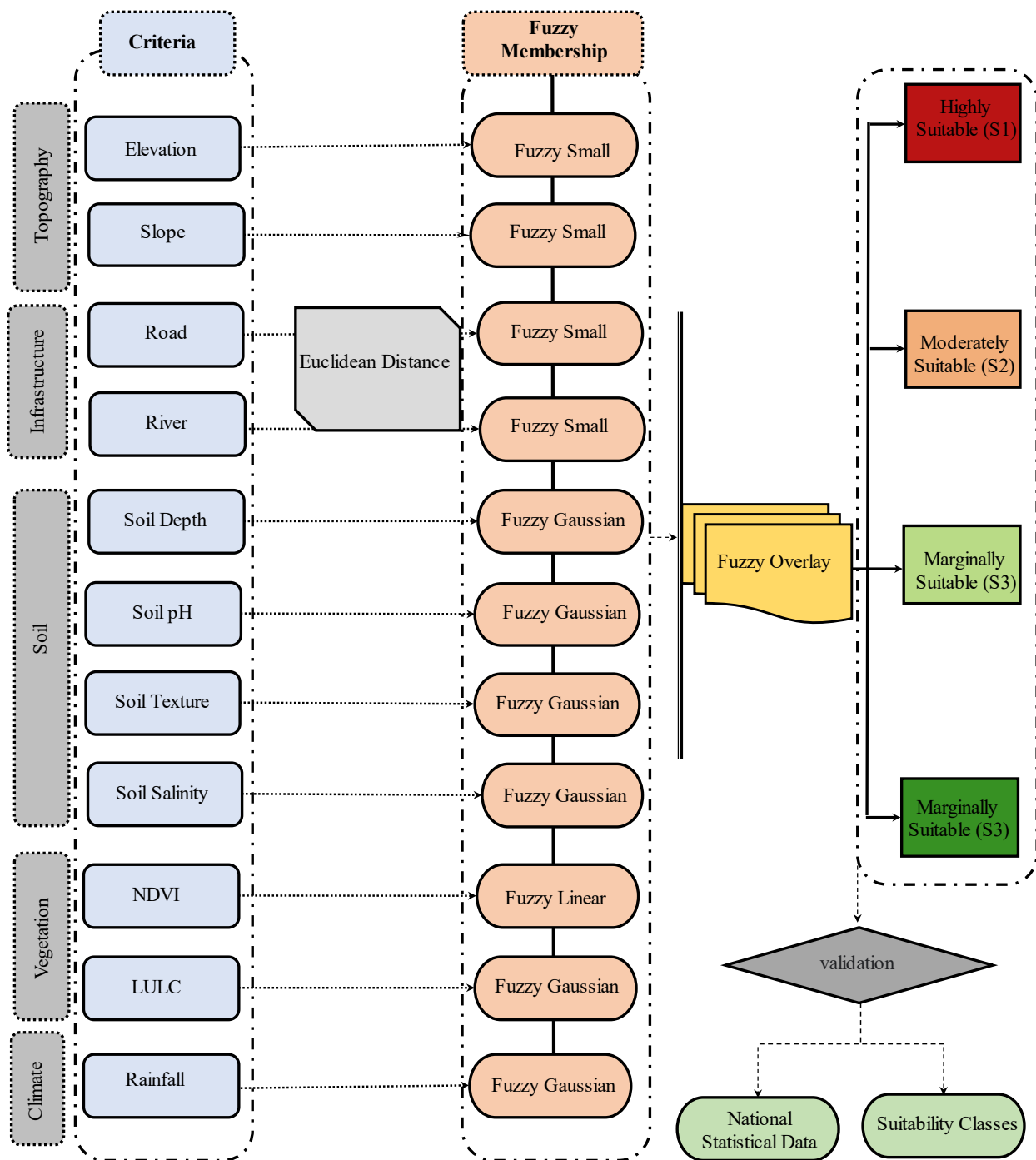


Figure 6.4 Research framework for vineyard suitability analysis based on a fuzzy algorithm

6.2.3.10 Soil pH

Soil pH values between 6.0 and 6.8 provide the optimum availability of nutrients in vineyard soils. Soil pH of less than 5.0 increases the aluminum solubility within the root zone and precipitates essential micronutrients such as iron out of the soil solution.

In this study, all topographical parameters such as elevation, slope and aspect were developed from the USGS EROS archive of digital elevation-shuttle radar topography mission (SRTM) (**Table 6.2**). The study area had two different paths; therefore, two images were mosaicked using ArcGIS Pro®. Further mask operations were conducted to find the study area.

6.2.3.11 Distance from River

Different rivers and water channels have flow in Kabul Province. Most of these rivers in all districts feed by snowmelt runoffs from the Paghman mountains in the west, the Qorugh Mountain in the southwest, the Shir Darvazeh, Asmayee, and Aliabad mountains are in the center, the Safi Mountain in the northeast, and the southeastern Bagrami, Shina, Lathaband and Tang Gharo dynasties (Series or chain of mountain). The most popular river is the Kabul River that flows from the Paghman Mountain toward South Pass about 70 km west of Kabul. It flows in an easterly direction, past Kabul, through Jalalabad city, and then on to Dakka where it enters Pakistan territory and finally runs into the Indus at the Attock region. The river distance was calculated from the polyline and then changed to raster. After changing to raster, the Euclidean distance was calculated from the nearest river to each vineyard (Purnamasari et al., 2019b). This criterion is important for accessing water for irrigation purposes. According to the expert suggestion, proximity from river or water bodies more than 1 km is the ideal distance. The nearer to river cause more humidity and it will cause fungal disease for the vineyard (*Ghulam Rasoul Samadi. Interview. Conducted by Sara Tokhi Arab, 24th July 2021*) (**Table 6.2**).

6.2.3. 12 Soil Salinity

This parameter is very important for the vineyard assessment. Soil salinity is mostly caused by poor irrigation practices in most under developing countries. Subsequently, the accumulation of the salt in the root zone of grapevines happens. Soil salinity can have drastic effects on their growth and yield. If the salt concentration is very high in the soil it kills the vine. Since Afghanistan is a dry area, therefore, the soil salinity increases during the dry periods, since absence of flushed out of salts from the soil (De Clercq et al., 2009; Aragues et al., 2014). Soil salinity dataset was collected from the FAO office in Kabul Afghanistan (**Table 6.2**).

6.2.3.13 Soil Organic Matter

Organic matter improves soil structure, moisture retention and fertility. Three percent organic matter is considered ideal for grapes. It also balances various chemical and biological processes and helps to maintain soil quality parameters at an ideal level in the vineyards (Goldammer, 2018). The organic matter mostly influences soil aggregation and related to pore space distribution and has the same effect as clay on water holding capacity (Saxton and Rawls, 2006) (**Table 6.2**). The dataset was collected from the FAO office in Kabul.

6.2.3.14 Land Use Map

A land use map was used to identify the locations of all vineyards in Kabul Province. Land use maps were obtained from the FAO geo spatial local office. The land use classes were aggregated into 11 generalized and self-explanatory classes. Similar land use classes were merged to the same class based on the ability of land to change to vineyards in the future. There were 11 classes and reclassified to 4 categories based on suitability classes (Worqlul et al., 2017) (**Table 6.2**).

6.2.3.15 Distance from Road

This criterion is important to access to market to sell the product or buy inputs for vineyard management. Different types of roads exist in Kabul Province, such as expressways, major roads, minor roads, and non-standard roads which include the urban and rural roads (Kabul Province master plan). Previous research proved that the proximity of vineyards to roads and industrial areas causes metal accumulation in the soil and causes soil pollution (Deluisa, 1996). *Therefore, suggestions from experts were considered to select more than 1000 m location of vineyards from main roads considered as suitable areas (Ghulam Rasoul Samadi. Interview. Conducted by Sara Tokhi Arab, 24th July 2021).* The road distance was calculated from the polyline and then changed to raster. After changing to raster, used the Euclidean distance to calculate the proximity of the nearest paved road to each vineyard (Purnamasari et al., 2019a).

6.2.3.16 Population Density

The number of people per unit area is called population density. When the population density increases in a region, there is a chance of land use conversion, from agricultural and forest areas to settlements and other services. Population density has a direct relationship with water scarcity and climate change. Several studies provide that density increases across the continent should lead to a significant increase in the extent of water-stressed zones, especially in overpopulated regions (Le Blanc and Perez, 2008;

Gong et al., 2012). The population density map was developed by the World Bank group to estimate the number of people per grid square with the national total adjusted to match the United Nations (UN) population division estimation (Worqlul et al., 2017).

6.2.3.17 Benefit-Cost Ratio (BCR)

The benefit-cost ratio is a measure of efficiency that compares a vineyard's benefit to its cost. A higher benefit-cost ratio value means a grape grower can produce more benefit using fewer costs (Wali et al., 2016). The benefit and cost of all the vineyards were collected through field survey in December 2020. Subsequently, the BCR was calculated through the below expression:

$$\text{Benefit-Cost Ratio} = \frac{\text{Total benefit earned from vineyard}}{\text{Total cost of production required in vineyard}} \quad (6.8)$$

The benefit-cost ratio was added to a separate sheet as a tabular form for all 100 vineyards. After that, the waypoints (x, y coordinate) of benefit-cost ratio were generated. The benefit-cost ratio higher value showed the suitable, lower value showed the less suitable. More than 1.2 considered as a suitable and less than 1.2 considered non-suitable vineyards.

6.2.3.18 Distance from Market

Access to the market is a very important criterion for vineyard site selection especially for underdeveloping countries, which mostly does not have access to modern storage and packing systems. Since table grapes are very perishable therefore access to regional, national, and local markets is very essential. Access to the markets offers opportunities for higher returns to the growers. Vineyard distance to the market was collected through the field survey in December 2020. The tabular form of 100 vineyards was prepared in Microsoft Excel® then market distance was inserted to the location of each vineyard in ArcGIS Pro® (Worqlul et al., 2017). All the criteria further descriptions and sources are described in Table 2 and the criteria classification thresholds are explained in appendix 6.1.

6.2.4 Regional Scales Criteria

The research was conducted in three steps: first step infrastructure, soil, vegetation, and climate variables were organized for vineyard suitability analysis as shown in the research flowchart (Figure 6.4). The criterion maps, such as (a) elevation, (b) slope, (c) river, (d) road, (e) soil depth, (f) pH, (g) soil texture, (h) soil salinity, (i) NDVI, (j) LULC, and (k) rainfall. In this research, different sources

were used to obtain the datasets, such as FAO, readily available sources, and Google earth engine for downloading big datasets of Landsat 8 OLI and rainfall. All primary suitability criteria were resampled to same resolution as Landsat 8 OLI 30 m. Second, the fuzzy membership function was applied to each criterion based on previous literatures (**Figure 6.8**). Third, in the ArcGIS® environment, the fuzzy gamma was applied to overlay all the criteria (**Bellman and Zadeh, 1970**). Finally, the validation was done with ground reference datasets (**Figure 6.16**).

6.2.5 Criteria Reclassification and Weighted Linear Combination for Micro to Macro

Reclassification was done in ArcGIS Pro® in order to create a new single classified raster map from the main raster. The raster maps of each criteria were classified based on reference to four classes: highly suitable, moderately suitable, marginally suitable and not suitable each classes were explained (**Appendix 6.1 and Figure 6.5 and 6.6**).

6.2.6 Analytical Hierarchy Process (AHP)

AHP was developed by Saaty (1985) to provide a framework for solving multi-criterion decision problems based on relative importance assigned to each criterion. In this research, the criteria were chosen based on their importance for physical and socio-economic for vineyards suitability under the dry condition of Afghanistan. We selected a total of 20 sub-criteria from two main criteria. Since the AHP has three main steps as the development of pairwise comparison matrix, computation of weight criterion and estimation of consistency ratio (CR) (**Table 6.5**). Therefore, the first step is the pairwise comparison matrix development from the 14 criterion for physical and 6 criterion for socio-economic were chosen. Subsequently, three questionnaires were developed to obtain the experts' opinions relative importance of each criterion.

Two AHP questionnaires were designed to collect the expert' opinions regarding the physical and socio-economic criterion of vineyards in Kabul Province. The third one used to know the influenced of each in total. The intensity of importance of each criterion was scaled from 1 to 9. In the scale, 1 is showed equal to importance and 9 is referred to the extremely importance of criteria. On the contrarary, the opposite is 1/9 means extremely less importance. The consistency index (CI) showed the level of deviation from consistency and was computed using the following expression (Saaty and Kearns, 2014) (**Table 6.3, Table 6.4 and Table 6.5**).

Table 6.2 List of data and source of datasets for table grapes land suitability analysis

No	Data	Description	Data Source
1	Land use map	Derived from Spot (10 m color), Google Earth (2.5m 1m, /0.6m color) and Arial Photographs (1m color/ 0.5m B and W).	FAO, 2016
2	Slope map		DEM SRTM USGS, 2014 & 2015
3	Elevation map	The Shuttle Radar Topography Mission (SRTM), resolution 1-ARC	DEM SRTM USGS, 2014 & 2015
4	Aspect map		DEM SRTM USGS, 2014 & 2015
5	Rainfall map	Resample to 30m resolution	JAXA Rainfall GSMAP, 2016-2020
6	Land surface temperature map	Derived from 30m (band10 and band11)	Lansat 8 Scenes USGS, 2016-2020
7	NDVI map	Derived from 30m resolution (band 4	Lansat 8 USGS, 2016-
8	NDMI	and band 5)	2020
9	Soil pH		FAO, 2020
10	Topsoil texture		FAO, 2020
11	Topsoil types		FAO, 2020
12	Topsoil depth	Afghanistan soil atls, Scale 1:50 000	FAO, 2020
13	Soil texture		FAO, 2020
14	Soil organic matter (OM)		FAO, 2020
15	Topsoil salinity		FAO2020
16	Road map	1:250,000	AIMS, OSM OCHA, 2019
17	River map	Scale 1:50,000	AIMS OSM OCHA, 2019
18	Population density	Spatial resolution 0.000833333 decimal degrees (approximate 100m at the equator)	World Bank Group, 2017
19	Distance from national market	GPS point	Field survey, 2020
20	Distance from local market	GPS point	Field survey, 2020
21	Vineyard's locations	Polygon	FAO, 2016
22	Benefit- cost ratio	GPS points	Field survey, 2020

$$CI = \frac{\lambda_{\max} - n}{n - 1} \quad (6.9)$$

where λ_{\max} is the maximum eigen value and n is the number of criteria or sub-criteria in the matrix of pairwise comparison (Tables 5.2 and 5.3).

CR is the ratio of CI to the average random inconsistency index (RI) for the same order matrix and was computed using the following expression:

$$CR = \frac{CI}{RI} \quad (6.10)$$

where CI is the consistency index and RI is the random index (**Table 6.5**). When the CR value was less than 10% the matrices consistent and AHP can be continued. If the CR bigger than 10%, the assesment required revision because the materix is not consistent.

$$S_i = \sum_{i=1}^n C_i \times W_n \quad (6.11)$$

where C_i is the criterion i that was reclassified and W_n is the number of criteria n that were wieghted. The score (weight) of each criterion was calculated in excel from the AHP (**Tables 6.2, 6.3 and 6.4**). Finally, the ArcGIS Pro[®] was used to combine the spatial data with S_i in order to generate a land suitability map.

6.2.7 Dataset and Criteria Conversion (Fuzzification)

In the fuzzification method, the datasets of various ranges and unites were transformed into a common scale (0–1). The fuzzy small, large, linear, and gaussian were assigned to biophysical, climatic, infrastructure, topographic, and soil-related criteria. The fuzzy small transformation function was used when the small values of the input raster have high fuzzy membership. The defined midpoint identifies the crossover point (assigned a membership of 0.5), with values greater than the midpoint having a lower chance of membership and values less than the midpoint having a higher chance of membership (**Equation 6.12**). The fuzzy large transformation function was used when the larger input values were more likely to be members of the set. The specified midpoint recognizes the crossover point (assigned a membership of 0.5), with values greater than the midpoint possessing a greater chance of being a member of the set and values less than the midpoint possessing a declining membership (**Equation 6.13**). Fuzzy linear shows the linear relationship in datasets and minimum values were assigned to 0 and maximum values were assigned to 1 (**Equation 6.14**). Fuzzy gaussian showed the normal distribution of datasets. The midpoint was assigned 1, and the remaining datasets moved in positive and negative directions. The input value membership was decreased when data moved from the midpoint (**Equation 6.15**). All fuzzy membership functions had a midpoint ($f2$) and spread ($f1$).

$$\mu_{(x)} = \frac{1}{1 + \left(\frac{x}{f_2}\right)^{f_1}} \quad (6.12)$$

$$\mu_{(x)} = \frac{1}{1 + \left(\frac{x}{f_2}\right)^{-f_1}} \quad (6.13)$$

$$\mu(x) = \begin{cases} 0 & x \leq a \\ \frac{x-a}{b-a} & a < x < b \\ 1 & x \geq b \end{cases} \quad (6.14)$$

$$\mu(x) = e^{(-f_1 \times (x-f_2)^2)} \quad (6.15)$$

6.2.7.1 Elevation

In this study, elevation data was obtained from SRTM DEM and taken from the USGS website (**Table 1**). This criterion was important because direct impact on grapevine phenology. The elevation dataset was converted using a fuzzy small function from low, ranging from 0 to a high of 6998 m (Stanchi et al., 2013). The range of elevation was selected based on the expert's field experience since the study area's elevation was very high. Fuzzy small selected the optimal elevation was selected in a range of 1500 m. The smaller values were considered optimum in arrange of 1500 m. The elevation range changed from 0 to 1, where 0 denotes the least suitable areas and 1 denotes the most suitable areas (**Figure 6.8-a**).

6.2.7.2 Slope

It relates to the vineyard's degree of inclination, a slight to moderate slope can be good for grape production. The gaussian function was assigned to each pixel of slope. In the study area, 5-15% slope was considered the optimal slope based on previous studies (Stanchi et al., 2013; Badr et al. 2018; Arab et al. 2022). In this process, the optimum elevation was assigned at the peak of the function. More or less than the ideal range was not good for growing grapes (**Figure 6.8-b and Table 6.1**).

6.2.7.3 River

There is a significant impact on vineyard production, especially in a country like Afghanistan, where water scarcity is widely observed due to its geographical location. Based on previous studies and field experience, up to 1 km from rivers was considered the optimum distance. In this regard, fuzzy small membership functions were assigned to each river's pixel criteria. The near area value changed to 1, and further locations were assigned to 0 (**Figure 6.8-c & Table 6.1**) (Purnamasari et al., 2019).

6.2.7.4 Road

Roads are an important parameter in facilitating the access of growers to input and output markets (**Table 6.1**). Based on previous studies and a field expert's experience, up to 1000 m from the road was

selected as optimal for vineyard suitability. The fuzzy small membership function was assigned to roads. The closer the road was assigned 1 and the further distance was assigned 0 (**Figure 6.8-d**) (Purnamasari et al., 2019, Arab et al., 2022).

6.2.7.5 Soil datasets

Several important soil variables were chosen, such as soil pH, soil depth, soil texture, and soil salinity. All these variables were obtained from the FAO soil database (**Table 6.1**). Fuzzy gaussian membership was assigned for all soil components. The soil pH range in the study area was 7.4–8.8. The optimum range was considered to be 6.5-8 (USAID, 2016). Soil texture was categorized for study areas into 9 classes based on FAO classification. Based on reference, the sandy loam, loam, and coarse sandy loam were selected with higher scores because the clay or silt soils had less water holding capacity in the root zone of grapevine (FAO, 2020). Poor irrigation and drainage are the primary cause of soil salinity in the study area because it is mostly prone to drought (Goes et al., 2016). The saline category is assigned a value of 0 and the less saline category is assigned a value of 1. 2 ECe dS/m is not saline soil (**De Pascale and Barbieri, 1995**). The fuzzy gaussian was used to assign all soil parameters. The optimal level is considered the peak of distribution, which is less than or higher than the range considered 0 (Park et al., 2021; Arab et al., 2022; Goldammer, 2018; Rameshkumar et al., 2006; Badr et al., 2018) (**Figure 6.8 e-h**).

6.2.7.6 Normalized Difference Vegetation Index (NDVI)

Google earth engine environment was used to calculate composite NDVI scenes from Landsat 8 OLI (Tire 1, 8-day composite) from April to October for five years (2016–2020). Finally, the average of all NDVI from 2016 to 2020 was considered for the suitability analysis. Further analysis was carried out with ArcGIS® 10.8. The fuzzy linear membership function was assigned. The higher NDVI is given a value of 1, and the lower NDVI is given a value of 0 (Alwan et al., 2020) (**Figure 6.8-i**).

6.2.7.7 Land Use Land Cover (LULC)

The LULC datasets were obtained from FAO (**Table 2**). For instance, LULC consisted to different classes: for instance, vineyards, irrigated and non-irrigated agricultural land, forest and shrubs, rangeland, barren land and sand cover, permanent snow, build up, water and marshland. The majority of Afghanistan's land is covered in sand and rock, with only 12% suitable for agricultural activities. Fuzzy gaussian membership was given to LULC. The maximum vineyard and agricultural land

membership is 1. However, the minimum membership function for the building, road, and water body is 0 (Worqlul et al., 2017) (**Figure 6.8-j**).

6.2.7.8 Rainfall

The rainfall data was collected yearly from the website of time-series rainfall estimates from rain gauges and satellite observations (CHIRPS). Following that, the five-year mean was used in this calculation. Based on previous studies, the optimum rainfall for grapevine is about 500mm with that reference fuzzy gaussian was used (Ted, 2018; USAID, 2016). The optimum rainfall was assigned to 1, that was less or greater than that assigned to 0 (**Figure 6.8-k**).

6.2.7.9 Fuzzy Overlay

The fuzzy overlay was used for multicriteria to show the likelihood of a feature belonged to various sets. The fuzzy gamma was used to develop the final suitability map. The fuzzy gamma developed the links between the numerous input criteria rather than merely returning the value of a single membership set, according to fuzzy OR and fuzzy AND (**Equation 6.16**).

$$\mu(x)=(\text{fuzzySum})^y \times (\text{fuzzySum})^{1-y} \quad (6.16)$$

The suitable vineyards were classified based on land index. The presently not suitable and permanently not suitable areas were classified considered in the similar class to locate highly, moderately and marginal areas. In this fuzzy method, a land index was calculated and converted from 0-1 fuzzy value to be multiplied by 100. The suitability classes were determined by the value of the land index: S1 Highly suitable land 75-100, moderately suitable land 75-50, S3 marginally suitable land 50-25 and N not suitable land 25-0.

6.2.7.10 Validation of Suitability Map with Ground Reference Data

The total yield of 2020 for each province was collected from the statistical book of the Islamic Republic of Afghanistan (**Figure 6.7**). The average yield of in each Provinces were calculated from total yield divided by total vineyard area. Furthermore, a subsequent regression analysis was done between the grape yield and the land suitability index.

Table 6.3 Parirwise comparison matirx for grape based on physical criterion to evaluate in Kabul Province of Afghanistan

Criteria	Soil Type	Soil pH	Soil Depth	Soil Texture	Soil Organic Matter	Soil Salinity	NDVI	NDMI	Rainfall	Slop	Elevation	LST	Land Cover	Aspect
Soil Type	1	1/2	1/2	1	1	2	5	5	1	4	2	3	4	5
Soil pH	2	1	1	1	1	4	7	4	4	6	4	4	7	9
Soil Depth	2	1	1	1	1	2	3	5	1	9	8	8	6	8
Soil Texture	1	1	1	1	1	2	8	8	2	7	7	6	6	6
Soil Organic Matter	1	1	1	1	1	5	7	7	2	6	6	7	7	8
Soil Salinity	1/2	1/4	1/2	1/2	1/5	1	5	6	1	9	7	3	8	9
NDVI	1/5	1/7	1/3	1/8	1/7	1/5	1	1	1	2	2	2	9	9
NDMI	1/5	1/4	1/5	1/8	1/7	1/6	1	1	1	1	2	2	7	9
Rainfall	1	1/4	1	1/2	1/2	1	1	1	1	9	9	5	9	9
Slop	1/4	1/6	1/9	1/7	1/6	1/9	1/2	1	1/9	1	2	2	3	3
Elevation	1/2	1/4	1/8	1/7	1/6	1/7	1/2	1/2	1/9	1/2	1	1	2	2
LST	1/3	1/4	1/8	1/6	1/7	1/3	1/2	1/2	1/5	1/2	1	1	3	3
Land Cover	1/4	1/7	1/6	1/6	1/7	1/8	1/9	1/7	1/9	1/3	1/2	1/3	1	1
Aspect	1/5	1/9	1/8	1/6	1/8	1/9	1/9	1/9	1/9	1/3	1/2	1/3	1	1
Sum	10.4	6.3	7.2	7	6.7	18.2	39.7	40.3	14.6	55.6	52	44.6	73	82

$$CI = \frac{(\lambda_{max} - n)}{(n - 1)}$$

$$RI = 1.57$$

$$\text{Maximum Eigen value} = 15.82$$

$$n = 14$$

$$CR = 0.09$$

Table 6.4 Normalized matrix of the criteria for grapes based on socio-economic criterion under the dry condition

Criteria	Distance from road	Distance from river	Population density	Benefit- cost ratio	Distance from local market	Distance from national market
Distance from road	1	2	1/2	3	8	8
Distance from river	1/2	1	1	1	6	2
Population density	2	1	1	6	9	6
Benefit- cost ratio	1/3	1	1/6	1	1	2
Distance from local market	1/8	1/6	1/9	1	1	1
Distance from national market	1/8	1/2	1/6	1/2	1	1
Sum	4.0833	5.6667	2.9444	12 1/2	26	20

$$CI = \frac{(\lambda_{max} - n)}{(n - 1)}$$

$$RI = 1.24$$

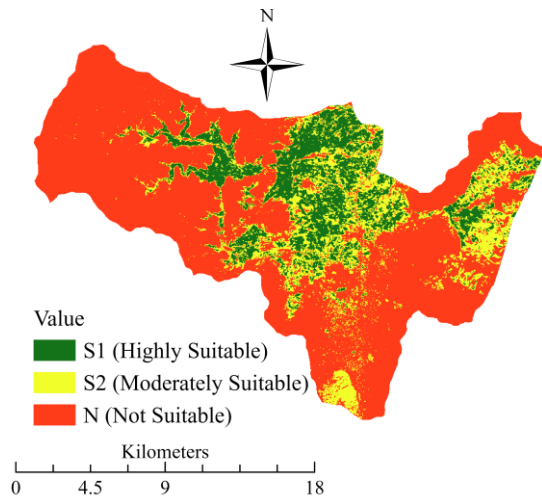
Maximum Eigen value = 6.44

$$n = 6$$

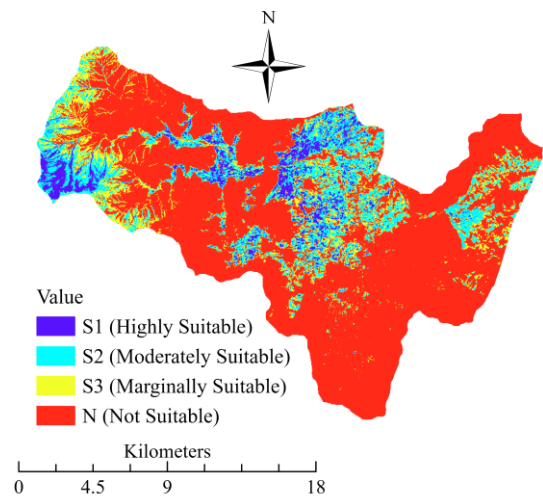
$$CR = 0.071$$

Table 6.5 Value of random consistency index (RI) (Aguaron, 2003)

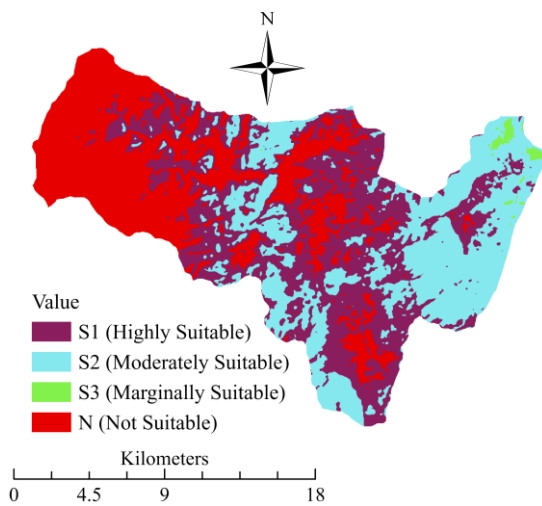
n	3	4	5	6	7	8	9	10	11	12	13	14	15
RI	0.525	0.882	1.115	1.252	1.341	1.404	1.452	1.484	1.513	1.535	1.555	1.570	1.583



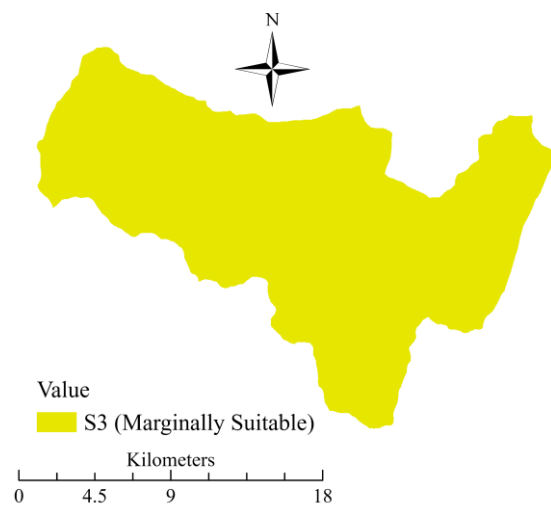
(a) NDVI



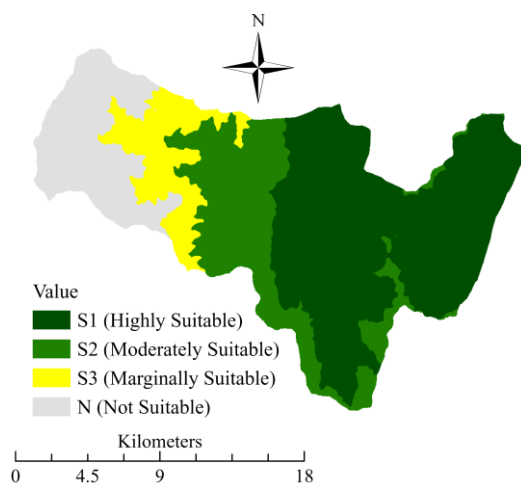
(b) NDMI



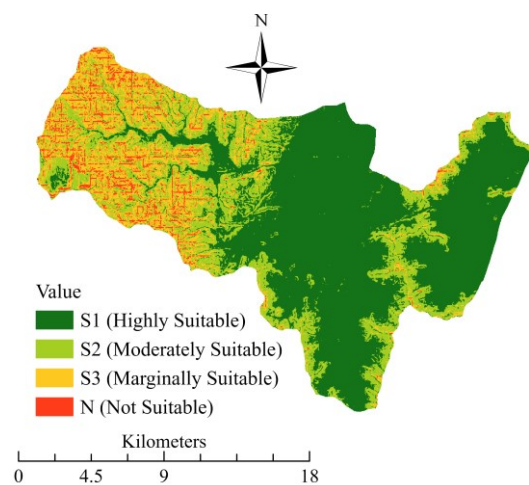
(c) LST



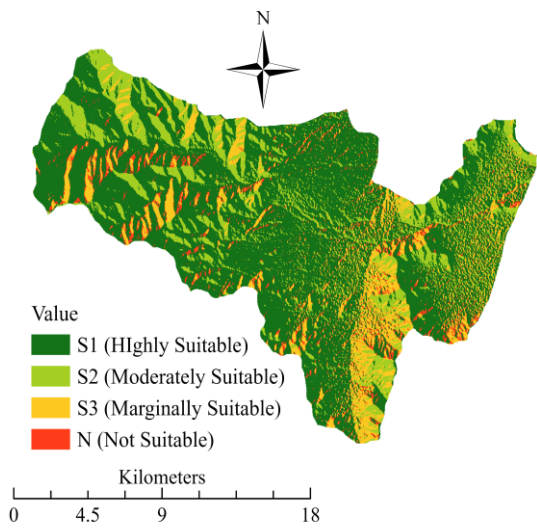
(d) Rainfall



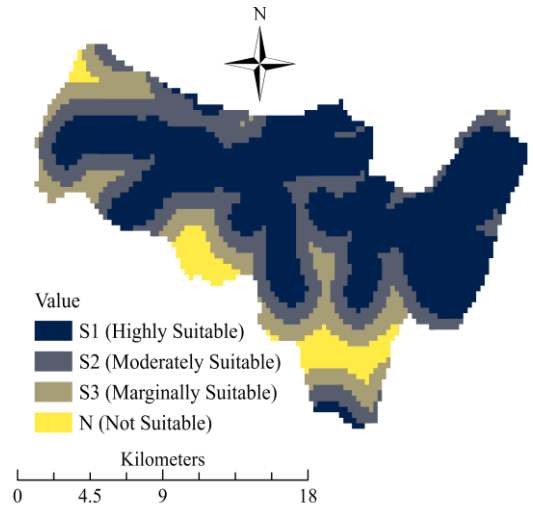
(e) Elevation



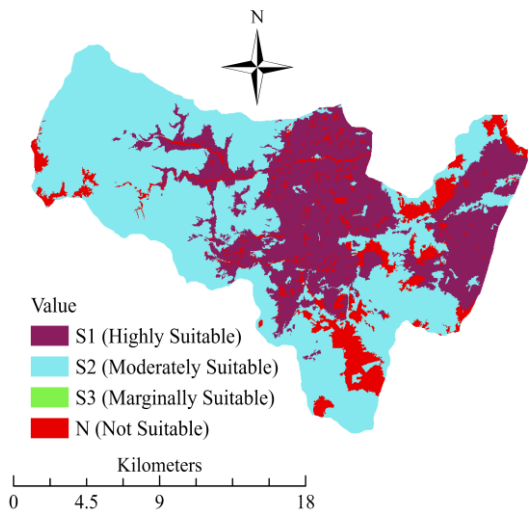
(f) Slope



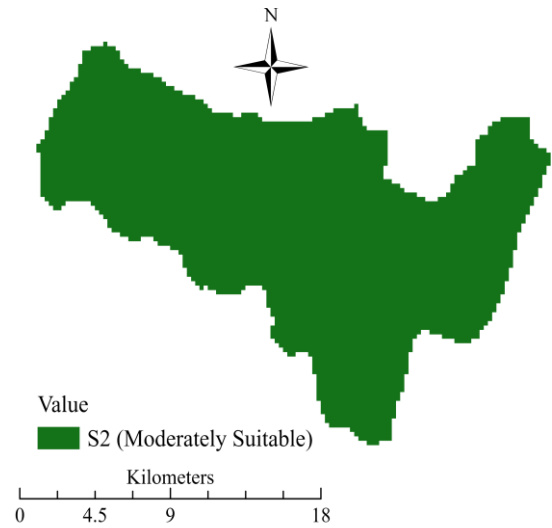
(g) Aspect



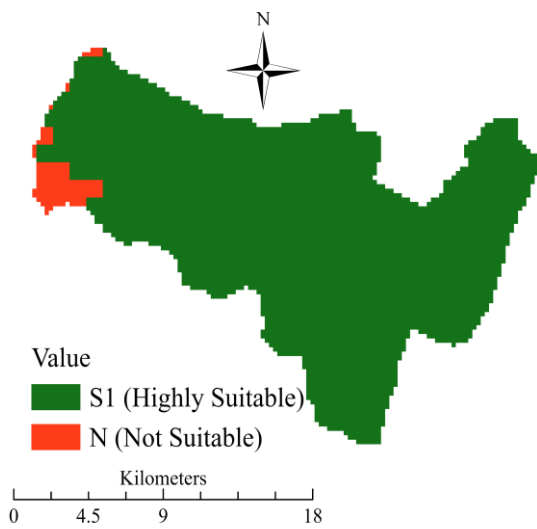
(h) Distance from river



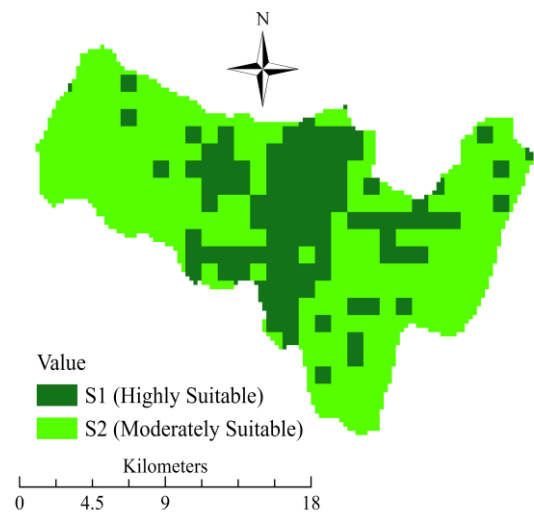
(i) Land cover



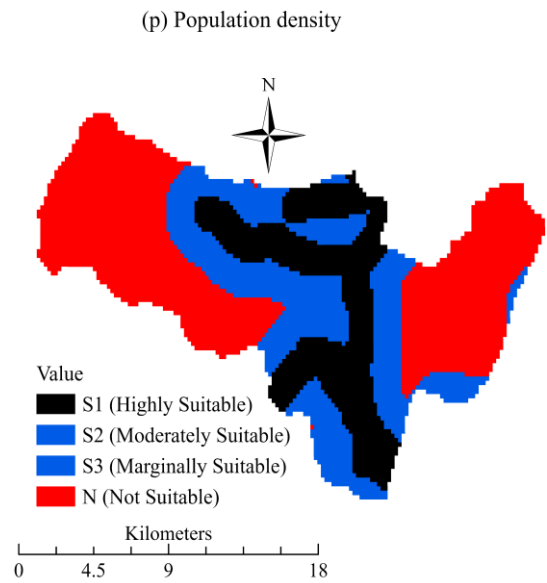
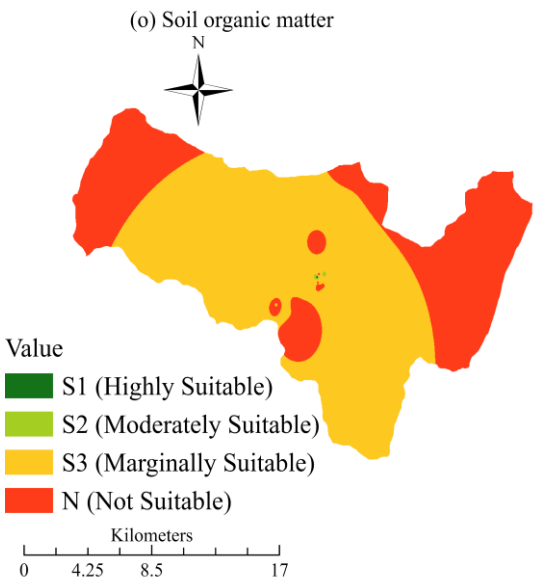
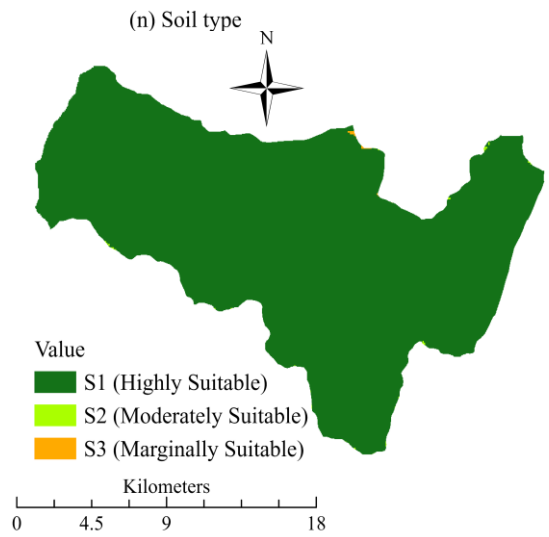
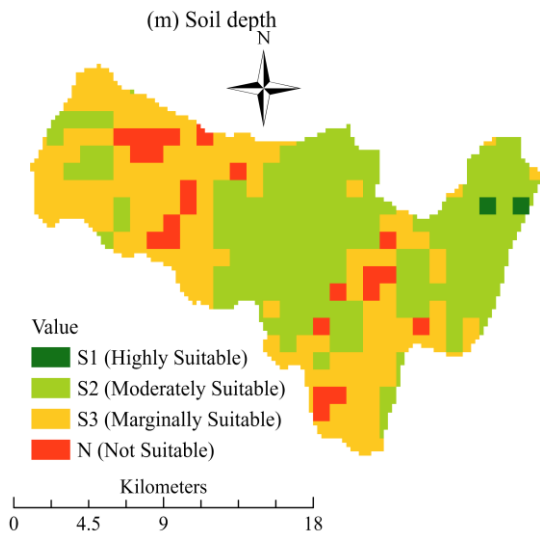
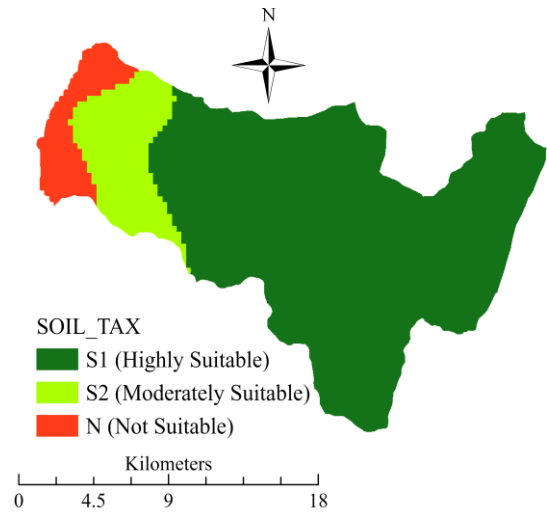
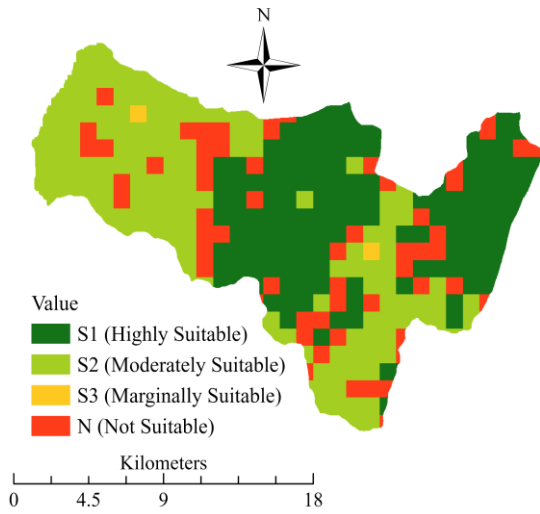
(j) Soil pH



(k) Soil texture

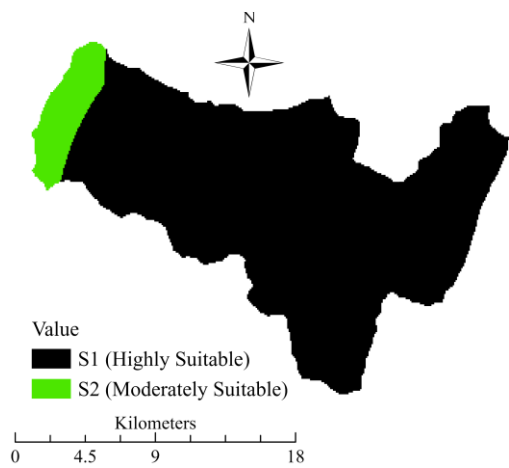


(l) Soil salinity

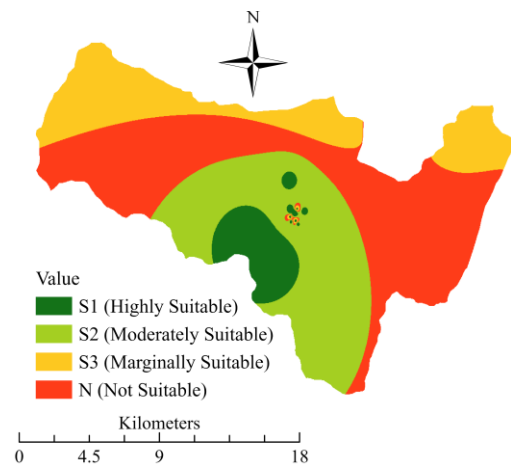


(q) Benefit-cost ratio

(r) Distance from road

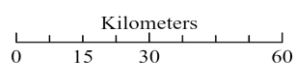
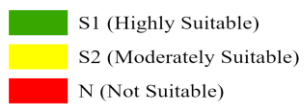
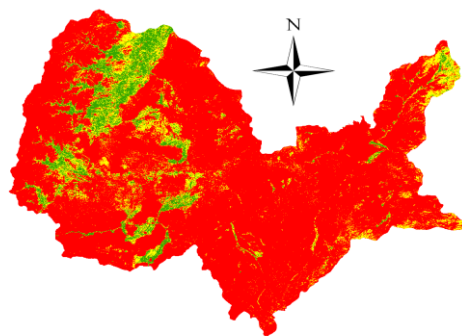


(s) Distance from local market

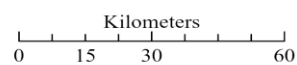
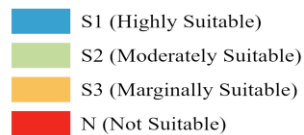
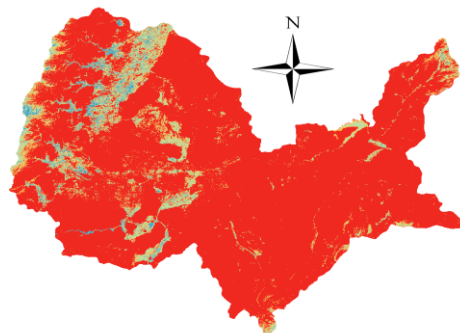


(t) Distance from national market

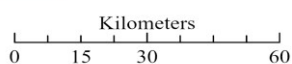
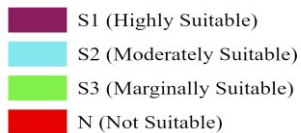
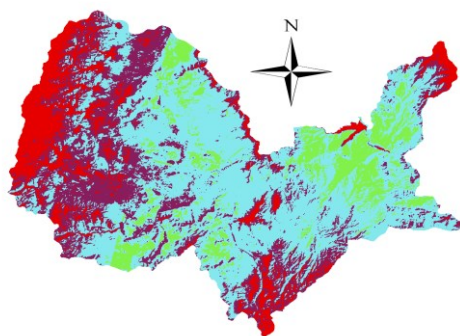
Figure 6.5 Reclassification of criteria for micro- scale (a-o) for physical criterion and from (p-t) for socio-economic criterion for vineyards suitability analysis



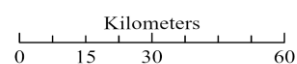
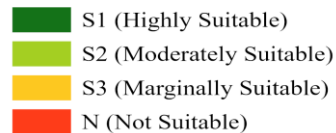
(a) NDVI



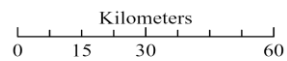
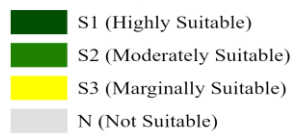
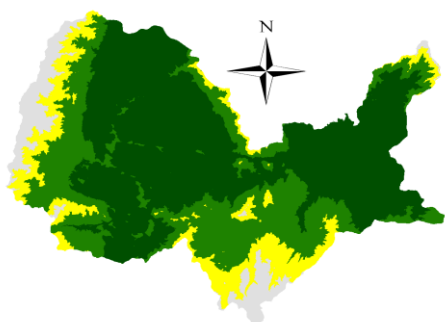
(b) NDMI



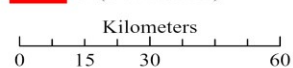
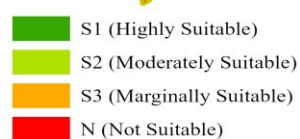
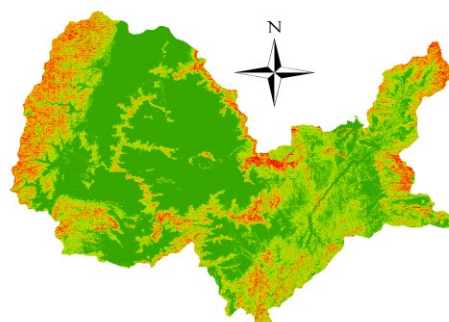
(c) LST



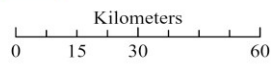
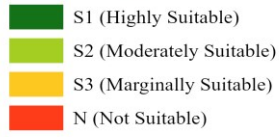
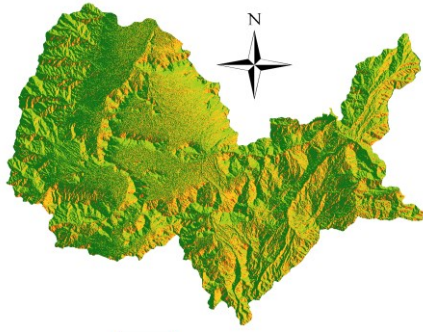
(d) Rainfall



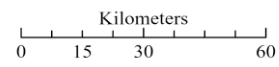
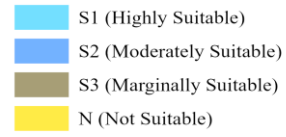
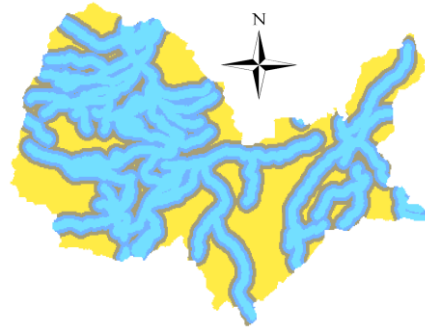
(e) Elevation



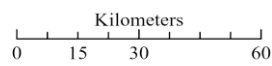
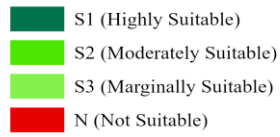
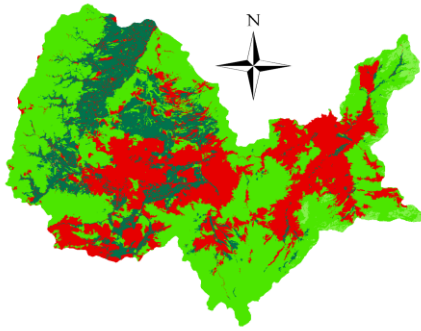
(f) Slope



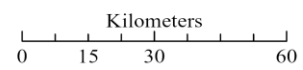
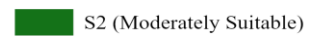
(g) Aspect



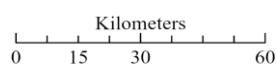
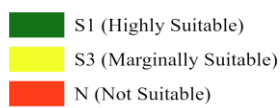
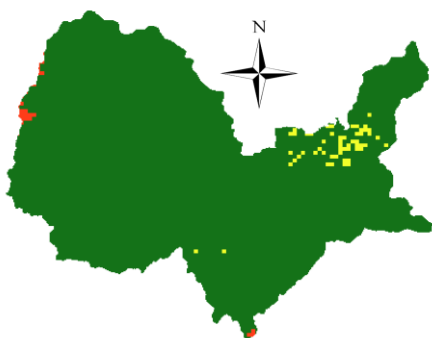
(h) Distance from river



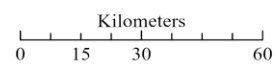
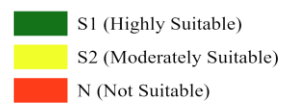
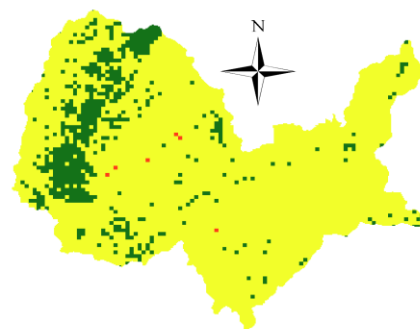
(i) Land cover



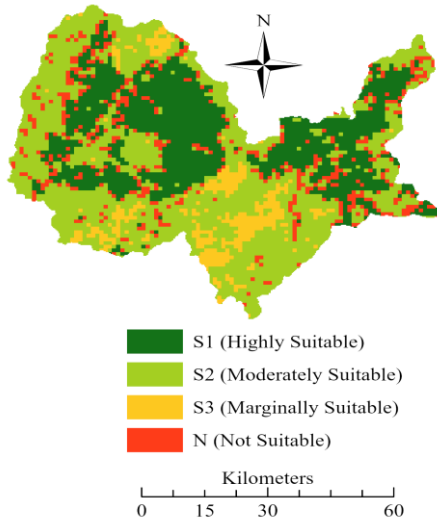
(j) Soil pH



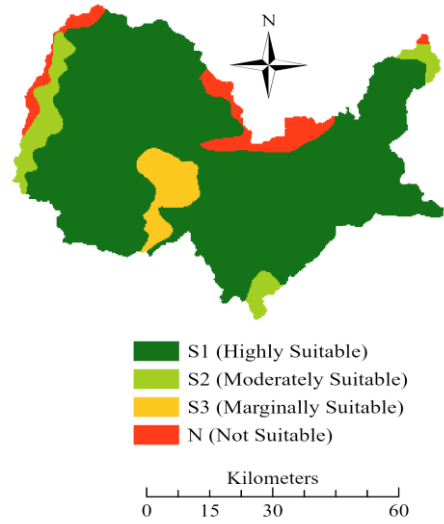
(k) Soil texture



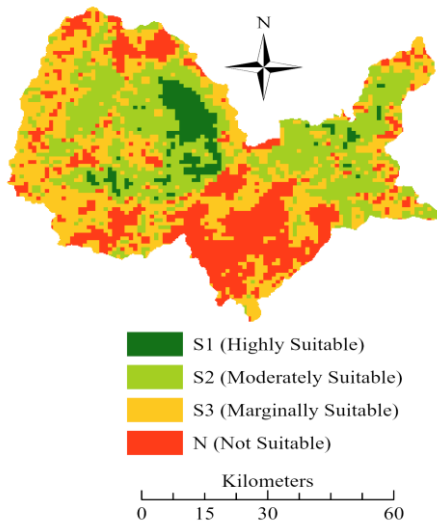
(l) Soil salinity



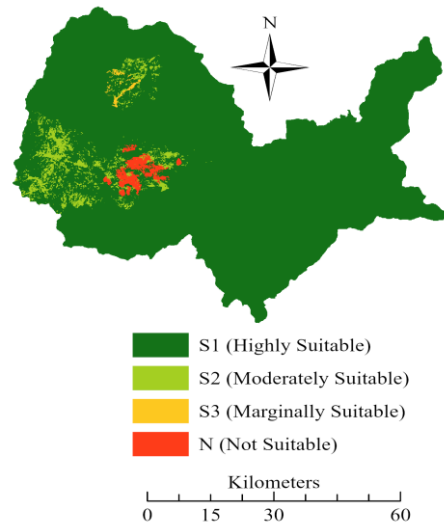
(m) Soil depth



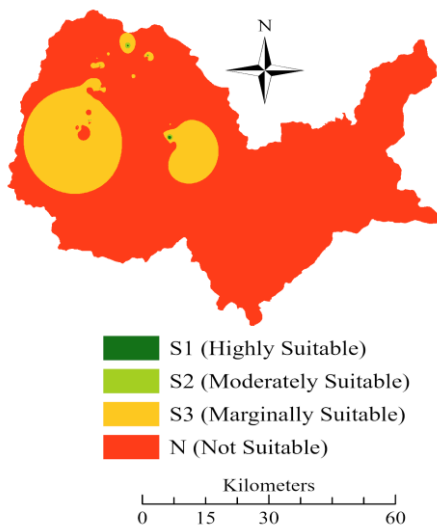
(n) Soil type



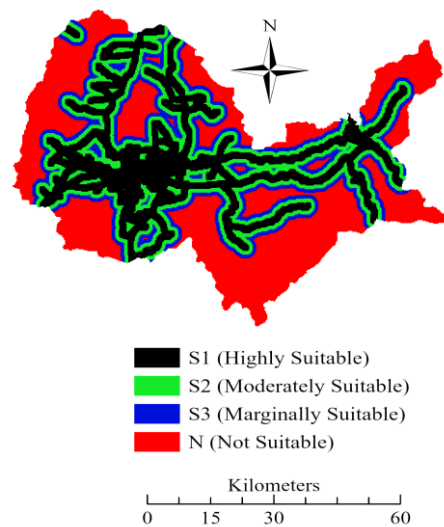
(o) Soil organic matter



(p) Population density



(q) Benefit-cost ratio



(r) Distance from road

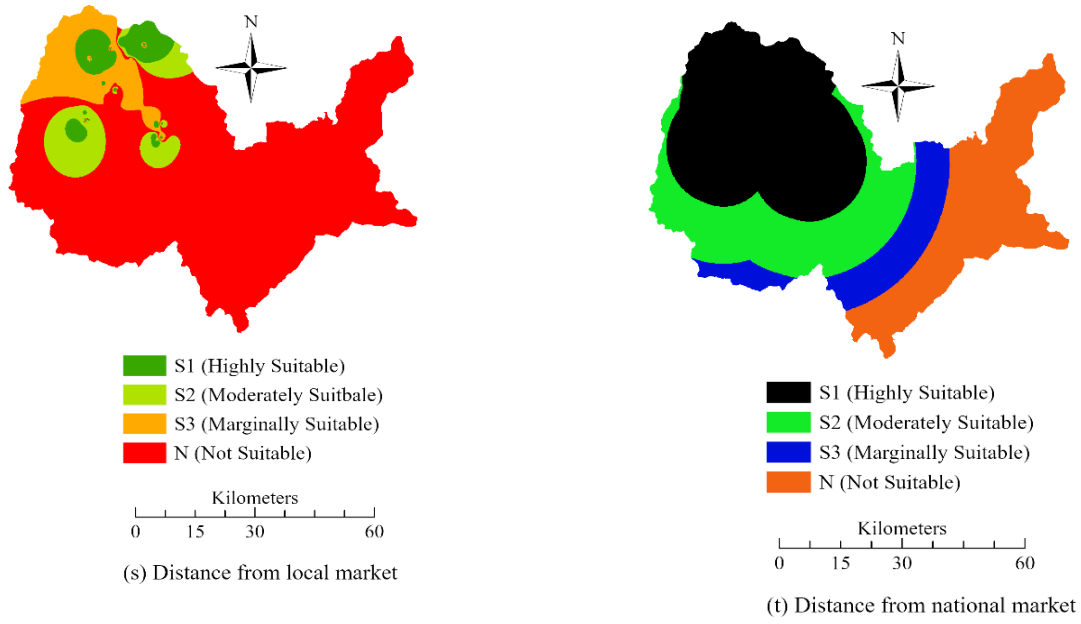


Figure 6.6 Reclassification of criteria for macro-scale (a-o) for physical criterion and from (p-t) for socio-economic criterion for vineyards suitability analysis

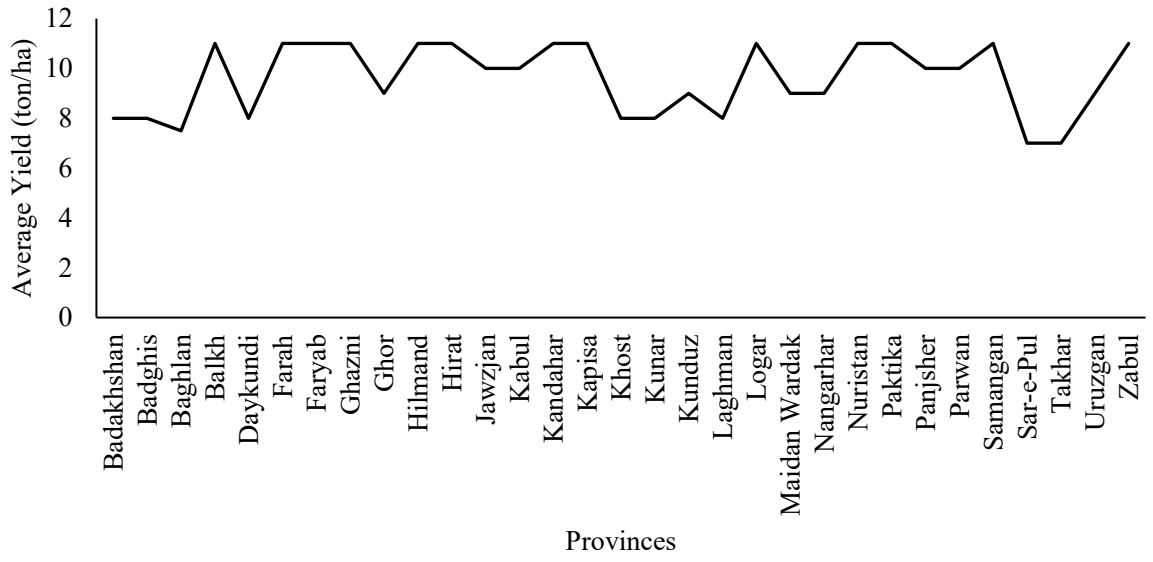
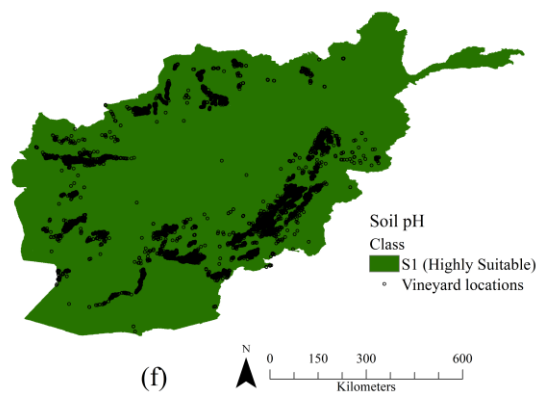
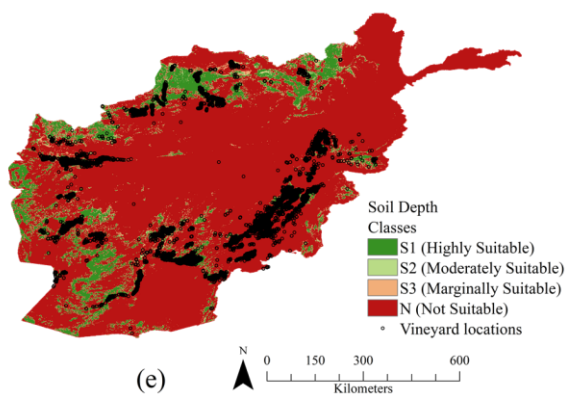
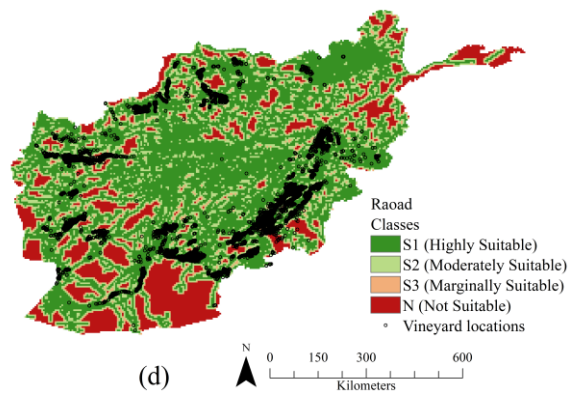
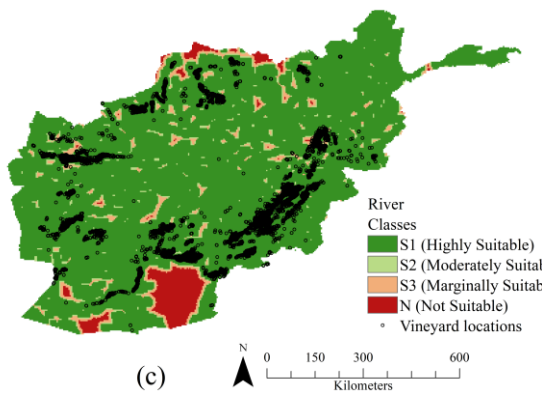
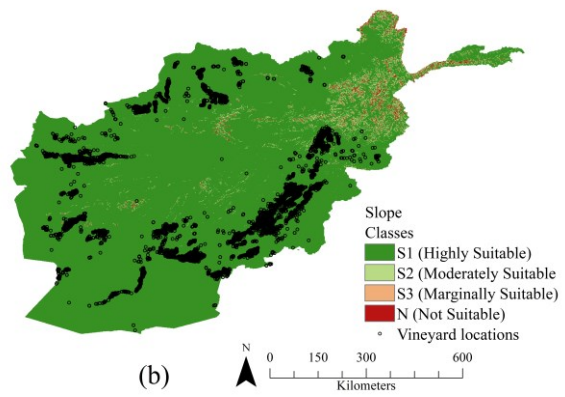
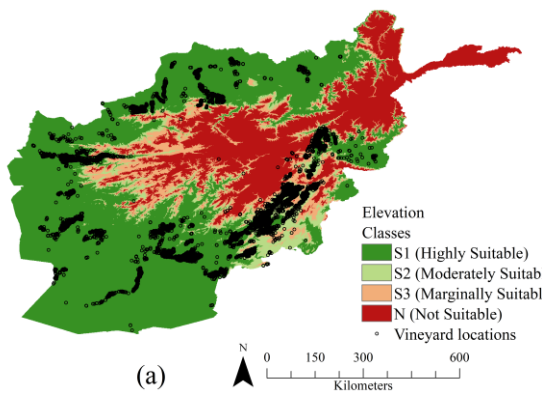


Figure 6.7 Average yield of table grapes (ton/ha) in Afghanistan during 2020



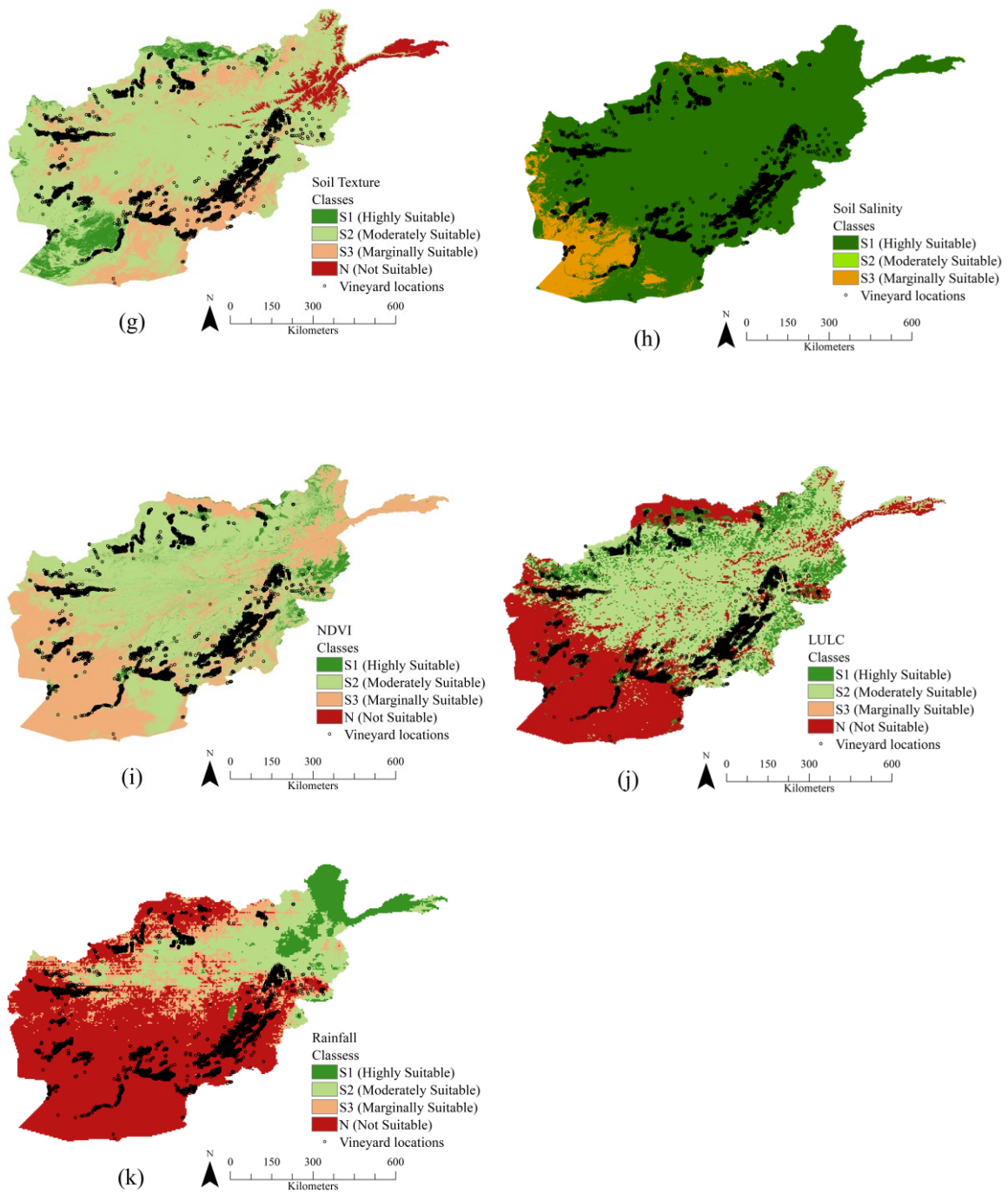


Figure 6.8 Reclassification of the criterion used for suitability analysis (a-k)

6.3 Results

6.3.1 Reclassification of Criteria for Micro to Macro Scales

The raster and vector layers were reclassified based on suitability classes into highly suitable, moderately suitable, marginally suitable and not suitable categories for micro and macro scales (**Figure 6.5 and 6.6**). The reclassification of all the criteria were done based on references (**Appendix 6.1**). In the reclassification of criteria, vegetation indices, NDVI reported that 6.4% of lands (30489 ha) were highly suitable. However, in climatic variables, rainfall had the highest percentage for area coverage for the highly suitable areas during the study periods (**Figure 6.5 and 6.6 (a-c)**).

Moreover, the reclassification of topographic criterion reported that 52.7 % of land were located in the highly suitable category (**Figure 6.5 and 6.6 (d-g)**). Again, soil texture covered 98% (6601.7ha) and soil types 82.7% (381497.9 ha) located in highly suitable category (**Figure 6.4 6.5 (i-o)**). However, in the case of the socio-economic criterion, there were six parameters considered for reclassification. Among them, population density referred to the highest percentage (94.9%) of lands that belonged to high suitable areas (**Figure 6.5 and 6.6 (p-t)**). The results indicated that population density was the important criterion because the average population is important for proper agricultural intensification in vineyard operations.

6.3.2 Analytical Hierarchy Process Weights (AHP)

In this study, the suitable area was monitored in the vineyards of Kabul Province using the weighted overlay method. First, each parameter was reclassified referring to the previous research, and then the AHP weight was assigned based on the expert's opinions (**Table 6.6 and Table 6.7**). The AHP results for physical criterion were indicated that soil texture (13.2%) was the most influenced, followed by organic matter (11.9%), soil pH (11%), soil depth (10.6), soil salinity (8.2%), rainfall (7.6%), NDVI (5.6%), soil type (5.6%), LST (5.1%), NDMI (4.8%), aspect (4.8%), land cover (4.7%), elevation (3.4%) and with the least influenced by the slope (3.2%). Moreover, the AHP determined weight for the socio-economic parameters and the highest weight was observed for the distance from the road (22.4%), followed by distance from the national market (18.8%), distance from river (17.1%), population density (16.4%), the distance from local market (13.3%) and the benefit- cost ratio (12%). The integrated average weights were assigned from the experts' opinions and reported that the physical criterion had an influence of 58%, and the socio-economics criterion had 42% for table grape production (**Table 6.6 and Table 6.7**).

Table 6.6 AHP weights according the expert's opinions for physical criterion

No	Criteria	A (35)	B (16)	C (9)	D (8)	E (12)	Mean	Weight
1	Soil Type	0.090	0.013	0.048	0.073	0.015	0.06	5.6
2	Soil pH	0.145	0.022	0.132	0.143	0.061	0.11	11.0
3	Soil Depth	0.131	0.027	0.145	0.123	0.145	0.11	10.6
4	Soil Texture	0.134	0.090	0.159	0.145	0.020	0.13	13.2
5	Soil Organic Matter	0.144	0.039	0.134	0.160	0.080	0.12	11.9
6	Soil Salinity	0.088	0.014	0.126	0.101	0.172	0.08	8.2
7	NDVI	0.043	0.081	0.065	0.040	0.161	0.06	5.7
8	NDMI	0.040	0.065	0.046	0.043	0.078	0.05	4.8
9	Rainfall	0.091	0.066	0.058	0.087	0.127	0.08	7.6
10	Slop	0.024	0.067	0.018	0.020	0.041	0.03	3.2
11	Elevation	0.021	0.080	0.015	0.019	0.026	0.03	3.4
12	LST	0.023	0.132	0.031	0.020	0.019	0.05	5.1
13	Land Cover	0.013	0.149	0.011	0.014	0.031	0.05	4.7
14	Aspect	0.012	0.155	0.011	0.013	0.023	0.05	4.8
Sum		1.00	1.00	1.00	1.00	1.00	1.00	100
Overall weight		0.8	0.6	0.6	0.5	0.4	0.58	58

* A-E indicated the expert numbers and number in parenthesis indicated the years of working experiences in the Agriculture sector for each of the experts, respectively

Table 6.7 AHP weights according the expert's opinions for socio-economic criteris

No	Criteria	A (35)	B (16)	C (9)	D (8)	E (12)	Mean	Weight
1	Distance from road	0.286	0.386	0.227	0.087	0.133	0.22	22.4
2	Distance from river	0.175	0.283	0.330	0.026	0.040	0.17	17.1
3	Population density	0.355	0.063	0.329	0.037	0.037	0.16	16.4
4	Benefit- cost ratio	0.089	0.144	0.039	0.192	0.136	0.12	12.0
5	Distance from local market	0.044	0.074	0.038	0.131	0.380	0.13	13.3
6	Distance from to national market	0.051	0.049	0.037	0.528	0.275	0.19	18.8
Sum		1.00	1.00	1.00	1.00	1.00	1.00	100
Overall weight		0.20	0.40	0.40	0.50	0.60	0.42	42

* A-E indicated the expert numbers and number in parenthesis indicated the years of working experiences in the Agriculture sector for each of the experts, respectively

6.3.3 Land Suitability Analysis

Suitable conditions were determined and reclassification was done for suitability analysis according to Appendix Table 6.1. First, the physical criterion map was developed using an AHP-based weighted overlay in the ArcGIS® environment. The results indicated that 22% of lands (100.8 ha) were highly, 27% (121.6 ha) moderately, 31% (141.3 ha) marginally and 20% (455.8 ha) lands were not suitable for grape production at micro-scale of Shakardar District. However the macro-scale results indicated that 11% of lands (739.17 ha) were highly, 25% (1654.5 ha) moderately, 36% (2376.4 ha) marginally and 28% (1892.8 ha) lands were not suitable for grape production in the Kabul Province (**Figure 6.9 and 6.10**). According to the physical criterion, the highly suitable lands were located in the north and east regions of Kabul Province. Furthermore, the socio-economic criterion also considered AHP-based weights for developing the suitability map based on the socio-economic criteria. The findings revealed at micro-scale that 29% (95.5 ha) of lands were highly suitable for grape production, 25% (82 ha) were moderately suitable, 37% (123.8 ha) were marginally suitable, and 9% (0.0009 ha) were not suitable for grape production and in macro-scale of Kabul Province 16% (764.6 ha) of lands were highly suitable for grape production, 18% (861.7 ha) were moderately suitable, 28% (1385.3 ha) were marginally suitable, and 38% (1870.7 ha) were not suitable for grape production in Kabul Province (**Figure 6.11 and 6.12**). The socio-economic criterion is not directly related to grape production, however, it has an important role in limiting table grape production.

Furthermore, the combined suitability map was developed from the physical and socio-economic maps by considering average weights from the experts opinions from micro to macro scales. Both maps were overlaid based on the overall percentage of influence. According to the combined land suitability results, the most suitable areas were 46% highly, 50% moderately, and 4% marginally for grape production at micro-scale. However, at macro scale the most suitable areas were 13% highly, 26% moderately, 29% marginally and 33% not suitable for grape production in the Kabul Province of Afghanistan (**Figure. 6.13 and 6.14**). Lastly, not suitable and marginal lands were identified from the combined land suitability map to support the growers by providing subsidies specially marginal and not suitable lands for production. According to the final suitability map out of 358 vineyards at micro-level 27 vineyards were located in a highly suitable areas and 86 vineyards were located in moderately and 2 vineyards in marginally ares. However, at macro-level out of 1759 vineyards, 1112 vineyards were located in a highly suitable areas and 549 vineyards were located in moderately suitable areas, 75 vineyards in marginally suitable areas and 23 in not suitable areas (**Table 6.8**).

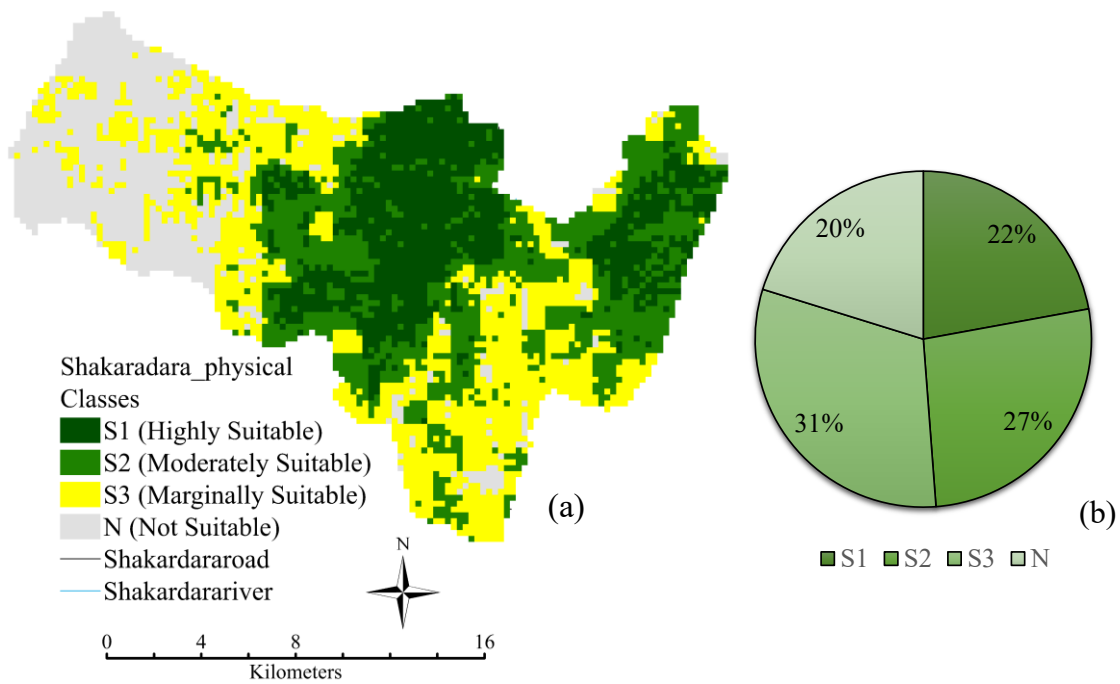


Figure 6.9 (a) Land suitability analysis for grape production based on physical criterion at micro-Scale (Shakardara District) and (b) pie chart showing the percentage of land for each of the four suitability classes.

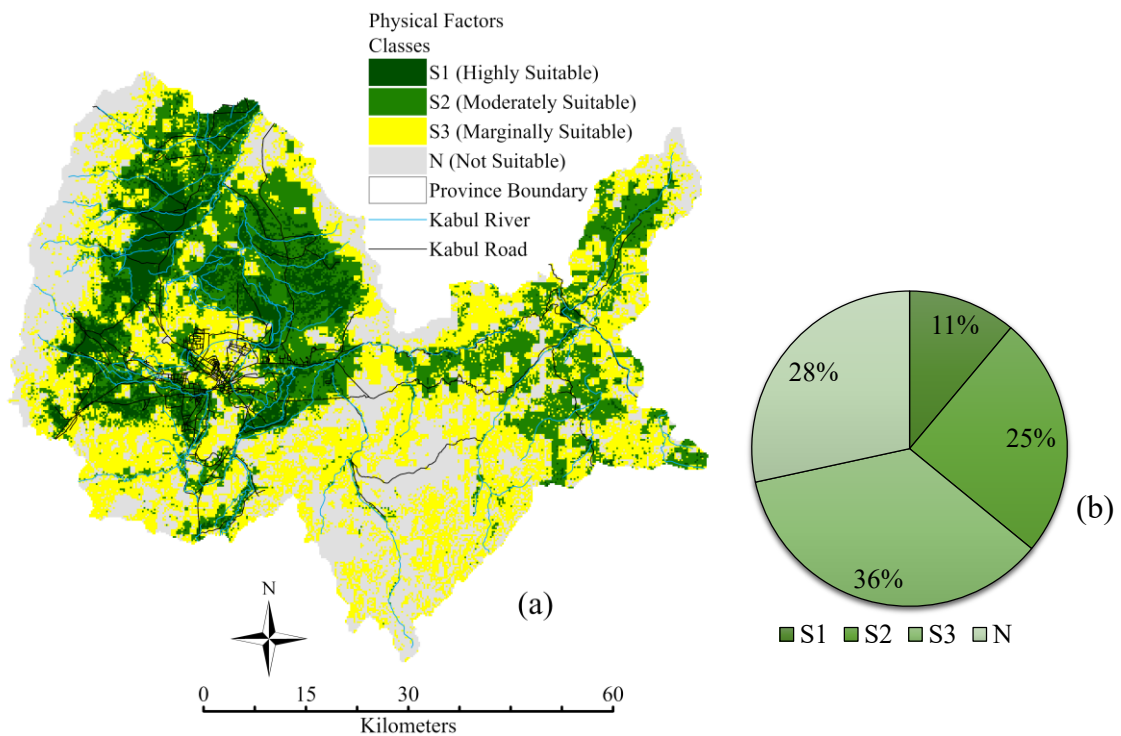


Figure 6.10 (a) Land suitability analysis for grape production based on physical criterion at macro-scale (Kabul Province) (b) pie chart showing the percentage of land for each of the four suitability classes.

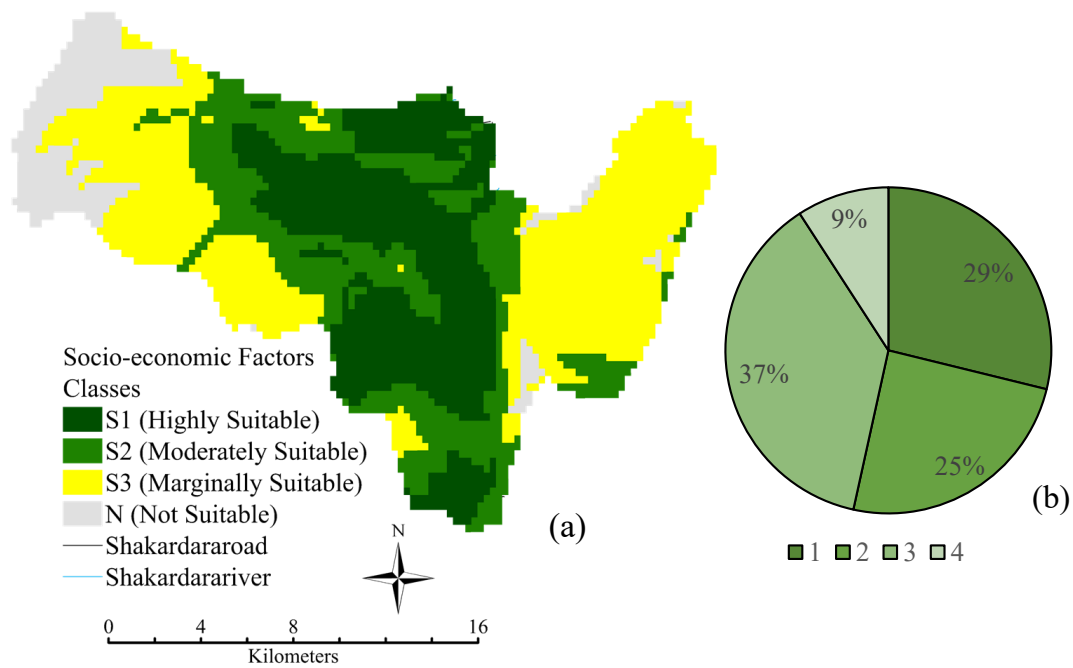


Figure 6.11 (a) Land suitability map for grape production based on socio-economical criterion at micro-scale and (b) pie chart showing the percentage of land for each of the four suitability classes.

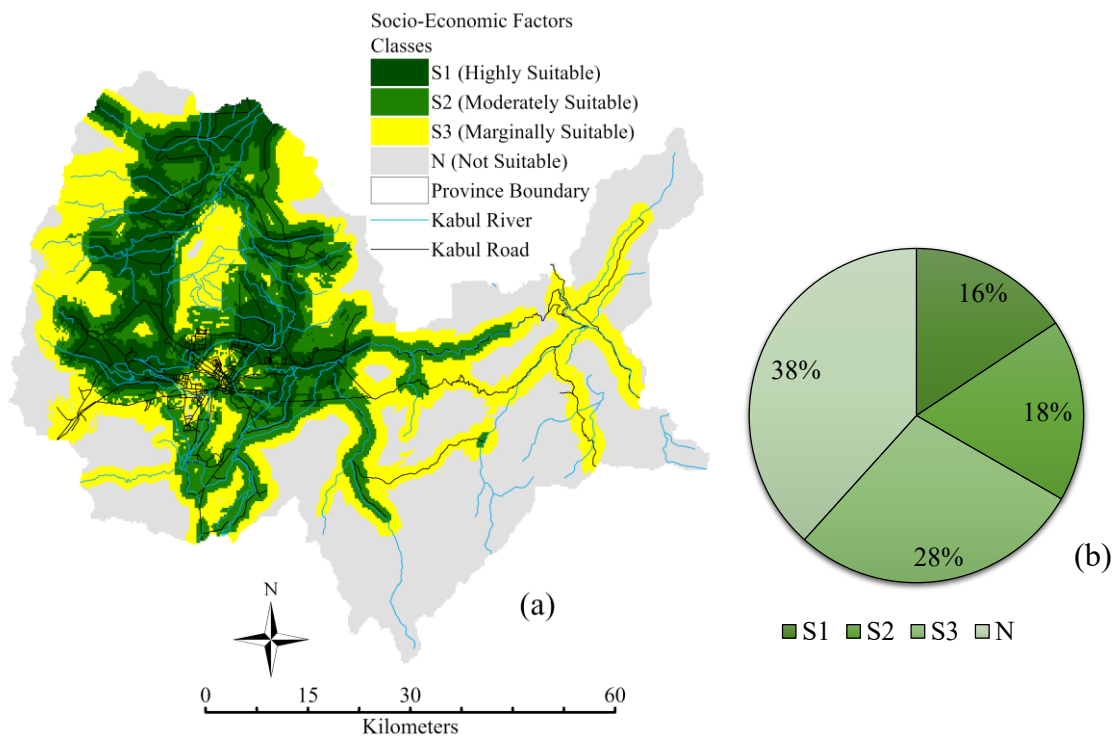


Figure 6.12 (a) Land suitability map for grape production based on socio-economical criterion at macro-scale and (b) pie chart showing the percentage of land for each of the four suitability classes.

Table 6.8 Vineyards suitability classes based on combined physical and socio-economic factors at micro and marco scales

Classes	Area%		Surveyed Vineyards		Vineyards Area (ha)	
	Micro-scale	Macro-scale	Micro-scale	Macro-scale	Micro-scale	Macro-scale
S1	46	13	27	1112	818	8223.90
S2	50	26	86	549	615	2200.59
S3	4	29	2	75	14	152.69
N	0	32	0	23	0	22.766
Total	100	100	358	1759	1447	10599.96

6.3.4 Reclassification of Criteria for Regional Scale

6.3.4.1 Fuzzy Overlay Analysis

In this research, eleven fuzzy layers: elevation, slope, river, road, soil depth, soil pH, soil texture, soil salinity, NDVI, LULC, and rainfall were used for vineyard suitability analysis. First, the criteria were reclassified based on a fuzzy membership function (**Figure 6.8 (a-k)**). This was done based on references and previous literature. Subsequently, the fuzzy overlay method was used to develop the suitable region, the area and percentage of area coverage were calculated per pixel (**Table 6.9**) for all Afghanistan. The fuzzy suitability results indicated that in overall Afghanistan 23% (15760144 ha) of land in highly, 44% (30307470 ha) moderately, 22% (15403607 ha) marginally and 11% (7370025 ha) were not suitable for grape production in Afghanistan. To confirm the present vineyard locations, the results indicated that 90.3% (80466 ha) of the vineyards were located in the highly, 7.3% (6533 ha) moderately, 2.4% (2124 ha) marginally, and 0.01% (5 ha) not suitable areas in Afghanistan (**Figure 6.15 Table 6.10**).

Table 6.9 Potential areas belonging to the suitable classes based on fuzzy algorithms for Afghanistan

Suitability			
Classes	Pixels	Area (ha)	Area (%)
S1	174763186	15760144	23
S2	336077507	30307470	44
S3	170809566	15403607	22
N	81725718	15403607	11
Total			100

Table 3.10 Potential areas belonging to the suitable classes based on fuzzy algorithms for Afghanistan
Vineyard locations of each suitability class in Afghanistan

Suitability Classes	Pixels	Vineyards Area (ha)	Vineyard Area (%)
S1	892282	80466	90.3
S2	72447	6533	7.3
S3	23553	2124	2.4
N	57	5	0.013
Total			100

6.3.4.2 Fuzzy Suitability Validation

Ground validation of the suitability map is significant for confirming each suitable vineyard and extending the vineyard areas for the future in Afghanistan. However, obtaining a large number of ground datasets in the country's current condition is very difficult. Consequently, the model validation was done by evaluating and testing the proxy of ground data. In the context of this study, validation was performed using regression analysis between the average vineyard area from the land suitability index and the average yield of grapes in each province (**Figure 6.16**). The result indicated a good agreement between the land suitability index and grape yield. The correlation coefficients were 0.74 on the regional scale.

6.4 Discussion

Synthesizing Landsat 8 OLI and TIRS scenes, metrological, topographic, soil and socio-economic datasets were used to develop a land suitability map for grape production from micro to regional scales. The expert's judgment from micro to macro scales indicated that the soil texture and soil pH were the most important criterion while producing the grapes (13% and 11%). In socio-economic criteria, the distance from the road and distance from the national market was observed as the most essential criterion (22% and 18%). Previous studies also implied that the physical properties of vineyards, such as soil are critically important for the grape's quality and productivity (Zdruli et al., 2014). These two socio-economic indicators above mentioned were significant because of carrying the inputs to vineyards and transporting fresh grapes to the market in the study areas. The findings from micro to macro scales indicated that most of the vineyards were located in the north part of Kabul Province.

However, based on fuzzy suitability assessment, indicated that highly suitable regions were mostly located in the southern agroclimatology with some parts of the central zone and northern zone. These

regions include Kabul, Logar, Khandahar, Kapisa, Ghazni, Zabul, Uruzgan, Kandahar, Herate, Badghis, Frayah, Jawzjan, Balkh, Kunduz, and Takhar provinces. According to the findings of the study, there was 23% of land in Afghanistan with potential for vineyard extension. However, only 0.13% of the land area is currently under vineyard production practices. Some provinces have the highest potential for vineyard extension, such as Badghis, Faryab, Herat and Takher. The government could act to increase vineyards since the suitable areas exceed the reality. Because grapes are an industrial crop and fresh grapes play an important role in growers' farm income and international trade in Afghanistan. The extension of vineyards will support farmers' livelihoods and be a good replacement for opium cultivation, especially in southern provinces. Besides, to improve grape grower households' income and livelihood, implementing a national subsidy program is very important for grape production based on land suitability and access to facilities and infrastructure. In most countries, especially underdeveloped countries, the government has tried to reduce production costs, increase the welfare of farmers and their competitive power in global markets by providing a proper subsidy scheme to them.

Currently, in Afghanistan, there is no specific subsidy scheme for grape growers. Although agricultural subsidies are an essential aspect of agricultural production and play an important role in international trade. Therefore, a subsidy program can be introduced to increase grape production regionally by considering land suitability based on physical and socio-economic criteria that influence production.

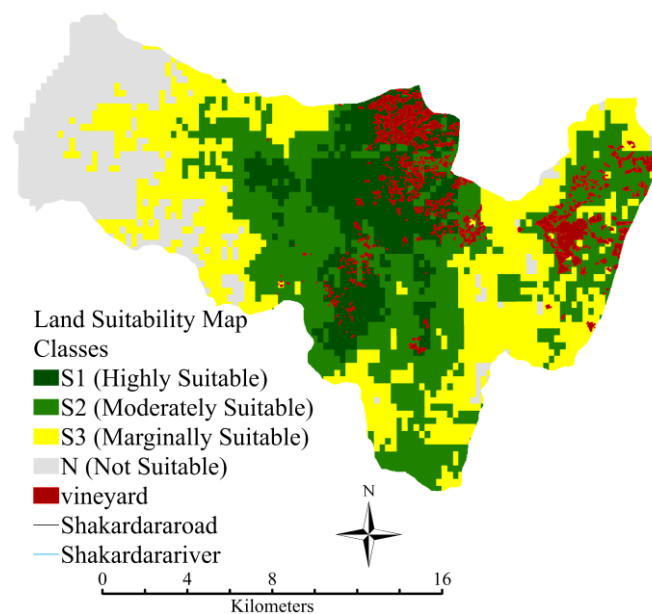


Figure 6.13 Land suitability analysis combining physical and socio economic for grape production in Shakaradara District

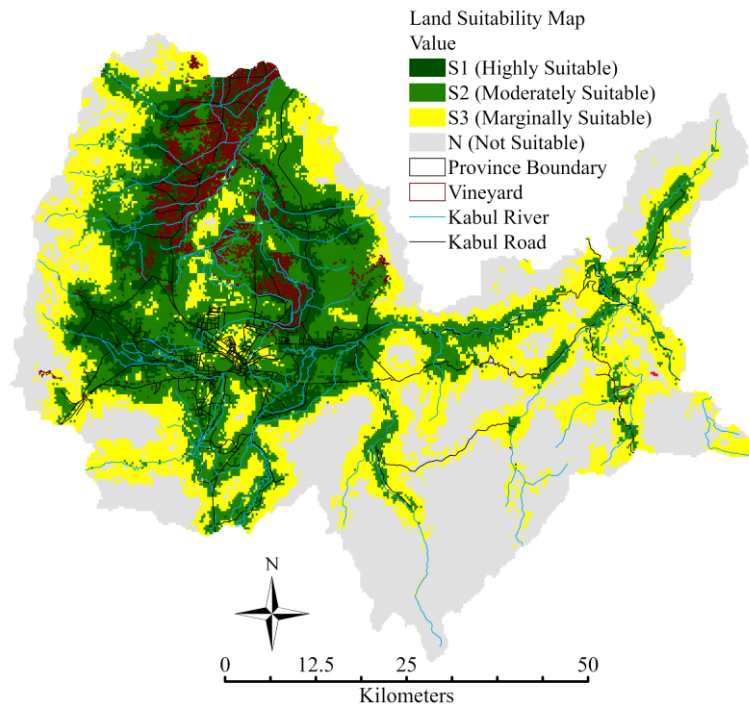


Figure 6.14 Land suitability analysis combining physical and socio economic for grape production in Kabul Province

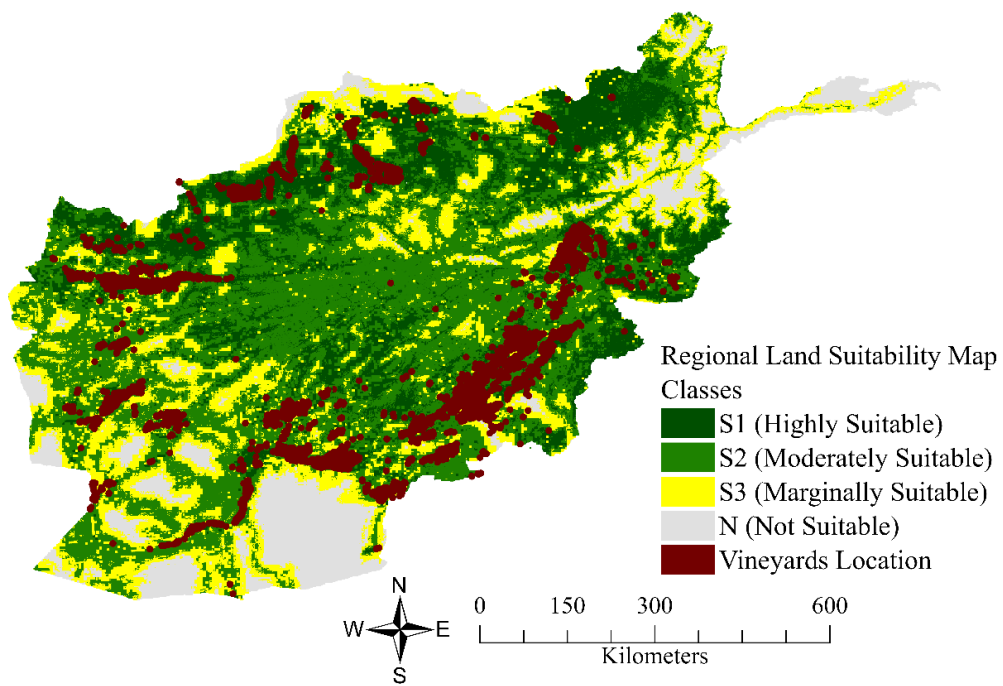


Figure 6.15 Suitable areas for table grape production in Afghanistan based on fuzzy multicriteria decision analysis

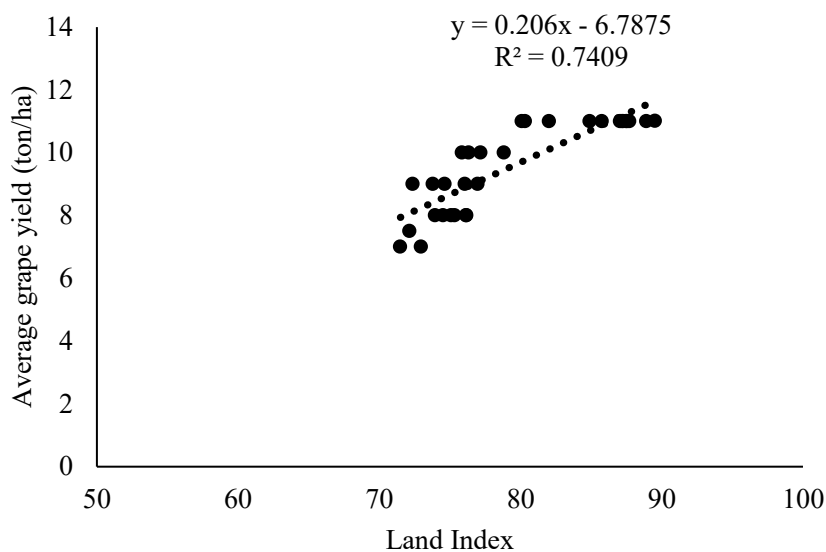


Figure 6.16. Validation of the fuzzy-based land suitability score referring to the average grape yield from different provinces in Afghanistan

6.5 Conclusions

Appropriate selection of physical and socio-economic criteria is important for land suitability analysis to increase table grape production and productivity. The socio-economic criteria significantly influence the livelihoods of vineyard growers and their decisions on whether to grow table grapes. Therefore, this study carried out the selection of multiple criteria to develop a land suitability model on a provincial to regional scales to find out the suitable areas for table grape production. The multi-criteria decision analysis was performed for suitability assessment using twenty criteria, fourteen focusing on the physical criterion and six for the socio-economic criterion for micro to macro scales. However, for regional scales eleven biophysical criterion were considered. The suitability model used the FAO land use/land cover layer and masked the restricted zones for selecting the vineyard area. Through this research, we found that only 11% physically, 15% socio-economically, and 13% of lands in a combination of both physical and socio-economic criteria were highly suitable for grape production in the Kabul Province. However, the regional scale suitability result indicated that 23% of the area was highly suitable. The validation results showed that the land suitability model had 74% accuracy at the regional scale. In the analysis, we have found that less than 1% of highly suitable area were used for vineyard. Therefore, there are significant opportunity to increase the production of table grapes another 21% highly suitable areas. This research has the potential to be applied toward determining the suitable areas on a regional scale with similar environmental conditions. Furthermore, inclusion of socio-economic criteria in regional land suitability analysis can support the vineyard growers with the allocation of subsidies to increase the total production of table grapes and the livelihoods of growers.

Chapter 7

Overall Conclusions

Grapes are more susceptible to climate change and vulnerable to droughts, with lower production in southeast Asian countries, including Afghanistan. During drought periods, grapes suffer from poor berry development and production losses in drought-prone regions of Afghanistan. Therefore, drought assessment and intervention are required to reduce the effects of drought on vineyards and sustain farmers' livelihoods. Satellite remote sensing datasets comprising vegetation, soil, and climatic parameters could be trained using machine learning algorithms to anticipate long-term changes in yield assessment and weather forecasts for grower interventions. In this regard, yield evaluation in drought-prone areas was done by using satellite remote sensing-based time series datasets and a machine learning approach to assess grape growers during drought periods. The research goal was broken down into four specific targets: predicting yield using machine learning at the micro-scale, estimating yield loss using a composite drought index at the macro-scale, assessing the severity of drought in vineyards at the regional-scale, and assessing the land's suitability from micro to the regional scales.

7.1. Yield Prediction using Machine Learning at Micro-scale

The first objective of this study attempted to create a predictive yield model based on satellite remote sensing and machine learning approaches. Since the growth stages of the grapevine have a significant impact on vineyard yield perdition. Therefore, yield perdition of grapes has a significant impact on monitoring of vineyard production and yield prediction throughout the season, especially during the drought-affected years at the district levels studied. This study was performed at the micro level. In this study, NDVI, LAI, and NDWI were utilized to forecast grape output across the growing season. The findings suggested that in 2017 and 2019, the NDVI had the highest performance ($r^2=0.79$) of all the vegetative indices; however, in 2019, the LAI reliability ($r^2=0.79$) was greater than the other indices. According to the ANN-based machine-learning results, the NDVI had the highest identifying effectiveness ($R = 0.94$) in 2017, 2018 ($R = 0.95$), and 2019 ($R = 0.92$). This study developed a model for predicting grape yields and creating yield maps with regional variability. Predicting yield of grapes at different stages could help stabilize the import, export, and marketing strategies during the grape's yield losses due to extreme events.

7.2. Yield loss Assessment Using Composite Drought Index at Macro-scale

In this study, yield loss assessment was performed at a macro scale using a composite drought index derived from satellite remote sensing-based time-series datasets. As a result, the CDI was used to

monitor drought in Kabul Province vineyards from 2016 to 2020. In this regard, a satellite-based composite drought index (CDI) was developed from five climatic (precipitation condition index, temperature), agricultural (normalized difference vegetation index and normalized difference moisture index) and drought indices (vegetation condition index, temperature condition index, and deviation of NDVI from long term mean) at micro scale. The PCA was used for weighting each index in order to create a single map for one year. A precise and accurate drought risk map was prepared with a high accuracy level of 64.74%. According to the CDI, drought in Kabul Province was observed to be moderate to severe between 2016 and 2018. The yield loss results indicated that the 2018 (4.9 ton/ha) yield losses were much greater than the 2016 (3.4 ton/ha) losses in severely drought-affected vineyards. This research will support and help grape growers and the government to support farmers during the severe drought conditions by providing a subsidy in Kabul Province, Afghanistan.

7.3. Vineyard Drought Severity Assessment at Regional Scale

The primary objective of this research was to evaluate drought severity in the berry growth stage through the veraison stages of growth. Since the traditional method for drought assessment is not so effective, using satellite images and satellite-based climatic datasets was a cost-effective method. In this study, drought severity was attempted at regional using SVI and SPI for the years 2013 to 2021 in Afghanistan. Since the datasets were big, the Google Earth engine was used to utilize the raw datasets. The total table grape yield ton per hectare for all provinces was collected from the statistical department of Islamic Republic of Afghanistan. Finally, the depth map validation was done with the table grape yield. The results showed that the drought intensity was extremely high throughout Afghanistan between 2018 and 2021. In 2018, 4785.03 hectares and in 2021, 1825.83 hectares were extremely affected by drought. Based on research findings, the coefficient of determination (r^2) was high in June ($r^2=0.79$) and July ($r^2=0.71$). However, in August, it is very low because it is near to harvest time. Therefore, more water causes fungal disease in grapes and causes yield loss. This research could help governments and policymakers assist farmers by providing a drought severity-based subsidy scheme.

7.4. Land Suitability Assessment from Micro to Regional scales

This study's primary objective was to determine the quality of vineyard soil after systemic and localized drought from a micro to regional scales using satellite remote sensing and multi-criteria decision analysis. In this search, two methods were used for suitability analysis for micro to regional scales. This intervention was utilized to evaluate land suitability based on soil, climate, vegetation, and socio-economic indicators in order to reallocate subsidies based on land suitability or extend the area of

vineyards based on soil quality. Thus, this research used a variety of variables to construct a land suitability model at a micro-to-macro level to identify potential sites for table grape cultivation. Twenty variables were used in the multi-criteria decision analysis for suitability evaluation. Fourteen were for the physical and six were for the socio-economic indicators. However, in the regional-scale suitability method, eleven biophysical and climatic criteria were used. The finding suggested that 46% were high, 50% moderately, and 4% marginally suitable at the micro-scale and just 13% of fields were highly, 26% moderately, 29% marginally, and 33% not suitable for grape production based on a combination of both physical and socioeconomic criteria at macro-scale. Almost 60% of vineyards located in marginally suitable regions or in unsuitable regions at the macro-scale need government support to increase their productivity. The fuzzy suitability finding showed that 23% highly, 44% moderately, 22% marginally and 11% not suitable for grapes production in all over Afghanistan. This research has the potential to be used to identify appropriate sites with similar environmental conditions. A further study will be required to validate the regional scale to suitability region based on the field survey and farmers prospective. In this regard, different agroclimatology variables will be used to develop a regional suitability map. A subsidy scheme based on drought severity is required following the identification of marginally and unsuitable vineyard locations. These integrated models might be employed in table grape production logistics and decision making.

7.5 Future Contributions

Calculating yield loss due to natural disasters based on satellite remote sensing is very important for underdeveloped countries, especially countries like Afghanistan, where field security makes it difficult to get data from the ground. In recent years, different high-resolution satellites and analyzing platforms have been used for this purpose. Farmers and stakeholders may use the data to determine if their lands are suitable for farming. This information may be used by associations to provide their members with knowledge and policy recommendations. Farmers will also find benefits in better understanding and managing their holdings or in creating more precise cost estimations. Finally, the data may be used to create estimations, inventories, and action plans for academics studying data needs, drought, and climate change. Additionally, being familiar with the creation, training, and evaluation of machine learning models as well as publications may aid emerging agricultural machine learning researchers in properly setting up and monitoring their machine learning programs, leading to the creation of thorough mid-term best-practice guidelines. In the long term, we anticipate that this research will aid us in understanding and proposing improvements in the evasion of an early warning system using machine learning and artificial intelligence.

Acknowledgement

Firstly, I would like to convey praise to a magnificent deity for his unending love, support, and advocating for me throughout my doctoral studies. Without the help, direct supervision, and encouragement of many people, I would not have been able to get my doctorate.

My sincere and deepest appreciation goes to my respected academic and research supervisor, Dr. Tofael Ahamed, for his valuable guidance, critical remarks, invaluable assistance, and prompt reaction to all my academic concerns. Of course, without his supervision and guidance, I would not be able to achieve my PhD and develop myself as a scientist. Thank you so much for everything!!!

I would like to express my heartfelt thanks to Associate Professor Ryozo Noguchi and Professor Matsushita Shusuke for their guidance, motivation, and suggestions. Their insightful inquiries and suggestions constantly help me improve my studies. Furthermore, I would like to convey my heartfelt appreciation and thanks to Professor Atsushi Ishii, Professor Toshiharu Enomae, and Yutaka Kitamura, who were on the advisory and examination committees, for their insightful remarks and ideas that helped to improve my research and dissertation.

I would be glad to thank my fellow labmates, Dr. Nazia Muhsin, Dr. Md. Monjurul Islam, Dr. Pengbo Gao, Dr. Animesh Chandra Das, Dr. Rubaiya Binte Mostafiz, Dr. Nety Nurda, Dr. Iqbal Habibie, Dr. Md. Monirul Islam, Md. Shamsuzzoha, Kazi Faiz Alam, Munira Hayati and Yun Yan Xie for their continuous support, stimulating discussions, and suggestions during Zemi (Seminar). I consider myself fortunate to have made such excellent friends.

I would like to convey my heartfelt appreciation to my Kabul University colleague, Mr. Tariq Salari, and a group of farmers and Kabul University students who helped me collect ground reference data from Shakardara District and Kabul Province, Afghanistan. Their kind assistance and fieldwork aided in the correlation of satellite datasets with ground reference datasets. Furthermore, I would like to thank the United States Geological Survey (USGS), Japan Aerospace Exploration Agency (JAXA), Climate Hazards Group Infrared Precipitation with Station Data (CHIRPS), World Food Organization (FAO), and Afghanistan Geodesy and Cartography Head Office (AGCHO) for providing satellite, GIS and climatic datasets available to student and researcher worldwide. Moreover, I acknowledge the usage of the U.S. Geological Survey product by the name of LANDSAT/LC08/C01/T1_8DAY_NDVI and the Google Earth Engine developers for creating such a great platform for large data analysis.

Thank you to the University of Tsukuba in Japan for allowing me to do my study there, in addition, I would like to express my gratitude to the More Jobs Better Lives (MJBL) Japanese foundation, which has provided me with a scholarship to continue my study at the University of Tsukuba. In addition, I would like to express my gratitude to the admiring personnel at the University of Tsukuba's Graduate

School of Life and Environmental Sciences for their help on different occasions during my study period at this university.

Finally, I am extremely grateful to my family for their support, inspiration, acceptance, and patience during my PhD program. My parents deserve special recognition for their love, sacrifices, and prayers for my education and achievements. A special thanks to my father-in-law's spiritual and financial support. Without his support, our survival would not have been possible in Japan. A heartfelt thanks to my mother-in-law, brothers and sisters. In addition, my grateful thanks to my lovely spouse, Dr. Ahmad Shekib Arab, and my daughters, Sana Arab and Husna Arab, for your unlimited love, care, and support. I could not have done my PhD journey without your support, suggestions, and companionship. There are no words to convey how much I love you.

With Thanks
Sara Tokhi Arab

References

- Acharya, T. D., and Yang, I. T. (2015). Vineyard suitability analysis of Nepal. *International Journal of Environmental Sciences*, 6(1), 13.[10.6088/ijes.6002](https://doi.org/10.6088/ijes.6002).
- Adger, W.N., Safra de Campos, R., Siddiqui, T., Franco Gavonel, M., Szaboova, L., Rocky, M.H., Bhuiyan, M.R.A. and Billah, T. (2021). Human security of urban migrant populations affected by length of residence and environmental hazards. *Journal of Peace Research*, 58, 50-66. <https://doi.org/10.1177/0022343320973717>.
- Afghanistan Central Statistics Organization (2013). Central statistics organization of Afghanistan's statistical yearbook. Islamic Republic of Afghanistan National Statistics and Information Authority, Kabul Afghanistan (35). 2015.
- Afghanistan Central Statistics Organization (2014). Central statistics organization of Afghanistan's statistical yearbook. Islamic Republic of Afghanistan National Statistics and Information Authority, Kabul Afghanistan (36). 2015.
- Afghanistan Central Statistics Organization (2015). Central statistics organization of Afghanistan's statistical yearbook. Islamic Republic of Afghanistan National Statistics and Information Authority, Kabul Afghanistan (37). 2016.
- Afghanistan Central Statistics Organization (2016). Central statistics organization of Afghanistan's statistical yearbook. Islamic Republic of Afghanistan National Statistics and Information Authority, Kabul Afghanistan (38). April 2017.
- Afghanistan Central Statistics Organization (2017). Central statistics organization of Afghanistan's statistical yearbook. Islamic Republic of Afghanistan National Statistics and Information Authority, Kabul Afghanistan (39). 2018.
- Afghanistan Central Statistics Organization (2018). Central statistics organization of Afghanistan's statistical yearbook. Islamic Republic of Afghanistan National Statistics and Information Authority, Kabul Afghanistan (40). July 2019. https://rise.esmap.org/data/files/library/afghanistan/Electricity%20Access/Afghanistan_Statistical-Yearbook-2018-19_compressed.pdf. Last access 12 March 2022.
- Afghanistan Central Statistics Organization (ACSO) (2019). Central Statistics Organization of Afghanistan's Statistical Yearbook of 2018-2019. Islamic Republic of Afghanistan National Statistics and Information Authority, Kabul Afghanistan.
- Afghanistan Central Statistics Organization (ACSO) (2020). Central statistics organization of Afghanistan's statistical yearbook of 2018-2019. Islamic Republic of Afghanistan National Statistics and Information Authority, Kabul Afghanistan (42). April

202.<https://invest.gov.af/theme3/wp-content/uploads/2021/06/Afghanistan-Statistical-Yearbook-first-Version.pdf>.

- Aguaron, J., Escobar, M. T., & Moreno-Jiménez, J. M (2003). Consistency stability intervals for a judgement in AHP decision support systems. *European Journal of Operational Research*, 145(2), 382-393. [https://doi.org/10.1016/S0377-2217\(02\)00544-1](https://doi.org/10.1016/S0377-2217(02)00544-1)
- Agutu, N.O., Awange, J.L., Zerihun, A., Ndehedehe, C.E., Kuhn, M. and Fukuda, Y. (2017). Assessing multi-satellite remote sensing, reanalysis, and land surface models' products in characterizing agricultural drought in East Africa. *Remote sensing of environment*, 194, pp.287-302. <https://doi.org/10.1016/j.rse.2017.03.041>
- Aich, V., Akhundzadah, N.A., Knuerr, A., Khoshbeen, A.J., Hattermann, F., Paeth, H., Scanlon, A., Paton, E.N. (2017). Climate change in Afghanistan deduced from reanalysis and coordinated regional climate downscaling experiment (cordex)—South Asia simulations, *J. Clim.* 5, 38. <https://doi.org/10.3390/cli5020038>.
- Aich, Valentin and Khoshbeen, Ahmad Jamshed. (2016). *AFGHANISTAN: CLIMATE CHANGE SCIENCE PERSPECTIVES*. Kabul: National Environmental Protection Agency & UN Environment. https://postconflict.unep.ch/publications/Afghanistan/UNEP_AFG_CC_Science_perspectives.pdf.
- Akıncı, H., Özalp, A.Y. and Turgut, B. (2013). Agricultural land use suitability analysis using GIS and AHP technique. *Computers and electronics in agriculture*, 97, pp.71-82. <https://doi.org/10.1016/j.compag.2013.07.006>.
- Ali, I., Cawkwell, F., Dwyer, E., Barrett, B. and Green, S. (2016). Satellite remote sensing of grasslands: from observation to management. *Journal of Plant Ecology*. 9, 649-671. <https://doi.org/10.1093/jpe/rtw005>.
- Almadani, M.A. (2022). Drought Assessment Using Standardized Precipitation Index (SPI) Case Study: Sulphur Springs Tampa FL. In *Proceedings of the 3rd International Conference on Green Environmental Engineering and Technology* (pp. 133-146). Springer, Singapore. https://doi.org/10.1007/978-981-16-7920-9_16
- Alsafadi, K., Bi, S., Bashir, B., Hagra, A., Alatrach, B., Harsanyi, E., Alsalman, A. and Mohammed, S. (2022). Land suitability evaluation for citrus cultivation (*Citrus* spp.) in the southwestern Egyptian delta: a GIS technique-based geospatial MCE-AHP framework. *Arabian Journal of Geosciences*, 15(3), pp.1-17. <https://doi.org/10.1007/s12517-022-09592-4>.

- Alwan, I. A., Aziz, N. A., & Hamoodi, M. N. (2020). Potential water harvesting sites identification using spatial multi-criteria evaluation in Maysan Province, Iraq. *ISPRS International Journal of Geo-Information*, 9(4), 235.
- Anderson, M.C., Hain, C., Wardlow, B., Pimstein, A., Mecikalski, J.R. and Kustas, W.P. (2011). Evaluation of drought indices based on thermal remote sensing of evapotranspiration over the continental United States. *Journal of Climate*, 24(8), pp.2025-2044.
<https://doi.org/10.1175/2010JCLI3812.1>
- Andresen, J. A., and Baule, W. J. (2020). Perennial systems (temperate Fruit Trees and Grapes) agroclimatology. *Linking Agriculture to Climate, Agronomy Monography*, 60, 425-452.
<https://doi.org/10.2134/agronmonogr60.2016.0016>.
- Anjum SA, Xie X, Wang L, et al. (2011) Morphological, physiological and biochemical responses of plants to drought stress. *Afr J Agric Res* 6: 2026-2032.
- Anyamba, A., & Tucker, C. J. (2012). Historical perspective of AVHRR NDVI and vegetation drought monitoring. *Remote sensing of drought: Innovative monitoring approaches*, 23, 20.
<https://digitalcommons.unl.edu/cgi/viewcontent.cgi?article=1217&context=nasapub>
- Arab, A.S., Nakamura, K., Seino, K., Hemat, S., Mashal, M.O. and Tashiro, Y. (2019). Lipid and Diabetic Profiles of School Teachers in Afghanistan Facing Food Insecurity and Their Association with Knowledge Relating to Healthy Lifestyle. *Food and Nutrition Sciences*, 10, 678-693.
[10.4236/fns.2019.106050](https://doi.org/10.4236/fns.2019.106050).
- Arab, S.T., Noguchi, R. and Ahamed, T. (2022). Yield loss assessment of grapes using composite drought index derived from landsat OLI and TIRS datasets. *Remote Sensing Applications: Society and Environment*, p.100727. <https://doi.org/10.1016/j.rsase.2022.100727>
- Arab, S.T., Noguchi, R., Matsushita, S. and Ahamed, T. (2021). Prediction of grape yields from time-series vegetation indices using satellite remote sensing and a machine-learning approach. *Remote Sensing Applications: Society and Environment*, 22, 100485.
<https://doi.org/10.1016/j.rsase.2021.100485>.
- Arab, S.T., Salari, T., Noguchi, R., Ahamed, T. (2022). Land Suitability Analysis for Grape (*Vitis vinifera* L.) Production Using Satellite Remote Sensing, GIS, and Analytical Hierarchy Process. In: Ahamed, T. (eds) *Remote Sensing Application. New Frontiers in Regional Science: Asian Perspectives*, vol 59. Springer, Singapore. https://doi.org/10.1007/978-981-19-0213-0_6
- Aragues, R., Medina, E. T., Clavería, I., Martínez-Cob, A., & Faci, J. (2014). Regulated deficit irrigation, soil salinization and soil sodification in a table grape vineyard drip-irrigated with moderately

- saline waters. *Agricultural water management*, 134, 84-93.
<https://doi.org/10.1016/j.agwat.2013.11.019>.
- Araujo, J. A., Abiodun, B. J., & Crespo, O. (2016). Impacts of drought on grape yields in Western Cape, South Africa. *Theoretical and applied climatology*, 123(1), 117-130.
<https://doi.org/10.1007/s00704-014-1336-3>.
- Aswathi, P. V., Nikam, B. R., Chouksey, A., & Aggarwal, S. P. (2018). Assessment and monitoring of agricultural drought in Maharashtra using meteorological and remote sensing-based indices. *ISPRS annals of Photogrammetry, Remote Sensing & Spatial Information Sciences*, 4(5).<https://pdfs.semanticscholar.org/cdad/7a4a02093556b4ee09e5c981048a08bf2f95.pdf>. Last access 5 May 2022.
- Aulia, M.R., Setiawan, Y. and Fatikhunnada, A. (2016). Drought Detection of West Java's Paddy Field Using MODIS EVI Satellite Images (Case Study: Rancaekek and Rancaekek Wetan). *Procedia Environmental Sciences*, 33, pp.646-653.
<https://doi.org/10.1016/j.proenv.2016.03.119>
- Avena, G.C., Ricotta, C. and Volpe, F. (1999). The influence of principal component analysis on the spatial structure of a multispectral dataset. *International Journal of Remote Sensing*, 20, 3367-3376. <https://doi.org/10.1080/014311699211381>.
- Badamassi, M. B. M., El-Aboudi, A., & Gbetkom, P. G. (2020). A New Index to Better Detect and Monitor Agricultural Drought in Niger Using Multisensor Remote Sensing Data, *Professional Geographer*, 72(3), 421-432. <https://doi.org/10.1080/00330124.2020.1730197>.
- Badr, G., Hoogenboom, G., Moyer, M., Keller, M., Rupp, R., & Davenport, J. (2018). Spatial suitability assessment for vineyard site selection based on fuzzy logic. *Precision Agriculture*, 19(6), 1027-1048. DOI: [10.1007/s11119-018-9572-7](https://doi.org/10.1007/s11119-018-9572-7).
- Ballesteros, R., Intrigliolo, D. S., Ortega, J. F., Ramírez-Cuesta, J. M., Buesa, I., & Moreno, M. A. (2020). Vineyard yield estimation by combining remote sensing, computer vision and artificial neural network techniques. *Precision Agriculture*, 21(6), pp1242-1262.
<https://doi.org/10.1007/s11119-020-09717-3>.
- Baluja, J., Diago, M.P., Balda, P., Zorer, R., Meggio, F., Morales, F. and Tardaguila, J. (2012). Assessment of vineyard water status variability by thermal and multispectral imagery using an unmanned aerial vehicle (UAV). *Irrigation Science*. 30, 511-522. <https://doi.org/10.1007/s00271-012-0382-9>.

- Barnston, A. G., and Livezey, R. E. (1987). Classification, seasonality and persistence of low-frequency atmospheric circulation patterns. *Monthly weather review*, 115, 1083-1126. [https://doi.org/10.1175/1520-0493\(1987\)115<1083:CSAPOL>2.0.CO;2](https://doi.org/10.1175/1520-0493(1987)115<1083:CSAPOL>2.0.CO;2).
- Basile, A., Albrizio, R., Autovino, D., Bonfante, A., De Mascellis, R., Terribile, F., and Giorio, P. (2020). A modelling approach to discriminate contributions of soil hydrological properties and slope gradient to water stress in Mediterranean vineyards. *Agricultural Water Management*, 241, 106338. DOI: [10.1016/j.agwat.2020.106338](https://doi.org/10.1016/j.agwat.2020.106338).
- Bayissa, Y. A., Tadesse, T., Svoboda, M., Wardlow, B., Poulsen, C., Swigart, J., & Van Andel, S. J., (2019). Developing a satellite-based combined drought indicator to monitor agricultural drought: A case study for Ethiopia. *GIScience & Remote Sensing* 56, 718-748. <https://doi.org/10.1080/15481603.2018.1552508>.
- Bhattacharya, S., Halder, S., Nag, S., Roy, P. K., & Roy, M. B. (2021). Assessment of Drought Using Multi-Parameter Indices. *Advances in Water Resources Management for Sustainable Use*, 131, 243.
- Biasi, R., Brunori, E., Ferrara, C. and Salvati, L., (2019). Assessing impacts of climate change on phenology and quality traits of *Vitis vinifera* L.: The contribution of local knowledge, *Plants*, 8, 121. <https://doi.org/10.3390/plants8050121>.
- Bobeca, N., Poni, S., Hilbert, G., Renaud, C., Gomès, E., Delrot, S., Dai, Z. (2015). Differential responses of sugar, organic acids and anthocyanins to source-sink modulation in Cabernet Sauvignon and Sangiovese grapevines, *Front, Plant Sci.*, 6, 382. <https://doi.org/10.3389/fpls.2015.00382>.
- Bonfante, A., Agrillo, A., Albrizio, R., Basile, A., Buonomo, R., De Mascellis, R., ... and Terribile, F. (2015). Functional homogeneous zones (fHZs) in viticultural zoning procedure: an Italian case study on Aglianico vine. *Soil*, 1(1), 427-441. <https://doi.org/10.5194/soil-1-427-2015>.
- Bota, J., Tomás, M., Flexas, J., Medrano, H. and Escalona, J.M. (2016). Differences among grapevine cultivars in their stomatal behavior and water use efficiency under progressive water stress. *Agricultural Water Management*, 164, pp.91-99. <https://doi.org/10.1016/j.agwat.2015.07.016>
- Bramley, R.G.V., and Hamilton, R.P. (2004). Understanding variability in Winegrape production systems: 1. Within vineyard variation in yield over several vintages. *Aust. J. Grape Wine Res*, 10, 32-45. <https://doi.org/10.1111/j.1755-0238.2004.tb00006.x>.

- Briglia, N., Williams, K., Wu, D., Li, Y., Tao, S., Corke, F., ... & Nuzzo, V. (2020). Image-based assessment of drought response in grapevines. *Frontiers in Plant Science*, 11, 595. <https://doi.org/10.3389/fpls.2020.00595>
- Brown, D. (2013). Soil sampling vineyards and guidelines for interpreting the soil test results. Michigan State University Extension. Retrieved, 2(15), 08. https://www.canr.msu.edu/news/soil_sampling_vineyards_and_guidelines_for_interpreting_the_soil_test_result.
- Burden, F. and Winkler, D. (2008). Bayesian regularization of neural networks. *Artificial neural networks*. 458, 23-42. https://doi.org/10.1007/978-1-60327-101-1_3.
- Cardell, M. F., Amengual, A., & Romero, R. (2019). Future effects of climate change on the suitability of wine grape production across Europe. *Regional Environmental Change*, 19(8), 2299-2310. <https://doi.org/10.1007/s10113-019-01502-x>.
- Casanova, M., Messing, I., and Joel, A. (2000). Influence of aspect and slope gradient on hydraulic conductivity measured by tension infiltrometer. *Hydrological processes*, 14(1), 155-164. [https://doi.org/10.1002/\(SICI\)1099-1085\(200001\)14:1<155::AID-HYP917>3.0.CO;2-J](https://doi.org/10.1002/(SICI)1099-1085(200001)14:1<155::AID-HYP917>3.0.CO;2-J)
- Chalmers, Y.M., Krstic, M.P., Downey, M.O., Dry, P.R. and Loveys, B.R. (2008). Impacts of sustained deficit irrigation on quality attributes and flavonoid composition of Shiraz grapes and wine. *Acta Horticulturae*. 163-169. <http://hdl.handle.net/102.100.100/118801?index=1>.
- Chang, S., Wu, B., Yan, N., Davdai, B., & Nasanbat, E. (2017). Suitability assessment of satellite-derived drought indices for Mongolian grassland. *Remote Sensing*, <https://doi.org/10.3390/rs9070650>.
- Chen, F., Jia, H., and Pan, D. (2019). Risk Assessment of Maize Drought in China Based on Physical Vulnerability. *J. Food Qual.* 2019. <https://doi.org/10.1155/2019/9392769>.
- Chen-jing, F.A.N., Shi-guang, S.H.E.N., Si-hui, W.A.N.G., Guang-hui, S.H.E. and Xin-yi, W.A.N.G. (2011). Research on urban land ecological suitability evaluation based on gravity-resistance model: A case of Deyang city in China. *Procedia Engineering*, 21, pp.676-685. <https://doi.org/10.1016/j.proeng.2011.11.2064>.
- Cook, B. I., & Wolkovich, E. M. (2016). Climate change decouples drought from early wine grape harvests in France. *Nature Climate Change*, 6(7), 715-719. <https://doi.org/10.1038/nclimate2960>
- Dai, A., 2011. Drought under global warming: a review. *Wiley Interdisciplinary Reviews: Climate Change*, 2(1), pp.45-65. <https://doi.org/10.1002/wcc.81>
- Dai, F.C., Lee, C.F. and Zhang, X.H. (2001). GIS-based geo-environmental evaluation for urban land-use planning: a case study. *Engineering geology*, 61(4), pp.257-271.

[https://doi.org/10.1016/S0013-7952\(01\)00028-X](https://doi.org/10.1016/S0013-7952(01)00028-X).

- Darra, N., Psomiadis, E., Kasimati, A., Anastasiou, A., Anastasiou, E., & Fountas, S. (2021). Remote and proximal sensing-derived spectral indices and biophysical variables for spatial variation determination in vineyards. *Agronomy*, 11(4), 741. <https://doi.org/10.3390/agronomy11040741>.
- Das, A.C., Noguchi, R. and Ahamed, T., 2020. Integrating an expert system, GIS, and satellite remote sensing to evaluate land suitability for sustainable tea production in Bangladesh. *Remote Sensing*, 12(24), p.4136. <https://doi.org/10.3390/rs12244136> tea
- De Clercq, W. P., Van Meirvenne, M., & Fey, M. V. (2009). Prediction of the soil-depth salinity-trend in a vineyard after sustained irrigation with saline water. *Agricultural water management*, 96(3), 395-404. <https://doi.org/10.1016/j.agwat.2008.09.002>.
- De Pascale, S., & Barbieri, G. (1995). Effects of soil salinity from long-term irrigation with saline-sodic water on yield and quality of winter vegetable crops. *Scientia Horticulturae* , 64 (3), 145-157. [https://doi.org/10.1016/0304-4238\(95\)00823-3](https://doi.org/10.1016/0304-4238(95)00823-3) .
- Delay, E., Piou, C. and Quéno, H. (2015). The mountain environment, a driver for adaptation to climate change. *Land Use Policy*, 48, pp.51-62. <https://doi.org/10.1016/j.landusepol.2015.05.008>
- Deluisa, A., Giandon, P., Aichner, M., Bortolami, P., Bruna, L., Lupetti, A., ... & Stringari, G. (1996). Copper pollution in Italian vineyard soils. *Communications in soil science and plant analysis*, 27(5-8), 1537-1548. <https://doi.org/10.1080/00103629609369651>.
- Deng, F., Li, X., Wang, H., Zhang, M., Li, R. and Li, X. (2014). GIS-based assessment of land suitability for alfalfa cultivation: A case study in the dry continental steppes of northern China. *Spanish Journal of Agricultural Research*, (2), pp.364-375.
- Deo, R. C., Tiwari, M. K., Adamowski, J. F., & Quilty, J. M. (2017). Forecasting effective drought index using a wavelet extreme learning machine (W-ELM) model. *Stochastic environmental research and risk assessment*, 31(5), 1211-1240. <https://doi.org/10.1007/s00477-016-1265-z>.
- Di Vittori, L., Mazzoni, L., Battino, M. and Mezzetti, B. (2018). Pre-harvest factors influencing the quality of berries. *Scientia Horticulturae*. 233, 310-322. <https://doi.org/10.1016/j.scienta.2018.01.058>.
- Dokoozlian, N.K. and Hirschfeld, D.J. (1995). The influence of cluster thinning at various stages of fruit development on Flame Seedless table grapes. *American journal of enology and viticulture*, 46(4), pp.429-436. <http://www.ajevonline.org/cgi/content/abstract/46/4/429>
- Dukat, P., Bednorz, E., Ziemlińska, K. and Urbaniak, M. (2022). Trends in drought occurrence and severity at mid-latitude European stations (1951–2015) estimated using standardized precipitation (SPI) and precipitation and evapotranspiration (SPEI) indices. *Meteorology and Atmospheric*

- Physics, 134(1), pp.1-21. <https://doi.org/10.1007/s00703-022-00858-w>
- Edwards. DC, and McKee TB. (1997). Characteristics of 20th Century Drought in the United States at Multiple Time Scales. Climatology Report No. 97–2. Colorado State University, Fort Collins. CO, USA. 155.
- Elaalem, M., Comber, A. and Fisher, P. (2011). A comparison of fuzzy AHP and ideal point methods for evaluating land suitability. Transactions in GIS, 15(3), pp.329-346. <https://doi.org/10.1111/j.1467-9671.2011.01260.x>.
- Enquist, B.J., and Ebersole, J.J. (2006). Effects of Added Water on Photosynthesis of *Bistorta Vivipara*: The Importance of Water Relations and Leaf Nitrogen in Two Alpine Communities. Arct. Antract. Alp. Res. 26, 29. <https://doi.org/10.2307/1551873>.
- Etchebarne, F., Ojeda, H., Deloire, A. (2009). Grape berry mineral composition in relation to vine water status & leaf area/fruit ratio. In Grapevine Molecular Physiology & Biotechnology: Second Edition. Springer Netherlands, pp. 53–72. https://doi.org/10.1007/978-90-481-2305-6_3
- Field, C.B., Barros, V., Stocker, T.F. and Dahe, Q. eds. (2012). Managing the risks of extreme events and disasters to advance climate change adaptation: special report of the intergovernmental panel on climate change. Cambridge University Pres. <http://dx.doi.org/10.1136/jech-2012-201045>.
- Food and Agriculture Organization (FAO) and Ministry of Agriculture, Irrigation and Livestock’s (MAIL) (2019). Afghanistan Drought Risk Management Strategy. https://reliefweb.int/sites/reliefweb.int/files/resources/Afghanistan_Drought-Risk-Management_Strategy9Feb2020.pdf Last access 12 March 2022.
- Food and Agriculture Organization (FAO) (2016). Land Cover ATLAS. The Islamic Republic of Afghanistan. <https://www.fao.org/publications/card/en/c/cc0ac143-38ed-41f0-b7c6-2342ffa7f0e6/> Last access 12 March 2022.
- Food and Agriculture Organization (FAO) (2021). Report: Climate change-related disasters a major threat to food security, Rome.
- Food and Agriculture Organization (FAO). (1976). A Framework for Land Evaluation; FAO: Rome, Italy., 1976. <http://www.fao.org/3/x5310e/x5310e00.htm> Last access 5 May 2022.
- Food and Agriculture Organization of the United Nation (FAO) (2019). FAO’s work on climate change United Nations Climate Change Conference, 2019. 1-40. <http://www.fao.org/3/ca7126en/ca7126en.pdf>.

- Food and Agriculture Organization of the United Nation (FAO) (2020). Grape production in Asia Pacific in 2019, by country. Survived by FAO. <https://www.statista.com/statistics/679330/asia-pacific-grape-production-by-country/#statisticContainer>. Last access 20 October 2021.
- Food and Agriculture Organization of the United Nation (FAO) and International Organization of Vine and Wine Intergovernmental Organization (OIV). (2016). TABLE AND DRIED GRAPES, Non - Alcoholic products of the vitivinicultural sector intended for human consumption. Pp.17042. <http://www.fao.org/3/a-i7042e.pdf>.
- Food and Agriculture Organization of the United Nations (FAO). (1999). Production Variability and Losses. In: R. Gomme, eds. Special: Agroclimatic Concepts. Sustainable Development Department (SD), Food Agriculture Organization of the United Nations (FAO). http://www.fao.org/nr/climpag/agroclim/losses_en.asp. Last access 8 February 2021.
- Ford, T.W. and Quiring, S.M. (2019). Comparison of contemporary in situ, model, and satellite remote sensing soil moisture with a focus on drought monitoring. *Water Resources Research*, 55(2), pp.1565-1582. <https://doi.org/10.1029/2018WR024039>
- Funk, C., Peterson, P., Landsfeld, M., Pedreros, D., Verdin, J., Shukla, S., ... & Michaelsen, J. (2015). The climate hazards infrared precipitation with stations—a new environmental record for monitoring extremes. *Scientific data*, 2(1), 1-21. <https://doi.org/10.1038/sdata.2015.66>.
- Gambetta, G.A., Herrera, J.C., Dayer, S., Feng, Q., Hochberg, U. and Castellarin, S.D., 2020. The physiology of drought stress in grapevine: towards an integrative definition of drought tolerance. *Journal of experimental botany*, 71(16), pp. 4658-4676. <https://doi.org/10.1093/jxb/eraa245>
- Gao, B.C. (1996). NDWI—A normalized difference water index for remote sensing of vegetation liquid water from space. *Remote sens. Environ.* 58, 257-266. [https://doi.org/10.1016/S0034-4257\(96\)00067-3](https://doi.org/10.1016/S0034-4257(96)00067-3).
- Gemitzi, A., Dalampakis, P., and Falalakis, G. (2021). Detecting geothermal anomalies using Landsat 8 thermal infrared remotely sensed data. *International Journal of Applied Earth Observation and Geoinformation*, 96, 102283. <https://doi.org/10.1016/j.jag.2020.102283>.
- Ghozat, A., Sharafati, A., & Hosseini, SA (2022). Satellite-based monitoring of meteorological drought over different regions of Iran: Application of the CHIRPS precipitation product. *Environmental Science and Pollution Research*, 29 (24), 36115 -36132. <https://doi.org/10.1007/s11356-022-18773-3>

- Gilliams, S., Van Orshoven, J., Muys, B., Kros, H., Heil, G. W., & Van Deursen, W. (2005). AFFOREST sDSS: a metamodel based spatial decision support system for afforestation of agricultural land. *New Forests*, 30(1), 33-53. <https://doi.org/10.1007/s11056-004-0761-z/>.
- Goes, B. J. M., Howarth, S. E., Wardlaw, R. B., Hancock, I. R., & Parajuli, U. N. (2016). Integrated water resources management in an insecure river basin: a case study of Helmand River Basin, Afghanistan. *International Journal of water resources Development*, 32(1), 3-25.
- Goldammer, T. (2018). *Grape Grower's Handbook—A Guide to Viticulture for Wine Production*. APEX Publishers: Centreville, VA, USA. 3rd Edition, 484. <http://www.wine-grape-growing.com/>.
- Gong, J., Liu, Y., & Chen, W. (2012). Land suitability evaluation for development using a matter-element model: a case study in Zengcheng, Guangzhou, China. *Land Use Policy*, 29(2), 464-472. <https://doi.org/10.1016/j.landusepol.2011.09.005>.
- Gorelick, N., Hancher, M., Dixon, M., Ilyushchenko, S., Thau, D. and Moore, R. (2017). Google Earth Engine: Planetary-scale geospatial analysis for everyone. *Remote sensing of Environment*, 202, pp.18-27. <https://doi.org/10.1016/j.rse.2017.06.031>
- Goñi, O., Fernandez-Caballero, C., Sanchez-Ballesta, M.T., Escribano, M.I. and Merodio, C. (2011). Water status and quality improvement in high-CO₂ treated table grapes. *Food chemistry*, 128, 34-39. <https://doi.org/10.1016/j.foodchem.2011.02.073>.
- Grassano, N., Tedone, L., Verdini, L. and De Mastro, G. (2011). Evaluation of rapeseed cultivation suitability in Apulia with GIS-multicriteria analysis. *Italian Journal of Agronomy*, 6(2), pp.e16-e16. <https://doi.org/10.4081/ija.2011.e16>
- Guo, H., Wang, R., Garfin, G.M., Zhang, A. and Lin, D. (2021). Rice drought risk assessment under climate change: Based on physical vulnerability a quantitative assessment method. *Science of The Total Environment*, 751, 141481. <https://doi.org/10.1016/j.scitotenv.2020.141481>.
- Habibie, M.I., Noguchi, R., Shusuke, M. and Ahamed, T., 2019. Land suitability analysis for maize production in Indonesia using satellite remote sensing and GIS-based multicriteria decision support system. *GeoJournal*, 86(2), pp.777-807. <https://doi.org/10.1007/s10708-019-10091-5>
- Hadri, A., Saidi, M. E. M., & Boudhar, A. (2021). Multiscale drought monitoring and comparison using remote sensing in a Mediterranean arid region: a case study from west-central Morocco. *Arabian Journal of Geosciences*, 14(2), 1-18. DOI: [10.1007/s12517-021-06493-w](https://doi.org/10.1007/s12517-021-06493-w).
- Han, H., Bai, J., Yan, J., Yang, H., & Ma, G. (2019). A combined drought monitoring index based on multi-sensor remote sensing data and machine learning. *Geocarto International*, 36, 1161-1177. <https://doi.org/10.1080/10106049.2019.1633423>.
- Han, Z., Huang, Q., Huang, S., Leng, G., Bai, Q., Liang, H., Wang, L., Zhao, J. and Fang, W. (2021).

- Spatial-temporal dynamics of agricultural drought in the Loess Plateau under a changing environment: Characteristics and potential influencing factors. *Agricultural Water Management*, 244, 106540. <https://doi.org/10.1016/j.agwat.2020.106540>.
- Hardisky, M.A., Klemas, V. and Smart, M. (1983). The influence of soil salinity, growth form, and leaf moisture on the spectral radiance of *Spartina alterniflora*. 49, 77-83 https://www.asprs.org/wp-content/uploads/pers/1983journal/jan/1983_jan_77-83.pdf.
- Hashemzadeh Ghalhari, M., Vafakhah, M. and Damavandi, A.A. (2022). Agricultural drought assessment using vegetation indices derived from MODIS time series in Tehran Province. *Arabian Journal of Geosciences*, 15(5), pp.1-13. <https://doi.org/10.1007/s12517-022-09741-9>
- Hashim, H., Abd Latif, Z., & Adnan, N. A. (2019). Urban vegetation classification with NDVI threshold value method with very high resolution (VHR) PLEIADES Imagery. *Int. Arch. Photogramm. Remote Sens. Spat. Inf. Sci*, 237-240. DOI: [10.5194/isprs-archives-XLII-4-W16-237-2019](https://doi.org/10.5194/isprs-archives-XLII-4-W16-237-2019).
- Heim Jr, R.R., 2002. A review of twentieth-century drought indices used in the United States. *Bulletin of the American Meteorological Society*, 83(8), pp.1149-1166. <https://doi.org/10.1175/1520-0477-83.8.1149>
- Hermans, K. and McLeman, R. (2021). Climate change, drought, land degradation and migration: exploring the linkages. *Current Opinion in Environmental Sustainability*, 50, pp.236-244. <https://doi.org/10.1016/j.cosust.2021.04.013>.
- Hernández, M., Borges, A. A., & Francisco-Bethencourt, D. (2022). Mapping stressed wheat plants by soil aluminum effect using C-band SAR images: implications for plant growth and grain quality. *Precision Agriculture*, 1-21. <https://doi.org/10.1007/s11119-022-09875-6>.
- Hoheisel, G.A. and Moyer, M. (2015). Grapevine management under drought conditions. <http://hdl.handle.net/2376/5377>.
- Hossain, M. S., & Das, N. G. (2010). GIS-based multi-criteria evaluation to land suitability modelling for giant prawn (*Macrobrachium rosenbergii*) farming in Companigonj Upazila of Noakhali, Bangladesh. *Computers and electronics in agriculture*, 70(1), 172-186. <https://doi.org/10.1016/j.compag.2009.10.003>.
- Huete, A.R. (1988). A soil-adjusted vegetation index (SAVI). *Remote sensing of environment*, 25(3), pp.295-309. [https://doi.org/10.1016/0034-4257\(88\)90106-X](https://doi.org/10.1016/0034-4257(88)90106-X).
- IPCC. (2019): *Climate Change and Land: an IPCC special report on climate change, desertification, land degradation, sustainable land management, food security, and greenhouse gas fluxes in terrestrial ecosystems* [P.R. Shukla, J. Skea, E. Calvo Buendia, V. Masson-Delmotte, H.-O. Pörtner, D. C. Roberts, P. Zhai, R. Slade, S. Connors, R. van Diemen, M. Ferrat, E. Haughey,

- S. Luz, S. Neogi, M. Pathak, J. Petzold, J. Portugal Pereira, P. Vyas, E. Huntley, K. Kissick, M. Belkacemi, J. Malley, (eds.)]. In press. <https://www.ipcc.ch/site/assets/uploads/2019/11/SRCCL-Full-Report-Compiled-191128.pdf>. Last access 5 May 2022.
- Iacono, M. J., Mlawer, E. J., Clough, S. A., & Morcrette, J. J. (2000). Impact of an improved longwave radiation model, RRTM, on the energy budget and thermodynamic properties of the NCAR community climate model, CCM3. *Journal of Geophysical Research: Atmospheres*, 105(D11), 14873-14890. <https://doi.org/10.1029/2000JD900091>.
- Iltis, C., Moreau, J., Pecharová, K., Thiéry, D., Louâpre, P. (2020). Reproductive performance of the European grapevine moth *Lobesia botrana* (Tortricidae) is adversely affected by warming scenario. *J. PEST Sci*, 93, 679-689. <https://link.springer.com/article/10.1007/s10340-020-01201-1>.
- International Organization for Migration (IOM), 2021. CBNA R14 — Afghanistan — Community-Based Needs Assessment. <https://displacement.iom.int/reports/cbna-r14-afghanistan-community-based-needs-assessment-summary-results-november-december>. Last access 12 March 2022.
- Islam, M. M., Matsushita, S., Noguchi, R., & Ahamed, T. (2021). Development of remote sensing-based yield prediction models at the maturity stage of boro rice using parametric and nonparametric approaches. *Remote Sensing Applications: Society and Environment*, 22, 100494. <https://doi.org/10.1016/j.rsase.2021.100494>.
- Jafari, S. and Zaredar, N. (2010). Land Suitability Analysis using Multi Attribute Decision Making Approach. *International journal of environmental science and development*, 1(5), p.441. DOI: [10.7763/IJESD.2010.V1.85](https://doi.org/10.7763/IJESD.2010.V1.85).
- Jayawardhana, W. G. N. N., & Chaturange, V. M. I. (2020). Investigate the sensitivity of the satellite-based agricultural drought indices to monitor the drought condition of paddy and introduction to enhanced multi-temporal drought indices. *Journal of Remote Sensing and GIS*, 9, 272.
- Jia, G., Shevliakova, E., Artaxo, P., Noblet-Ducoudré, D., Houghton, R., House, J., Kitajima, K., Lennard, C., Popp, A., Sirin, A. and Sukumar, R. (2019). Land-climate interactions. In *Climate Change and Land*. (pp. 131-247). https://www.ipcc.ch/site/assets/uploads/2019/11/05_Chapter-2.pdf.
- Jiang, H. and Eastman, J.R. (2000). Application of fuzzy measures in multi-criteria evaluation in GIS. *International Journal of Geographical Information Science*, 14(2), pp.173-184. <https://doi.org/10.1080/136588100240903>

- Johnson G.E., Achutuni V.R., Thiruvengadachari S., Kogan F. (1993). The Role of NOAA Satellite Data in Drought Early Warning and Monitoring: Selected Case Studies. In: Wilhite D.A. (eds) Drought Assessment, Management, and Planning: Theory and Case Studies. Natural Resource Management and Policy, vol 2. Springer, Boston, 31-49. Norwell Mass https://doi.org/10.1007/978-1-4615-3224-8_3.
- Johnson, L.F., Roczen, D.E., Youkha Tian na, S.K., Nemani, R.R., Bosch, D.F. (2003). Mapping vineyard leaf area with multispectral satellite imagery. *Comput. Electron Agric*, 38, 33-44. [https://doi.org/10.1016/S0168-1699\(02\)00106-0](https://doi.org/10.1016/S0168-1699(02)00106-0).
- Jones, B. M., Kolden, C. A., Jandt, R., Abatzoglou, J. T., Urban, F., & Arp, C. D. (2009). Fire behavior, weather, and burn severity of the 2007 Anaktuvuk River tundra fire, North Slope, Alaska. *Arctic, Antarctic, and Alpine Research*, 41(3), 309-316. <https://doi.org/10.1657/1938-4246-41.3.309>.
- Jones, E.G., Wong, S., Milton, A., Sclauzero, J., Whittenbury, H., McDonnell, M.D., 2020. The impact of pan-sharpening and spectral resolution on vineyard segmentation through machine learning. *Rem. Sens.* 12, 934. <https://doi.org/10.3390/rs12060934>.
- Junges, A.H., Fontana, D.C., Anzanello, R., Bremm, C. (2017). Normalized difference vegetation index obtained by ground-based remote sensing to characterize vine cycle in Rio Grande do Sul, Brazil. *Ciênc. Agrotec*, 4, 543-553. <https://doi.org/10.1590/1413-70542017415049016>.
- Kamir, E., Waldner, F., Hochman, Z. (2020). Estimating wheat yields in Australia using climate records, satellite image time series and machine learning methods. *ISPRS J. Photogramm. Remote Sens.* 160, 124-135. <https://doi.org/10.1016/j.isprsjprs.2019.11.008>.
- Kanellou, E., Domenikiotis, C., Tsiros, E. and Dalezios, N.R. (2008). Satellite-based drought estimation in Thessaly. *Eur Water*, 23(24), pp.111-122.
- Karnieli, A., Agam, N., Pinker, R.T., Anderson, M., Imhoff, M.L., Gutman, G.G., Panov, N. and Goldberg, A. (2010). Use of NDVI and land surface temperature for drought assessment: Merits and limitations. *Journal of climate*, 23(3), pp.618-633. DOI: [10.1175/2009JCLI2900.1](https://doi.org/10.1175/2009JCLI2900.1).
- Keyantash, J.A. and Dracup, J.A. (2004). An aggregate drought index: Assessing drought severity based on fluctuations in the hydrologic cycle and surface water storage. *Water Resources Research*, 40. <https://doi.org/10.1029/2003WR002610>.
- Khan, M.S., Semwal, M., Sharma, A., Verma, R.K. (2020). An artificial neural network model for estimating Mentha crop biomass yield using Landsat 8 OLI. *Precis, Agri*, 21, 18-33. <https://doi.org/10.1007/s11119-019-09655-9>.
- Knipper, K. R., Kustas, W. P., Anderson, M. C., Alfieri, J. G., Prueger, J. H., Hain, C. R., ... & Sanchez, L. (2019). Evapotranspiration estimates derived using thermal-based satellite remote sensing

- and data fusion for irrigation management in California vineyards. *Irrigation Science*, 37(3), 431-449. <https://doi.org/10.1007/s00271-018-0591-y>.
- Kogan, F., Guo, W., Yang, W. (2019). Drought and food security prediction from NOAA new generation of operational satellites. *Geomatics, Natural Hazards, and Risk*, 10, 651–666. <https://doi.org/10.1080/19475705.2018.1541257>.
- Kogan, F.N. (1990). Remote sensing of weather impacts on vegetation in non-homogeneous areas. *International Journal of Remote Sensing*, 11, 1405-1419. <https://doi.org/10.1080/01431169008955102>.
- Kogan, F.N. (1995a). Application of vegetation index and brightness temperature for drought detection. *Advances in space research*. 15, .91-100. [https://doi.org/10.1016/0273-1177\(95\)00079-T](https://doi.org/10.1016/0273-1177(95)00079-T).
- Kogan, F.N. (1995b). Droughts of the late 1980s in the United States as derived from NOAA polar-orbiting satellite data. *Bulletin of the American Meteorological Society*, 76(5), pp.655-668. [https://doi.org/10.1175/1520-0477\(1995\)076<0655:DOTLIT>2.0.CO;2](https://doi.org/10.1175/1520-0477(1995)076<0655:DOTLIT>2.0.CO;2).
- Kogan, F.N. (1997). Global droughts watch from space. *Bulletin of the American Meteorological Society*, 78(4), pp.621-636 [https://doi.org/10.1175/15200477\(1997\)078<0621:GDWFS>2.0.CO;2](https://doi.org/10.1175/15200477(1997)078<0621:GDWFS>2.0.CO;2).
- Krishnan, S.P.T. and Gonzalez, J.L.U., 2015. Building your next important thing with google cloud platform: A guide for developers and enterprise architects. USA: A press.
- Kurtser, P., Ringdahl, O., Rotstein, N., Berenstein, R. and Edan, Y. (2020). In-field grape cluster size assessment for vine yield estimation using a mobile robot and a consumer level RGB-D camera. *IEEE Robot. Autom. Lett.* 5, 2031-2038. <https://doi.org/10.1109/lra.2020.2970654>.
- Kurtural, S.K. (2007). Vineyard site selection. University of Kentucky Cooperative Extension Service. https://simpson.ca.uky.edu/files/vineyard_site_selection_in_ky_based_on_climate_and_soil_properties.pdf.
- Kılıc, O.M., Ersayın, K., Gunal, H., Khalofah, A. and Alsubeie, M.S. (2022). Combination of fuzzy-AHP and GIS techniques in land suitability assessment for wheat (*Triticum aestivum*) cultivation. *Saudi Journal of Biological Sciences*, 29(4), pp.2634-2644. <https://doi.org/10.1016/j.sjbs.2021.12.050>.
- Lamb, D.W., Weedon, M.M., and Bramley, R.G.V. (2004). Using remote sensing to predict grape phenolics and colour at harvest in a Cabernet Sauvignon vineyard: timing observations against vine phenology and optimizing image resolution. *Aust. J. Grape Wine Res.* 10, 46–54. <https://doi.org/10.1111/j.1755-0238.2004.tb00007.x>.
- Law, B.E., Waring, R.H. (1994). Remote sensing of leaf area index and radiation intercepted by

- understory vegetation. *Ecol. Appl.* 4, 272-279. <https://doi.org/10.2307/1941933>.
- Le Blanc, D., and Perez, R. (2008). The relationship between rainfall and human density and its implications for future water stress in Sub-Saharan Africa. *Ecological Economics*, 66(2-3), 319-336. DOI: [10.1016/j.ecolecon.2007.09.009](https://doi.org/10.1016/j.ecolecon.2007.09.009).
- Leng, G., & Hall, J. (2019). Crop yield sensitivity of global major agricultural countries to droughts and the projected changes in the future. *Science of the Total Environment*, 654, 811-821. <https://doi.org/10.1016/j.scitotenv.2018.10.434>.
- Lesk, C., Rowhani, P. and Ramankutty, N. (2016). Influence of extreme weather disasters on global crop production. *Nature*, 529, 84-87. <https://doi.org/10.1038/nature16467>.
- Li, C., Li, H., Li, J., Lei, Y., Li, C., Manevski, K., & Shen, Y. (2019). Using NDVI percentiles to monitor real-time crop growth. *Computers and Electronics in Agriculture*, 162, 357-363. <https://doi.org/10.1016/j.compag.2019.04.026>.
- Li, Y., Ye, W., Wang, M. and Yan, X. (2009). Climate change and drought: a risk assessment of crop-yield impacts. *Climate research*, 39, 31-46. <https://doi.org/10.3354/cr00797>.
- Liu, S., Marden, S., & Whitty, M. (2013). Towards automated yield estimation in viticulture. In *Proceedings of the Australasian Conference on Robotics and Automation*, Sydney, Australia (Vol. 24, pp. 2-6).
- Liu, S., and Whitty, M. (2015). Automatic grape bunch detection in vineyards with an SVM classifier. *J. Appl. Log.* 13, 643-653. <https://doi.org/10.1016/j.jal.2015.06.001>.
- Liu, X., Zhu, X., Zhang, Q., Yang, T., Pan, Y., & Sun, P. (2020). A remote sensing and artificial neural network-based integrated agricultural drought index: Index development and applications. *Catena*, 186, 104394. <https://doi.org/10.1016/j.catena.2019.104394>
- Lopez-Fornieles, E., Brunel, G., Devaux, N., Roger, J. M., & Tisseyre, B. (2022). Is It Possible to Assess Heatwave Impact on Grapevines at the Regional Level with Time Series of Satellite Images? *Agronomy*, 12(3), 563.
- Loveland, T. R., & Irons, J. R. (2016). Landsat 8: The plans, the reality, and the legacy. *Remote Sensing of Environment*, 185, 1-6. <https://doi.org/10.1016/j.rse.2016.07.033>.
- Mackay, D.J. (1992). Bayesian interpolation. *Neural computation*. 4,415-447. <https://doi.org/10.1162/neco.1992.4.3.415>.
- Macpherson, G.L., Johnson, W.C., and Liu, H. (2017). Viability of karezes (ancient water supply systems in Afghanistan) in a changing world. *Appl. Water Sci.* 7, 1689-1710. <https://doi.org/10.1007/s13201-015-0336-5>.

- Maes, W.H. and Steppe, K. (2012). Estimating evapotranspiration and drought stress with ground-based thermal remote sensing in agriculture: a review. *Journal of Experimental Botany*, 63(13), pp.4671-4712. <https://doi.org/10.1093/jxb/ers165>
- Mainali, J. and Pricope, N.G. (2017). High-resolution spatial assessment of population vulnerability to climate change in Nepal. *Applied Geography*, 82, pp.66-82. <https://doi.org/10.1016/j.apgeog.2017.03.008>.
- Matsa, M. (2021). Impact of Climate Change in Zimbabwe. In *Climate Change and Agriculture in Zimbabwe*. Springer, Cham. 21-30. https://doi.org/10.1007/978-3-030-51346-7_3.
- McKee, T.B., Doesken, N.J. and Kleist, J. (1993). The relationship of drought frequency and duration to time scales. In *Proceedings of the 8th Conference on Applied Climatology*. 17, 179-183. <https://climate.colostate.edu/pdfs/relationshipofdroughtfrequency.pdf>.
- Meggio, F., Zarco-Tejada, P.J., Núñez, L.C., Sepulcre-Cantó, G., González, M.R., and Martín, P. (2010). Grape quality assessment in vineyards affected by iron deficiency chlorosis using narrow-band physiological remote sensing indices. *Remote Sens. of Environ*, 114, 1968-1986. <https://doi.org/10.1016/j.rse.2010.04.004>.
- Meng, L., Ford, T. and Guo, Y. (2017). Logistic regression analysis of drought persistence in East China. *International Journal of Climatology*, 37(3), pp.1444-1455. <https://doi.org/10.1002/joc.4789>
- Meza, I., Siebert, S., Döll, P., Kusche, J., Herbert, C., Eyshi Rezaei, E., Nouri, H., Gerdener, H., Popat, E., Frischen, J. and Naumann, G. (2020). Global-scale drought risk assessment for agricultural systems. *Natural Hazards and Earth System Sciences*, 20, 695-712.
- Mikaili, O. and Rahimzadegan, M., 2022. Investigating remote sensing indices to monitor drought impacts on a local scale (case study: Fars province, Iran). *Natural Hazards*, pp.1-19. <https://doi.org/10.1007/s11069-021-05146-1>
- Ming, B., Guo, Y., Tao, H., Liu, G., Li, S., Wang, P. (2015). SPEIPM-based research on drought impact on maize yield in North China Plain. *Journal of Integrative, Agriculture* 14, 660–669. [https://doi.org/10.1016/s2095-3119\(14\)60778-4](https://doi.org/10.1016/s2095-3119(14)60778-4).
- Modica, G., Laudari, L., Barreca, F., & Fichera, C. R. (2014). A GIS-MCDA Based Model for the Suitability Evaluation of Traditional Grape Varieties: The Case-Study of ‘Mantonico’Grape (Calabria, Italy). *International Journal of Agricultural and Environmental Information Systems (IJAEIS)*, 5(3), 1-16. [10.4018/ijaeis.2014070101](https://doi.org/10.4018/ijaeis.2014070101).
- Mollalo, A., Sadeghian, A., Israel, G.D., Rashidi, P., Sofizadeh, A. and Glass, G.E. (2018). Machine learning approaches in GIS-based ecological modeling of the sand fly *Phlebotomus papatasi*, a

- vector of zoonotic cutaneous leishmaniasis in Golestan province, Iran. *Acta tropica*. 188, 187-194. <https://doi.org/10.1016/j.actatropica.2018.09.004>.
- Monteiro, A.L., de Freitas Souza, M., Lins, H.A., da Silva Teófilo, T.M., Júnior, A.P.B., Silva, D.V. and Mendonça, V. (2021). A new alternative to determine weed control in agricultural systems based on artificial neural networks (ANNs). *Field Crops Research*, 263, p.108075. <https://doi.org/10.1016/j.fcr.2021.108075>.
- Morisette, J.T., Baret, F., Privette, J.L., Myneni, R.B., Nickeson, J.E., Garrigues, S., Shabanov, N.V., Weiss, M., Fernandes, R.A., Leblanc, S.G., Kalacska, M. (2006). Validation of global moderate-resolution LAI products: A framework proposed within the CEOS land product validation subgroup. *IEEE Trans. Geosci. Remote Sens.* 44, 1804-1817. <https://doi.org/10.1109/TGRS.2006.872529>.
- Muhsin, N., Ahamed, T. and Noguchi, R. (2018). GIS-based multi-criteria analysis modeling used to locate suitable sites for industries in suburban areas in Bangladesh to ensure the sustainability of agricultural lands. *Asia-Pacific Journal of Regional Science*, 2, 35-64. <https://doi.org/10.1007/s41685-017-0046-0>.
- Nguyen, H., Nguyen, T., Hoang, N., Bui, D., Vu, H., & Van, T. (2020). The application of LSE software: A new approach for land suitability evaluation in agriculture. *Computers and Electronics in Agriculture*, 173, 105440. <https://doi.org/10.1016/j.compag.2020.105440>.
- Niaz, M. A., Faiz, M. A., & Yongxia, W. (2021). Development of an integrated weighted drought index and its application for agricultural drought monitoring. *Arabian Journal of Geosciences*, 14(6), 1-12. <https://doi.org/10.1007/s12517-021-06879-w>.
- Olatunji, O. M., Horsfall, I. T., Ukoha-Onuoha, E., & Osa-aria, K. (2022). Application of hybrid ANFIS-based non-linear regression modeling to predict the% oil yield from grape peels: Effect of process parameters and FIS generation techniques. *Cleaner Engineering and Technology*, 6, 100371. <https://doi.org/10.1016/j.clet.2021.100371>.
- Parfitt, J., Barthel, M., Macnaughton, S. (2010). Food waste within food supply chains: quantification and potential for change to 2050. *Philosophical transactions of the royal society B: Biol. Sci.* 365, 3065-3081. <https://doi.org/10.1098/rstb.2010.0126>.
- Park, S., Jeon, S., Kim, S., & Choi, C. (2011). Prediction and comparison of urban growth by land suitability index mapping using GIS and RS in South Korea. *Landscape and urban planning*, 99(2), 104-114. [10.1016/j.landurbplan.2010.09.001](https://doi.org/10.1016/j.landurbplan.2010.09.001).

- Patakas, A., Noitsakis, B., & Chouzouri, A. (2005). Optimization of irrigation water use in grapevines using the relationship between transpiration and plant water status. *Agriculture, Ecosystems & Environment*, 106(2-3), 253-259. <https://doi.org/10.1016/j.agee.2004.10.013>.
- Paterson, R. R. M., & Lima, N. (2011). Further mycotoxin effects from climate change. *Food Research International*, 44(9), 2555-2566.
- Pathak, T.B., Maskey, M.L., Dahlberg, J.A., Kearns, F., Bali, K.M., Zaccaria, D. (2018). Climate change trends and impacts on California agriculture: a detailed review. *Agron*, 8, 1-27. <https://doi.org/10.3390/agronomy8030025>.
- Paul, M., Negahban-Azar, M., Shirmohammadi, A., & Montas, H. (2020). Assessment of agricultural land suitability for irrigation with reclaimed water using geospatial multi-criteria decision analysis. *Agricultural Water Management*, 231, 105987. DOI: 10.1016/j.agwat.2019.105987.
- Permanhani, M., Costa, J.M., Conceição, M.A.F., De Souza, R.T., Vasconcellos, M.A.S. and Chaves, M.M. (2016). Deficit irrigation in table grape: eco-physiological basis and potential use to save water and improve quality. *Theoretical and Experimental Plant Physiology*, 28,85-108. <https://doi.org/10.1007/s40626-016-0063-9>.
- Peters, A. J., Walter-Shea, E. A., Ji, L., Vina, A., Hayes, M., & Svoboda, M. D. (2002). Drought monitoring with NDVI-based standardized vegetation index. *Photogrammetric engineering and remote sensing*, 68(1), 71-75.
- Pokhrel, Y., Felfelani, F., Satoh, Y., Boulange, J., Burek, P., Gädeke, A., Gerten, D., Gosling, S.N., Grillakis, M., Gudmundsson, L. and Hanasaki, N. (2021). Global terrestrial water storage and drought severity under climate change. *Nature Climate Change*, 11(3), pp.226-233. <https://doi.org/10.1038/s41558-020-00972-w>.
- Potopová, V., Štěpánek, P. Možný, M., Türkott, L. Soukup, J. (2015). Performance of the standardized precipitation evapotranspiration index at various lags for agricultural drought risk assessment in the Czech Republic. *Agric, For. Meteorol*, 202, 26–38 <https://doi.org/10.1016/j.agrformet.2014.11.022>.
- Potopová, V., Trnka, M., Hamouz, P., Soukup, J. and Castraveţ, T. (2020). Statistical modelling of drought-related yield losses using soil moisture-vegetation remote sensing and multiscalar indices in the south-eastern Europe. *Agricultural Water Management*, 236, 106168. <https://doi.org/10.1016/j.agwat.2020.106168>.
- Prodhan, F. A., Zhang, J., Bai, Y., Sharma, T. P. P., & Koju, U. A. (2022). Monitoring of drought condition and risk in Bangladesh combined data from satellite and ground meteorological observations. *IEEE Access*, 8, 93264-93282.

- Purnamasari, R.A., Ahamed, T. and Noguchi, R. (2019a). Land suitability assessment for cassava production in Indonesia using GIS, remote sensing and multi-criteria analysis. *Asia-Pacific Journal of Regional Science*, 3(1), pp.1-32. <https://doi.org/10.1007/s41685-018-0079-z>.
- Purnamasari, R.A., Noguchi, R. and Ahamed, T. (2019b). Land suitability assessments for yield prediction of cassava using geospatial fuzzy expert systems and remote sensing. *Computers and Electronics in Agriculture*, 166, 105018. <https://doi.org/10.1016/j.compag.2019.105018>.
- Purnamasari, R.A., Noguchi, R. and Ahamed, T. (2022). Land suitability assessment for cassava production in Indonesia using GIS, remote sensing, and multi-criteria analysis. In *Remote Sensing Application* (pp. 99-132). Springer, Singapore.
- Pôças, I., Tosin, R., Gonçalves, I., Cunha, M. (2020). Toward a generalized predictive model of grapevine water status in Douro region from hyperspectral data. *Agric. For. Meteorol*, 280, 107793. <https://doi.org/10.1016/j.agrformet.2019.107793>.
- Quarmby, N.A., Milnes, M., Hindle, T.L., and Silleos, N. (1993). The use of multi-temporal NDVI measurements from AVHRR data for crop yield estimation and prediction. *Int. J. Remote Sens*, 14, 199-210. <https://doi.org/10.1080/01431169308904332>.
- Qureshi AS, Akhtar M. (2004). A survey of drought impacts and coping measures in Helmand and Kandahar provinces of Afghanistan. IWMI internal report, Afghanistan. <https://agris.fao.org/agris-search/search.do?recordID=QL2010000958>.
- Qureshi, A. S. (2002). Water resources management in Afghanistan: The issues and options, Work. Pap. 49, Int. Water Manage. Inst., Colombo, Sri Lanka. http://www.iwmi.cgiar.org/Publications/Working_Papers/working/WOR49.pdf.
- Radočaj, D., Jurišić, M., Gašparović, M. and Plaščak, I. (2020). Optimal soybean (*Glycine max* L.) land suitability using gis-based multicriteria analysis and sentinel-2 multitemporal images. *Remote Sensing*, 12(9), p.1463. <https://doi.org/10.3390/rs12091463>.
- Raksapatcharawong, M., Veerakachen, W., Homma, K., Maki, M. and Oki, K. (2020). Satellite-based drought impact assessment on rice yield in Thailand with SIMRIW– RS. *Remote Sensing*, 12(13), p.2099. <https://doi.org/10.3390/rs12132099>.
- Rameshkumar, S., Vadivelu, S., Reddy, R., Naidu, L., Hegde, R., & Srinivas, S. (2006). Land suitability for grape cultivation and its economic evaluation in Rajanukunte watershed, Karnataka. <http://isslup.in/wp-content/uploads/2018/09/Land-suitability-for-grape-cultivation-and-its.pdf>.
- Regional Rural Economic Regeneration Strategies (RRERS) provincial profile, Kabul Province https://www.ecoi.net/en/file/local/1152622/1222_1197553692_kabul-provincial-profile.pdf. Last

access 5 May 2022.

- Ribeiro, A. F., Russo, A., Gouveia, C. M., & Páscoa, P. (2019). Modelling drought-related yield losses in Iberia using remote sensing and multiscale indices. *Theoretical and Applied Climatology*, 136(1), 203-220. <https://doi.org/10.1007/s00704-018-2478-5>.
- Ridley, W., & Devadoss, S. (2021). The Effects of COVID-19 on Fruit and Vegetable Production. *Applied Economic Perspectives and Policy*, 43(1), 329-340. <https://doi.org/10.1002/aep.13107>.
- Romano, G., Dal Sasso, P., Liuzzi, G.T. and Gentile, F. (2015). Multi-criteria decision analysis for land suitability mapping in a rural area of Southern Italy. *Land use policy*, 48, pp.131-143. <https://doi.org/10.1016/j.landusepol.2015.05.013>
- Rouse, R.W.H, Haas, J.A.W.Deering, D. W. (1974). Monitoring Vegetation System in the Great Plains with ERTS. Conference Paper, NASA. Goddard Space Flight Center 3d ERTS-1 Symp 1, 309–317. <https://ntrs.nasa.gov/search.jsp?R=19740022614>.
- Roy, J. and Saha, S. (2018). Assessment of land suitability for the paddy cultivation using analytical hierarchical process (AHP): A study on Hinglo river basin, Eastern India. *Modeling Earth Systems and Environment*, 4(2), pp.601-618. <https://doi.org/10.1007/s40808-018-0467-4>
- Rötter, R.P. Höhn, J. Trnka, M. Fronzek, S. Carter, T.R. Kahiluoto, H. (2013). Modeling shifts in agroclimatic and crop cultivar response under climate change. *Ecol. Evol*, 3, 4197–4214. <https://doi.org/10.1002/ece3.782>.
- Saaty, T. L., & Kearns, K. P. (2014). *Analytical planning: The organization of system* (Vol. 7). Elsevier.
- Saaty, T.L. (1980). The analytic hierarchy process (AHP). *The Journal of the Operational Research Society*, 41(11), pp.1073-1076.
- Santos, T.T., de Souza, L.L., dos Santos, A.A., Avila, S. (2020). Grape detection, segmentation, and tracking using deep neural networks and three-dimensional association. *Comput. Electron, Agr.* 170, 105247. <https://doi.org/10.1016/j.compag.2020.105247>.
- Savage, M., Dougherty, B., Hamza, M., Butterfield, R. and Bharwani, S. (2009). *Socio economic impacts of climate change in Afghanistan*. Stockholm Environment Institute: Oxford, UK. <https://www.weadapt.org/sites/weadapt.org/files/legacy-new/placemarks/files/5345354491559sei-dfid-afghanistan-report-1-.pdf>.
- Saxton, K. E., & Rawls, W. J. (2006). Soil water characteristic estimates by texture and organic matter for hydrologic solutions. *Soil science society of America Journal*, 70(5), 1569-1578. <https://doi.org/10.2136/sssaj2005.0117>.
- Schwalm, C. R., Anderegg, W. R., Michalak, A. M., Fisher, J. B., Biondi, F., Koch, G., Litvak, M., Ogle,

- K., Shaw, J.D., Wolf, A. and Huntzinger, D.N. (2017). Global patterns of drought recovery. *Nature*. 548, 202-205. <https://doi.org/10.1038/nature23021>.
- Sellers, P.J. (1985). Canopy reflectance, photosynthesis, and transpiration. *International journal of remote sensing*, 6, 1335-1372. <https://doi.org/10.1080/01431168508948283>.
- Sepulcre-Canto, G., Horion, S.M.A.F., Singleton, A., Carrao, H. and Vogt, J. (2012). Development of a Combined Drought Indicator to detect agricultural drought in Europe. *Natural Hazards and Earth System Sciences*, 12, 3519-3531. <https://doi.org/10.5194/nhess-12-3519-2012>.
- Serrano Porta, L., González Flor, C., & Gorchs Altarriba, G. (2014). Assessment of grape yield and composition using reflectance-based indices in rainfed vineyards. *Agronomy Journal*, 118(15), 1309-1316. <http://hdl.handle.net/2117/87054>.
- Shahab, M., Roberto, S.R., Ahmed, S., Colombo, R.C., Silvestre, J.P., Koyama, R., de Souza, R.T. (2020). Relationship between anthocyanins and skin color of table grapes treated with abscisic acid at different stages of berry ripening. *Sci. Hort.* 259, p.108859. <https://doi.org/10.1016/j.scienta.2019.108859>.
- Shahzaman, M., Zhu, W., Bilal, M., Habtemicheal, B.A., Mustafa, F., Arshad, M., Ullah, I., Ishfaq, S. and Iqbal, R. (2021). Remote sensing indices for spatial monitoring of agricultural drought in South Asian countries. *Remote Sensing*, 13(11), p.2059. <https://doi.org/10.3390/rs13112059>
- Shamsuzzoha M, Noguchi R, Ahamed T (2021) Damaged area assessment of cultivated agricultural lands affected by cyclone bulbul in coastal region of Bangladesh using Landsat 8 OLI and TIRS datasets. *Remote Sens Appl Soc Environ* 23:100523. <https://doi.org/10.1016/j.rsase.2021.100523>
- Shashikant, V., Mohamed Shariff, A. R., Wayayok, A., Kamal, M. R., Lee, Y. P., & Takeuchi, W. (2021). Utilizing TVDI and NDWI to Classify Severity of Agricultural Drought in Chuping, Malaysia. *Agronomy*, 11(6), 1243. <https://doi.org/10.3390/agronomy11061243>.
- Shukla, P.R., Skea, J., Calvo Buendia, E., Masson-Delmotte, V., Pörtner, H.O., Roberts, D.C., Zhai, P., Slade, R., Connors, S., Van Diemen, R. and Ferrat, M. (2019). IPCC, 2019. Climate Change and Land: an IPCC special report on climate change, desertification, land degradation, sustainable land management, food security, and greenhouse gas fluxes in terrestrial ecosystems. file:///F:/Second_paper_review/SRCCL-Full-Report-Compiled-191128.pdf.
- Sok, K., Visessri, S. and Heng, S. (2022). Assessing Impacts of Drought on Agriculture and Food Security in the Baribo Basin, Cambodia. 10.20944/preprints202201.0444.v1

- Spinoni, J., Vogt, J.V., Naumann, G., Barbosa, P. and Dosio, A. (2018). Will drought events become more frequent and severe in Europe? *International Journal of Climatology*, 38(4), pp.1718-1736. <https://doi.org/10.1002/joc.5291>
- Stanchi, S., Godone, D., Belmonte, S., Freppaz, M., Galliani, C., & Zanini, E. (2013). Land suitability map for mountain viticulture: A case study in Aosta Valley (NW Italy). *Journal of Maps*, 9(3), 367-372. <https://doi.org/10.1080/17445647.2013.785986>
- Steiner, F., McSherry, L., & Cohen, J. (2000). Land suitability analysis for the upper Gila River watershed. *Landscape and urban planning*, 50(4), 199-214. [10.1016/S0169-2046\(00\)00093-1](https://doi.org/10.1016/S0169-2046(00)00093-1).
- Sun, F., Mejia, A., Zeng, P. and Che, Y. (2019). Projecting meteorological, hydrological and agricultural droughts for the Yangtze River basin. *Science of the Total Environment*, 696, 134076. <https://doi.org/10.1016/j.scitotenv.2019.134076>.
- Sun, L., Gao, F., Anderson, M.C., Kustas, W.P., Alsina, M.M., Sanchez, L., Sams, B., McKee, L., Dulaney, W., White, W.A., Alfieri, J.G. (2017). Daily mapping of 30 m LAI and NDVI for grape yield prediction in California vineyards. *Rem. Sens*, 9, 317. <https://doi.org/10.3390/rs9040317>.
- Tagarakis, A., Liakos, V., Fountas, S., Koundouras, S., & Gemtos, T. A. (2013). Management zones delineation using fuzzy clustering techniques in grapevines. *Precision Agriculture*, 14(1), 18-39. <https://doi.org/10.1007/s11119-012-9275-4>.
- Taghizadeh-Mehrjardi, R., Nabiollahi, K., Rasoli, L., Kerry, R., & Scholten, T. (2020). Land suitability assessment and agricultural production sustainability using machine learning models. *Agronomy*, 10(4), 573. <https://doi.org/10.3390/agronomy10040573>.
- Tamiminia, H., Salehi, B., Mahdianpari, M., Quackenbush, L., Adeli, S., & Brisco, B. (2020). Google Earth Engine for geo-big data applications: A meta-analysis and systematic review. *ISPRS Journal of Photogrammetry and Remote Sensing*, 164, 152-170. <https://doi.org/10.1016/j.isprsjprs.2020.04.001>
- Tanre, D., Deuze, J.L., Herman, M., Santer, R., and Vermote, E. (2005). Second Simulation Of The Satellite Signal In The Solar Spectrum. *IEEE Trans. Geosci. Remote Senc.* 35 (3), 187–187. <https://doi.org/10.1109/igarss.1990.688308>.
- Tariq, A., Riaz, I., Ahmad, Z., Yang, B., Amin, M., Kausar, R., Andleeb, S., Farooqi, M.A. and Rafiq, M. (2020). Land surface temperature relation with normalized satellite indices for the estimation of spatio-temporal trends in temperature among various land use land cover classes of an arid Potohar region using Landsat data. *Environmental Earth Sciences*, 79, 40. <https://doi.org/10.1007/s12665-019-8766-2>.

- Tashayo, B., Honarbakhsh, A., Akbari, M. and Eftekhari, M. (2020). Land suitability assessment for maize farming using a GIS-AHP method for a semi-arid region, Iran. *Journal of the Saudi Society of Agricultural Sciences*, 19(5), pp.332-338.
- Taylor, J. W. (2000). A quantile regression neural network approach to estimating the conditional density of multiperiod returns. *Journal of Forecasting*, 19(4), 299-311. [https://doi.org/10.1002/1099-131X\(200007\)19:4<299::AID-FOR775>3.0.CO;2-V](https://doi.org/10.1002/1099-131X(200007)19:4<299::AID-FOR775>3.0.CO;2-V)
- Ted, G. (2018). *The grape grower's handbook: a complete guide to viticulture for wine production*. Apex. 3rd ed. <https://www.amazon.com/Grape-Growers-Handbook-Viticulture-Production/dp/0967521254>.
- Teixeira, A.D.C., Bastiaanssen, W.G.M., Bassoi, L.H. (2007). Crop water parameters of irrigated wine and table grapes to support water productivity analysis in the São Francisco River basin, Brazil. *Agric. Water Manag.*, 94, 31-42. <https://doi.org/10.1016/j.agwat.2007.08.001>.
- The Sustainable Development Goals (SDGs) Report. (2019). <https://unstats.un.org/sdgs/report/2019/The-Sustainable-Development-Goals-Report-2019.pdf>. Last access 8 February 2022.
- Tian, H., Wang, T., Liu, Y., Qiao, X., Li, Y. (2020). Computer vision technology in agricultural automation—A review. *Inf. Process Agric*, 7, 1-19. <https://doi.org/10.1016/j.inpa.2019.09.006>.
- Tisseyre, B., Ojeda, H., Taylor, J. (2007). New technologies and methodologies for site-specific viticulture. *J. Intl. Sci. Vin.* 41, 63-76. <https://doi.org/10.20870/oeno-one.2007.41.2.852>.
- Tombesi, S., Frioni, T., Poni, S. and Palliotti, A., 2018. Effect of water stress “memory” on plant behavior during subsequent drought stress. *Environmental and Experimental Botany*, 150, pp.106-114. <https://doi.org/10.1016/j.envexpbot.2018.03.009>
- Touma, D., Ashfaq, M., Nayak, M. A., Kao, S. C., and Duffenbaugh, N. S. (2015). A multi-model and multi-index evaluation of drought characteristics in the 21st century. *Journal of Hydrology*, 526, 196-207. <https://doi.org/10.1016/j.jhydrol.2014.12.011>.
- Tucker, C.J. (1979). Red and photographic infrared linear combinations for monitoring vegetation. *Remote sensing of Environment*, 8(2), pp.127-150. [https://doi.org/10.1016/0034-4257\(79\)90013-0](https://doi.org/10.1016/0034-4257(79)90013-0).
- Tucker, C.J., Justice, C.O. and Prince, S.D. (1986). Monitoring the grasslands of the Sahel 1984-1985. *International Journal of Remote Sensing*, 7(11), pp.1571-1581. <https://doi.org/10.1080/01431168608948954>
- UN Environment Program. (2009), Projected losses in food production due to climate change by 2080. <https://reliefweb.int/map/world/projected-losses-food-production-due-climate-2080>.

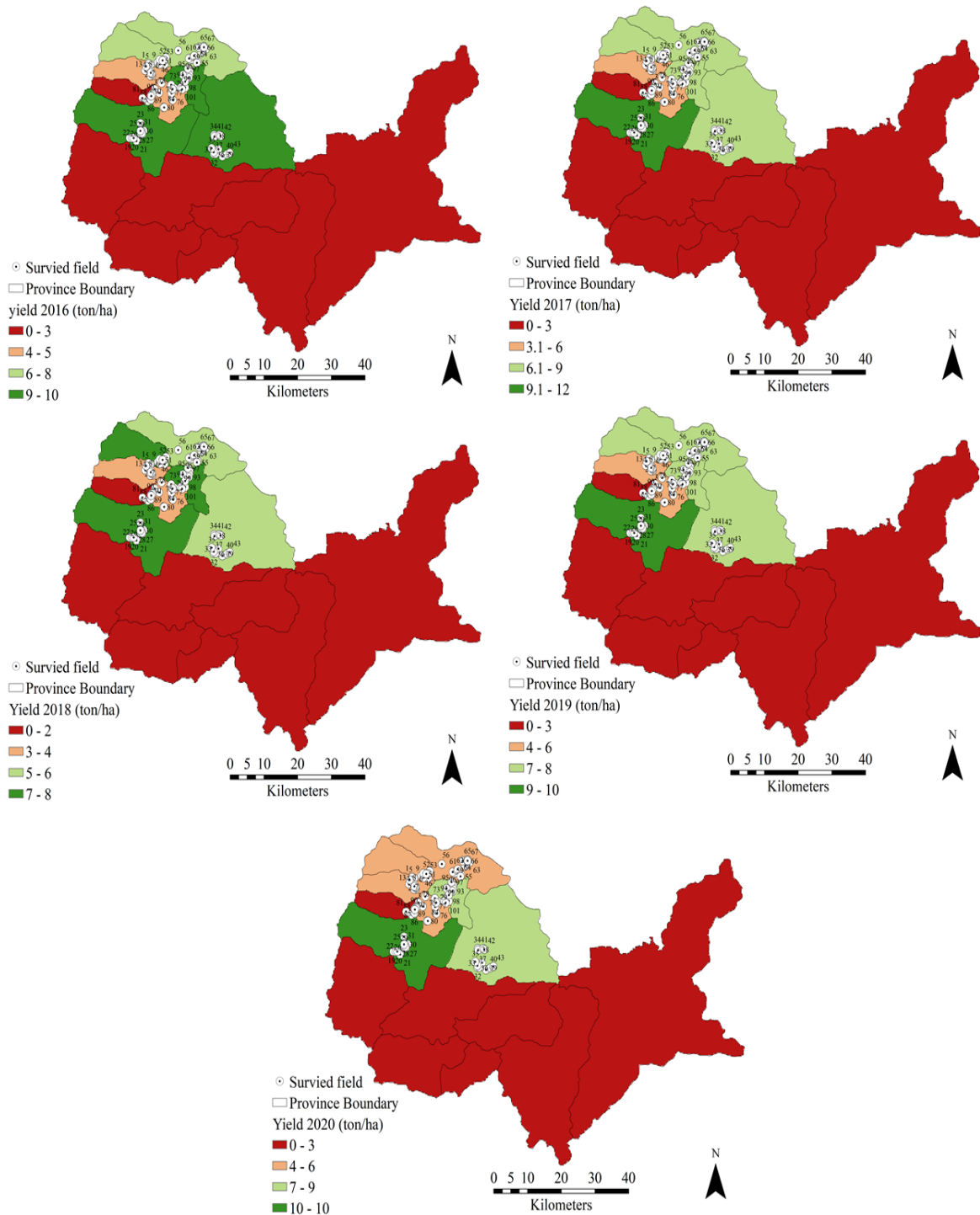
- change-2080 Last access 8 February 2022.
- UNHCR (2002). UNHCR Sub-Office Central Region District profile. https://www.ecoi.net/en/file/local/1350659/10565_accord368_shakardara.pdf. Last access 8 February 2022.
- USAID, Commercial Horticulture and Agricultural Marketing Program and Roots of Peace (2016). Best Practices for GRAPE Production and Marketing in Afghanistan. Guide offers tips on cultivation, harvesting and marketing techniques to improve sales of Afghan produce on international export markets pp 1-37.
- WWF Germany. (2019). Drought risk–The global thirst for water in the era of climate crisis. WWF Germany. https://wwfint.awsassets.panda.org/downloads/drought_risk_wwf.pdf last access 09 February 2022.
- Wali, E., Datta, A., Shrestha, R. P., & Shrestha, S. (2016). Development of a land suitability model for saffron (*Crocus sativus* L.) cultivation in Khost Province of Afghanistan using GIS and AHP techniques. *Archives of Agronomy and Soil science*, 62(7), 921-934. <https://doi.org/10.1080/03650340.2015.1101519>.
- Walt, S. M. (2018). LAND COVER ATLAS, Foreign Policy. <https://ufdc.ufl.edu/AA00003612/00001/4j>. Last access 8 February 2022.
- Wang, L., Ma, Y., Yan, J., Chang, V., & Zomaya, AY (2018). PipsCloud: High performance cloud computing for remote sensing big data management and processing. *Future Generation Computer Systems*, 78, 353-368. <https://doi.org/10.1016/j.future.2016.06.009>
- Wang, L., Wang, P., Liang, S., Qi, X., Li, L. and Xu, L. (2019). Monitoring maize growth conditions by training a BP neural network with remotely sensed vegetation temperature condition index and leaf area index. *Computers and Electronics in Agriculture*, 160, pp.82-90. <https://doi.org/10.1016/j.compag.2019.03.017>
- Wang, L., Wang, P., Liang, S., Zhu, Y., Khan, J., & Fang, S. (2020). Monitoring maize growth on the North China Plain using a hybrid genetic algorithm-based back-propagation neural network model. *Computers and Electronics in Agriculture*, 170, 105238. <https://doi.org/10.1016/j.compag.2020.105238>.
- Wilhite, D. A., Sivakumar, M. V., & Pulwarty, R. (2014). Managing drought risk in a changing climate: The role of national drought policy. *Weather and climate extremes*, 3, 4-13. <https://doi.org/10.1016/j.wace.2014.01.002>.
- Wilhite, D.A. and Glantz, M.H. (1985). Understanding: the drought phenomenon: the role of definitions. *Water international*, 10(3), pp.111-120. <https://doi.org/10.1080/02508068508686328>

- Wilhite, D.A. (2000). Drought as a natural hazard: concepts and definitions. Published in *Drought: A Global Assessment*, Vol. I, chap. 1, pp. 3–18 (London: Routledge, 2000).
- Wolf, TK., Boyer JD. (2005). Vineyard site selection.
https://vtechworks.lib.vt.edu/bitstream/handle/10919/50983/463-020_pdf.pdf Last access 12 March 2022.
- World bank, Afghanistan Multi-hazard risk assessment (2018). Washington, DC: World Bank.
<https://www.gfdrr.org/en/publication/afghanistan-multi-hazard-risk-assessment>. Last access 8 February 2022.
- Worqlul, A. W., Dile, Y. T., Jeong, J., Adimassu, Z., Lefore, N., Gerik, T., Srinivasan, R., & Clarke, N. (2019). Effect of climate change on land suitability for surface irrigation and irrigation potential of the shallow groundwater in Ghana. *Computers and Electronics in Agriculture*, 157, 110–125. <https://doi.org/10.1016/j.compag.2018.12.040>
- Worqlul, A. W., Jeong, J., Dile, Y. T., Osorio, J., Schmitter, P., Gerik, T., ... & Clark, N. (2017). Assessing potential land suitable for surface irrigation using groundwater in Ethiopia. *Applied Geography*, 85, 1-13. <https://doi.org/10.1016/j.apgeog.2017.05.010> .
- Wu, X., Wang, P., Ma, Y., Gong, Y., Wu, D., Yang, J., & Huo, Z. (2021). Standardized relative humidity index can be used to identify agricultural drought for summer maize in the Huang-Huai-Hai Plain, China. *Ecological Indicators*, 131, 108222. <https://doi.org/10.1016/j.ecolind.2021.108222>.
- Wójtowicz, M., Wójtowicz, A. and Piekarczyk, J. (2016). Application of remote sensing methods in agriculture. *Communications in biometry and crop science*, 11(1), pp.31-50. <https://digitalcommons.unl.edu/droughtfacpub/69/>. Last access 12 March 2022.
- Xie, Z., Phinn, SR, Game, ET, Pannell, DJ, Hobbs, RJ, Briggs, PR, & McDonald-Madden, E. (2019). Using Landsat observations (1988–2017) and Google Earth Engine to detect vegetation cover changes in rangelands-A first step towards identifying degraded lands for conservation. *Remote Sensing of Environment*, 232, 111317. <https://doi.org/10.1016/j.rse.2019.111317>
- Xu, Y., Ramanathan, V., & Washington, W. M. (2016). Observed high-altitude warming and snow cover retreat over Tibet and the Himalayas enhanced by black carbon aerosols. *Atmospheric Chemistry and Physics*, 16(3), 1303-1315. <https://doi.org/10.5194/acp-16-1303-2016>.
- Xu, Y., Zhang, Y. and Chen, J. (2021). Migration under economic transition and changing climate in Mongolia. *Journal of Arid Environments*. 185, 104333. <https://doi.org/10.1016/j.jaridenv.2020.104333>.

- Yagci, A. L., Di, L., Deng, M., Han, W., & Peng, C. (2011). Agricultural drought monitoring from space using freely available MODIS data and impacts on cotton commodity. *Pecora 18—Forty Years of Earth Observation... Understanding a Changing World*, 9. <http://www.asprs.org/pecora18/proceedings/Yagci.pdf>. Last Access 5 May 2022.
- Yamoah, C. F., Walters, D. T., Shapiro, C. A., Francis, C. A., & Hayes, M. J. (2000). Standardized precipitation index and nitrogen rate effects on crop yields and risk distribution in maize. *Agriculture, ecosystems & environment*, 80(1-2), 113-120. [https://doi.org/10.1016/S0167-8809\(00\)00140-7](https://doi.org/10.1016/S0167-8809(00)00140-7)
- Yao, N., Li, L., Feng, P., Feng, H., Liu, D.L., Liu, Y., Jiang, K., Hu, X., Li, Y. (2020). Projections of drought characteristics in China based on a standardized precipitation and evapotranspiration index and multiple GCMs. *Sci. Total Environ*, 704, 135245. <https://doi.org/10.1016/j.scitotenv.2019.135245>.
- Yin, L., Clark, M.D., Burkness, E.C., Hutchison, W.D. (2019). Grape phylloxera (Hemiptera: Phylloxeridae), on cold-hardy hybrid wine grapes (*Vitis* spp.): A review of pest biology, damage, and management practices. *J. Integr. Pest Manag.* 10, 16. <https://doi.org/10.1093/jipm/pmz011>.
- Zdruli, P., Calabrese, J., Ladisa, G., & Otekhile, A. (2014). Impacts of land cover change on soil quality of manmade soils cultivated with table grapes in the Apulia Region of south-eastern Ital, *Catena*, 121, 13-21. DOI: [10.1016/j.catena.2014.04.015](https://doi.org/10.1016/j.catena.2014.04.015).
- Zhang, A. and Jia, G. (2013). Monitoring meteorological drought in semiarid regions using multi-sensor microwave remote sensing data. *Remote Sensing of Environment*, 134, 12-23. <https://doi.org/10.1016/j.rse.2013.02.023>.
- Zhang, J. (2004). Risk assessment of drought disaster in the maize-growing region of Songliao Plain, China. *Agriculture, ecosystems & environment*, 102(2), pp.133-153. <https://doi.org/10.1016/j.agee.2003.08.003>.
- Zhang, J., Mishra, A. K., Hirsch, S., & Li, X. (2020). Factors affecting farmland rental in rural China: Evidence of capitalization of grain subsidy payments. *Land Use Policy*, 90, 104275. <https://doi.org/10.1016/j.landusepol.2019.104275>.
- Zhang, J., Mu, Q., & Huang, J. (2016). Assessing the remotely sensed Drought Severity Index for agricultural drought monitoring and impact analysis in North China. *Ecological Indicators*, 63, 296-309. <https://doi.org/10.1016/j.ecolind.2015.11.062>
- Zhang, L., Chu, Q. Q., Jiang, Y. L., Fu, C., & LEI, Y. D. (2021). Impacts of climate change on drought risk of winter wheat in the North China Plain. *Journal of Integrative Agriculture*, 20(10), 2601-2612. [https://doi.org/10.1016/S2095-3119\(20\)63273-7](https://doi.org/10.1016/S2095-3119(20)63273-7).

- Zhang, T., Su, X., Zhang, G., Wu, H., Wang, G. and Chu, J. (2022). Evaluation of the impacts of human activities on propagation from meteorological drought to hydrological drought in the Weihe River Basin, China. *Science of The Total Environment*, 819, p.153030. <https://doi.org/10.1016/j.scitotenv.2022.153030>.
- Zhang, X., Chen, N., Li, J., Chen, Z. and Niyogi, D. (2017). Multi-sensor integrated framework and index for agricultural drought monitoring. *Remote Sensing of Environment*, 188, pp.141-163. <https://doi.org/10.1016/j.rse.2016.10.045>.
- Zhu, X., Hou, C., Xu, K. and Liu, Y. (2020). Establishment of agricultural drought loss models: A comparison of statistical methods. *Ecological Indicators*, 112, 106084. <https://doi.org/10.1016/j.ecolind.2020.106084>.
- Zhu, Z., Woodcock, C.E. (2012). Object-based cloud and cloud shadow detection in Landsat imagery. *Remote Sens. Environ*, 118, 83–94. <https://doi.org/10.1016/j.rse.2011.10.028>.

Appendices



Appendix 4.1 Yield maps shows the ground reference data and GPS points collected from Kabul Province through surveys.

Appendix 4.2 Variation in yield in severely drought-affected vineyards in percent and tons in 2016

FID	Drought classes	latitude	longitude	Drought composite index 2016	Yield (ton/ha) 2016	Predicted yield (ton/ha)	Losses (%)	Losses (ton/ha)
7	2	34.807582	69.061695	0.1824	7	7.7	-9.6	-0.7
10	2	34.78959	69.074149	0.1721	5	2.8	43.8	2.2
11	2	34.793774	69.071657	0.1820	3.5	6.5	-85.8	-3.0
14	2	34.634556	69.034192	0.1458	2.8	1.5	47.9	1.3
15	2	34.633661	69.032658	0.1242	1.1	1.0	3.4	0.0
17	2	34.656974	69.052773	0.1614	1.7	1.7	-3.0	-0.1
21	2	34.633463	69.03284	0.1773	5.3	5.0	6.5	0.3
29	2	34.650874	69.043925	0.1986	5.6	9.0	-61.5	-3.4
30	2	34.651399	69.047035	0.1826	11.9	7.8	34.4	4.1
46	2	34.81469	69.089129	0.1645	2.8	1.7	38.2	1.1
47	2	34.809187	69.107673	0.1938	14	10.4	25.9	3.6
59	2	34.82382	69.172991	0.1711	3.4	2.5	24.3	0.8
67	2	34.849625	69.212477	0.1589	1.4	1.8	-26.4	-0.4
75	2	34.76698	69.099934	0.1373	1	1.1	-12.1	-0.1
88	2	34.725339	69.062947	0.1659	2.6	1.8	31.5	0.8
92	2	34.793473	69.175309	0.1988	10.5	9.0	14.4	1.5
94	2	34.765873	69.158607	0.1928	10	10.5	-4.8	-0.5

Appendix 4.3 Variation in yield in moderately drought-affected vineyards in percent and tons in 2016

FID	Drought classes	latitude	longitude	Drought composite index 2016	Yield (ton/ha) 2016	Predicted Yield (ton/ha)	Losses (%)	Losses (ton/ha)
1	3	34.81169	69.06475	0.2112	0.6	1.0	-78.6	-0.4
2	3	34.78426	69.07432	0.2305	6.3	4.7	26.2	1.6
3	3	34.78391	69.06963	0.2328	2.8	3.9	-40.5	-1.1
4	3	34.80882	69.06958	0.2385	2.8	2.7	4.5	0.1
5	3	34.80892	69.07033	0.2191	0.3	0.6	-100.0	-0.3
6	3	34.78762	69.07402	0.2479	5.6	4.9	12.8	0.7
8	3	34.79612	69.05603	0.2112	1	2.0	-100.0	-1.0
9	3	34.81159	69.06469	0.2312	5.6	4.4	20.5	1.2
12	3	34.79081	69.07098	0.2099	4.2	4.1	3.4	0.1
13	3	34.80548	69.05848	0.2179	2.2	1.7	24.4	0.5
18	3	34.65826	69.04799	0.2992	25	23.5	6.1	1.5
20	3	34.63964	69.02115	0.2096	1.4	2.0	-42.9	-0.6
22	3	34.64016	69.02539	0.2584	10	10.2	-1.7	-0.2
23	3	34.67438	69.04297	0.2704	20	15.2	24.0	4.8
24	3	34.65833	69.04413	0.2340	2.5	3.5	-44.9	-1.1
27	3	34.64961	69.04862	0.2036	0	1.9	0.0	-1.9
28	3	34.65602	69.04641	0.2995	26	23.5	9.7	2.5
31	3	34.65676	69.04295	0.2457	1.4	2.0	-42.9	-0.6
37	3	34.61676	69.23316	0.2117	4.2	3.3	21.1	0.9
43	3	34.60591	69.28156	0.2199	1.1	2.0	-78.6	-0.9
44	3	34.82612	69.11177	0.2495	5.6	5.7	-1.2	-0.1
48	3	34.81058	69.09507	0.2497	7.7	5.8	25.1	1.9
50	3	34.81966	69.10696	0.2217	3	3.3	-9.5	-0.3
51	3	34.81907	69.09848	0.2322	0.6	1.0	-78.6	-0.4
52	3	34.82069	69.0947	0.2028	0.8	1.2	-41.7	-0.4
54	3	34.83759	69.20596	0.2428	5.6	3.1	45.1	2.5
55	3	34.81735	69.19552	0.2621	15	11.5	23.3	3.5
56	3	34.84224	69.14399	0.2458	2	4.0	-99.9	-2.0
57	3	34.84931	69.19973	0.2394	2	2.7	-32.7	-0.7
58	3	34.82095	69.17767	0.2651	3.4	5.0	-48.8	-1.6
61	3	34.82793	69.1844	0.2069	10.1	4.0	60.2	6.1
62	3	34.83003	69.18646	0.2456	11.2	3.9	65.0	7.3
64	3	34.81356	69.19386	0.2705	11.2	15.3	-36.2	-4.1

65	3	34.85171	69.21214	0.2215	4.5	3.2	29.0	1.3
66	3	34.84902	69.21174	0.2188	3.5	1.9	44.6	1.6
68	3	34.76068	69.12376	0.2193	1.2	2.1	-76.9	-0.9
69	3	34.74413	69.09288	0.2054	0.8	2.0	-150.0	-1.2
70	3	34.76027	69.12325	0.2000	0	-1.2	0.0	1.2
71	3	34.7292	69.12714	0.2451	10	3.7	62.6	6.3
73	3	34.76275	69.12551	0.2380	0.2	1.0	-31.7	-0.8
74	3	34.75036	69.13116	0.2397	1.4	2.7	-90.1	-1.3
76	3	34.72791	69.1296	0.2033	1.2	1.6	-35.7	-0.4
77	3	34.74312	69.1262	0.2440	1.4	2.0	-42.9	-0.6
78	3	34.75297	69.08113	0.2657	18	12.9	28.6	5.1
79	3	34.75315	69.12924	0.2355	1.4	2.0	-42.9	-0.6
80	3	34.71092	69.10456	0.2349	7	3.3	53.1	3.7
81	3	34.73253	69.04863	0.2054	3.2	3.3	-1.8	-0.1
84	3	34.71068	69.10661	0.2332	6.8	3.8	44.1	3.0
85	3	34.74096	69.07524	0.2240	1.2	2.0	-66.7	-0.8
86	3	34.72848	69.0703	0.2479	1.2	2.0	-66.7	-0.8
87	3	34.72757	69.07141	0.2292	0.2	0.4	-66.7	-0.2
89	3	34.72889	69.07079	0.2171	0.4	0.8	-100.0	-0.4
91	3	34.73684	69.07225	0.2193	0.1	0.2	-42.9	-0.1
93	3	34.79305	69.17482	0.2283	9	5.1	43.7	3.9
100	3	34.80073	69.16992	0.2215	10.5	3.2	69.7	7.3

Appendix 4.4 Variation in yield in severely drought-affected vineyards in percent and tons in 2018

FID	Drought classes	latitude	longitude	Drought composite index 2018	Yield (ton/ha) 2018	Predicted Yield (ton/ha)	Losses (%)	Losses (ton/ha)
1	2	34.81169	69.06475	0.1348	0.8	1.2	-44.9	-0.4
9	2	34.81159	69.06469	0.1348	0.0	1.2	0.0	-1.2
12	2	34.79081	69.07098	0.1520	5.6	5.7	-1.3	-0.1
14	2	34.63456	69.03419	0.1122	2.1	2.6	-22.4	-0.5
15	2	34.63366	69.03266	0.1229	0.7	0.7	0.6	0.0
16	2	34.64035	69.01387	0.1145	2.9	1.9	35.3	1.0
19	2	34.6402	69.01426	0.1708	4.5	8.3	-85.5	-3.8
20	2	34.63964	69.02115	0.1024	1.1	1.4	-32.3	-0.3
21	2	34.63346	69.03284	0.1409	1.5	2.0	-100.0	-1.0
22	2	34.64016	69.02539	0.2010	20	24.9	-24.4	-4.9
31	2	34.65676	69.04295	0.1460	0.9	0.5	41.5	0.4
32	2	34.60382	69.23861	0.1904	24.5	15.6	36.5	8.9
34	2	34.64711	69.23964	0.1307	3.5	1.8	49.1	1.7
44	2	34.82612	69.11177	0.1508	5.6	4.9	12.9	0.7
57	2	34.84931	69.19973	0.1348	3.5	1.2	65.1	2.3
61	2	34.82793	69.1844	0.1905	10.1	14.8	-47.1	-4.7
62	2	34.83003	69.18646	0.1975	10.1	8.9	11.3	1.1
68	2	34.76068	69.12376	0.1152	2.4	1.7	29.8	0.7
70	2	34.76027	69.12325	0.1156	0.2	0.4	-100.0	-0.2
72	2	34.75565	69.13278	0.0903	2.2	2.2	0.3	0.0
73	2	34.76275	69.12551	0.1042	1.6	2.1	-31.1	-0.5
85	2	34.74096	69.07524	0.1353	0.4	0.7	-75.0	-0.3
86	2	34.72848	69.0703	0.1484	1.6	2.6	-60.2	-1.0
88	2	34.72534	69.06295	0.1037	2.3	1.9	17.1	0.4
96	2	34.78586	69.17391	0.1906	10.	14.4	-44.4	-4.4
97	2	34.77912	69.17211	0.1698	7	7.7	-9.8	-0.7

Appendix 4.5 Variation in yield in moderately drought-affected vineyards in percent and tons in 2018

FID	Drought classes	latitude	longitude	Drought composite index 2018	Yield (ton/ha) 2018	Predicted Yield (ton/ha)	Losses (%)	Losses (ton/ha)
4	3	34.80882	69.06958	0.2359	1.7	3	-78.6	-1.3
5	3	34.80892	69.07033	0.2000	0.1	0.2	-100.0	-0.1
7	3	34.80758	69.0617	0.2300	7.4	4	45.7	3.4
13	3	34.80548	69.05848	0.2300	1.4	2.8	-100.0	-1.4
23	3	34.67438	69.04297	0.2546	11	7.3	33.3	3.7
25	3	34.65371	69.04333	0.2526	10.5	7.4	29.8	3.1
26	3	34.65519	69.04602	0.2658	11	8.7	20.9	2.3
27	3	34.64961	69.04862	0.2821	18	14.2	21.2	3.8
33	3	34.60374	69.24359	0.2498	12	7.1	40.6	4.9
35	3	34.61446	69.25129	0.2274	5	3.3	34.3	1.7
36	3	34.60769	69.23904	0.2557	10.5	7.2	31.1	3.3
38	3	34.64359	69.24063	0.2141	2	3.7	-82.8	-1.7
39	3	34.59808	69.26179	0.2496	1.5	2.0	-33.3	-0.5
40	3	34.60256	69.27399	0.2200	1	1.8	-80.0	-0.8
41	3	34.64712	69.25391	0.2166	0.5	0.9	-83.7	-0.4
42	3	34.64489	69.25708	0.2786	18	19.5	-8.3	-1.5
46	3	34.81469	69.08913	0.2538	2.8	5.0	-78.6	-2.2
47	3	34.80919	69.10767	0.2684	17	11.8	30.7	5.2
50	3	34.81966	69.10696	0.2100	4.5	3.4	23.6	1.1
52	3	34.82069	69.0947	0.2200	0.6	1.0	-58.7	-0.4
53	3	34.81918	69.10264	0.2200	7.7	3.0	61.3	4.7
54	3	34.83759	69.20596	0.2400	7.7	6.0	22.3	1.7
55	3	34.81735	69.19552	0.2500	10	7.1	28.5	2.9
56	3	34.84224	69.14399	0.2500	2	4.0	-100.0	-2.0
58	3	34.82095	69.17767	0.2100	3.4	3.4	-2.3	-0.1
59	3	34.82382	69.17299	0.2600	3.4	6.6	-97.0	-3.3
60	3	34.84566	69.2174	0.2400	9	6.0	33.3	3.0
63	3	34.84546	69.21777	0.2500	8	7.1	10.7	0.9
66	3	34.84902	69.21174	0.2400	3.5	6.0	-70.9	-2.5
71	3	34.7292	69.12714	0.2400	7	6.0	14.6	1.0
74	3	34.75036	69.13116	0.2300	1.4	2.0	-42.9	-0.6
75	3	34.76698	69.09993	0.2300	1.9	3.0	-60.7	-1.1
76	3	34.72791	69.1296	0.2200	5.4	3.0	44.5	2.4

77	3	34.74312	69.1262	0.2300	2.1	4.0	-90.2	-1.9
78	3	34.75297	69.08113	0.2300	7.0	4.0	42.9	3.0
80	3	34.71092	69.10456	0.2700	16	14.1	11.8	1.9
81	3	34.73253	69.04863	0.2563	3.6	7.2	-97.8	-3.5
84	3	34.71068	69.10661	0.2561	3	6.0	-97.8	-3.0
89	3	34.72889	69.07079	0.2223	0.4	0.8	-80.5	-0.4
91	3	34.73684	69.07225	0.2000	0.2	0.4	-77.6	-0.2
92	3	34.79347	69.17531	0.2494	9.5	7.1	25.6	2.4
93	3	34.79305	69.17482	0.2574	9	7.0	22.6	2.0
98	3	34.75637	69.16274	0.2575	9	7.0	22.6	2.0
99	3	34.75632	69.14972	0.2686	7.5	12.1	-61.3	-4.6
100	3	34.80073	69.16992	0.2562	9	7.2	20.5	1.8

Appendix 6.1 Criteria classification for vineyard suitability analysis based on physical and socio-economics criterion

Criteria	Suitability Classes	Threshold Value	References
NDVI	S1	0.2 - 0.5	Hashim et al., 2019
	S2	0.5 - 0.8	
	S3	0.8 - 0.9	
	N	> 0.199	
NDMI	S1	0.6 - 0.8	Zhang et al., 2016
	S2	0.4 - 0.6	
	S3	0.4 - 0.2	
	N	> 0.2	
LST	S1	25-30 °C	Stanchi et al., 2013 and USAID, 2016
	S2	30 - 36	
	S3	36 - 43	
	N	< 20	
Rainfall	S1	500 mm	Ted, 2018
	S2	-	
	S3	-	
	N	<800mm	
Elevation	S1	800 - 2000 m	Stanchi et al., 2013
	S2	2000 - 2500	
	S3	2500 - 3000	
	N	> 3000	
Slope	S1	0-10°	Stanchi et al., 2013
	S2	10-25°	
	S3	25-35°	
	N	35-44°	
Aspect	S1	North, Northeast, East	Modica et al. 2014
	S2	South, Southeast, Southwest	
	S3	West, Northwest	
	N	North	
Soil PH	S1	5.5 - 6.5	Brown, 2013
	S2	4 - 8.5	
	S3	6.5-8.0	
	N	< 5.0 and < 8.0	
Topsoil texture	S1	Sandy loam, Loam, very fine sandy loam, Loam very fine sand, Coarse sandy loam	Badr et al., 2018
	S2	Silt loam, Loamy sand, Loamy fine sand, Loamy coarse sand	
	S3	Silt, Silty clay loam, Silty clay, Clay loam, Sandy clay loam	
	N	Clay	
Topsoil types	S1	CMe (Eutric CAMBISOLS), CMg (Gleyic CAMBISOLS) CMu (Humic CAMBISOLS), CMx (Chromic CAMBISOLS), LVx (Chromic LUVISOLS).	Acharya and Yang, 2015
	S2	CMo (Ferralic CAMBISOLS), GLe (Eutric GLEYSOLS), PHc (Calcaric PHAEZEMS), PHh (Haplic PHAEZEMS RGD).	

	S3	RGd (Dystric REGOSOLS), RGi (Gelic REGOSOLS), FLc (Calcic FLUVISOLS), LPi (Gelic LEPTOSOLS), RGe (Eutric REGOSOLS)	
	N	Rock outcrop Glacier, inland ice Lake, inland water	
Topsoil depth	S1	> 50 cm	Rameshkumar et al.,2006
	S2	20-50	
	S3	-	
	N	< 20	
Soil organic matter (OM)	S1	Rich soil organic matter	Goldammer, 2018
	S2	-	
	S3	-	
	N	Poor soil organic matter	
Soil salinity	S1	Slight saline	Park et al., 2021
	S2	Moderately saline	
	S3	N/A	
	N	Strongly saline	
Distance from road	S1	1000 m	Purnamasari et al., 2019
	S2	1000-2000	
	S3	2000-3000	
	N	>3000	
Distance from river	S1	1000	
	S2	1000-15000	
	S3	< 500	
	N	>1000	
Population density	S1	Medium	Steiner et al., 2000
	S2	Low	
	S3	-	
	N	High	
Distance from local market	S1	<2 km	Hossain et al.,2010
	S2	2-4	
	S3	4-5	
	N	>5	
Distance from national market	S1	0- 5 km	Nguyen et al., 2020
	S2	5 – 10 km	
	S3	>10	
	N	-	
Benefit- cost ratio	S1	Above 1.2	Wali, et al., 2016
	S2	-	
	S3	-	
	N	Below 1.2	

Additional Appendices A

University of Tsukuba, Japan

Survey 1

Vineyard Survey questionnaire for Shakardara district

Kabul province, Afghanistan

Farmer Name								
Village Name								
Coordinates	Latitude							
	Longitude							
	Latitude							
	Longitude							
	Latitude							
	Longitude							
	Latitude							
	Longitude							
	Latitude							
	Longitude							
1. Information about agricultural operations in vineyard.								
Total area of vineyard in hectare or jerib								
Harvest Time	Month				Day			
Number of Vine in vineyard								
Type of cultivar								
Yield per vine	Kg or tone				Total vineyard			
					yield			
2017						2017		
2018						2018		
2019						2019		
Land clearing time	Month				Day			
Planting time	Month				Day			
Fertilizer	types	Month	Day	Amount	Irrigatio n Time	Month	day	frequency

Pruning time		Month	Frequency		Soil types			
A mount of Rainfall from planting up to harvesting (March-September)		1.enough water during planting to harvesting		2.insufficient amount of water during planting to harvesting				
Temperature ranges from planting up to harvesting (March-September)								
2.infromation about pre-harvest losses due to natural disaster or others								
Please circle vineyard Field suffered damage by.								
No.	Cultivar	Number of losses	Type of natural disaster	Year				
1			Drought 1.Extreme drought 2.Severe Drought 3.Moderate drought 4.Mild drought 5.No drought					
	Cultivar		Type of natural disaster	Year	Type of Diseases			
2			Diseases 1.Diseases affect all field 2.Half field 3.None		1.leaf roll virus 2.fanleaf diseases 3.Enation diseases			
3			Insect 1. Insect affect all field 2.Half field		1. Grape Berry Moth 2. Grape Phylloxera 3. Grape Rootworm 4. Grape Flea Beetle 5. Grape Cane Girdler			

			3.None		6.Grape Cane Gallmaker 7. Grape Root Borer 8. Redbanded Leafroller
When drought happened?	Month		Day		
When flood happened?	Month		Day		
When disease affected your vineyard?	Month		Day		
When insect attacked your vineyard?	Month		Day		
Losses due to drought	kg		Per vine or total vineyard		
Losses due to flood	kg		Per vine or total vineyard		
Losses due to insect	kg		Per vine or total vineyard		
Other sources of loss	kg		Per vine or total vineyard		
Government support (subsidy) during the losses	amount		Month		
Production purpose for market or family	Kg for market		Kg for family consumption		
Grape price per kg					

Additional Appendices B

University of Tsukuba, Japan

Survey 2

Awareness of and opinion of farmers about grapes subsidy Questionnaire

Introduction

To fulfill the requirement of PhD degree we would like to do research in the University of Tsukuba and through this field survey in the Kabul province of Afghanistan to know about the farmers awareness and opinion about the agricultural subsidy. The finding of this research will support government to establish subsidy program for farmers in Afghanistan and it also assist producers in dealing with the repercussions of natural disasters and diseases affecting grapes production and in sustaining their livelihoods.

Code:..... Household Head Name:.....

Age:..... Major Occupation:.....

Secondary occupation:..... Education level:.....

No. of family members:.....

Telephone: ----- Date of interview: -----

Village: ----- District: -----

GPS Location:

Longitude:

Latitude:

I. Household socio-economic information

1. Off-farm jobs: No Yes (specify)-----
2. How many of your family members depend on farming? -----
3. Do you have membership in cooperative? Yes No
4. Are you the current landowner? Yes No
5. What type of landownership are you using?.....
6. Owned agricultural land area: (jerib)
7. Total land for grapes cultivation: (jerib)
8. Which type of Agricultural Land you are having? Irrigated Non-Irrigated Semi
 Irrigated

II. Perception of Threat

1. Please rate the most common catastrophes and its frequency in your area during the previous five years.

<input type="checkbox"/> Flood.....	<input type="checkbox"/> Drought.....	<input type="checkbox"/> Storm.....
<input type="checkbox"/> Landslide.....	<input type="checkbox"/> Agricultural pests and epidemics.....	<input type="checkbox"/> Other(specify).....

2. How probable or unlikely is it that you will directly experience natural disasters or diseases that disrupt grape production?

- 0 = This will not happen to me
- 1 = Extremely doubtful
- 2 = Unbelievable
- 3 = Disinterested
- 4 = Likely
- 5 = Highly likely
- 6 = This will undoubtedly happen to me

3. How essential is it for you to prevent or mitigate the negative repercussions of natural disasters or diseases that harm grape production?

- 0= it makes no difference
- 1= Not essential
- 2= Slightly essential
- 3= Neutral
- 4 = quite significant
- 5= Very essential
- 6 = incredibly essential

4. How do you rate your personal capacity to defend yourself from nature disasters or infections that harm grape production?

- 0 = I am not able to protect myself
- 1 = I can scarcely defend myself
- 3= Neutral
- 2= I can defend myself to some extent
- 4 = I can protect myself perfectly
- 5 = I am quite good at protecting myself
- 6 = I can absolutely depend on myself

5. What was the observed and expected production in your farm?

Yield	2020	2019	2018	2017	2016
Expected Yield					
Observed Yield					

Enumerator Name:

Date:

Additional Appendices C

University of Tsukuba, Japan

Graduate School of Life and Environmental Sciences

AHP Questionnaire for Vineyard Suitability Analysis base on Physical criteria

SURVEY QUESTIONNAIRE																																																
<p>This study's main goal is to assess Afghanistan's physical suitability for grape cultivation, mainly in Kabul Province. Please fill in the below criteria based on its influence</p> <p>Guidelines:</p> <p>1. Use the following scale to compare one criterion in a row to another in a column.</p> <div style="text-align: center; margin: 10px 0;"> <table border="1" style="display: inline-table; border-collapse: collapse;"> <tr> <td style="padding: 2px 5px;">1/9</td><td style="padding: 2px 5px;">1/8</td><td style="padding: 2px 5px;">1/7</td><td style="padding: 2px 5px;">1/6</td><td style="padding: 2px 5px;">1/5</td><td style="padding: 2px 5px;">1/4</td><td style="padding: 2px 5px;">1/3</td><td style="padding: 2px 5px;">1/2</td><td style="padding: 2px 5px;">1</td><td style="padding: 2px 5px;">2</td><td style="padding: 2px 5px;">3</td><td style="padding: 2px 5px;">4</td><td style="padding: 2px 5px;">5</td><td style="padding: 2px 5px;">6</td><td style="padding: 2px 5px;">7</td><td style="padding: 2px 5px;">8</td><td style="padding: 2px 5px;">9</td> </tr> <tr> <td style="padding: 2px 5px;">Extreme</td><td style="padding: 2px 5px;">Strong</td><td style="padding: 2px 5px;">Moderate</td><td style="padding: 2px 5px;">Weak or Slight</td><td style="padding: 2px 5px;">Equal</td><td style="padding: 2px 5px;">Weak or Slight</td><td style="padding: 2px 5px;">Moderate</td><td style="padding: 2px 5px;">Strong</td><td style="padding: 2px 5px;">Extreme</td><td colspan="8"></td> </tr> </table> <div style="display: flex; justify-content: space-around; margin-top: 5px;"> ← → </div> <div style="display: flex; justify-content: space-around; margin-top: 5px;"> LEAST IMPORTANT MORE IMPORTANT </div> </div> <p>2. Please compare soil type cell A24 to soil pH cell E24. If you consider soil type more important than soil pH, please add 1/9 in the column E25. Or if you think both are equal, please add 1.</p> <p>3.</p> <p>4. CR is very crucial, and it determines whether the expert's judgment is consistent or not. Therefore, the CR result should be less than 0.1.</p> <p>Note: please fill in the color area of the table only.</p>															1/9	1/8	1/7	1/6	1/5	1/4	1/3	1/2	1	2	3	4	5	6	7	8	9	Extreme	Strong	Moderate	Weak or Slight	Equal	Weak or Slight	Moderate	Strong	Extreme								
1/9	1/8	1/7	1/6	1/5	1/4	1/3	1/2	1	2	3	4	5	6	7	8	9																																
Extreme	Strong	Moderate	Weak or Slight	Equal	Weak or Slight	Moderate	Strong	Extreme																																								
Criteria	Soil Type	Soil pH	Soil Depth	Soil Texture	Organic Matter	Soil Salinity	NDVI	NDMI	Rainfall	Slop	Elevatio	LST	Land Cover	Aspect																																		
Soil Type	1																																															
pH Soil		1																																														
Depth Soil			1																																													
Texture Soil				1																																												
Organic Matter					1																																											
Soil Salinity						1																																										
NDVI							1																																									
NDMI								1																																								
Rainfall									1																																							
Slop										1																																						
Elevation											1																																					
LST												1																																				
Land Cover													1																																			
Aspect														1																																		
<p>CI = 0 RI = 1.24 CR = 0 Name: Affiliation: Address:</p> <p style="text-align: right;">Signature:</p>																																																

Additional Appendices D

University of Tsukuba, Japan

AHP Questionnaire for Vineyard Suitability Analysis based on Socio-economic Criteria

SURVEY QUESTIONNAIRE																																								
This study's main goal is to assess Afghanistan's socio-economic suitability for grape cultivation, mainly in Kabul Province. Please fill in the below criteria based on its influence Guidelines: Guidelines: 1. Use the following scales to compare one criterion in a row to another in a column.																																								
<table border="1" style="margin: auto; border-collapse: collapse;"> <tr> <td style="padding: 2px 5px;">1/9</td><td style="padding: 2px 5px;">1/8</td><td style="padding: 2px 5px;">1/7</td><td style="padding: 2px 5px;">1/6</td><td style="padding: 2px 5px;">1/5</td><td style="padding: 2px 5px;">1/4</td><td style="padding: 2px 5px;">1/3</td><td style="padding: 2px 5px;">1/2</td><td style="padding: 2px 5px;">1</td><td style="padding: 2px 5px;">2</td><td style="padding: 2px 5px;">3</td><td style="padding: 2px 5px;">4</td><td style="padding: 2px 5px;">5</td><td style="padding: 2px 5px;">6</td><td style="padding: 2px 5px;">7</td><td style="padding: 2px 5px;">8</td><td style="padding: 2px 5px;">9</td> </tr> <tr> <td style="padding: 2px 5px;">Extreme</td><td style="padding: 2px 5px;">Strong</td><td style="padding: 2px 5px;">Moderate</td><td style="padding: 2px 5px;">Weak or Slight</td><td style="padding: 2px 5px;">Equal</td><td style="padding: 2px 5px;">Weak or Slight</td><td style="padding: 2px 5px;">Moderate</td><td style="padding: 2px 5px;">Strong</td><td style="padding: 2px 5px;">Extreme</td><td colspan="8"></td> </tr> </table> <div style="display: flex; justify-content: space-around; margin-top: 5px;"> ← LEAST IMPORTANT MORE IMPORTANT → </div>							1/9	1/8	1/7	1/6	1/5	1/4	1/3	1/2	1	2	3	4	5	6	7	8	9	Extreme	Strong	Moderate	Weak or Slight	Equal	Weak or Slight	Moderate	Strong	Extreme								
1/9	1/8	1/7	1/6	1/5	1/4	1/3	1/2	1	2	3	4	5	6	7	8	9																								
Extreme	Strong	Moderate	Weak or Slight	Equal	Weak or Slight	Moderate	Strong	Extreme																																
2. Please compare distance from road to distance cell A24 distance from river cell E23. If you consider distance from road more important than distance from river, please add 1/9 in the column E24. Or if you think both are equal, please add 1. 3. CR is very essential, and it determines whether the expert's judgment is consistent or not. Therefore, the CR result should be less than 0.1.																																								
Note: Please fill in the color area of the table only																																								
Criteria	Distance from road	Distance from river	Population Density	Revenue cost Ratio	Distance from Local Market	Distance from National Market																																		
Distance from road	1																																							
Distance from river		1																																						
Population Density			1																																					
Revenue cost Ratio				1																																				
Distance from Local Market					1																																			
Distance from National Market						1																																		
CI = 0 RI = 1.24 CR = 0 Name: _____ Affiliation: _____ Address: _____																																								
Signature:																																								

Additional Appendices E

University of Tsukuba, Japan

Graduate School of Life and Environmental Sciences

AHP Questionnaire for vineyard suitability based on Physical and Socio-economic criteria

Which factor is the most important for grapes production in Afghanistan?	
Please write your answer in percentage	
a. Physical Factors (%)	b. Socii-economic factors (%)